Kinderklinik und Kinderpoliklinik im Dr. von Haunerschen Kinderspital

Dissertation

zum Erwerb des Doctor of Philosophy (Ph.D.) an der

Medizinischen Fakultät der

Ludwig-Maximilians-Universität zu München

Elucidation of novel monogenic disorders in children with intestinal inflammation

vorgelegt von:

David Illig

aus:

Bad Neustadt a.d. Saale, Deutschland

Jahr:

2022

Mit Genehmigung der Medizinischen Fakultät der

Ludwig-Maximilians-Universität zu München

First supervisor: *Prof. Dr. med. Dr. sci. nat. Christoph Klein*

Second supervisor: *Dr. med. Daniel Kotlarz, PhD*

Third supervisor: *Prof. Dr. phil. nat. Carolin Daniel*

Dean: Prof. Dr. med. Thomas Gudermann

Datum der Verteidigung:

30.03.2022

“The most exciting phrase to hear in science, the one that heralds the most discoveries, is not "Eureka!", but "That’s funny...".”

Isaac Asimov

Gewidmet in Liebe

meiner Frau, meiner Familie

und meinen guten Freunden.

Gewidmet in Dankbarkeit

allen Patienten.

Ihr Schicksal wird mich immer

begleiten und motivieren.

Table of content

Abstract

Gastrointestinal disorders manifesting with chronic intestinal inflammation are grouped as inflammatory bowel diseases (IBD). The pathogenesis of IBD is influenced by genetic predisposition, dysregulation of the immune system, the intestinal microbiome, and environmental factors. Very early onset IBD (VEO-IBD; disease onset below 6 years of age) is a life-threatening, often intractable form of IBD. VEO-IBD is often the first sign of an underlying inborn error of immunity and can be caused by rare monogenic disorders. To provide rationale arguments for treatment decisions and develop personalized therapies, genetic diagnosis and elucidation of detailed pathomechanisms is critical. However, most patients lack definitive genetic diagnosis and in patients with known defects the molecular pathomechanisms remain largely elusive.

To identify novel mutations in known and yet unknown genes, our laboratory performed a whole-exome sequencing-based screen on one of the internationally largest cohorts of VEO-IBD patients. In this screen, novel mutations in the genes (i) *IL2RG*, (ii) *CD33*, and (iii) *TREM2* were identified in three independent families. The aim of my dissertation was to unravel the underlying molecular pathomechanisms of novel mutations in these three genes and analyze their functional consequences on immune cell phenotypes by using innovative human disease model systems.

(i) A novel mutation in *IL2RG* could be identified in two siblings, which was predicted to produce an early frameshift and cause a severe SCID phenotype. However, detailed expression analysis could show that the frameshift mutation was partly rescued by a cryptic intronic splice site. Functional analysis demonstrated that the mutant IL-2Rγ caused defective IL-4 and IL-21 signaling, but normal IL-2, IL-7, and IL-15 responses. As a phenotypic correlate, I could detect a defective B cell differentiation and an atypical SCID phenotype reminiscent of *IL21R* deficiency.

(ii) Detailed immunophenotyping of peripheral blood cells from a patient with compound heterozygous mutations in *CD33* demonstrated an aberrant and increased expression of CD33 in various immune cell populations. Studies on patient cells and CRISPR/Cas9-engineered iPSC-derived hematopoietic cells revealed an altered CD33 isoform expression pattern, increased myeloid differentiation of CD33-mutated hematopoietic progenitor cells, as well as defective bacterial killing and an increased production of IL-1β in response to immune alarmins in macrophages.

(iii) The homozygous *TREM2* mutation identified in a patient was shown to cause altered molecular weight of TREM2 protein in immunoblotting studies. Functional assays showed that the TREM2 mutation led to defective pro-inflammatory cytokine secretion and aberrant M1 macrophage polarization upon stimulation of macrophages with LPS indicating impaired TLR4-mediated signaling in human TREM2 deficiency. Furthermore, TREM2 deficiency was associated with an reduced capacity of hematopoietic stem and progenitor cells to differentiate towards macrophages.

Taken together, I could identify novel mutations in three candidate genes for intestinal inflammation, that encode cell surface receptors expressed on innate and adaptive immune cells and that affect the function of hematopoietic cells in humans. My studies shed light on the molecular mechanisms regulating expression and function of these three candidates. Furthermore, I could show that the identified mutations alter functional responses of different immune cells and might contribute to intestinal inflammation in these patients. This dissertation will facilitate a better understanding of important mechanisms in immunity, help to unravel novel pathomechanisms in common immune-related disorders, and might allow identification of therapeutic strategies in future.

List of figures

List of tables

List of abbreviations

3SL	3’-Sialyllactose
AD	Alzheimer's disease
ADA	Adenosine deaminase
ADAM	A disintegrin and metalloprotease
AIM2	Absent in melanoma 2
AJ	Adherens junction
AJC	apical junctional complex
AK2	Adenylate kinase 2
AKT	AKT serine/threonine kinase
ALS	Amyotrophic lateral sclerosis
AML	Acute myeloid leukemia
AMP	Antimicrobial peptide
AP-1	Activator protein 1
APLAID	PLCγ2-associated antibody deficiency
ApoE	Apolipoprotein E
APS	Ammonium peroxodisulfate
ASC	Apoptosis-associated speck-like protein containing a CARD
Aβ	Amyloid beta
BAD	BCL2 associated agonist of cell death
BAX	BCL2 associated X, apoptosis regulator
BCL2	B-Cell CLL/Lymphoma 2
bFGF	Basic fibroblast growth factor
BMP4	Bone morphogenetic protein 4
BSA	Bovine serum albumin
CARD	Caspase recruitment domain family member
Cas9	CRISPR-associated protein 9
CASP	Caspase
CCL	C-C motif chemokine ligand
CCRC Hauner	Comprehensive Childhood Research Center at the Dr. von Hauner’s Childrens Hospital
CD	Cluster of differentiation
CGD	Chronic granulomatous disease
CLR	C type lectin
CMP	Cytidine monophosphate
CNS	Central nervous system
CrD	Crohn's disease
CRISPR	Clustered regularly interspaced short palindromic repeats
CSF	Cerebrospinal fluid
CSF-1R	Colony stimulating factor 1 receptor
CST	Cell Signaling Technologies
CTLA-4	Cytotoxic T-lymphocyte-associated protein 4
CTP	Cytidine triphosphate
DAG	Diacalyglycerol
DAMP	Danger-associated molecular pattern
DAP12	DNAX-activating protein of 12 kDa
DC	Dendritic cell
DCLR1C	DNA cross-link repair 1C
DMEM	Dulbecco's Modified Eagle's Medium

DMSO	Dimethyl sulfoxide
DNA	Deoxyribonucleic acid
dNTP	Deoxy nucleoside triphosphate
DSMZ	German Collection of Microorganisms and Cell Cultures GmbH
DSS	Dextran sulfate sodium
ECM	Extracellular matrix
EDTA	Ethylenediaminetetraacetic acid
EEN	Exclusive enteral nutrition
EO-IBD	Early-onset inflammatory bowel disease
ERK	Extracellular signal-regulated kinase
FBS	Fetal bovine serum
FcεRI	High-affinity IgE receptor
FLT3	Fms like tyrosine kinase 3
FOXN1	Forkhead box N1
FOXP3	Forkhead box P3
FTD	Frontotemporal dementia
GATA3	GATA binding protein 3
G-CSF	Granulocyte colony-stimulating factor
GFP	Green fluorescent protein
GM-CSF	Granulocyte-macrophage colony stimulating factor
GO	Gemtuzumab ozogamicin
GPR65	G protein-coupled receptor 65
GRB2	Growth factor receptor bound protein 2
GSDMD	Gasdermin D
GWAS	Genome-wide association studies
HDR	Homologous-directed repair
HSCT	Hematopoietic stem cell transplantation
HSPC	Hematopoietic stem or progenitor cell
IBD	Inflammatory bowel disease
IBD-U	IBD-unclassified
ICOS	Inducible T cell co-stimulator
IEC	Intestinal epithelial cell
IFN	Interferon
Ig	Immunoglobulin
IL	Interleukin
IL10R	Interleukin-10 receptor
IL-13Rαl	Interleukin-13 receptor subunit alpha 1
IL-15R	Interleukin-15 receptor
IL-15Rα	Interleukin-15 receptor subunit alpha
IL17RA	Interleukin-17 receptor alpha
IL-21R	Interleukin-21 receptor
IL23R	Interleukin 23 receptor
IL2RG	Interleukin-2 receptor subunit gamma
IL-2R	Interleukin-2 receptor
IL-2Rα	Interleukin-2 receptor alpha
IL-2Rβ	Interleukin-2 receptor beta
IL-2Rγ	Interleukin-2 receptor gamma
IL-4R	Interleukin-4 receptor
IL-4Rα	Interleukin-4 receptor subunit alpha
IL6ST	Interleukin-6 cytokine family signal transducer

IL-7R	Interleukin-7 receptor
IL7RA	Interleukin-7 receptor subunit alpha
IL-7Rα	Interleukin-7 receptor subunit alpha
IL-9R	Interleukin-9 receptor
IL-9Rα	Interleukin-9 receptor subunit alpha
ILC	Innate lymphoid cell
InsP3	Inositol-1,4,5-trisphosphate
iPSC	Induced pluripotent stem cell
IRF	Interferon response factor
ITAM	Immunoreceptor tyrosine-based activation motif
ITIM	Immunoreceptor tyrosine-based inhibitory motif
JAK	Janus kinase
KD	Knock-down
KI	Knock-in
KO	Knock-out
LB	Luria/Miller
LOAD	Late-onset Alzheimer’s disease
LP	Lamina propria
LPS	Lipopolysaccharide
MAG	Myelin-associated glycoprotein
MAPK	Mitogen-activated protein kinase
M-CSF	Macrophage colony-stimulating factor
MDP	Muramyl dipeptide
MDS	Myelodysplastic syndromes
MDSC	Myeloid-derived suppressor cells
MHC	Major histocompability complex
MNP	Mononuclear phagocyte
mRNA	messenger ribonucleic acid
mTOR	Mammalian target of rapamycin
MyD88	Myeloid differentiation primary response 88
Neu5Ac	N-acetylneuraminic acid
NF-κB	Nuclear factor kappa-light-chain-enhancer of activated B cells
NHD	Nasu-Hakola-Disease
NK	Natural killer
NKT	Natural killer T
NLR	NOD like receptor
NLRC	NLR family CARD domain containing
NLRP	NLR family pyrin domain containing
NOD2	Nucleotide-binding oligomerization domain-containing protein 2
PAMP	Pathogen-associated molecular pattern
PBMC	Peripheral blood mononuclear cells
PBS	Phosphate-buffered saline
PCR	Polymerase chain reaction
PD	Parkinson’s disease
PFA	Paraformaldehyde
PI3K	Phosphoinositide 3-kinase
PIC	Protease inhibitor cocktail
PID	Primary immunodeficiency
PKC	Protein kinase C
PLCγ	Phospholipase C gamma

PLOSL	Polycystic lipomembranous osteodysplasia with sclerosing leukoencephalopathy
PMA	Phorbol 12-myristate 13-acetate
PMSF	Phenylmethylsulfonylfluorid
PNP	Purine nucleoside phosphorylase
PRDM1	PR/SET domain 1
PRR	Pattern recognition receptor
PTPN	Protein tyrosine phosphatase non-receptor type
PVDF	Polyvinylidene fluoride
qRT-PCR	Quantitative reverse transcription polymerase chain reaction
RAG	Recombination activating
RAGE	Receptor for advanced glycation end-products
RFP	Red fluorescent protein
RIPK	Receptor-interacting serine/threonine-protein kinase
RNA	Ribonucleic acid
RORγt	Retinoic acid receptor-related orphan receptor-γt
ROS	Reactive oxygen species
RPMI	Roswell Park Memorial Institute
S100A9	S100 calcium binding protein A9
SAMP	Self-associated molecular pattern
SCF	Stem cell factor
SCID	Severe combined immunodeficiency
SDS	Sodium dodecyl sulfate
SEM	Standard error of the mean
SH2	Src homology 2
SHIP1	SH2 domain containing inositol polyphosphate 5-phosphatase 1
SHP	Src homology region 2 domain-containing phosphatase
Siglec	Sialic acid binding immunoglobulin type lectins
SNP	Single nucleotide polymorphism
SOCS3	Suppressor of cytokine signaling 3
ST3Gal4	ST3 beta-galactoside alpha-2,3-sialyltransferase 4
ST6Gal1	ST6 beta-galactoside alpha-2,6-sialyltransferase 1
STAT	Signal transducer and activator of transcription
sTREM2	Soluble TREM2
SYK	Spleen associated tyrosine kinase
T-bet	T-box expressed in T cells
TEMED	Tetramethylethylenediamine
T_{FH}	T follicular helper cells
TFS	Thermo Fisher Scientific
TGF-β	Transforming growth factor beta
TH	T helper
TJ	Tight junction
TLR	Toll-like receptor
TNFAIP3	TNF alpha induced protein 3
TNF-α	Tumor necrosis factor α
TPO	Thrombopoietin
Tregs	Regulatory T cells
TREM	Triggering receptor expressed on myeloid cells
TRIM22	Tripartite Motif Containing 22
TTC7A	Tetratricopeptide repeat domain 7A

TYK2	Tyrosine Kinase 2
UC	Ulcerative colitis
Vav	Vav guanine nucleotide exchange factor
VEGF	Vascular endothelial growth factor
VEO-IBD	Very-early onset inflammatory bowel disease
WES	Whole-exome sequencing
WT	Wild-type
ZAP70	Zeta chain of T cell receptor associated protein kinase 70

1. Introduction

1.1 Inflammatory bowel diseases

Inflammatory bowel diseases (IBD) are hallmarked by chronic gastrointestinal inflammation and commonly present with diarrhea, abdominal pain, fever, rectal bleeding, and weight loss.[1-5] Approximately 6.8 million people globally suffer from IBD, which poses a significant burden for health systems worldwide.[6, 7] The majority of patients (3.6 million) is located in Europe and the United States and IBD was considered a disease of western countries historically.[3, 6, 8] However, in the last centuries the incidence and prevalence of IBD also increased in developing countries.[8, 9]

Crohn's disease (CrD) and ulcerative colitis (UC) are the common forms of IBD.[2, 4] CrD usually manifests with disseminated transmural inflammation in the complete gastrointestinal tract and UC affects continuous regions in the rectum and the colon.[2, 3, 10] Histologically, CrD is characterized by infiltrating T cells and macrophages and UC presents with micro-abscesses formed by neutrophils in the intestinal epithelium.[2, 8, 10] Furthermore, loss of goblet cell-derived mucus and cryptitis can be more often observed in UC.[2, 8, 10] To categorize patients that do not fit into the CrD-UC dichotomy, IBD-unclassified (IBDU) was described as a third group.[11-13] However, recent findings indicate that IBD is more heterogenous and can present with a wide spectrum of phenotypes.[11, 12]

With a peak age of onset of 15-30 years, IBD is usually diagnosed in young adults, but IBD patients suffer from a chronic and relapsing disorder over their whole life.[2, 3, 5, 14] Of note, IBD symptoms (e.g., diarrhea, urgency, and tenesmus), certain treatments (e.g., ostomy), as well as prolonged hospitalization can cause a major impact on the life quality and mental health of IBD patients.[5] Individual, economical, and social consequences of IBD are exacerbated by physical, neurological, dermatological, ophthalmological, hepatic, biliary, skeletal, and immunological co-morbidities as well as an increased risk for colorectal cancer.[8, 10-12, 15] Classical treatment options for IBD comprise different immunomodulators (e.g., aminosalicylates, corticosteroids, cyclosporine A, methotrexate, and thiopurines), but biologics (e.g., monoclonal antibodies targeting tumor necrosis factor α (TNF-α), α4 integrins, the common p40 subunit, and the interleukin (IL-) 6 receptor) gained importance for the treatment of IBD.[8, 16, 17] These monoclonal

antibodies were a breakthrough in IBD therapy and can induce long-term clinical remission in many patients, but they still have major drawbacks including (i) the requirement of combination therapies with immunosuppressant drugs, (ii) development of anti-drug antibodies, (iii) loss of response over time, (iv) adverse effects (e.g., infections, arthralgia), as well as (v) high numbers of non-responsive patients.[17, 18] Furthermore, comprehensive data on long-term adverse effects and withdrawal strategies for biologics are still missing.[17] Despite medical and scientific progress, IBD can still be lethal and between 50 - 80 % of CrD patients require surgical intervention in the first 10 years after diagnosis.[5, 15, 17, 19, 20] Therefore, further research on the molecular pathomechanisms is needed to identify novel and curative treatment options.

1.1.1 Pathogenesis of IBD

The intestine represents a large contact area between the environment and the inner body.[21, 22] Consequently, one of the main tasks of the intestinal epithelium is to build a tight barrier protecting our body from potential exterior hazards. However, the gastrointestinal barrier cannot be completely impermeable, as it needs to allow uptake of nutrients and secretion of waste products.

The intestine is colonized by commensal microbes that help to fulfill its digestive and protective functions in healthy humans, but can pose a significant threat when the intestinal barrier is disturbed.[21, 22] To further protect the inner body from pathogens overcoming the intestinal barrier, the gastrointestinal tract is equipped with specialized immune cells that form a multilayer surveillance system.[1, 3, 22] These immune processes need to be tightly regulated to tolerate the presence of commensal microbes and rapidly destroy pathogens at the same time. Small dysbalances can result in detrimental effects and diseases like IBD. In particular, aberrant immune responses towards environmental or microbial agents may cause chronic gastrointestinal inflammation.[3, 23] Therefore, genetic, immunological, epithelial, environmental, and microbial aspects need to be considered in IBD pathogenesis (**Figure 1**).[1-4, 11]

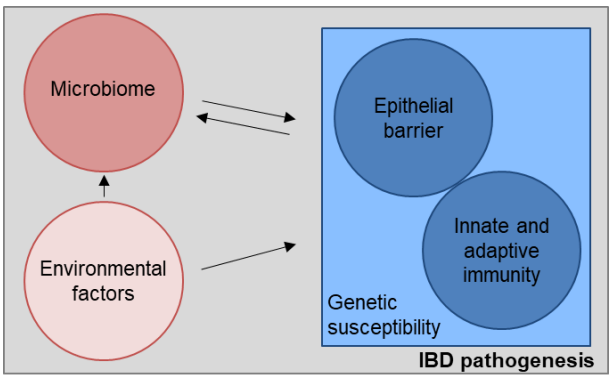

Figure 1: Pathogenesis of IBD is multifactorial.
IBD is caused by dysregulation of environmental factors, the microbiome, epithelial barrier function, or immunity in a genetically susceptible host. Dysbiosis can be trigger and result of disturbed intestinal homeostasis. Figure modified from [2]

1.1.2 Genetic susceptibility

An inheritable component has long been recognized in IBD pathogenesis, since one of the major risk factors for IBD is an affected first-degree relative.[2, 4, 24] Furthermore, studies demonstrated a higher concordance of disease in monozygotic twins compared to dizygotic twins indicating that genetic susceptibility plays a major role in IBD pathogenesis.[3, 4, 25-27] Although these studies showed that the association of IBD and genetic factors is stronger for CrD than UC, both share certain genetic risk factors (**Figure 2A**).[1-4, 25, 26]

Further evidence for the role of genetic predisposition in intestinal inflammation was provided by animal models including IBD (non-)susceptible mouse strains, genetically engineered mice, and chemically-induced models.[4, 28, 29] Nearly all of these experimental models result in aberrant function of innate (including intestinal epithelial cells) and adaptive immune cells indicating the importance of intestinal immune dysbalance in IBD pathogenesis (see also sections 1.1.5 and 1.1.6).[28, 29] Of note, the development of intestinal inflammation is dependent on the presence of microbiota in most of the animal models, as germ-free mice usually do not develop disease (see also section 1.1.4).[29]

Genetic susceptibility for IBD in humans was proven by linkage and association studies identifying genetic loci associated with CrD and UC pathogenesis.[28, 30-34] Replicated loci include *nucleotide-binding oligomerization domain-containing protein 2* (*NOD2*), class II major histocompability complexes (MHC), and IBD5.[28, 30-34] NOD2 is a cytosolic sensor for muramyl dipeptide (MDP), which is a peptidoglycan present in the cell wall of most bacteria, and thus is involved in recognition of bacteria by innate immune and epithelial cells.[1, 3, 11, 35-37] Despite being a strong genetic risk factor, homozygosity for a *NOD2* single nucleotide polymorphism (SNP)

does not invariably lead to CrD suggesting an influence of environmental factors in IBD pathogenesis.[3]

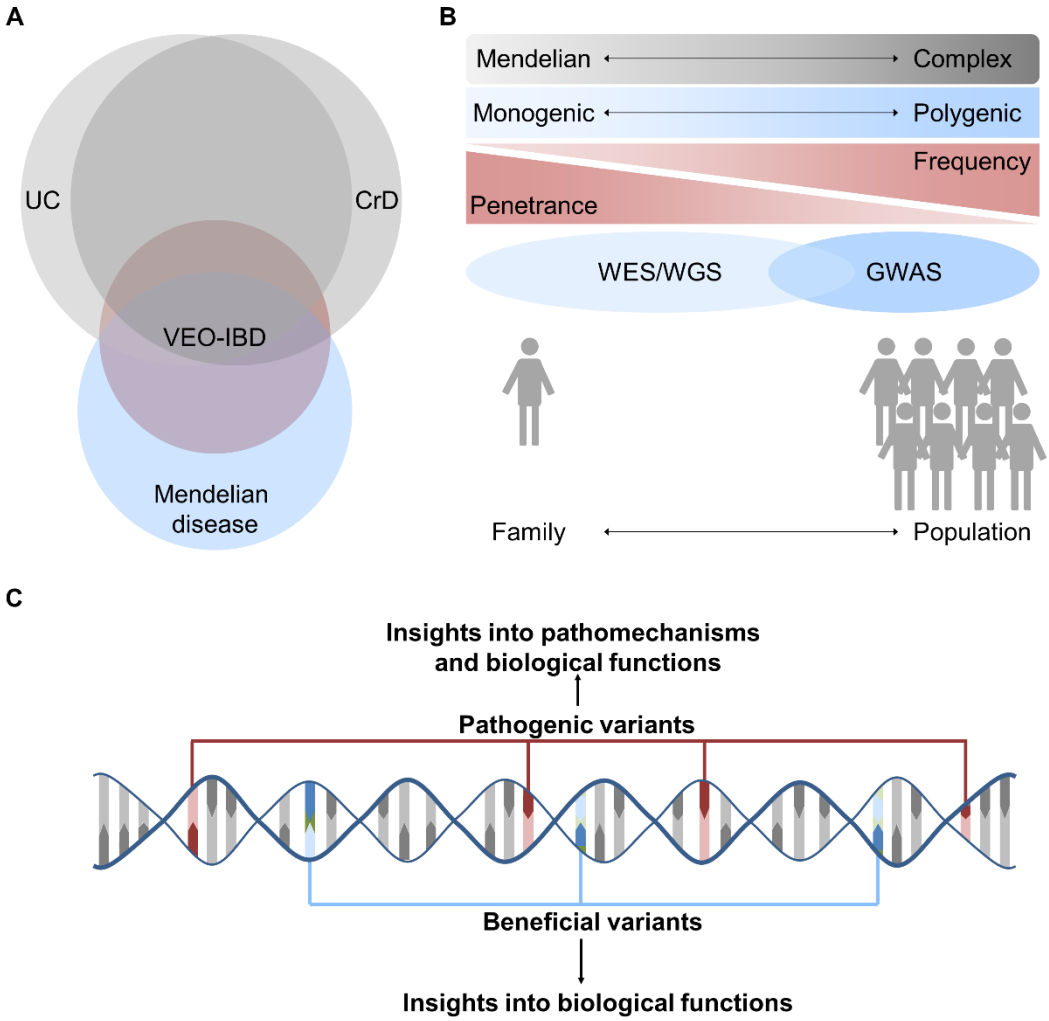

Figure 2: Genetics of IBD.
(A) CrD and UC share many risk factors for IBD pathogenesis, but also have specific subtype risk factors. Mendelian inheritance modes are more frequent for VEO-IBD. (B) Whereas rare mendelian diseases are caused by monogenic causes with high penetrance and severe consequences for protein function, more frequent diseases are caused by polygenic factors and show complex inheritance modes. (C) Functional studies on genetic variants provided insights into central biological functions of intestinal immunity and helped to understand pathogenesis of various diseases. Figure based on [11,38]

Our understanding of genetic risk factors for IBD and other diseases was significantly expanded by genome-wide association studies (GWAS).[38-40] In total, 240 genetic loci have been associated with IBD pathogenesis.[11, 12, 23, 41] Of note, the majority of these loci (i.e., ~ 67.5 % in a large study [42]) is associated with CrD as well as UC and only a few loci modify the risk for one specific type indicating common (genetic) pathomechanisms between CrD and UC (**Figure 2A**).[38, 42]

Identification of interleukin 23 receptor (*IL23R)* as IBD risk factor was one of the first and major contributions made by GWAS. The most significant SNP in *IL23R* (R381Q) reduces the risk of CrD and UC up to three times.[38, 43] R381Q was later shown to be a loss-of-function allele, which reduces IL-23R-mediated signaling and affects the number and function of T helper (T_H) 17 cells.[38, 44-46] These functional studies on the R381Q allele linked the IL-23/IL-17 pathway to IBD development, but also increased our understanding of fundamental processes in IL-23 and IL-17 signaling demonstrating the potential of functional genomics for science and medicine.[11, 38] Furthermore, these data provided rationale arguments for the usage of anti-p40 (common IL-12 and IL-23 subunit) for the treatment of IBD.[11, 38, 47, 48]

Although GWAS helped to determine important mechanisms in IBD, these approaches are limited to known SNPs with higher frequency, moderate effects on pathogenesis (e.g., 7.5 % or 14 % for UC and CrD), and lower penetrance (**Figure 2B**).[11, 28, 38, 42, 49] With cost-effective availability of next-generation sequencing technologies, less frequent and previously unknown SNPs with stronger effects could be associated with IBD pathogenesis.[11, 38, 50] Since the coding regions of genes are estimated to contain 85 % of strong effect variants, whole exome sequencing (WES) is a powerful tool to identify these highly penetrant, but rare variants (**Figure 2B**).[11, 38, 50]

In most cases, IBD is inherited in a non-mendelian fashion indicating that genetic susceptibility is determined by polygenic risk factors and IBD is thus considered a complex genetic disease.[38] From an evolutionary perspective, moderate effect SNPs (i.e., no effect, advantageous or disadvantageous) are not subject to selection pressure, as their effect is probably not influencing the individuum or the population.[38] Therefore, many variants with moderate effect are present in the (“healthy”) human genome, but only some combinations of certain alleles cause a phenotype and thus predispose to a certain disease. However, susceptibility to a genetic disorder depends not only on the number and strength of certain risk factors, but also on protective variants (**Figure 2C**). Pathogenic and beneficial genetic factors for a specific disorder are thus in a homeostasis in each individuum and need to be considered for understanding disease pathogenesis and gain insights into molecular mechanisms of immunology and pathology.

Overall, the genetic loci identified by different techniques were enriched in several important pathways including microbe effectors, epithelial barrier regulators, adaptive immunity, cellular

stress pathways, fibrosis, cytokine networks, and inflammasome regulators (**Figure 3**).[11] These pathways and their role in IBD pathogenesis will be discussed in detail in sections 1.1.5 and 1.1.6.

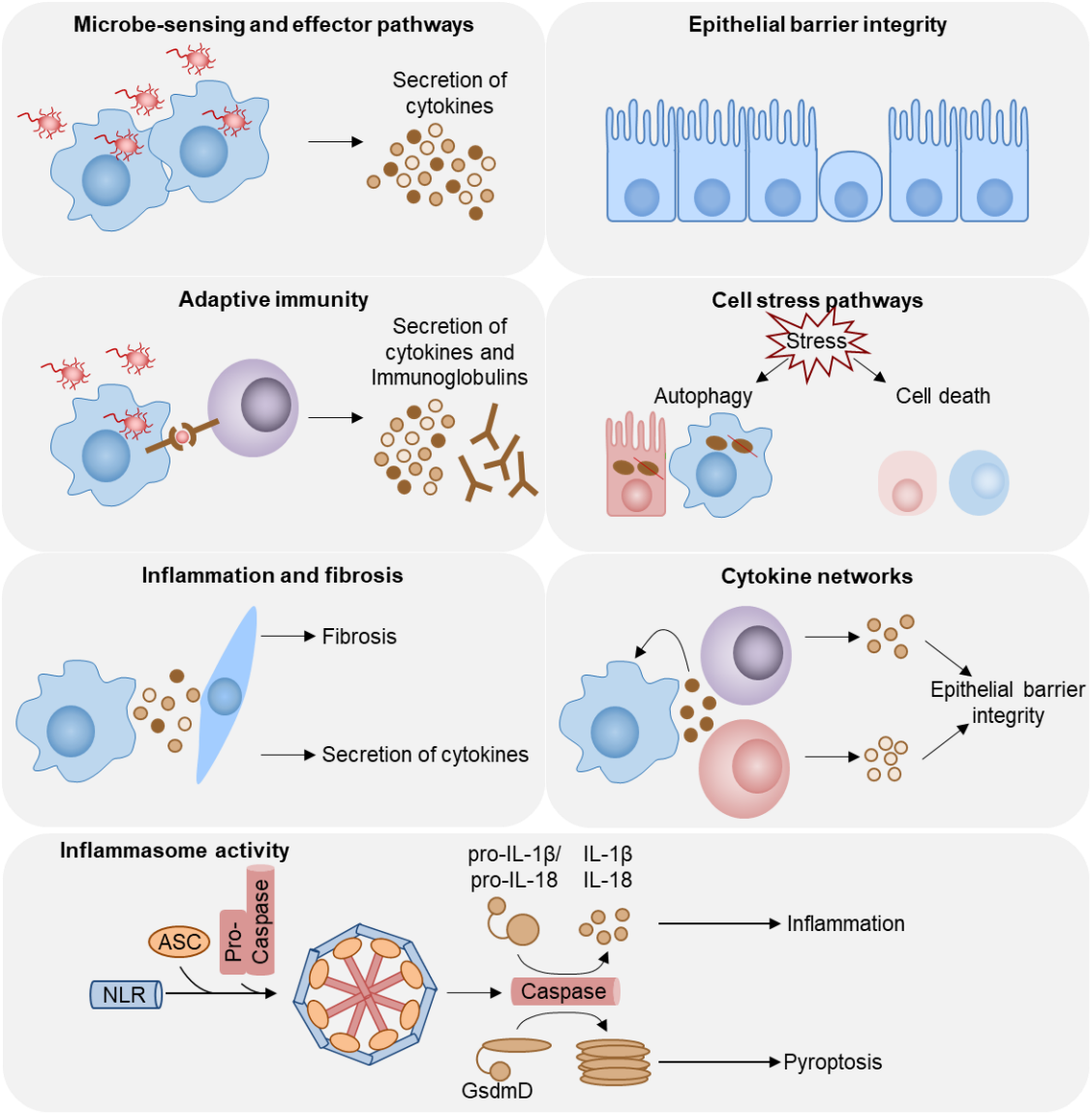

Figure 3: Genetics reveal important pathways involved in IBD pathogenesis. Figure based on [11]

1.1.3 Pediatric IBD

IBD in children is substantially different from adult forms and pediatric IBD mostly results in more severe disease.[38, 51, 52] The pediatric IBD population itself shows considerable heterogeneity and different groups based on the disease onset have been defined: Neonatal IBD (≤ 28 days of age), infantile onset IBD (< 2 years of age), very-early onset (VEO)-IBD (< 6 years of age), early-onset (EO)-IBD (< 10 years of age), and pediatric-onset IBD (< 17 years of age).[53] In line, the proportion of IBDU is higher in pediatric IBD (34 % in infantile onset IBD vs. 21 % in VEO-IBD vs. 6 % in adult patients).[38, 54]

Childhood and adolescence represent a critical time window for physical, psychological, social, and emotional development.[52] Therefore, pediatric IBD poses more challenges to treating physicians. In detail, physical development is impeded by long-lasting high levels of pro-inflammatory cytokines, nutritional shortage, and exposure to steroidal drugs, which can also result in other medical complications.[52, 55-58] Psychological development and well-being is affected by stigmatized symptoms (e.g., diarrhea), unclear healing perspectives, and reduced quality of life.[5, 52] Lastly, long-term hospitalization and increased sickness absence in school hinder social and emotional development in patients.[5, 52] Altogether, additional complications, unique disease behavior, and biological characteristics warrant the design of therapeutic options specifically adapted to children.

Pediatric IBD differs also from a genetic point of view, since the proportion of monogenic diseases is higher in children.[12, 59] In detail, around 8 % of patients with VEO-IBD and around 14 % of patients with infantile onset are estimated to suffer from monogenic IBD.[12, 59] In 2009, the first truly monogenic form of IBD, IL-10R deficiency, was described in pediatric patients.[60] Afterwards more than 75 different monogenic defects causing IBD(-like) symptoms have been identified, which can be categorized into the following groups: (1) epithelial barrier, (2) adaptive immunity, (3) hyperinflammatory and autoinflammatory disorders, (4) phagocytosis, and (5) regulation of immune responses.[12, 53, 61-64] Of note, these groups largely overlap with genetic loci identified in polygenic IBD and insights from pediatric IBD help to understand pathomechanisms in adult IBD as well as other immune-related diseases. Functional studies on monogenic defects not only defined novel concepts of immunology and biology, but also helped to identify novel treatment options for these patients. New therapies include hematopoietic stem cell transplantation (HSCT), which has been established as curative treatment for IL10R deficiency and other defects caused by primary immunodeficiencies (PID).[12, 53, 60, 63, 65] However, HSCT is associated with risks and for many monogenic diseases curative treatments are not available. Therefore, it is still necessary to further investigate pathomechanisms in monogenic forms of IBD, which can help to identify individualized or general therapeutic options for IBD.

1.1.4 Environmental and microbiotic influences on IBD pathogenesis

The low concordance in twin studies as well as temporal and geographical changes of IBD epidemiology suggest a contribution of environmental factors in IBD pathogenesis.[1, 25, 26, 66

Although the contribution of external influences is a long established fact, specific risk factors, their causality, and especially the underlying pathomechanisms are still poorly understood.[67] Elucidation of risk factors is also hindered by technical and conceptual limitations. For example, environmental factors presumably play a role in pathogenesis long before the patient develops symptoms, but retrospective evaluation of environmental exposure is often not possible.[67, 68] Furthermore, external influences might not be an on-off switch for pathology, but rather the accumulation of exposures to (multiple) risk factors modifies disease.[67] Despite these limitations, different environmental factors (e.g., antibiotics, smoking, diet, stress, hypoxia) have been proposed to play a role in IBD pathogenesis (**Figure 4**).[1, 66, 67]

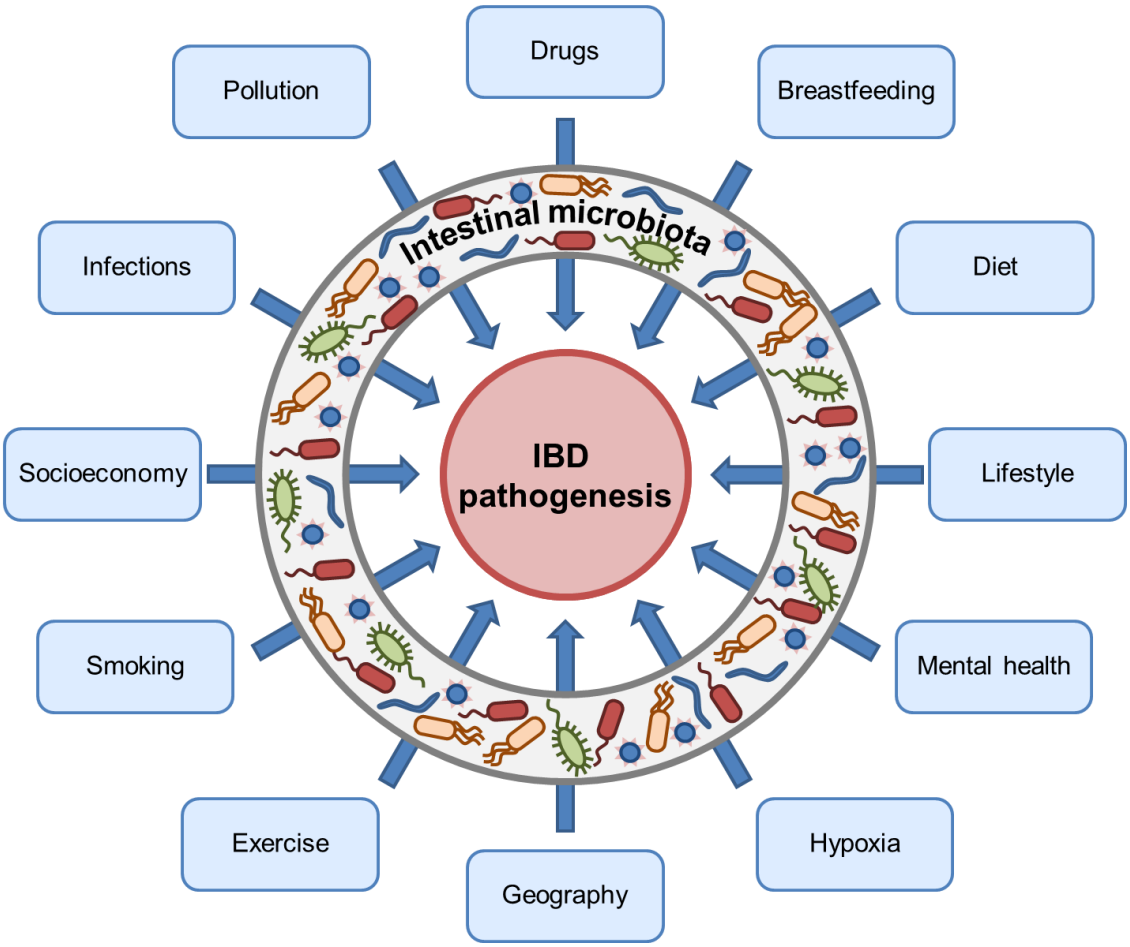

Figure 4: Environmental and microbiotic influences play a role in IBD pathogenesis.
Different environmental factors influence intestinal homeostasis directly or by causing dysbiosis of the intestinal microbiome. Figure based on [66]

Many of these environmental factors can influence intestinal homeostasis directly but can also affect the gut microbiota adding further complexity to the role of external factors in IBD pathogenesis (**Figure 4**).[66, 69-71] The importance of the intestinal microbial flora for IBD

pathogenesis is well established, as the development of intestinal inflammation in experimental mouse models is fully dependent on the presence of commensal intestinal microbiota.[1, 29] Furthermore, intestinal inflammation can cause dysbiosis in IBD patients, which might result in advantages for pathogens or render commensal symbionts pathogenic.[66, 72-74] Ultimately, dysbiosis can thus amplify and exacerbate disease.

Analogous to European and North American countries in the mid of the last century, industrialization and urbanization is paralleled by a rise of IBD prevalence in developing countries over the last decades confirming the role of environmental factors in IBD pathogenesis.[1, 66, 67, 75, 76] Urban surroundings, for example, increase the risk of IBD, which is presumably caused by differences in pollution, diet, hygiene, and lifestyle between rural and urban areas.[66, 75, 77] Of note, the risk of developing IBD is highest for people living in urban areas during their childhood and adolescence indicating that IBD diagnosed in adults might be influenced by exposure to certain risk factors at a very different age.[66, 77]

Usage of antibiotics in childhood is one of the proven risk factors for IBD pathogenesis.[66, 78-80] An obvious mechanism for the role of antibiotics in IBD is their effect on the intestinal microbiome and different studies in humans could show that antibiotic administration has short-term and long-term effects on composition of human gut bacteria, which might result in dysbiosis.[66, 81, 82]

Based on the digestive function of the gastrointestinal tract, diet is an obvious risk candidate for IBD pathogenesis. However, identification of protective or fatal nutrients is often hindered by (i) the complexity of human eating behavior, (ii) high variation in studies, and (iii) difficulties in retrospective assessments.[66, 67] Animal models have helped to provide links between diet and intestinal inflammation, since different studies showed that certain dietary components can contribute to colitis development.[66, 67, 83, 84] In humans, studies on vegans/vegetarians showed that different alimentation can lead to dysbiosis, which, in turn, can cause intestinal inflammation.[85, 86] Importantly, exclusive enteral nutrition (EEN) has become an important tool to induce remission in pediatric CrD demonstrating the role of diet in pathogenesis as well as sustainment of disease.[52, 87-89]

Since many people experience intestinal symptoms during episodes of stress, mental health is a well-known modulator of intestinal functions and homeostasis. The central nervous system (CNS) can regulate the function of different cell types in the intestine such as epithelial, immune, and

neuronal cells, which can affect intestinal motility, secretion, and permeability as well as immune cell function.[67, 90] However, the CNS can also influence the intestinal microbiome via different signaling molecules.[67, 90] It seems obvious that stressful events or episodes can cause pro-inflammatory milieus in the gut and/or dysbiosis. Indeed, different studies could show that higher stress levels are associated with risk of relapse or aggravation of IBD.[67, 91, 92]

1.1.5 Role of the epithelial barrier in IBD

Loss of epithelial barrier integrity or function is one mechanism involved in IBD pathogenesis (**Figure 3**).[3, 11] Epithelial cells form physical barriers to separate the outside from the inside of the body and are thus the first line of defense of the host immune system against external threats (e.g., toxins, pathogens).[93, 94] The epithelial barrier also generates a safe distance between the commensal flora and the host immune system, which prevents non-desirable, chronic activation of intestinal immune cells by microbial antigens.[93, 94] However, intestinal epithelial cell (IEC) layers cannot be impermeable since they need to allow transport of nutrients and fluids across the barrier.[93, 94] To allow these controversial functions, IEC are linked by apical junctional complexes (AJCs) built by tight junctions (TJs) and adherens junctions (AJs), which seal the intercellular space and limit diffusion of particles from the gut lumen inside the body.[3, 93-96] Since TJs are critical for barrier function, their permeability is tightly, but dynamically regulated.[94, 96] Interestingly, several studies in animal models and humans could demonstrate dysregulated TJs and increased paracellular permeability in IBD.[3, 94, 96-101] Since TJ permeability is also modulated by pro-inflammatory cytokines (e.g., interferon (IFN)-γ and TNF-α), increased permeability might be a result of intestinal inflammation.[94, 96, 102] Vice versa, higher barrier permeability can be a source of immune activation due to increased detection of microbial or dietary antigens.[94, 96, 102] Of note, altered intestinal permeability can be also observed in healthy family members of IBD patients indicating genetic predisposition.[94, 97]

Besides physical separation, specialized IEC also generate a chemical barrier, which contributes to the protection from the environment. Goblet cells, secrete mucins that form a gel-like mucus layer, which slows movements and limits the contact between microbiota and host cells.[3, 11, 94, 103] Paneth cells, contribute to chemical barrier formation by production of antimicrobial peptides (AMPs), which regulate and control the microbiome.[3, 11, 95, 104, 105]

Important evidence for the role of IEC in intestinal homeostasis was provided by studies on pediatric IBD patients identifying multiple genetic deficiencies that affect epithelial cells. A prominent example are autosomal-recessively inherited mutations in tetratricopeptide repeat domain 7A (TTC7A), which result in VEO-IBD presenting with immunodeficiency, intestinal atresia, and variable extraintestinal manifestations.[106-110] Aberrant immune cell functions caused by TTC7A deficiency could be cured by HSCT, but the IEC-intrinsic defects remained after HSCT and resulted in relapse or death of the patients.[110, 111] Recently, the spectrum of genes affecting immune as well as epithelial cell compartments was expanded by patients suffering from caspase (CASP) 8 and receptor-interacting serine/threonine-protein kinase (RIPK) 1 deficiency, which both cause dysregulated cell death.[112-114] Data on the effect of HSCT in these patients is scarce and further research on epithelial defects is needed to identify and develop new therapeutic approaches for these patients.[114]

1.1.6 Role of intestinal hematopoietic cells in health and disease

The epithelial barrier separates the content of the gut lumen including microbial and dietary antigens from the inner body providing a first line of defense. If the barrier is compromised, luminal components can enter the compartments below the IEC barrier (**Figure 5**).[115] To protect the host against dangers, the lamina propria (LP) is patrolled by various immune cells, which can mount powerful response to invading pathogens and render the intestine an important human immune organ (**Figure 5**).[115-118]

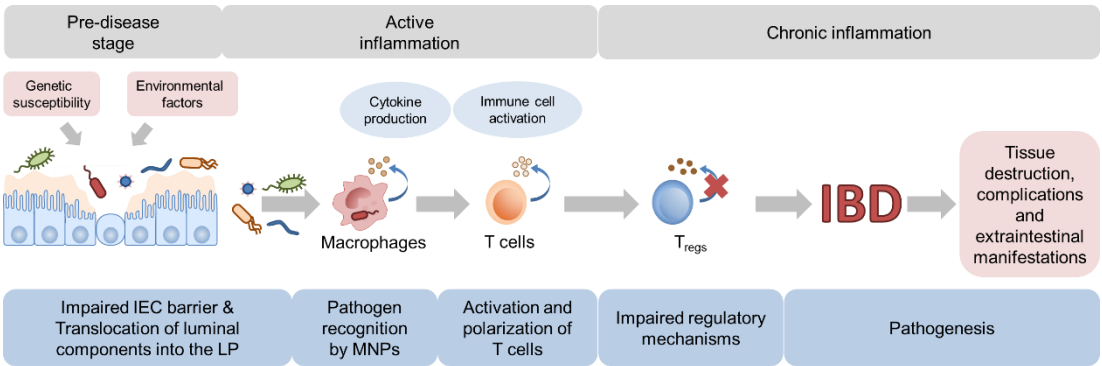

Figure 5: Immune mechanisms in IBD pathogenesis.
Genetic susceptibility, environmental factors, or dysbiosis can cause damages to intestinal epithelial cells (IECs), which results in translocation of luminal components into the lamina propria (LP). Mononuclear Phagocytes (MNP) recognize translocated components and activate adaptive immune responses. Failure of clearance of luminal components and/or regulation of immune responses results in chronic intestinal inflammation, which will lead to extraintestinal complications. Figure modified from [115]

Intestinal innate immune cells: Pathogen recognition and clearance

Mononuclear phagocytes (MNPs), which include monocytes, macrophages, and dendritic cells (DCs) can be considered the second line of defense against invading pathogens.[119] These innate immune cells are armed with a variety of functions and pathways to detect, take up, and destroy threats for the host.[11] Furthermore, MNPs serve as vanguard, which can mount complex adaptive immune responses upon detection of danger.[119] However, due to their unique surrounding intestinal MNPs need to tolerate microbial and dietary antigens without causing uncontrolled inflammation.[2, 119] Hence, MNPs contribute to establishment of tolerance, pathogen clearance, activation of adaptive immune responses, inflammation, and wound healing in the intestinal mucosa.[118, 119] To fulfill this complex functions, MNPs express a variety of pattern-recognition receptors that detect pathogen-associated molecular patterns (PAMPs) or danger-associated molecular patterns (DAMPs) and elicit intracellular signaling pathways resulting in expression of cytokines (e.g., IL-1β, IL-6, IL-8, IL-23, TNF-α), chemokines, adhesion molecules, and regulators of adaptive immune responses (e.g., cluster of differentiation (CD)40, CD80, CD86 and inducible T cell co-stimulator (ICOS)).[1-3] The importance of microbe detection mechanisms is exemplified by the association of variants with IBD risk in genes related to NOD2 function (e.g., *RIPK2, Tripartite Motif Containing 22 (TRIM22),* and *TNF Alpha Induced Protein 3 (TNFAIP3),* see also section 1.1.2) and variants in *Caspase Recruitment Domain Family Member (CARD) 9*, which is an adaptor protein for immunoreceptor tyrosine-based activation motif (ITAM)-containing surface receptors involved in microbe detection.[1-3, 11, 23, 120, 121] Taken together, pathogen-sensing pathways are important to maintain intestinal homeostasis and are deregulated in IBD pathogenesis (**Figure 3**).

Monocytes in the peripheral blood constitute 8 % of all leukocytes, but there are at least three different types including $CD14^{+}CD16^{-}$ classical monocytes, $CD14^{+}CD16^{+}$ intermediate monocytes, and $CD14^{-}CD16^{+}$ non-classical monocytes.[119, 122, 123] Monocytes differentiate from common myeloid progenitor cells in the bone marrow and travel to peripheral organs via the blood stream (**Figure 6**).[119, 124, 125]

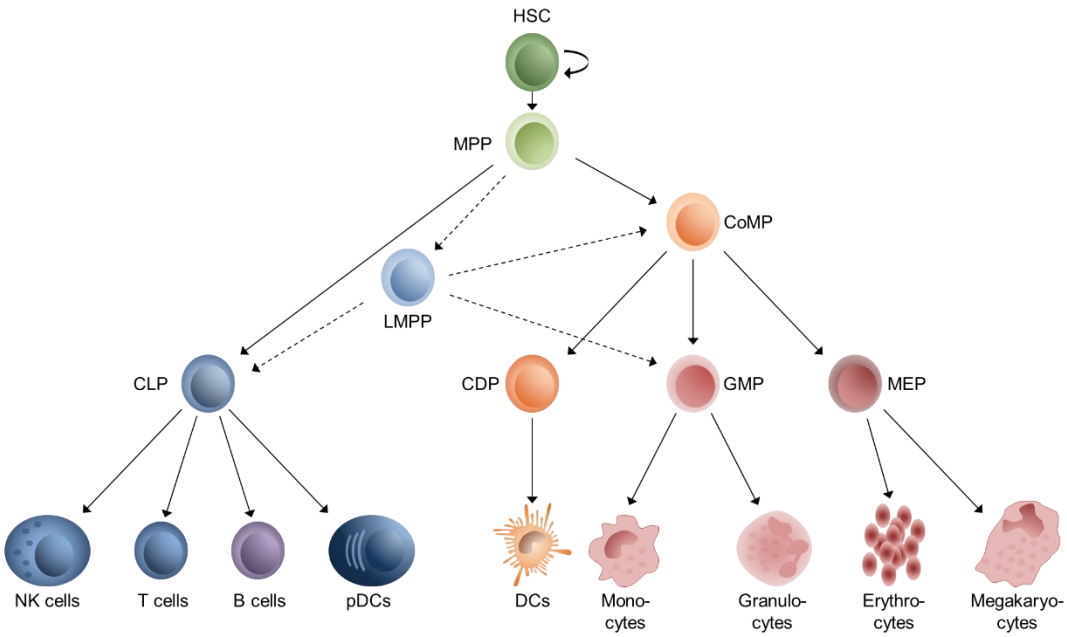

Figure 6: Schematic overview of hematopoiesis.
Figure based on [119, 124, 125]. HSC: Hematopoietic stem cell; MPP: multipotent progenitor; CoMP: Common myeloid progenitor; LMPP: Lymphoid-primed progenitor; CLP: Common lymphoid progenitor; CDP: Common dendritic cell progenitor; GMP: Granulocyte-Macrophage progenitor; MEP: Megakaryocyte-Erythrocyte progenitor; NK: natural killer cell; pDCs: plasmacytoid dendritic cells; DCs: Dendritic cells.

The majority of monocytes are short-lived classical monocytes, which mature to macrophages in peripheral organs based on the local environment of cytokines and growth factors.[119, 122, 126] Macrophages (i) remove pathogens, toxins, and cell debris, (ii) recycle metabolites, (iii) regulate tissue homeostasis, and (iv) are the primary sensors of internal dangers to the host.[127] Murine models have shown that macrophages play a prominent role in maintaining intestinal homeostasis.[2, 128, 129] In detail, mice with macrophages defective for *Signal Transducer And Activator Of Transcription (STAT) 3* or *IL10* knock-out (KO) mice demonstrate increased production of pro-inflammatory cytokines (e.g., IFN-γ, IL-1β, IL-6, IL-12, IL-23, and TNF-α) from macrophages.[2, 128, 129] Although the gut is one of the few organs where resident macrophages are permanently replenished from blood-derived monocytes, mature macrophages were shown to persist for more than 6 weeks in the gut.[119, 130] Interestingly, tissue-resident macrophages in other organs are derived from early progenitor cells during embryogenesis and are thus more long-lived than intestinal macrophages.[119, 131-135] Mature intestinal macrophages show strong phagocytic and endocytic properties, but they show significantly reduced cytokine and chemokine production in response to stimulation compared to monocytes, which probably indicates an anergic state of long-lived mature macrophages tolerant to the continuous presence of microbial and dietary

antigens in the gut.[119, 130] Comparable to IECs, mature intestinal macrophages also show down-regulation of important bacterial sensors like Toll-like receptor (TLR) 2 and TLR4 explaining reduced responsiveness to microbial stimuli.[119, 130] Furthermore, the intestinal microenvironment induces down-regulation of other pro-inflammatory molecules like triggering receptor expressed on myeloid cells (TREM) 1, which contributes to expression of different cytokines including TNF-α, IL-1β, IL-6, and C-C Motif Chemokine Ligand (CCL) 2, in mature intestinal macrophages.[119, 136, 137] Of note, TREM1 expression is increased in IBD patients and enhances experimental colitis.[137]

Nevertheless, intestinal macrophages are still the main source of pro-inflammatory cytokines (e.g., IFN-γ, TNF-α, IL-6, and IL-23), which are also increased in the LP of IBD patients.[1, 119, 138] Furthermore, the number of pro-inflammatory immature macrophages is increased in IBD patients.[1, 119, 138, 139] The higher presence of immature macrophages might be fueled by an increased extravasation of peripheral blood monocytes caused by changes in the intestinal cytokine/chemokine environment in IBD patients (see also cytokine networks).[119, 140, 141] Anti-TNF-α and anti-α4β7 therapies reverse this trend in IBD patients and reduce the number of pro-inflammatory, immature macrophages.[119, 142-144]

The functional dichotomy of macrophages in the intestine ranging from pathogen recognition and immune system activation to tolerance induction and intestinal homeostasis is fulfilled by a spectrum of intestinal macrophage subsets.[118, 119, 127, 130] Traditionally, macrophages have been divided into M1 pro-inflammatory and M2 anti-inflammatory macrophages, which are generated in response to TLR signaling and IFN-γ or IL-4 and IL-13, respectively.[118, 127] However, macrophages can be also functionally classified as host defense (corresponding to M1), wound healing, and immune regulatory macrophages.[118, 127]

Cytokine networks control intestinal homeostasis

Cytokine and chemokine networks determine the recruitment, differentiation, maturation, proliferation, and function of immune cells. Pro-inflammatory cytokines are mainly produced by LP macrophages and T cells upon loss of barrier integrity triggered by environmental factors in a genetically-predisposed host (**Figure 5** and sections 1.1.2, 1.1.4, and 1.1.5).[115] Genetic and animal studies demonstrated that dysregulation of cytokine networks results in inflammation and contributes to IBD pathogenesis (**Figure 3**).[11] The success of therapies targeting different cytokines (e.g., TNF-α and p40) in IBD treatment proves the importance of cytokines as driver of

intestinal inflammation.[115] Cytokine networks are complex and are continuously expanded by novel scientific insights, but, based on the clinical application, TNF-α, IL-1β, and IL-23 will be discussed below.

TNF-α is the most prominent example of dysregulated cytokines in IBD. TNF-α is produced by macrophages, T cells, fibroblasts, and adipocytes in the LP as a membrane-bound form and cleaved by a disintegrin and metalloprotease (ADAM) 17 generating soluble TNF-α.[115, 138, 145, 146] Levels of both forms are increased in IBD patients resulting in (i) activation of macrophages and T cells, (ii) induction of angiogenesis, (iii) loss of barrier integrity, and (iv) increased cell death.[115, 147-150] In response to TNF-α stimulation target cells up-regulate or release a variety of other cytokines/chemokines and effector molecules amplifying inflammatory responses and promoting intestinal inflammation.[151] Of note, uncleaved TNF-α bound to cell membranes seem to exert larger effects on intestinal inflammation than soluble TNF-α as indicated by reduced efficacy of clinical antibodies targeting solely soluble TNF-α.[115, 152, 153]

IL-1β is a prominent cytokine in hyperinflammatory diseases and its levels are also increased in IBD.[154-158] Furthermore, the concentration of IL-1β was shown to be a marker for IBD disease severity.[154, 155, 159, 160] In comparison to other cytokines, the secretion of IL-1β depends on the activity of inflammasomes, which are supramolecular complexes of various proteins.[155] To activate inflammasomes, two independent stimuli are necessary.[154, 155, 161] The first signal, which is also called priming, is usually induced by recognition of DAMPs or PAMPs by pattern recognition receptors (PRR) (e.g.,TLRs, C type lectins (CTLs), or NOD-like receptors (NLRs)).[154, 155, 161] Most of these priming signals lead to activation of nuclear factor kappa-light-chain-enhancer of activated B cells (NF-κB), activator protein 1 (AP-1), and interferon response factors (IRFs).[154, 155, 161] Ultimately, the priming signal results in expression of central inflammasome components including inflammasome-sensor proteins, pro-CASP1, pro-IL-1β and pro-gasdermin D (GSDMD).[154, 155, 161] The number of different inflammasome-sensor proteins with cell-type specific expression was expanded continuously over the last years and well-known examples include absent in melanoma 2 (AIM2), NLR family CARD domain-containing protein 4 (NLRC4), NLR family pyrin domain containing (NLRP) 1, NLRP3, NLRP6, and PYRIN.[162] Many inflammasome sensor proteins are implicated in pathology and especially immune and intestinal

diseases. For example, NLRP3 inflammasome activity was associated with IBD pathogenesis in animal models and humans.[154, 155, 163-169]

Inflammasome activation is inhibited until a second stimulus, which is detected by the inflammasome sensor proteins and is usually also a DAMP or PAMP.[162] For NLRP3 inflammasomes, these second activation signals include potassium efflux, lysosome leakage, reactive oxygen species (ROS), and/or mitochondrial dysfunction.[155, 161] Upon activation, inflammasome sensor proteins oligomerize and recruit CASP1 either directly or via the adaptor protein apoptosis-associated speck-like protein containing a CARD (ASC).[161, 162, 170] This oligomerization process triggers self-cleavage of pro-CASP1 molecules resulting in full activation and cleavage of effector molecules (e.g., pro-IL-1β, pro-IL-18 and pro-GSDMD).[161, 162, 171-173] Mature GSDMD forms a cell membrane pore and results in pyroptosis, which is a CASP1-mediated, pro-inflammatory form of cell death that is characterized by release of cytokines through membrane pores and subsequent cell lysis (i.e., IL-1β and IL-18).[161, 173-177] Released mature IL-1β has pleiotropic functions in intestinal immunity and is targeting a variety of immune cells, which promotes inflammation. For example, IL-1β recruits neutrophils to the intestinal LP and stimulates release of other pro-inflammatory cytokines like IL-6, IL-8, and TNF-α.[155] Furthermore, IL-1β induces polarization of pro-inflammatory T_H17 cells, which are important mediators of intestinal inflammation and link IL-1β levels produced by innate immune cells to adaptive immune responses (discussed in detail below, **Figure 7**).[154, 156]

The role of IL-1β in inflammation is shown by different human pathologies, which are characterized by excessive IL-1β production and present with detrimental hyperinflammation affecting different organs including the gut. For example, intestinal inflammation in chronic granulomatous disease (CGD), which causes increased susceptibility to infections and severe intestinal inflammation, can be treated with the IL-1 receptor antagonist anakinra.[11, 178] Further evidence for the role of IL-1β in IBD was provided by VEO-IBD patients with IL-10R defects, which also show elevated IL-1β levels.[168] Hence, IL-1β represents a central hub in cytokine networks between T cells and macrophages controlling intestinal homeostasis (**Figure 7**).

IL-12 and IL-23 represent key cytokines for the transmission of innate immune signals after recognition of PAMPs and DAMPs by MNPs towards the adaptive immune system.[115] Whereas IL-12, which is a heterodimer of p35 (encoded by *IL12A*) and p40 (encoded by *IL12B*), induces a

T_H1 fate, IL-23, which is composed of p19 (encoded by *IL23A*) and p40 subunits, is stimuating the generation of T_H17 cells.[11, 115, 179-184] *IL12B* was associated with an increased risk for IBD by GWAS and different members of the IL-12 cytokine family (i.e., IL-12 and IL-23) are upregulated in the tissue of CrD patients.[1, 11, 115, 185-188] The importance of IL-12/IL-23 cytokines is demonstrated by the efficacy of antibodies targeting the p40 subunit in clinical trials, which induced amelioration of disease in CrD patients and patients refractory to anti-TNFα treatment.[11, 47, 115]

Intestinal adaptive immune cells: Execution and regulation of immune responses

Activation of lymphocytes by MNPs mounts highly effective immune responses to clear pathogens and other threats. Failure of these clearance mechanisms can result in disease (e.g., immunodeficiency), but excessive adaptive immune responses due to lack of regulatory mechanisms can also cause tissue damage, exacerbation of intestinal inflammation, and ultimately intestinal pathology (**Figure 5**).[2, 11, 115] To control these critical immune responses, there are complex regulatory cytokine networks between innate immune cells (i.e., macrophages) and adaptive immune cells (i.e., $CD4^+$ T_H cells) (**Figure 7**).[127]

T cells, which can be considered the third line of defense, are activated by MNP-mediated presentation of antigens on MHC molecules. Antigen presentation is essential for pathogen clearance, resolution of inflammation, and intestinal homeostasis, as demonstrated by the association of genes encoding MHC class II proteins with risk for IBD (see also *HLA* locus in **Figure 3**).[11, 189] T cells are considered the pivot of IBD pathogenesis, since $CD4^+$ T_H cells critically orchestrate innate and adaptive immune responses in the gut and their type defines the pathomechanisms in IBD (**Figure 7**).[1, 2, 190] Although more T_H cell fates have been identified, T_H1, T_H2, and T_H17 cells play the major role in intestinal immunity and their function in IBD pathogenesis is well characterized. Interestingly, the cytokine networks shaping $CD4^+$ T_H cell polarization and responses differ in CrD and UC, since they are characterized by T_H1 and T_H2 responses, respectively.[1, 2, 115, 191-194]

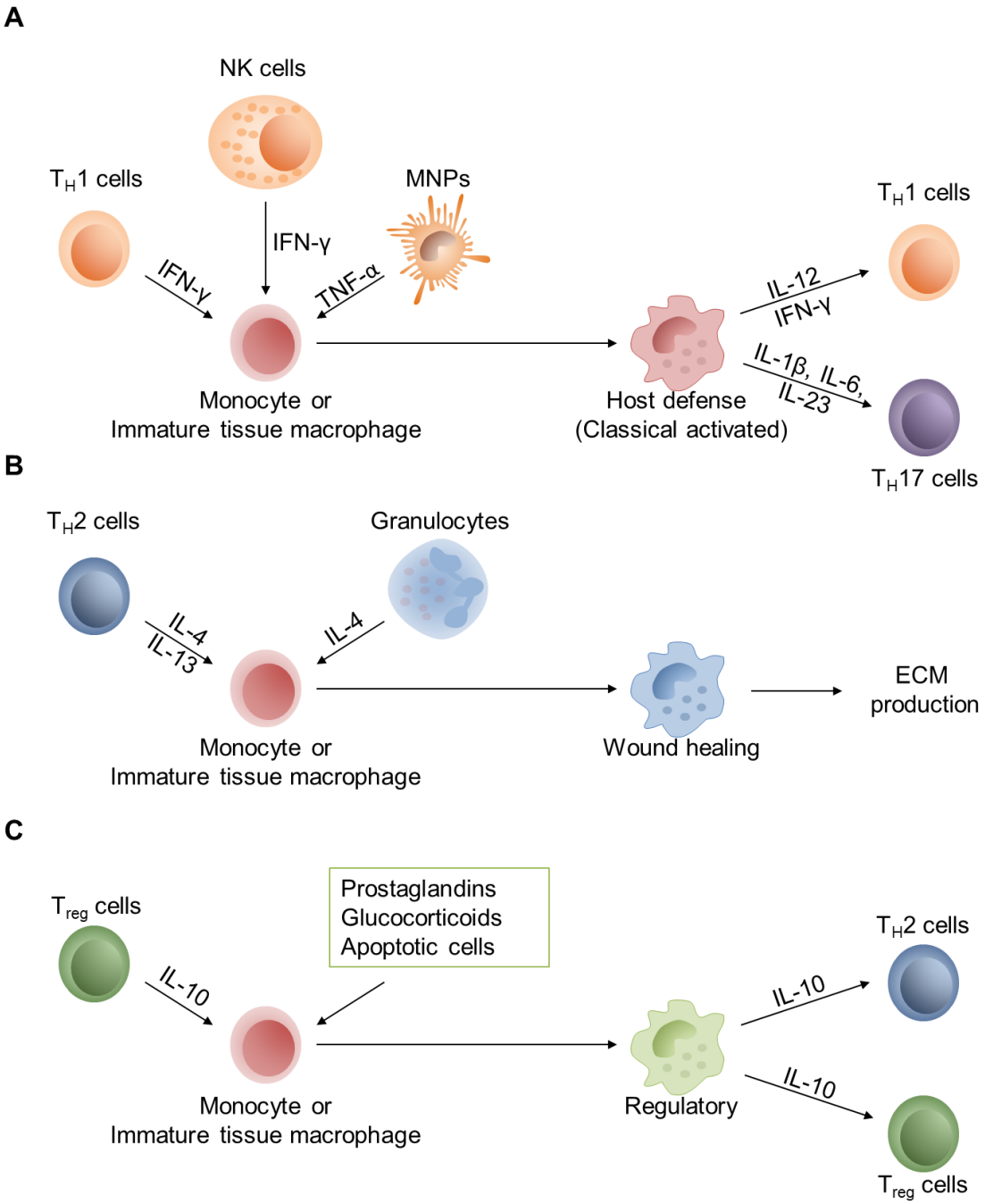

Figure 7: Regulatory cytokine networks between Macrophages and T cells.
(A) Pro-inflammatory cytokines (e.g., IFN-γ and TNF-α) induce differentiation of classically activated macrophages, which produce IL-1β, IL-6, IL-12, IL-23, and IFN-γ and stimulate polarization of T_H1 and T_H17 cells. (B) T_H2 cytokines like IL-4 and IL-13 stimulate development of wound healing macrophages that contribute to repair of epithelial damage. ECM = Extracellular matrix. (C) IL-10 in combination with other stimuli induces differentiation of regulatory macrophages that in turn contribute to IL-10 production, which is important for regulating immune responses. Figure modified from [127]

T_H1 cells are adapted to fight viruses and intracellular bacteria and their polarization is induced by an IL-12-dependent increase in IFN-γ expression.[182-184, 195-201] IFN-γ induces phosphorylation of STAT1, which results in expression of the T_H1 master transcription factor T-box expressed in T cells (T-bet).[195-197, 202, 203] Besides inducing T_H1 fate, IFN-γ is also the hallmark cytokine secreted

by T_H1 cells and stimulates phagocytosis, antigen presentation, ROS production, and pro-inflammatory polarization of macrophages, which help to fulfill the task of T_H1 immunity and clear intracellular pathogens.[197]

In contrast to CrD, UC is dominated by T_H2-like immune responses and cytokine networks.[1, 2, 115, 193, 194] T_H2 cells fulfill important roles in the defense against parasites and contribute to allergic reactions.[196, 204] They are characterized by expression of the transcription factor GATA binding protein 3 (GATA3) and secretion of IL-4, IL-5, and IL-13.[115, 196, 205-208] Of note, expression of GATA3 is upregulated in response to IL-4-mediated signaling via STAT6.[195, 209-213] The T_H2 hallmark cytokines IL-4 and IL-13 stimulate development of arginase-expressing macrophages, which produce precursors of extracellular matrix (ECM) components and contribute to wound healing (**Figure 7**).[127, 214-216] Excessive T_H2 responses and activity of wound-healing macrophages can result in increased collagen production and fibrosis, which is observed in IBD patients.[127, 215, 217, 218]

T_H17 cells critically contribute to protection against fungi and extracellular bacteria and are abundantly found in the intestinal mucosa.[115, 196, 219] T_H17 cells are characterized by the master transcription factor retinoic acid receptor-related orphan receptor-γt (RORγt; encoded by *RORC*) as well as secretion of IL-17 cytokines (e.g., IL-17A and IL-17F), which are enriched in the gut of IBD patients.[115, 196, 219-225] T_H17 polarization of naïve $CD4^+$ T cells is enhanced by IL-6, IL-21, and IL-23, but the most potent T_H17 fate-inducing cytokine is transforming growth factor beta (TGF-β), which was recently identified to be defective in VEO-IBD patients.[195, 196, 219, 222, 226] In contrast, T_H1 and T_H2 cytokines block the differentiation of T_H17 cells.[190, 227, 228] IL-17-induced signaling results in production of several pro-inflammatory cytokines including granulocyte-macrophage colony stimulating factor (GM-CSF), IL-1β, IL-6, and TNF-α, chemokines, as well as AMPs, which can feedback to IECs and MNPs.[115, 219, 229-232] Of note, several genetic studies have implicated the IL-23/T_H17 axis in intestinal inflammation, as several IBD risk genes have been identified to play a role in this axis including *RORC, IL23R, Interleukin-6 cytokine family signal transducer (IL6ST), G protein-coupled receptor 65 (GPR65), Interleukin-17 receptor alpha (IL17RA), Tyrosine kinase 2 (TYK2)* and *STAT3* (**Figure 3**).[11, 42]

Without resolution of inflammation, continuous T_H cell activity will result in chronic inflammation and disease (**Figure 5**).[115] Regulatory T cells (T_{regs}) play a critical role to shut down excessive or

autoreactive immune responses. At intestinal epithelial barriers T_{regs} prevent autoimmunity, but also dampen the immune response towards microbial and dietary triggers to ensure intestinal homeostasis.[233, 234] The variety of tasks for T_{regs} in the intestine is reflected by their frequency, which increases from 10 % of all $CD4^+$ T cells in other organs to 20 % in the small intestine and 30 % in the large intestine.[233, 235] Most T_{regs} express the transcription factor forkhead box P3 (FOXP3), anti-inflammatory cytokines like IL-10 and TGF-β, and inhibitory molecules like cytotoxic T-lymphocyte-associated protein 4 (CTLA-4).[233, 234, 236-240] Many of these characteristic markers for T_{regs} are dysfunctional in human diseases and most of these disorders cause severe gastrointestinal inflammation demonstrating the importance of T_{regs} for intestinal homeostasis.[60, 65, 226, 241, 242] T_{reg} numbers are reduced in the small intestinal LP upon removal of specific antigens, which indicates that small intestinal T_{regs} mostly regulate homeostasis towards dietary antigens.[233, 243] On the other hand, development of colonic T_{regs} depends largely on an intact microbiome, which is demonstrated by the reduced numbers of T_{regs} in the large intestinal LP of germ-free mice.[233, 235, 244] Therefore, T_{regs} represent a central hub controlling the cytokine environment in the intestine and innate as well as adaptive immune responses.

1.1.7 Immune defects in IBD

Currently there are at least 456 different genetic defects (including 26 preliminary recognized ones) known to cause PID in humans.[245, 246] Around one third of these inborn errors of immunity can present with gastrointestinal disease, which demonstrates the importance of a well-functioning immune system for intestinal homeostasis.[11, 247] Gut symptoms are often the first to be recognized in PID patients, which might be a consequence of the continuous collision between a malfunctioning immune response and the intestinal microbiome.[11] Importantly, these severe phenotypes and children with VEO-IBD represent model systems for studying immune pathomechanisms in IBD.

1.2 Role of IL-2Rγ-mediated signaling in immunity

A rare, but well-studied group of primary immunodeficiencies is severe combined immunodeficiency (SCID), which is characterized by absence of T cell populations and complete or partial dysfunction of other lymphoid populations (i.e., B and natural killer (NK) cells).[248-250] SCID patients present with severe, recurrent bacterial, fungal, and/or viral infections in the first

months of life causing death in the first year of life without treatment.[250-253] Of note, many SCID patients develop failure to thrive, chronic diarrhea, and suffer from gastrointestinal infections reminiscent of IBD, which indicates disturbed intestinal homeostasis due to dysregulated immune responses.[250, 251, 253, 254] Whereas all usual SCID forms show absence of T cells, different SCID forms can be grouped by their immunophenotype of B and NK cells ($T^-B^+NK^+$, $T^-B^-NK^+$, $T^-B^+NK^-$, and $T^-B^-NK^-$ forms).[251, 255, 256] This phenotypic variation is a result of different genetic entities and SCID phenotypes were shown to be caused by mutations in around 20 genes, which affect different immune cell mechanisms including defective hematopoiesis (e.g., *Adenylate kinase 2* (*AK2)*), lymphocyte survival (e.g., *adenosine deaminase (ADA), purine nucleoside phosphorylase (PNP)*), cytokine signaling (e.g, *interleukin 2 receptor subunit gamma* (*IL2RG), interleukin 7 receptor subunit alpha (IL7RA), janus kinase (JAK) 3*), T cell receptor function (e.g., *recombination activating (RAG) 1, RAG2, CD45, deoxyribonucleic acid (DNA) cross-link repair 1C (DCLR1C)*), and thymus function (e.g., *Forkhead Box N1 (FOXN1)*).[251, 252, 256] The majority of SCID cases (approximately 25 - 40 %) presents with mutations in the gene *IL2RG*, which encodes the γ-subunit of the IL-2 receptor (IL-2Rγ) and is also known as common gamma chain (γ_c), as it is also part of the receptors for IL-4, IL-7, IL-9, IL-15, and IL-21.[257-260] With more than 200 mutations, *IL2RG* harbors the largest number of distinct SCID-causing mutations, which are distributed over the complete gene.[256, 257, 261] Since *IL2RG* is located on the X chromosome, γ_c deficiency is also called X-linked SCID or SCID-X1.[257, 262, 263] Despite being a rare disease with an incidence of 1:40,000-75,000 per live births, SCID-X1 is the most common human inborn error of immunity.[256, 257, 264] Although there were also gene therapy approaches tested, the only curative treatment available is HSCT, which is associated with side effects and low efficacy especially in case no HLA-matched sibling is available.[257, 265-267]

1.2.1 Molecular mechanisms of IL-2Rγ signaling

Phenotypically, SCID-X1 is characterized by lack of T and NK cells and dysfunctional B cells ($T^-B^+NK^-$ SCID), which is caused by the lack of central cytokine pathways and their consequences for the development and/or function of different (non-)hematopoietic cells (**Figure 8**).[258] The γ_c cytokine family are cytokines with a four-helix bundle fold that all signal via heterodimeric or -trimeric receptors incorporating IL-2Rγ as shared subunit (**Figure 8**).[258, 268-274] Of note, IL-2Rγ is indispensable for signaling of all of these receptors.[258, 264] Upon ligand binding, all γ_c cytokine

receptors recruit JAK1 and JAK3, which activate different downstream signaling cascades resulting in phosphorylation of different STAT transcription factors (**Figure 8**).[258, 275-277] The central role of JAK/STAT signaling for γ_c cytokine receptors is demonstrated by humans with autosomal-recessive mutations in *JAK3*, which develop $T^-B^+NK^-$ SCID with similar phenotypes as SCID-X1 patients.[251, 258, 278, 279]

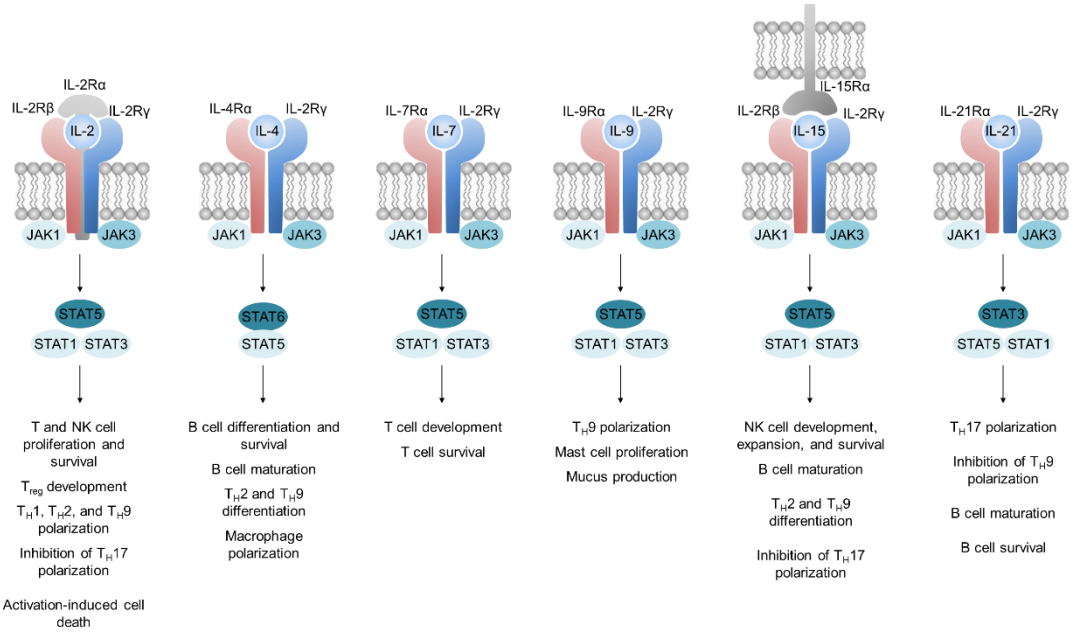

Figure 8: Overview of γ_c signaling pathways.
IL-2Rγ is the critical signaling subunit of interleukin-2 receptor (IL-2R), interleukin-4 receptor (IL-4R), interleukin-7 receptor (IL-7R), interleukin-9 receptor (IL-9R), interleukin-15 receptor (IL-15R), and interleukin-21 receptor (IL-21R) complexes, which are heterodimeric (IL-4R, IL-7R, IL-9R, and IL-21R) or heterotrimeric (IL-2R and IL-15R). Major downstream signaling molecules of γ_c receptors include JAK1, JAK3, STAT1, STAT3, STAT5, and STAT6 and their activation controls pleiotropic functions. Figure modified from [258, 264]

1.2.2 IL-2

In 1976 a soluble factor indispensable for growth of T cells was discovered, which was later named IL-2.[258, 280] IL-2 is predominantly produced by $CD4^+$ T_H cells and the interleukin-2 receptor (IL-2R) is one of the two heterotrimeric receptors in the γ_c cytokine family.[264, 274] Usually, IL-2 first binds to the α subunit of the IL-2R (IL-2Rα) and subsequently the β subunit (IL-2Rβ) as well as the IL-2Rγ subunit are recruited.[264, 281] IL-2Rα, IL-2Rβ, and IL-2Rγ are also called CD25, CD122, and CD132, respectively.[264] Three different cytokine-receptor combinations were shown to exist: (1) IL-2/IL-2Rα, (2) IL-2/IL-2Rβ/IL-2Rγ, and (3) IL-2/IL-2Rα/IL-2Rβ/IL-2Rγ.[264, 282] Interestingly, the affinities of the three receptor complexes to IL-2 differ substantially: low affinity for only IL-2Rα

($K_d \approx 10^{-8}$ M), intermediate affinity for IL-2Rβ/IL-2Rγ ($K_d \approx 10^{-9}$ M), and high affinity for IL-2/IL-2Rα/IL-2Rβ/IL-2Rγ ($K_d \approx 10^{-11}$ M).[264, 282] IL-2R-mediated signaling is mostly mediated by STAT5 and promotes (i) proliferation and survival of T and NK cells, (ii) T_{reg} development, as well as (iii) T_H1, T_H2, and T_H9 polarization (**Figure 8**).[258, 264, 283-286] Furthermore, IL-2 can inhibit T_H17 polarization and cause activation-induced cell death of T cells in large concentrations (**Figure 8**).[228, 258, 264] IL-2Rγ is expressed on a wide variety of cell types allowing different signaling processes, so target cell specificity for certain cytokines needs to be established by the unique subunits of the IL-2R. For IL-2, specificity is established by IL-2Rβ, which can be co-expressed with IL-2Rγ on different T, B, and NK cell subsets.[258, 264] Sensitivity to IL-2 signaling is regulated by expression of IL-2Rα.[287] Whereas IL-2Rα is constitutively expressed on T_{regs}, other T cell subsets acquire IL-2Rα expression only after activation.[287-292] Consequently, T_{regs} usually express the high affinity IL-2R and thus respond to lower IL-2 concentrations.[287, 293, 294] In line, mice lacking IL-2 or IL-2Rβ show impaired T_{reg} development causing lymphoproliferation and autoimmune disease, but still have functional effector T cells.[287, 295, 296] This demonstrates that IL-2 is critical for T_{reg} development, but at least partially dispensable for effector T cell function.[287, 295, 296] Interestingly, IL-2-deficient mice also develop UC-like disease due to the absence of T_{regs} and expansion of T_{regs} with low-dose IL-2 treatments was proven to ameliorate colitis in a mouse model of IBD and human autoimmune diseases in clinical settings demonstrating the importance of T_{regs} for intestinal homeostasis.[287, 296, 297] In summary, IL-2 mediates important survival and polarization signals for T and NK cells, but is not critical for their development, which indicates that loss of T and NK cells in SCID-X1 patients is caused by other γ_c cytokines.[258]

1.2.3 IL-4

Whereas IL-2 is primarily known to regulate T cells, IL-4 promotes B cell differentiation and function (**Figure 8**).[258, 298-300] However, IL-4 is also a key cytokine for polarization of T_H2 cells and wound-healing macrophages demonstrating the central role of γ_c cytokines in innate and adaptive immunity and the connectivity between these different cell populations (see section 1.1.6).[127, 212, 216, 258, 301, 302] IL-4 is produced by a variety of immune cell types including lymphocytes like $CD4^+$ T_H cells and natural killer T (NKT) cells as well as granulocytes and mast cells.[258, 303-310] From a mechanistic perspective, IL-4 is an exceptional γ_c cytokine, as it can also signal independent of IL-2Rγ and it induces phosphorylation of STAT6, which is unique in the family of

γ_c cytokines (**Figure 8**).[258, 303] IL-4 can be bound by two different heterodimeric receptors consisting of the Interleukin-4 receptor subunit alpha (IL-4Rα) and IL-2Rγ (type I interleukin-4 receptor (IL-4R)) or IL-4Rα and Interleukin 13 receptor subunit alpha 1 (IL-13RαI) (type II IL-4R).[258, 273, 303, 311-314] Of note, type I IL-4R expression is predominantly found in hematopoietic cells, but type II receptors are mostly found on non-hematopoietic cells.[258, 303] However, B cells and myeloid cells are responsive to IL-4 and IL-13, which is only possible if IL-4Rα and IL-13RαI are present on the surface of these cells indicating that these cells express both types of the IL-4R.[258, 303, 315, 316] SCID-X1 patients usually present with normal numbers of B cells, but impaired immunoglobulin (Ig) production, which might indicate that IL-4 contributes to B cell functionality, but is dispensable for their development.[258, 317, 318] However, IL-4-mediated signaling was shown to be still functional in B cells from SCID-X1 patients, which might be mediated by type II IL-4Rs independently of IL-2Rγ.[317-319] Pan-hypogammaglobulinemia and B cell dsyfunctions in SCID-X1 patients and also other SCID diseases might be also a consequence of dysfunctions of other γ_c cytokines (e.g., IL-21) or T_H and T follicular helper (T_{FH}) cells, which are indispensable for support of B cell development and function.[248, 317, 319]

1.2.4 IL-7

IL-7 is primarily produced by non-hematopoietic cells (e.g., stromal and epithelial cells) and is indispensable for T cell development.[258, 320, 321] IL-7 signals via a heterodimeric receptor consisting of Interleukin 7 receptor subunit alpha (IL-7Rα), which is also known as CD127, and IL-2Rγ (**Figure 8**).[258, 272, 320, 322] IL-7Rα is expressed during different developmental stages of B and T cells and constitutively in naïve T cells.[320, 323-330] Binding of IL-7 to its receptor induces STAT5- and phosphoinositide 3-kinase (PI3K)-mediated signaling and promotes expression of anti-apoptotic molecules (e.g., B-Cell CLL/Lymphoma 2 (BCL2)), but inhibits pro-apoptotic factors (e.g., BCL2 associated X, apoptosis regulator (BAX), BCL2 associated agonist of cell death (BAD)).[258, 320, 325, 331-335] Furthermore, IL-7 augments proliferation by blocking the cyclin-dependent kinase inhibitor p27.[320, 336] In total, IL-7-mediated signaling supports survival and proliferation of target cells.[320] In contrast to the IL-2R, IL-7Rα expression is down-regulated upon IL-7 stimulation and/or activation of T cells, which removes pro-survival signals from IL-7 in effector T cells and might allow deactivation of T cell responses.[320, 328] The essential role of IL-7 in T cell development is demonstrated by patients with mutations in the *IL7RA* gene encoding the IL-7Rα subunit, which

present with $T^-B^+NK^+$ SCID.[320, 321] Consequently, loss of T cells in SCID-X1 patients is probably mostly caused by impaired IL-7 signaling.

1.2.5 IL-9

IL-9 represents the hallmark cytokine of T_H9 cells and is predominantly produced by this $CD4^+$ T cell subset, but also T_{regs}, T_{FH}, mast cells, innate lymphoid cells (ILCs), and some B cells contribute to IL-9 production.[337-343] Binding of IL-9 to the heterodimeric Interleukin-9 receptor subunit alpha (IL-9Rα)-IL-2Rγ complex induces phosphorylation of STAT5 and contributes to (i) enhanced mucus production from goblet cells, (ii) mast cell proliferation, and (iii) recruitment of mast cells and eosinophils.[258, 271, 337, 344-348] IL-9 has been shown to increase inflammation in allergy and to contribute to anti-tumor responses.[258, 337, 349-351] Interestingly, T_H9 cells are increased in the LP of UC patients, which indicates an important role of IL-9 in intestinal inflammation.[258, 352, 353] Moreover, IL-9 induces (i) pro-inflammatory cytokine production by granulocytes, (ii) dysregulation of IEC barrier integrity, (iii) reduction of IEC proliferation and (iv) impairment of wound-healing demonstrating that IL-9 can promote intestinal inflammation and pathology.[258, 352, 353] In fact, mice deficient for IL-9 show less severe chemically-induced colitis, which makes IL-9 and T_H9 cells interesting candidates for novel therapies in IBD.[352] Since defects in other γ_c cytokines impair T cell development, the contribution of IL-9 deficiency to SCID remains unclear. However, mouse studies suggest that loss of IL-9 function might be rather beneficial.[352, 353]

1.2.6 IL-15

IL-15 is produced by hematopoietic MNPs and non-hematopoietic cells like epithelial cells, keratinocytes, fibroblasts, stromal cells, myocytes, and neural cells.[258, 354-363] IL-2R and IL-15R are the only heterotrimeric receptors of the γ_c family and both depend on the IL-2Rβ and IL-2Rγ subunit for signaling.[258, 269, 354, 364] In contrast to IL-4Rα, IL-7Rα, IL-9Rα, and interleukin-21 receptor (IL-21R), the additional third subunits, IL-2Rα and interleukin-15 receptor subunit alpha (IL-15Rα), contain sushi domains and are thus structurally different from the others.[258, 365, 366] Together with their chromosomal proximity, the structural similarity between IL-2Rα and IL-15Rα might indicate that they developed from a gene duplication event.[258] However, IL-2Rα and IL-15Rα differ in the affinity to their respective cytokine.[364] Whereas IL-2 shows low affinity to

IL-2Rα, IL-15 is bound with high affinity by IL-15Rα.[364] Furthermore, IL-15 signaling was shown to be mostly mediated *in trans*, which means that the IL-15Rα bound to IL-15 interacts with IL-2Rβ-IL-2Rγ complexes on a different cell (**Figure 8**).[258, 364, 367, 368] In these neighboring cells, IL-15 induces phosphorylation of STAT5, which controls the development, survival, proliferation, and function of different cytotoxic immune cells including $CD8^+$ memory T cells, NK, and NKT cells.[258, 270, 354, 364, 367-374] In fact, IL-15 is indispensable for their development, as $Il15^{-/-}$ and $Il15ra^{-/-}$ mice show absence of $CD8^+$ memory T cells and NK cells.[258, 270, 354, 364, 375] Therefore, defective IL-15 signaling likely causes the loss of NK cells in SCID-X1 patients.

1.2.7 IL-21

IL-21 is mostly secreted by T_H17, T_{FH}, and NKT cells, but can be also expressed in other $CD4^+$ T cell populations and other hematopoietic cells.[258, 318, 376-380] The heterodimeric IL-21R consists of the IL-21Rα subunit and the common IL-2Rγ subunit and primarily induces phosphorylation of STAT3 upon activation (**Figure 8**).[258, 268, 378, 379, 381-383] IL-21 signaling contributes to (i) induction of T_H17 cell polarization, (ii) T_{FH} cell development, (iii) inhibition of T_H9 and T_{reg} generation, and (iv) proliferation and memory formation of $CD8^+$ T cells, and (v) cytotoxicity of NK cells.[181, 258, 318, 378, 384-394] For innate immune cells, IL-21 can (i) induce apoptosis of DCs, (ii) promote phagocytosis of macrophages, and (iii) inhibit pro-inflammatory molecule secretion from mast cells.[318, 395, 396] However, the most important functions of IL-21 are affecting B cells. First, IL-21-mediated activation of STAT3 and PR/SET domain 1 (PRDM1) was shown to be essential for the development of plasmablasts from naïve B cells indicating a critical role for IL-21 in B cell maturation (**Figure 8**).[258, 317, 318] Furthermore, IL-21 modulates Ig production of B cells, which was demonstrated by $IL21R^{-/-}$ mice and in SCID-X1 patients after HSCT.[317, 318] Whereas IgG1 subtypes are reduced in $Il21r^{-/-}$ mice, IgE serum levels are increased.[318, 319] Of note, $Il21r^{-/-}Il4^{-/-}$ mice show impaired IgE production indicating that increased IgE in single Il21r-deficient mice is controlled by IL-4.[318, 319] IL-21 signaling controls important functions relevant to intestinal inflammation including activation of the IL-23/T_H17-axis.[397-399] The importance of IL-21 for intestinal homeostasis is demonstrated by (i) an increased concentration in the LP of IBD patients, (ii) SNPs associated with IBD pathogenesis in genes linked to IL-21 signaling (e.g., *IL21, STAT3, IL23R*, *RORC)* (**Figure 3**), and (iii) pediatric patients with mutations in the *IL21R* gene, which present with recurrent respiratory and gastrointestinal infections, diarrhea, cholangitis, and liver

disease.[11, 318, 397, 399-402] Interestingly, IL-21R deficiency was also associated with chronic infections with cryptosporidium, which can cause intestinal pathology.[318, 400] In line with experiments from mice and SCID-X1 patients, IL-21R-deficient patients developed normal numbers of B cells, but aberrant function of B cells in response to IL-21.[318, 400] Analogous to murine models, IL-21R-deficient patients also showed increased IgE production and decreased IgG upregulation upon IL-21 stimulation.[318, 400] Furthermore, defective T cell proliferation and function as well as cytotoxicity of NK cells could be observed.[318, 400]

1.2.8 Atypical SCID

SCID is characterized by impaired T cell development caused by mutations in different genes and increased susceptibility to infections. However, several studies reported patients with mutations in SCID genes that present with normal or even increased numbers of T cells, milder phenotypes and/or later onset of disease.[248, 252] These specific phenotypes were classified as atypical or “leaky” SCID.[248, 252] Whereas classic SCID is defined by a disease onset in the first year of life, onset of atypical SCID can be delayed up to adulthood.[252] Atypical SCID forms are caused by hypomorphic mutations, somatic reversion, somatic mosaicism, or maternal engraftment.[248, 252, 403-405] From a genetic perspective, atypical forms are often caused by mutations in *ADA, RAG1/2*, or *IL2RG*.[252] Analogous to classical SCID, atypical SCID is also characterized by recurrent infections, which most frequently include pneumonia, but more rarely also result in systemic bacterial, fungal, or viral infections.[252] Furthermore, atypical SCID can present with autoimmune cytopenia, lymphoproliferation, skin rashes, and importantly IBD.[252] Most patients with atypical SCID show lymphopenia with low numbers of $CD3^+$ and $CD4^+$ cells, but $CD8^+$ cells were less often affected.[252] Moreover, most patients have normal Ig levels.[252] Phenotypic heterogeneity, late disease onset, unknown mutations, complex genotype-phenotype correlations, and less severe symptoms can complicate diagnosis of atypical SCID. Since the curative treatment HSCT has the highest success rate in younger patients unaffected by infections, delayed diagnosis and treatment might have severe consequences for the affected patients warranting an early identification of atypical SCID.

1.3 CD33-mediated inhibition of immune cells

Homeostasis is central for the operability of most biological systems in the human body and many of the most prevalent diseases in modern human society (e.g., diabetes, allergy, autoimmunity, atherosclerosis, neurodegenerative disorders) might be caused by loss of homeostasis and lead to chronic inflammation.[406] Maintaining homeostasis at the intestinal barrier is very challenging, as intestinal immune cells need to maintain homeostasis, establish tolerance for commensal microbial and dietary antigens, but also need to be prepared for invading pathogens. Analogous to activating receptors, immune cells express a variety of inhibitory receptors, which (i) regulate activating signals, (ii) reestablish homeostasis by deactivating the immune response, (iii) prevent autoimmunity, and (iv) avoid unnecessary activation.[407] Inhibitory receptors also allow immune cells to differentiate between background noise and actual threats by providing a threshold for activation (threshold receptors), but also shut down actively ongoing immune responses (negative feedback receptors).[407] Most inhibitory receptors are characterized by an immunoreceptor tyrosine-based inhibitory motif (ITIM), which is the counterpart of ITAMs in activating receptors and is fulfilling its inhibitory function by recruiting phosphatases.[407-415] An important protein family containing a variety of inhibitory receptors is formed by sialic acid binding immunoglobulin type lectins (Siglecs) and CD33 represents a prototype of this family.[416, 417]

1.3.1 Sialic acids

Sialic acids are the most frequent terminal sugar on complex glycans in eucaryotes and are also found ubiquitously in the human body, which allows them to mediate pleiotropic functions.[418] Sialic acids are named based on their discovery in saliva mucins (Greek: síalon) and are derivatives of neuraminic acid, which is a nine-carbon sugar that is rarely found in nature as a free molecule.[419, 420] In humans the term sialic acid mostly refers to N-acetylneuraminic acid (Neu5Ac), which is a N-substituted form of neuraminic acid with an acetyl group at position 5 of the carbon backbone.[416, 417, 419, 421-424] For activation, Neu5Ac is transferred onto cytidine triphosphate (CTP) in the nucleus by CMP-Neu5Ac synthetase generating cytidine monophosphate (CMP)-sialic acid conjugates, which are then transported into the golgi apparatus.[419, 421, 425-429] Here, various sialyltransferases catalyze the transfer of sialic acids via α2,3-, α2,6-, or α2,8-linkage onto glycans found on proteins, lipids, or other molecules.[419, 421, 429] Mice that lack an important enzyme in sialic acid biogenesis (UDP-GlcNAc 2-epimerase) die during early embryogenesis exemplifying the

importance of sialic acids for mammalian development.[418, 430] Furthermore, functional deficiencies in sialyltransferases (e.g., ST3 beta-galactoside alpha-2,3-sialyltransferase 4 (St3Gal4) and ST6 beta-galactoside alpha-2,6-sialyltransferase 1 (ST6Gal1)) can result in defects in immunity demonstrating the importance of sialic acids for immune cells.[431, 432] Of note, sialic acids are usually added as the last sugar molecule on complex glycans and thus represent a “cap”, which can be recognized by Siglecs.[416, 421, 429]

1.3.2 Siglecs

Siglecs can be mostly found on the surface of innate immune cells allowing regulation of activating surface receptors like TLRs and NLRs.[416, 421] However, nearly all immune cell types (except resting T cells) express at least one Siglec demonstrating the central role of Siglecs in regulating immunity.[416] Based on their evolutionary proximity and conservation, the Siglec protein family is divided into two groups.[416, 417, 421, 433] The first group has a low sequence similarity, but is found in most mammals and includes Siglec-1 (also known as Sialoadhesin or CD169), Siglec-2 (CD22), Siglec-4 (myelin-associated glycoprotein, MAG), and Siglec-15.[416, 417, 421] The second group is named CD33-related Siglecs based on their prototype member and is characterized by high sequence similarity and variability across species and includes Siglec-3 (also named CD33), Siglec-5 to Siglec-11, Siglec-14, and Siglec-16.[416, 417, 421, 433] Of note, studies on CD33-related Siglecs are hindered by the lack of appropriate *in vivo* model systems, as humans express a more diverse repertoire of CD33-related Siglecs compared to other mammals, like mice and rats.[416, 417, 421, 433] Structurally, Siglecs are type I transmembrane proteins, which are characterized by a N-terminal ligand binding V-set Ig domain and C2-set Ig domains in their extracellular part.[416] Depending on the number of C2-set Ig domains, Siglecs can bind ligands *in cis* or *in trans*.[416, 417, 419, 421] However, due to the high concentration of sialic acids on the cell surface of mammalian cells (up to > 100 mM), Siglecs probably bind mostly to ligands *in cis*.[416, 434] Sialoadhesin (Siglec-1) contains 17 C2-set Ig domains and probably binds ligands *in trans* representing an exception in the Siglec family.[416, 435]

Sialic acids serve as self-associated molecular pattern (SAMP) and Siglecs allow immune cells to differentiate between self and non-self.[416, 417, 421, 436] Most Siglecs provide a constant inhibitory signal to immune cells, which dampens activation and is only overcome upon recognition of a real threat.[416, 417, 419, 421] Upon binding of sialic acids, the ITIM and ITIM-like motifs in the intracellular

domain of inhibitory Siglecs are tyrosine phosphorylated by kinases of the Src family, which allows binding of the SH2-domain containing protein tyrosine phosphatase non-receptor type (PTPN) 6 (also known as Src homology region 2 domain-containing phosphatase (SHP)-1) and PTPN11 (also known as SHP-2).[416, 417, 419, 421, 437-439] PTPN6 and PTPN11 dephosphorylate many different downstream targets including central TLR and NLR signaling components, which results in inhibition of cellular activation, proliferation, cytokine production, and adhesion as well as increased cell death.[416, 417, 419, 421]

1.3.3 CD33

Although CD33 is the prototype of CD33-related Siglecs and shares many features with other Siglecs, it has some unique characteristics. In common with many other Siglecs, CD33 binds α2,3- and α2,6-linked sialic acids and contains one ITIM and one ITIM-like motif in its intracellular domain, which recruit PTPN6 and PTPN11 upon activation (**Figure 9C**).[417, 440-443] In humans, CD33 is the only inhibitory Siglec with a single C2-set domain, which generates the smallest possible extracellular domain for Siglecs and positions the ligand binding domain close to the cell surface (**Figure 9B**).[416, 444] Therefore, it is likely that CD33 preferably binds ligands *in cis* rather than *in trans*.[416, 444]

CD33 is expressed by different myeloid populations including monocytes, macrophages, and DCs.[416, 417, 421, 443, 445] Whereas other Siglecs are expressed only in fully differentiated cells, CD33 starts to be expressed on the surface of progenitor cells during myelopoiesis indicating a potential inhibitory role during myelopoiesis.[416, 446-449] In fact, activation of CD33 substantially inhibits proliferation and differentiation of myeloid progenitors as well as monocyte-derived DCs *in vitro*.[446-448] Furthermore, CD33 activity was linked to apoptosis of cells during differentiation.[446-448] CD33 is a commonly used marker for myeloid progenitor cells, monocytes, and macrophages, but recent evidence showed that CD33 can be also expressed by activated lymphoid cells including T and NK cells indicating a broader function of CD33 in regulating immunity.[450, 451]

Previous studies have identified two major isoforms of CD33 (**Figure 9A**).[450-453] Whereas the canonical, larger isoform is built by 7 exons and is named CD33M (**Figure 9A**), the smaller, less frequent isoform is named CD33m and is characterized by skipping of exon 2, which encodes the V-set domain of CD33 (**Figure 9B**).[450, 452, 453] In contrast to CD33M, which is expressed on the plasma membrane, CD33m has been suggested to be located in peroxisomes or other

intracellular vesicular structures.[452, 453] However, in over-expression models CD33m was also detected on the cell surface.[444, 453] Since the V-set domain was shown to mediate ligand binding, CD33m was proposed to be a loss-of-function form of CD33, but recent evidence suggests that CD33m has a V-set-independent function or might result in a gain-of-function.[444, 452-455]

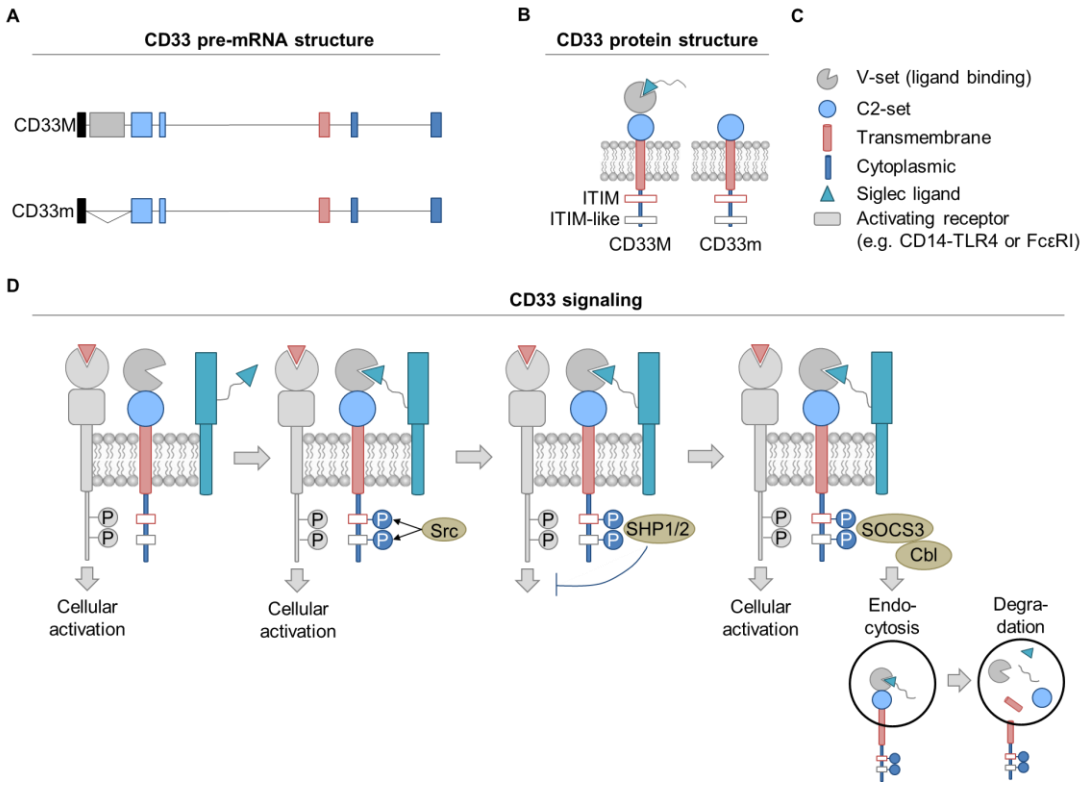

Figure 9: Structure and signaling of CD33.
Schematic overview of CD33 (A) messenger ribonucleic acid (mRNA) and (B) protein. (C) Figure legend for schemes. (D) CD33 mediates inhibitory signals via recruitment of SHP1 (PTPN6) and SHP2 (PTPN11) phosphatases. CD33 signaling is turned off by endocytosis and degradation. Information on mRNA structure obtained from *Ensemble Genome Browser* (https://grch37.ensembl.org/index.html; Human reference genome GRCh37.p13). Figure modified from [416, 421, 442, 451]

CD33 is considered a threshold receptor, which is constitutively active and prevents unwanted activation of immune cells by generating a barrier that activating signals have to overcome before the immune cell reacts.[407] In line, knock-down (KD) or antibody-mediated inhibition of CD33 in human peripheral blood monocytes results in release of pro-inflammatory cytokines (e.g., IL-8, TNF-α, and IL-1β), which would disturb homeostasis without a real trigger.[456] Similarly, removal of cell surface sialic acids by neuraminidase treatment also causes release of pro-inflammatory cytokines.[456] Mechanistically, pro-inflammatory cytokine release upon CD33 inhibition was mediated by p38 Mitogen-Activated Protein Kinase (MAPK) and regulated by PI3K.[456] As discussed above, Siglecs inhibit activating receptors like TLRs and NLRs to prevent autoimmunity

and tissue damage caused by excessive immune responses. In the case of CD33, studies have shown that CD33 can inhibit signaling of TLR4, which detects different PAMPs but is mostly known as receptor for lipopolysaccharide (LPS) from bacterial cell walls.[442] In detail, CD33 was shown to bind sialic acids on the surface of the TLR4 co-receptor CD14, which is involved in binding and presentation of LPS and other PAMPs.[442] Presence of CD33 reduced the presentation of LPS from CD14 to TLR4 and the uptake of LPS presumably via inhibition of NF-κB-mediated signaling.[442]

To allow appropriate activation of the immune system and clearance of pathogens in case of infections, the inhibitory signals of CD33 need to be overwritten and turned off. To overcome CD33-mediated inhibition, PAMPs (e.g., LPS) induce expression of suppressor of cytokine signaling 3 (SOCS3), which can bind to phosphorylated tyrosines in the ITIM motifs of CD33 and competes with PTPN6 and PTPN11 (**Figure 9C**).[457-459] SOCS3 recruits other proteins to form an E3 ubiquitin ligase complex that induces ubiquitination of CD33.[457-459] Ultimately, ubiquitination increases endocytosis of CD33 and targets CD33 and SOCS3 for proteasomal degradation thereby counteracting the inhibitory functions of CD33 (**Figure 9C**).[457-459] SOCS3 was shown to control several important signaling pathways in innate and adaptive immune cells and its absence increases macrophage activation and results in more severe inflammation in different disease models.[460, 461] Importantly, SOCS3 expression is also increased in different colitis models and loss of SOCS3 results in enhanced dextran sulfate sodium (DSS)-induced colitis, which links CD33 regulatory pathways and intestinal inflammation.[460]

1.3.4 Siglecs and CD33 in health and disease

Role of Siglecs in intestinal immunity

In aqueous solutions with neutral pH carboxy groups of sialic acids are deprotonated and are negatively charged. Since the cell surface of many cells contains high concentrations of sialylated glycans, most cells present negative charges on their surface, which establishes repulsive forces between different cells.[419, 462] In the blood, negative charges established by sialic acids prevent aggregation of erythrocytes and provides a barrier between blood cells and vascular endothelial cells that is only overcome upon activation of extravasation.[419, 462]

Of note, sialic acids are also present on mucins and are thus a primary component of mucus, which provides a chemical and physical barrier against commensal and pathogenic bacteria at healthy epithelial surfaces.[419, 463-466] During intestinal inflammation and dysbiosis, microbiota (e.g., *Bacteroides vulgatus*) were shown to produce neuraminidase, which releases sialic acids from the surface of IECs fueling dysbiosis.[467] Inhibition of bacterial neuraminidase was shown to ameliorate chemically-induced colitis in mice indicating an important role of sialic acids in intestinal homeostasis.[467] Similarly, removal of sialyl(α2,3)lactose (also called 3'-Sialyllactose or 3SL) from feeding milk reduced severity of colitis induced by DSS or by KO of the *Il10* gene (spontaneous colitis).[468, 469] Mechanistically, 3SL was shown to induce the release of T_H1 and T_H17 cytokines from DCs in a TLR4-dependent fashion and these cytokines were shown to promote intestinal inflammation (see section 1.1.6).[469] Recently, 3SL was shown to bind to CD33, activate CD33 downstream signaling via PTPN6, and induce SOCS3-mediated degradation of CD33 via proteasomes suggesting that 3SL and/or sialic acid binding by CD33 could also play a role in intestinal homeostasis.[470] 3SL binding to CD33 also stimulated differentiation of megakaryocytes and induced apoptosis in myeloid cancer cell lines, which was abrogated in CD33 KD cell lines.[470]

Several pathogens (e.g., *Neisseria meningitidis, Haemophilus influenzae, Campylobacter jejuni, Pseudomonas aeruginosa* and group B *Streptococcus*) evolved sialic acids on their surface hijacking their role as SAMPs and suppressing immune activation.[417, 471-475] For example, sialic acids on the surface of group B *Streptococcus* were shown to activate Siglec-9, which inhibits oxidative burst reactions and extracellular trap formation resulting in less bacterial killing.[417, 476] Furthermore, Siglec-9 inhibited production of pro-inflammatory cytokines like IL-6 and IL-1β, but

increased the secretion of anti-inflammatory IL-10 demonstrating a central role of Siglecs in shaping the cytokine environment during homeostasis and infection.[417, 477]

The prototype Siglec CD33 was shown to modulate development of different human pathologies including acute myeloid leukemia (AML), Alzheimer's disease (AD), Allergy, and myelodysplastic syndrome (MDS) (**Figure 10**).

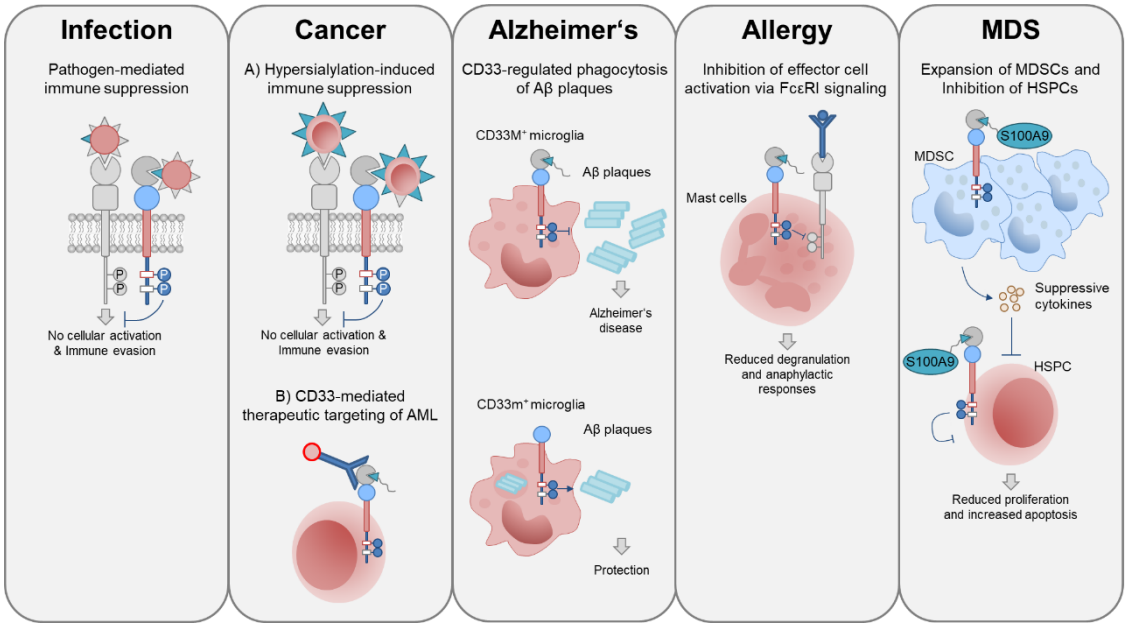

Figure 10: Siglecs and CD33 in disease.
Various pathogens and cancer cells have been shown to hijack Siglec-mediated immune suppression to evade recognition by the immune system. Siglecs are known to play important roles in different human pathologies (e.g Cancer, AD, allergy, and MDS) and are interesting therapeutic targets. Figure based on [416, 417, 419, 446-448, 478-483].

CD33 represent an important target in AML

Besides external threats, also internal threats, like cancer cells, hijack the function of Siglecs to suppress immunity.[419, 478] In fact, leukemia, ovarian cancer, colorectal cancer, and breast cancer cells were shown to be hypersialylated inhibiting the response of the immune system.[419, 478] Based on its expression pattern in myeloid progenitor cells as well as mature monocytes/macrophages and DCs, CD33 was identified as an attractive target for the treatment of AML and an anti-CD33 antibody coupled to the toxin calicheamicin (gemtuzumab ozogamicin; also known as GO or Mylotarg) was approved for the treatment of AML in the United States.[417, 484-486] GO binds to CD33 and induces endocytosis, which results in toxin-induced death of the targeted cell.[485] Although GO improved the survival of AML patients, it was withdrawn from the market in several countries due to safety concerns and adverse effects.[484, 487] Previously, CD33 was thought to be expressed

at much later stages of myeloid differentiation, but it was shown that CD33 can be already expressed in hematopoietic stem or progenitor cells (HSPC).[487] Targeting of these HSPC by GO might explain prolonged cytopenia observed in some patients after the treatment.[487] Discovery of the second CD33 isoform, CD33m, also raised questions regarding the efficacy of GO, as the targeted epitope of GO is in the V-set domain, which is lacking in CD33m.[484] Consequently, CD33m is not bound by GO and CD33m-expressing tumor cells might escape GO-mediated cytotoxicity building a potential reservoir for relapse.[484]

CD33 SNPs are associated with late-onset Alzheimer's disease (LOAD)

Around 28 million people worldwide suffer from AD, which makes AD the most frequent form of dementia.[419, 488] AD most commonly presents as LOAD, which is defined by a disease onset after 65 years of age.[488] GWAS implicated *CD33* as one of the most important genetic risk factors for LOAD pathogenesis.[419, 481, 489-491] In line, AD patients express increased levels of sialic acids and CD33.[419, 481] In the brain, CD33 is mostly expressed in microglia, which are macrophage-like cells and represent the tissue-resident innate immunity in the CNS.[492] Similar to IBD, over-reactive macrophages/microglia in the CNS contribute to pro-inflammatory environments causing chronic inflammation and tissue damage.[480] Importantly, AD is characterized by increased activation of NLRP3 inflammasomes and production of its downstream effectors IL-1β and IL-18.[480, 493, 494] In line, microglia and monocyte-like THP1 cells that lack CD33 or express CD33m showed increased Spleen Associated Tyrosine Kinase (SYK) and Extracellular Signal-Regulated Kinase (ERK) signaling activity and higher basal expression of *IL1B, IL6, IL8,* and *IL10* messenger ribonucleic acid (mRNA).[495] Microglia contribute to phagocytosis of Aβ, which might be defective or dysregulated in AD causing increased deposition of Aβ plaques in the brain.[481, 496] Recognition and clearance of DAMPs (e.g., Aβ) by microglia depends also on balanced signals between activating and inhibitory receptors during homeostasis and CD33 risk alleles might modify this balance.[481] Indeed, the identified LOAD risk allele in *CD33* was shown to augment the expression of CD33M on the surface of microglia and reduce the capacity of microglia to phagocytose Aβ plaques.[481] In contrast, the protective allele reduced CD33 surface expression and enhanced uptake of Aβ by microglia prompting the hypothesis that CD33-mediated signaling inhibits microglia phagocytosis and thus contributes to AD pathogenesis.[481] The protective allele was later shown to increase skipping of exon 2 and expression of the small CD33m isoform indicating that reduced sialic acid binding by CD33m might enhance phagocytosis of Aβ plaques.[481, 492, 497, 498]

Initially, it was hypothesized that CD33m represents a loss-of-function isoform due to the missing ligand binding domain, but a SNP generating a premature stop codon in exon 3 was not conferring protection to AD questioning the protective effect of CD33 loss.[492, 499] Recently, two different studies suggested that CD33m actually enhances phagocytosis of different substrates, which might be in line with a gain-of-function role of CD33m.[454, 455] However, possible mechanisms and functions of CD33m still remain elusive and their elucidation is complicated by controversial reports about the subcellular localization of CD33m.[444, 451-453, 492]

A possible hypothesis for the role of CD33m is that the ITIM motifs in the cytoplasmic tail of CD33 can also function as ITAMs.[444] In fact, the ITIM sequences in CD33 resemble the ITAM consensus sequence and similar ITIM sequences in other proteins have been shown to be able to recruit SYK and Zeta Chain Of T Cell Receptor Associated Protein Kinase 70 (ZAP70) that mediate activating signals.[444] Furthermore, CD33m could also change dimerization properties, as the lack of the V-set domain leaves important cysteine residues unpaired, which might allow unknown disulfide bridges.[444] Independent of the protective role of CD33m, increased CD33M expression is associated with increased risk and thus CD33M represents an interesting target for the treatment of AD. In fact, a gene therapy approach reducing CD33 expression was shown to ameliorate Aβ plaque burden and decrease the expression of microglial *CD11c, Tlr4, Il1b, Ccl2,* and *Tnfa*, which demonstrates the important role of CD33 in controlling microglial function.[500]

CD33 in allergy

Many widespread diseases are caused or triggered by modern lifestyle, which often leads to dysregulation of homeostatic processes including immune responses.[501] Allergies are a prime example of modern lifestyle-triggered dysregulation of immunity and represent a major disease burden affecting hundreds of million people worldwide.[482, 501] Allergic responses result in production of allergen-specific IgE antibodies that are bound by mast cells, eosinophils, and basophils via the high-affinity IgE receptor (FcεRI).[501, 502] Known allergens are recognized by FcεRI-bound IgE molecules, which induces cross-linking of several IgE-receptor complexes on the cell surface and results in release of cellular messengers like histamine, prostaglandins, and leukotrienes.[501, 502] The function of IgE was recently shown to depend largely on the presence of sialic acids, as desialylated IgE dampened mast cell degranulation and anaphylactic responses.[502] Interestingly, recruitment of CD33 to IgE-FcεRI complexes suppressed activation and cytokine release (i.e., TNF-α, IL-4, IL-6, and IL-13) of mast cells indicating an important

function of CD33 in regulation of FcεRI complexes and mast cell activation.[482] Importantly, CD33 ligands were able to prevent anaphylaxis and bronchoconstriction in transgenic animal models, which makes CD33 an attractive target for desensitization of mast cells during allergen immunotherapy.[482]

Role of CD33 in myelodysplastic syndromes

MDS is a type of neoplasm characterized by cytopenia, which is caused by hematopoiesis defects.[483, 503, 504] In the over 70 year old population, MDS represent one of the most frequent hematological disorders with an incidence greater than 20 per 100000 persons.[504, 505] Chronic inflammation and immune cell activation is assumed to be a driver of MDS phenotypes.[483] Continuous production of cytokines (e.g., GM-CSF, Macrophage Colony-stimulating factor (M-CSF), IL-1β, IL-6) also contributes to the development of myeloid-derived suppressor cells (MDSCs), which were found in high numbers in MDS patients.[483, 506] MDSCs, derive from granulocyte or monocyte progenitor cells, respectively, and have strong immunosuppressive capacity controlling activation of T, B, and NK cells in a variety of pathologies (e.g., cancer, autoimmunity).[506] In line with their inhibitory role, human MDSCs express high levels of CD33, which is also used as marker to identify MDSCs.[483] In fact, activation of CD33 by the immune alarmin S100 Calcium Binding Protein A9 (S100A9) was shown to be associated with higher numbers of MDSCs in MDS patients.[483] In detail, binding of S100A9 to CD33 increased the release of TGF-β and IL-10, which are known to exert strong immunosuppressive effects and presumably inhibit proliferation of HSPC.[483] Moreover, transgenic over-expression of S100A9 in mice resulted in a MDS phenotype characterized by dysplastic cytopenia.[483] Vice versa, blocking of CD33 prevented this phenotype demonstrating the central role of the S100A9-CD33 axis in the development of MDSCs and pathogenesis of MDS.[483] Of note, increased numbers of MDSC were also observed in IBD patients and murine colitis models.[507]

S100A9 (also known as MRP14) is produced by monocytes and neutrophils and usually forms heterodimers with S100A8 (also known as MRP8).[508, 509] Since expression of S100 proteins is induced by a wide variety of stimuli including heat, infection, stress, and trauma, they are also known as immune alarmins, which activate various effector mechanism and serve as biomarker for several inflammatory diseases.[508] Importantly, S100 protein levels are also increased in IBD and are used routinely as marker for ongoing intestinal inflammation.[510, 511] Furthermore, S100A9

levels are also increased in the cerebrospinal fluid (CSF) of AD patients and might contribute to production of Aβ plaques via stimulation of TLR4.[480, 512, 513] Therefore, S100A8/A9 play an important role in the complete human body and serve as central alarmin and disease mediator.

S100A8/A9 proteins have intracellular and extracellular functions.[508] Intracellularly, S100 proteins bind divalent cations (e.g., Ca^{2+} and Zn^{2+}) and influence cytoskeletal rearrangements and oxidative burst responses.[508, 514-516] Extracellularly, S100A8/A9 can induce leukocyte recruitment, release of cytokines, proliferation, differentiation, and apoptosis of different target cells.[508, 517-523] The variability of S100A8/A9 is demonstrated by their binding to several receptors including Receptor For Advanced Glycation End-Products (RAGE), TLR4, and CD33.[483, 508]

Interestingly, blocking of NLRP3 inflammasomes and pyroptosis in HSPC of MDS patients ameliorated proliferative capacity indicating that inflammasomes might be the reason for the cytopenia observed in MDS.[524] Importantly, NLRP3 inflammasome activation and pyroptosis was triggered by S100A9, as removal of S100A9 with an CD33-IgG chimera showed similar effects and reduced levels of inflammasome effector molecules (e.g., CASP1 and IL-1β).[524]

1.4 TREM2

TREM2 is a cell surface receptor binding negatively charged sugars and lipids including DAMPs like phosphatidylserine, apolipoprotein E (ApoE), and Aβ.[492, 525] Initially, TREM2 was shown to recognize bacteria and is also known to bind PAMPs like LPS.[492, 525-527] As indicated by the name, TREM2 is expressed in myeloid cells including DCs, monocytes, macrophages, microglia, and osteoclasts.[528, 529] *TREM2* mRNA contains 5 exons and TREM2 protein is part of the Ig superfamily of receptors containing one V-set domain for ligand binding, a positively charged transmembrane domain, and a short intracellular C-terminal domain (**Figure 11A-C**).[527, 530, 531]

1.4.1 Dual function of TREM2 intracellular signaling

In contrast to CD33, TREM2 has no intracellular signaling motif and is thus dependent on interaction with DNAX-activating protein of 12 kDa (DAP12; also known as TYROBP) for mediating its signals inside the cell (**Figure 11C**).[528, 529, 532, 533] Conversely, DAP12, which exists as disulfide bond-linked homodimer on the cell surface, has a short extracellular domain and contains an intracellular ITAM motif (**Figure 11C**).[529, 534] The interaction of TREM2 and DAP12 is

stabilized by attraction between positively charged residues in TREM2 and negatively charged residues in DAP12 inside their respective transmembrane domains.[529, 533, 535] Of note, DAP12 is known to be the signaling partner of many other cell surface receptors including NK cell- and T cell-specific receptors and myeloid-specific receptors (e.g., TREM1) and mediates signaling of activating Siglecs (e.g., Siglec-14, see also section 1.3.2).[421, 528, 532, 536]

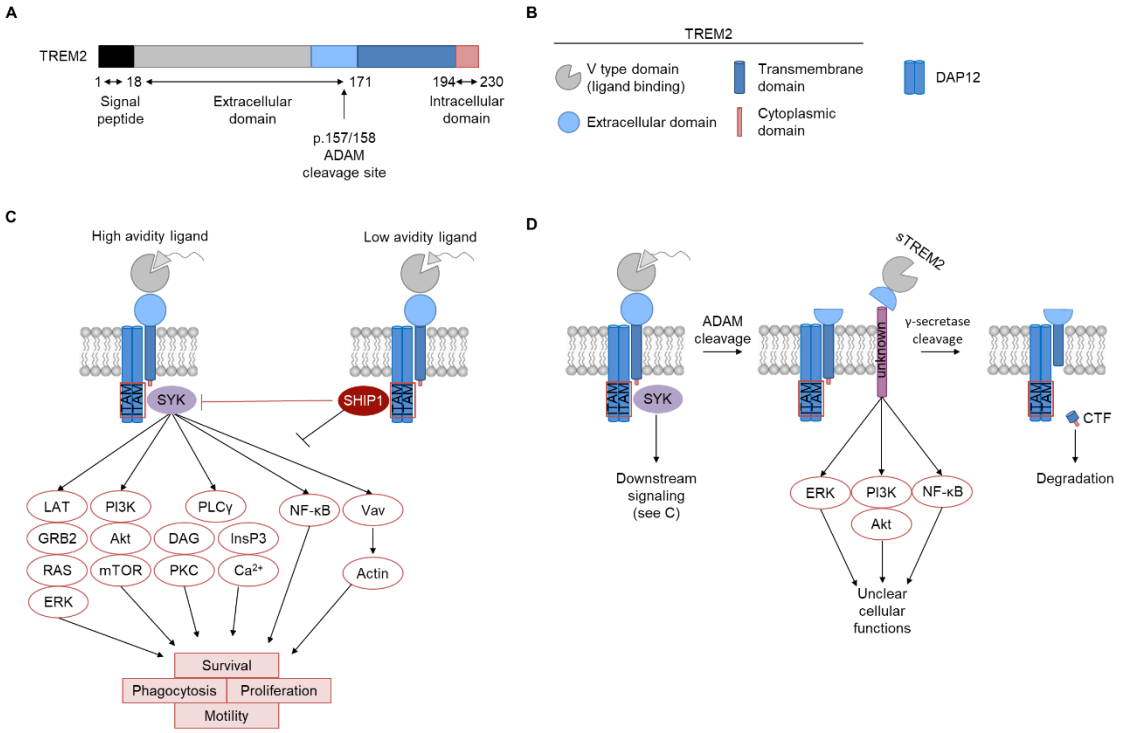

Figure 11: Overview of TREM2 structure and TREM2-DAP12-mediated signaling.
(A) Schematic overview of *TREM2* mRNA. (B) Figure legend. (C) Schematic overview of TREM2 signaling. TREM2 can induce (high avidity ligands) or inhibit (low avidity ligands) cellular activation via various intracellular signaling pathways controlling cell survival, proliferation, motility, and phagocytosis. (D) TREM2 signaling is turned off by ectodomain shedding. Information on mRNA structure obtained from *Ensemble Genome Browser* (https://grch37.ensembl.org/index.html; Human reference genome GRCh37.p13) and UniProt (https://www.uniprot.org/). Figure adapted from [528, 529, 537]

Activation of TREM2 or any other DAP12-associated cell surface receptor by ligand binding induces phosphorylation of tyrosines in the ITAM motifs of DAP12 dimers by Src kinases, which allows recruitment of Syk to the complex (**Figure 11C**).[528, 529, 538-541] SYK is known to activate several important signaling cascades including ERK, PI3K, Phospholipase C Gamma (PLCγ), NF-κB, and Vav Guanine Nucleotide Exchange Factor (Vav) in various cell types (**Figure 11C**).[528, 529, 538-541] In detail, phosphatidylinositol-3,4,5-trisphosphate generated by activated PI3K serves as membrane adaptor for several important signaling effectors like LAT,

which serves as platform for recruitment and activation of Growth Factor Receptor Bound Protein 2 (GRB2), PLCγ, and Vav.[528, 542-545] Active GRB2 induces ERK-mediated signaling, PLCγ produces the second messenger diacalyglycerol (DAG, activates Protein Kinase C (PKC)) and inositol-1,4,5-trisphosphate (InsP3, induces Ca^{2+} influx), and Vav mediates remodeling of the actin cytoskeleton (**Figure 11C**).[528, 529, 546, 547] Furthermore, PI3K also modulates AKT Serine/Threonine Kinase (AKT) and mammalian Target of Rapamycin (mTOR) signaling (**Figure 11C**).[528, 529] Ultimately, TREM2 signaling regulates cellular survival, proliferation, phagocytic activity, and motility of myeloid cells (**Figure 11C**).[525, 526, 529, 540, 548-550]

TREM2 and DAP12 were also shown to have inhibitory functions in cells and their opposing role is proposed to depend on the avidity of the ligand.[528, 529, 539] Whereas high avidity ligands induce the above-described activating signaling, low avidity ligands result in inhibition of similar signaling cascades.[528, 529, 539] Mechanistically, low avidity ligands might induce phosphorylation of a single tyrosine in the ITAM motif, which recruits the phosphatase PTPN6 instead of the kinase SYK to the TREM2-DAP12 complex.[444, 528, 529, 539] Analogous to CD33, PTPN6/11 and/or Src homology 2 (SH2) domain containing inositol polyphosphate 5-phosphatase 1 (SHIP1) activity causes dephosphorylation of downstream targets counteracting the activity of SYK and resulting in cellular inhibition.[528, 529, 539] However, the mechanisms behind the dual role of DAP12 are still controversial, might be cell type-specific, or include other signaling pathways.[528] For example, TREM2-DAP12-mediated activation of PLCγ might inhibit TLR signaling by depletion of phosphatidylinositol-4,5-diphosphate, which is a necessary adaptor for important TLR signaling components (e.g., MyD88).[528, 551] In line, TREM2-DAP12 signaling was shown to inhibit pro-inflammatory cytokine production in response to different TLR and Fc receptor ligands (e.g., LPS, CpG, Zymosan) in murine macrophages.[530, 552] Correspondingly, TREM2-deficient macrophages showed increased pro-inflammatory cytokine production.[530, 552]

1.4.2 Functions of soluble TREM2

In contrast to CD33, TREM2 activity is not regulated by endocytosis, but by digestion of the receptor on the cellular membrane. In a first step, TREM2 is cleaved by members of the ADAM family between His157 and Ser158 and the ectodomain is shedded from the cell surface (**Figure 11D**).[529, 537, 553] Since the ligand binding domain of TREM2 remains intact, the produced fragment is also called soluble TREM2 (sTREM2). Despite ADAM10 being able to cleave TREM2,

shedding is mostly attributed to ADAM17, which is also responsible for producing mature TNF-α (see also section 1.1.6).[529, 553] After ectodomain shedding, the residual transmembrane-cytoplasmic fragment of TREM2 is further cleaved by γ-secretase producing a C-terminal fragment (CTF) that can be further digested inside the cell (**Figure 11D**).[553-555] Although no specific receptor could be determined yet, stimulation of microglia with sTREM2 was shown to improve survival and induce expression of cytokines like IL-1β, IL-6, IL-10, and TNF-α (**Figure 11D**).[529, 554] Whereas survival advantages and inhibition of apoptosis were mediated by AKT-Glycogen synthase kinase beta (GSK)-β-catenin signaling, increased production of cytokines was dependent on the NF-κB pathway.[554] Besides intrinsic signaling functions, sTREM2 might also act as competitive antagonist of membrane-bound TREM2 by capturing TREM2 ligands and reducing the activation of TREM2-DAP12.[529, 554, 556] Of note, levels of sTREM2 in the CSF were shown to increase with age and were also found to be higher in patients with (early-stage) AD.[556-559] Since TREM2 shedding is induced by activation, increased levels of sTREM2 might indicate a change in microglial activation during aging and in early AD.[559]

1.4.3 TREM2 in health and disease

Many neurodegenerative disorders (e.g., AD, Parkinson's disease (PD), Frontotemporal dementia (FTD), Huntington's disease, and Amyotrophic lateral sclerosis (ALS)) are characterized by CNS inflammation, which might be mediated by innate immune cells and might be the cause for neurotoxicity and -degeneration (**Figure 12**).[479, 480]

In the CNS, innate immunity is established by microglia, which can be abundantly found in the brain.[479, 559, 560] Microglia in the CNS express PRRs and their over-reaction to different host factors (e.g., Aβ plaques, huntingtin, S100A8/A9, and chromogranin A) might cause chronic inflammation and result in neurotoxicity, which is reminiscent of the response of intestinal macrophages towards microbiota (see also section 1.1.6, **Figure 12**).[479, 480, 561-563] In line, many neurodegenerative diseases are characterized by increased levels of pro-inflammatory cytokines (e.g., TNF-α, IL-1β, IL-18, S100A9) and inflammasome activity (i.e., mostly NLRP3 inflammasomes), which are also markers for IBD (see section 1.1.6).[480, 494] Similar to IBD, IL-12/IL-23 cytokines are also upregulated in AD and contribute to increased Aβ production.[480, 564] Accumulation of unfolded proteins and aggregation of Aβ is a hallmark of neurodegenerative diseases like AD (**Figure 12**).[479] Upon binding of these proteins to PRRs on the microglia surface,

the aggregates are endocytosed.[479, 565, 566] Defective clearance of these accumulated proteins by microglia is a likely pathomechanism common to different diseases and changes in microglial function due to senescence or during ageing probably contribute to phagocytosis defects (**Figure 12**).[479, 567] However, neurodegeneration might be also promoted by inflammatory cytokine release upon activation of microglia by accumulated proteins.[479] Therefore, regulation of microglial/macrophage responses is critical to maintain homeostasis in the intestine, CNS, and other organs.

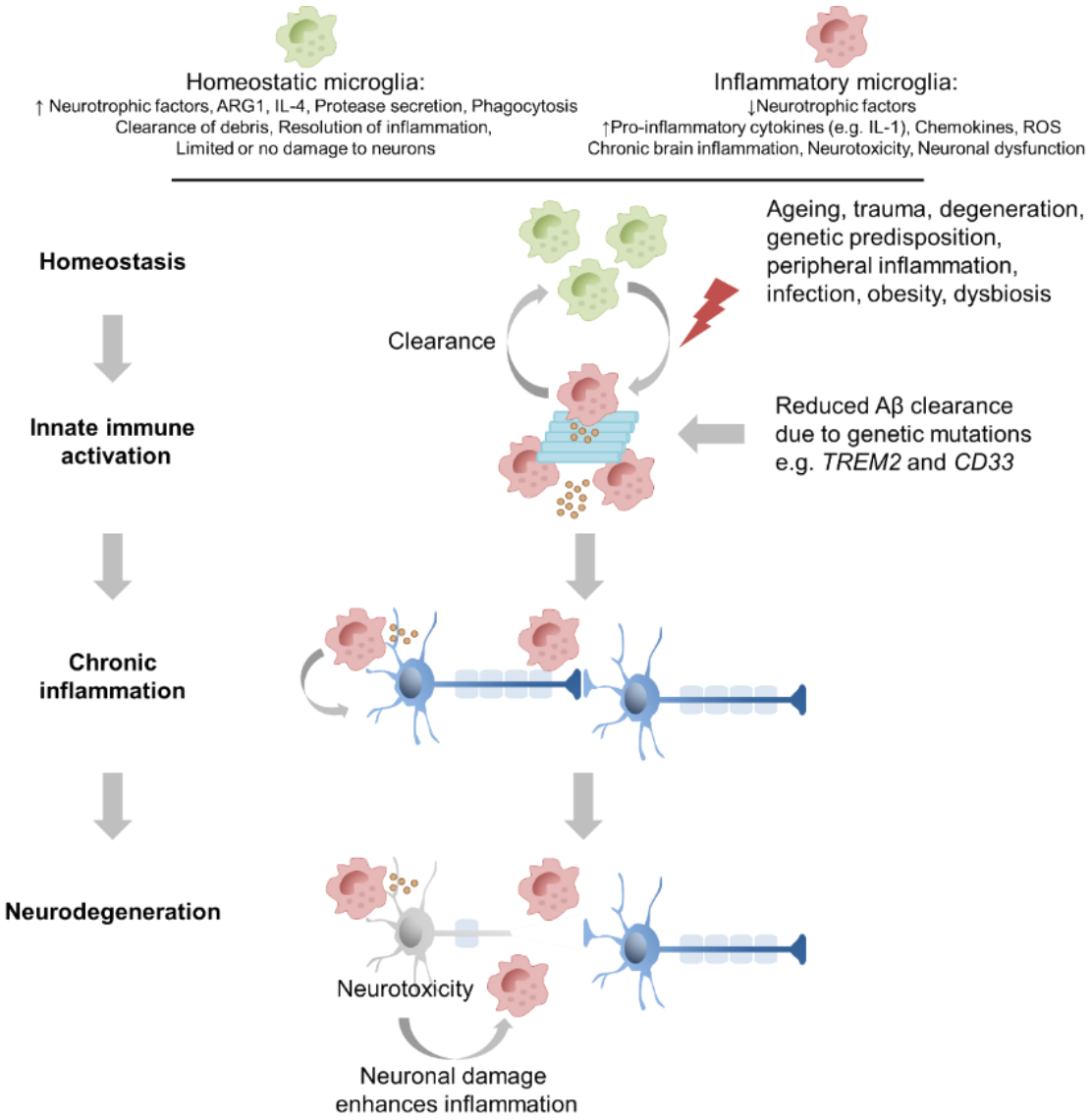

Figure 12: Microglial mechanisms in neurodegenerative disease.
Two different types (homeostatic vs. inflammatory microglia) of microglia control tissue homeostasis in the CNS. Different factors can cause dysregulation of balance between homeostatic and inflammatory microglia. Genetic susceptibility and other factors can result in reduced clearance of toxic protein aggregates, which can cause neurodegeneration. Figure adapted from [479, 480]

TREM2 mutations cause defects in macrophage-like cells leading to Nasu-Hakola-Disease

Autosomal recessive mutations in TREM2 and DAP12 have been shown to cause Nasu-Hakola-Disease (NHD), which is also known as polycystic lipomembranous osteodysplasia with sclerosing leukoencephalopathy (PLOSL).[529, 568, 569] NHD is a neurodegenerative disorder manifesting with dementia, osteoporosis, and bone cysts and usually is lethal before the age of 50.[529, 570, 571] However, symptoms of NHD usually manifest in much younger patients starting between 20-30 years of age.[568] The specific symptoms of NHD are most likely explained by the macrophage-like cell types affected by TREM2 deficiency, as TREM2 is expressed in microglia of the CNS and in osteoclasts found in bones.[529, 571, 572] Microglia in the CNS of NHD patients show an activated phenotype and probably contribute to neuronal loss in the white matter.[572, 573] Furthermore, TREM2 and DAP12 mutations were shown to affect differentiation and bone absorption of osteoclasts, which probably results in osteoporosis and bone cysts in NHD patients.[571]

DAP12 has also an important role in signaling of M-CSF via colony stimulating factor 1 receptor (CSF-1R).[550] In fact, mutant DAP12 impaired M-CSF-induced proliferation and survival of macrophages and also affected the capacity of myeloid progenitor cells to differentiate towards mature myeloid cells, which might explain defects in microglia and osteoclasts in NHD.[550] Some homozygous TREM2 mutations have been reported to cause “only” FTD, which manifests with an NHD-like phenotype without bone defects.[559, 574] However, why certain TREM2 mutations affect osteoclasts biology and some not remains unclear.

TREM2 function in AD

Several mutations in *TREM2* have been identified to cause NHD or FTD or increase the risk of neurodegenerative disorders like AD, PD, and ALS.[574-576] Although these variants probably result in loss-of-function of TREM2, they differ in their effect on the function of TREM2.[577] Whereas the FTD-causing mutations, p.T66M and p.Y38C, affect folding of TREM2 and prevent transport to the cell surface, the p.H157Y mutation causes increased shedding of TREM2, which results in reduced activity.[537, 574, 575] R47H, another mutation causing NHD and increasing the risk for AD, impairs lipid binding of TREM2 and thus also decreases activity of TREM2.[578, 579] Since p.T66M and p.Y38C prevent TREM2 to reach the cell surface, sTREM2 cannot be shedded from cells carrying these mutations. Consequently, patients homozygous for these mutations show no sTREM2 in the CSF.[575]

TREM2 defects have been shown to result in decreased phagocytic activity and chemotaxis as well as increased production of pro-inflammatory cytokines (e.g., IL-6, TNF-α, and CCL2) by microglia.[537, 549, 559, 575] From a pathomechanistic view, reduced phagocytosis and defective lipid sensing probably impacts the clearance of toxic Aβ plaques in the brain, which leads to toxic effects and neurodegeneration.[537, 549, 559, 575, 579] In line, TREM2-deficient microglia were also shown to display defective chemotaxis and reduced migratory capacity might exacerbate ineffective clearance of toxic misfolded proteins.[549] Furthermore, increased release of pro-inflammatory cytokines might cause enhanced tissue damage and neurotoxicity contributing to the pathogenesis of AD.[479, 559] In summary, TREM2 defects demonstrate the importance of microglia in the CNS and highlight that a chronic inflammatory environment can result in dramatic tissue damages and disease.

TREM2 in intestinal homeostasis

The role of TREM2 in regulation of phagocytosis and inflammatory cytokine secretion by microglia in the CNS is well studied. However, the role of TREM2 in other organs remains controversial. In the intestine, $TREM2^+$ cells are absent in healthy human mucosa, but can be detected in samples of IBD patients.[580, 581] In line, chemically-induced colitis induces up-regulation of TREM2 expression in the colon tissue of mice.[580, 581] In comparison to wild-type (WT) mice, *Trem2* KO mice showed reduced weight loss, disease activity, endoscopic, and histological scores upon induction of acute colitis.[580, 581] *Trem2*-deficient mice showed decreased mucosal expression of pro-inflammatory cytokines (e.g., IL-1β, TNF-α) and matrixmetalloproteinases in their mucosa in a colitis model.[580, 581] Surprisingly, $CD11c^+$ cells isolated from *Trem2* KO mice also showed reduced release of pro-inflammatory cytokines (e.g., IL-1β, IL-6, IL-12, and TNF-α) in response to different TLR ligands, which is in contrast to previous reports.[580, 581] Furthermore, $Trem2^{-/-}$ $CD11c^+$ were less effective in killing of *Salmonella typhimurium (S. typhimurium)* and induction of T cell proliferation.[580, 581]

Although presence of TREM2 might exacerbate acute colitis, TREM2 was also demonstrated to be important for efficient epithelial wound-healing in a murine colonic injury model.[582] In this model, loss of TREM2 was accompanied by increased production of T_H1 cytokines like TNF-α and IFN-γ, but reduced levels of T_H2 cytokines like IL-4 and IL-13, which is in line with inhibition of TLR signaling by TREM2 and indicates that TREM2 deficiency might also cause inflammatory

damages in the intestine.[582] Furthermore, Trem2 KO was shown to shift macrophage fates towards an pro-inflammatory M1 phenotype.[582]

In summary, TREM2 likely plays a critical role in regulation of innate immune responses in the intestine, but further research is needed to shed more light on its exact mechanisms.

CD33 and TREM2

As discussed above, CD33 and TREM2 are both associated with risk of AD and both modulate phagocytic as well as inflammatory activities of macrophages and microglia in the CNS.[492] However, AD risk polymorphisms lead to up-regulation of CD33 and loss of TREM2 function, which shows that CD33 and TREM2 have actually contrary effects on microglial function in the CNS.[492, 583] In fact, loss of CD33 improves cognition and reduces accumulation of Aβ plaques in AD mouse models, but loss of TREM2 causes accumulation of Aβ.[584] Of note, beneficial effects of reduced CD33 on Aβ accumulation and restoration of cognition were blocked by additional KO of Trem2 in AD mouse models, but effects of *Trem2* KO were unaffected by *Cd33* KO, which indicates that CD33 mediates its effect upstream of TREM2.[584] The opposing role of CD33 and TREM2 is also reflected on a transcriptional level, as *Cd33* KO resulted in increased expression of genes involved in phagocytosis and inflammation, but *Trem2* KO caused reduced expression.[584] Similarly, transcriptional changes caused by loss of *Cd33* in microglia are dependent on the presence of TREM2 confirming that CD33 acts upstream of TREM2 in microglia.[584] Of note, inflammasome-related genes were shown to be a central component of transcriptional changes induced by *Cd33/Trem2* KO in microglia identifying inflammasome dysregulation as an interesting candidate for CD33/TREM2-mediated pathogenesis.[584] However, CD33 and TREM2 do not affect each other's signaling directly, but share substantial overlapping signaling pathways, which are regulated by the opposing role of the kinase SYK and the phosphatases PTPN6/11 (**Figure 13**).[584]

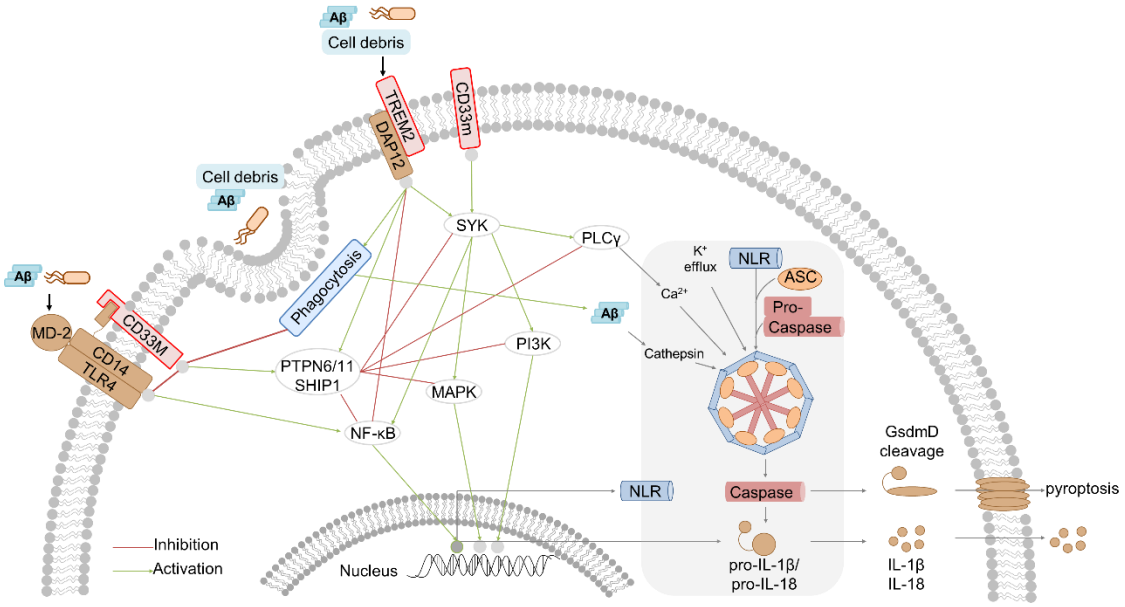

Figure 13: CD33 and TREM2 control overlapping signaling pathways.
CD33 and TREM2 can inhibit important signaling hubs via activation of phosphatases PTPN6 and PTPN11. TREM2 can activate similar pathways via SYK signaling. Most pathways converge at activation of inflammasomes and phagocytosis. Figure based on [479, 585]

Other TREM2 signaling components in intestinal disease

TREM2 signaling is controlled and mediated by the activity of SYK (**Figure 11C** and **Figure 13**). Recently, autosomal-dominant gain-of-function mutations in SYK have been identified to cause severe multi-organ inflammation with very-early onset IBD.[586] Inflammation affected skin, lung, joints, and liver of the patients, but also caused CNS inflammation in some of the patients.[586] The identified mutations caused increased activity of SYK which is in line with an autoinflammatory disease phenotype and indicates the importance of proper regulation of SYK signaling in immune and intestinal homeostasis.

Hematopoietic cell-specific PLCγ2 is another important downstream effector of TREM2 (**Figure 13**) and PLCγ2 KO mice exhibit immunodeficiency characterized by impaired B cell development and FcR signaling in mast cells, platelets, and macrophages.[577, 587] PLCγ2 has important functions in regulating human peripheral immunity, as loss-of-function and gain-of-function of PLCγ2 were shown to cause either detrimental immunodeficiency or autoinflammation and PLCγ2-associated antibody deficiency (APLAID), respectively.[577, 588, 589] Of note, APLAID frequently presents with enterocolitis indicating dysregulation of intestinal immunity.[588] Humans with dominant gain-of-function mutations in *PLCG2* present with absent (class-switched) B cells, hypogammaglobulinemia, early-onset skin inflammation, recurrent infections, and detrimental autoinflammation indicating that correct regulation of PLCγ2 signaling

is critical for the function of immune cells.[577, 588-590] Autoinflammatory diseases are caused by over-activation of innate immune cells (e.g., neutrophils and macrophages) and are mostly characterized by increased activity of inflammasomes and IL-1β production.[591] In line, *PLCG2* hypermorphic mutations also cause increased release of pro-inflammatory cytokines from macrophages and DCs.[592] Interestingly, hypermorphic mutations in *PLCG2* have been shown to also confer protection against AD connecting intestinal and brain inflammatory diseases.[577]

2. Objective

IBD is characterized by chronic intestinal inflammation and affects 6.8 million patients worldwide representing a global health burden.[6, 7] Life-threatening forms of IBD are seen in patients with VEO-IBD, which is defined by a disease onset before 6 years of age and can be caused by monogenic defects. VEO-IBD affects patients in important developmental phases, is accompanied by detrimental comorbidities, and is often refractory to therapy, which poses enormous risks for the patients and substantial challenges for treating physicians. Therefore, diagnosis of genetic causes and elucidation of underlying pathomechanisms is critical to provide rational arguments for treatment options. Furthermore, insights from studies on VEO-IBD patients can also help to understand pathomechanisms of common inflammatory diseases, which might allow definition of novel therapeutic avenues. Most monogenic defects in VEO-IBD cause dysregulation of intestinal immunity and many primary immunodeficiencies present with VEO-IBD indicating a central role of immune cells in the pathogenesis of IBD. Using a WES-based screen, we identified novel mutations in *IL2RG, CD33*, and *TREM2*, which are all known to control development and/or function of immune cells, as potential cause of VEO-IBD. The aim of this thesis was to elucidate how the identified mutations cause immune dysfunction and result in pathogenesis of IBD.

2.1 Specific aims: IL2RG

1. Identification of immune dysfunctions caused by a hypomorphic *IL2RG* mutation.
2. Elucidation of novel splicing mechanisms in *IL2RG* mRNA.
3. Evaluation of differential effects of the *IL2RG* defect on immune cell function.

2.2 Specific aims: CD33

1. Analysis of mechanisms controlling expression and function of CD33.
2. Deciphering the unexplored role of CD33 in hematopoiesis.
3. Elucidation of perturbed functional responses of CD33-deficient myeloid cells.

2.3 Specific aims: TREM2

1. Generation of model systems to study TREM2 deficiency.
2. Analysis of TREM2 functions in myelopoiesis.
3. Exploration of TREM2-dependent functional responses of macrophages.

3. Material and Methods

3.1 Materials

3.1.1 Antibodies and dyes

Antigen	Conjugate	Clone	Use	Order No.	Company
anti-goat IgG	HRP	-	WB	sc-2354	SCB
anti-goat IgG	HRP	-	WB	705-035-003	Dianova
anti-mouse	HRP	-	WB	554002	BD Biosciences
anti-mouse IgG	HRP	-	WB	405306	BioLegend
anti-rabbit IgG	AF488	-	FC	A11008	TFS
anti-rabbit IgG	AF633	-	FC	A21070	TFS
anti-rabbit IgG	HRP	-	WB	7074S	CST
anti-rabbit IgG	HRP	-	WB	W401B	Promega
β-Actin	HRP	C4	WB	sc-47778	SCB
Calnexin	-	Polyclonal	WB	SPA-860	Enzo
CASP1	-	Polyclonal	WB	BML-SA101-0100	Enzo
CASP1	-	EPR16883	WB	ab179515	Abcam
CCR4	PE-Cy7	L291H4	FC	359410	BioLegend
CCR6	BV786	11A9	FC	563704	BD Biosciences
CCR6	BV785	G034E3	FC	353422	BioLegend
CCR7	BV421	G043H7	FC	353208	BioLegend
CD3	APC-Fire750	SK7	FC	344840	BioLegend
CD3	BUV395	SK7	FC	564001	BD Biosciences
CD3	BUV496	UCHT-1	FC	612940	BD Biosciences
CD3	PacificBlue	SK7	FC	344824	BioLegend
CD3	-	OKT3	Stim.	16-0037-85	eBioscience
CD4	BV711	SK3	FC	563028	BD Biosciences
CD4	BUV395	RPA-T4	FC	564724	BD Biosciences
CD8	APCFire750	RPA-T8	FC	301066	BioLegend
CD8	BUV496	RPA-T8	FC	564804	BD Biosciences
CD8	BUV737	SK1	FC	612754	BD Biosciences
CD8	BUV737	SK1	FC	564629	BD Biosciences
CD8	PE-Cy5	RPA-T8	FC	561951	BD Biosciences
CD10	PE	HI10a	FC	555375	BD Biosciences
CD11c	BV421	B-ly6	FC	562561	BD Biosciences
CD11c	BV421	Bu15	FC	337226	BioLegend
CD11c	PE-Cy7	S-HCL-3	FC	371508	BioLegend
CD14	APC	M5E2	FC	301808	BioLegend

CD14	BB700	M5E2	FC	745790	BD Biosciences
CD14	BV650	M5E2	FC	301836	BioLegend
CD14	FITC	M5E2	FC	555397	BD Biosciences
CD16	APC	3G8	FC	561248	BD Biosciences
CD16	APC	3G8	FC	302012	BioLegend
CD19	BUV395	SJ25C1	FC	563549	BD Biosciences
CD19	PerCP-Cy5.5	HIB19	FC	302230	BioLegend
CD20	PE-Cy7	2H7	FC	560735	BD Biosciences
CD21	BUV737	B-Ly4	FC	612788	BD Biosciences
CD21	BUV737	B-Ly4	FC	564437	BD Biosciences
CD25	PE	M-A251	FC	555432	BD Biosciences
CD27	APC-R700	M-T271	FC	565116	BD Biosciences
CD27	BV785	O323	FC	302832	BioLegend
CD27	BV786	L128	FC	563327	BD Biosciences
CD28	BB700	L293	FC	745905	BD Biosciences
CD28	-	CD28.2	Stim.	302902	BioLegend
CD33	-	WM53	Stim.	MCA1271	BioRad
CD33	APC	WM53	FC	551378	BD Biosciences
CD33	PE	HIM3-4	FC	12-0339-41	eBioscience
CD33	PE-Cy7	P67.6	FC	333952	BD Biosciences
CD33	PE-Cy7	P67.6	FC	366618	BioLegend
CD34	BV421	561	FC	343610	BioLegend
CD38	APC	HB-7	FC	345807	BD Biosciences
CD38	APC	HB-7	FC	356606	BioLegend
CD38	BV650	HB-7	FC	356620	BioLegend
CD45	BV480	HI30	FC	566115	BD Biosciences
CD45	FITC	HI30	FC	304038	BioLegend
CD45	PE	HI30	FC	31255X	BD Biosciences
CD45RA	BUV737	HI100	FC	564442	BD Biosciences
CD45RA	BUV737	HI100	FC	612846	BD Biosciences
CD45RO	BB515	UCHL1	FC	564529	BD Biosciences
CD56	PE-CF594	NCAM16.2	FC	564849	BD Biosciences
CD57	BB515	NK-1	FC	565285	BD Biosciences
CD86	BV421	2331 (FUN1)	FC	562432	BD Biosciences
CD123	BV785	6H6	FC	306032	BioLegend
CD127	APC	A019D5	FC	351316	BioLegend
CD132	PE	AG184	FC	555900	BD Biosciences
CD163	PE	GHI/61	FC	333606	BioLegend
CD273	BV786	MIH18	FC	563843	BD Biosciences
CD274	APC	MIH1	FC	563741	BD Biosciences
CXCR3	PE-CF594	1C6	FC	562451	BD Biosciences

FVS780	-	-	FC	565388	BD Biosciences
IgD	BB515	IA6-2	FC	565243	BD Biosciences
IgG	-	G155-178	Stim.	553454	BD Biosciences
IgM	BV421	G20-127	FC	562618	BD Biosciences
IgM	BV421	UCH-B1	FC	747878	BD Biosciences
IL-1β	-	Polyclonal	WB	AF-201-NA	R&D
IL-2Rγ	-	Polyclonal	WB	PA5–26461	TFS
HLA-DR	BV711	G46-6	FC	563696	BD Biosciences
HLA-DR	BV711	L243	FC	307644	BioLegend
HLA-DR	PE-Cy7	G46-6	FC	560651	BD Biosciences
NLRP3	-	D2P5E	WB	13158S	CST
pSTAT3	AF488	4/P-STAT3	FC	557814	BD Biosciences
pSTAT3 (pY705)	-	D3A7	WB	9145S	CST
pSTAT5	PE-CF594	47/Stat5	FC	562501	BD Biosciences
pSTAT5 (pY694)	-	47/Stat5 (pY694)	WB	611965	BD Biosciences
pSTAT6 (pY641)	-	Polyclonal	FC	9361S	CST
S100A9	HRP	MRP 1H9	WB	sc-53187 HRP	SCB
STAT5	-	Polyclonal	WB	9363S	CST
STAT3	-	84/Stat3	WB	610190	BD Biosciences
TCR α-β	PE/Cy5	IP26	FC	306710	BioLegend
TCR γ-δ	PE	B1	FC	555717	BD Biosciences
TLR4	PE	TF901	FC	564215	BD Biosciences
TREM2	-	Polyclonal	WB	AF1828	R&D
TREM2	-	D8I4C	WB	91068	CST

Table 1: List of antibodies.
CST, Cell Signaling Technologies; SCB, Santa Cruz Biotechnologies; TFS, Thermo Fisher Scientific; FC, flow cytometry; Stim., Stimulation; WB, Western Blot.

3.1.2 Buffer recipes

Component	Manufacturer	Concentration	Mass/Volume
Tris base	Carl Roth	48 mM	5.82 g
Glycine	Carl Roth	39 mM	2.93 g
Methanol	Honeywell	20 % (v/v)	200 mL
dH_2O	-	-	to 1 L

Table 2: Formulation for Bjerrum Schafer-Nielsen buffer.

Component	Manufacturer	Volume
10X Cell lysis buffer	CST	100 µL
PIC	Sigma Aldrich	60 µL
PMSF	Alpha Diagnostics	10 µL
2 mM Na_3VO_4/dH_2O	Sigma Aldrich	830 µL

Table 3: Formulation for cell lysis buffer. CST, Cell Signaling Technologies.

Component	Manufacturer	Mass/Volume
Glycerol	Carl Roth	30 mL
Bromophenol blue	Carl Roth	10 mg
Adjust to pH 8.0		
dH_2O	-	to 100 mL

Table 4: Formulation for 6X DNA loading dye.

Component	Manufacturer	Mass/Volume
20 % SDS	Carl Roth	4 mL
Glycerol	Carl Roth	4 mL
1.0 M Tris HCl pH 6.8	Carl Roth	2 mL
Bromophenol blue	Carl Roth	5 mg

Table 5: Formulation for 6X Laemmli buffer.
Aliquots were stored at – 20 °C. Before usage, 4 % (v/v) β-mercaptoethanol (Sigma) was added freshly. SDS, Sodium dodecyl sulfate

Component	Manufacturer	Mass/Volume
LB-Medium (Luria/Miller)	Carl Roth	25 g
dH_2O	-	to 1 L

Table 6: Formulation for LB medium.

Component	Manufacturer	Mass/Volume
LB-Medium (Luria/Miller)	Carl Roth	25 g
Agar-agar Kobe 1	Carl Roth	15 g
dH_2O	-	to 1 L

Table 7: Formulation for LB plates.
Mixture was sterilized, cooled down under constant stirring, supplemented with antibiotics, and added to plates (10 mL per 10 cm petridish).

Component	Manufacturer	Mass/Volume
NaCl	Carl Roth	800 g
KCl	Carl Roth	20 g
Na_2HPO_4	Carl Roth	142 g
KH_2PO_4	Carl Roth	24.5 g
Adjust pH to 7.4		
dH_2O	-	to 1 L

Table 8: Formulation for phosphate-buffered saline (PBS).

Component	Manufacturer	Concentration
PBS	see **Table 8**	-
Tween 20	Applichem	0.05 % (v/v)

Table 9: Formulation for PBS-T washing buffer.

Component	Manufacturer	Concentration
Tris base	Carl Roth	25 mM
Glycine	Carl Roth	190 mM
SDS	Carl Roth	0.1 (v/v)
Adjust pH to 8.3		
dH_2O		

Table 10: Formulation for running buffer.

Component	Manufacturer	Concentration	Mass/Volume
Na_2HPO_4	Carl Roth	133 mM	13.49 g
KH_2PO_4	Carl Roth	133 mM	5.17 g
dH_2O			to 1 L

Table 11: Formulation for Sørenson buffer.

Component	Manufacturer	Concentration
Glycine	Carl Roth	200 mM
SDS	Carl Roth	1.0 (v/v)
Tween 20	Applichem	0.01 % (v/v)
Adjust pH to 2.2		
dH_2O		

Table 12: Formulation for stripping buffer.

Component	Manufacturer	Concentration
Tris base	Carl Roth	25 mM
Glycine	Carl Roth	190 mM
Ethanol or Methanol	VWR or Honeywell	10 % (v/v)
Adjust pH to 8.3		
dH_2O		

Table 13: Formulation for transfer buffer.

Component	Manufacturer	Mass/Volume
Tris base	Carl Roth	216 g
Boric acid	Carl Roth	110 g
0.5 M EDTA (pH 8.0)	Carl Roth	80 mL
dH_2O	-	to 2 L

Table 14: Formulation for Tris-boric acid-EDTA (TBE) buffer.

Component	Manufacturer	Concentration
Tris base	Carl Roth	10 mM
EDTA	Carl Roth	1 mM
Adjust pH to 8.0		
dH_2O	-	

Table 15: Formulation for Tris-EDTA (TE) buffer.

3.1.3 Chemicals

Product	Order Number	Company
Agar-Agar, Kobe I,	5210.2	Carl Roth
Agarose	A8963,0500	Applichem
Ammonium peroxodisulfate (APS)	A3678-25G	Sigma Aldrich
β-estradiol	E8875-1G	Sigma Aldrich
β-mercaptoethanol	M7522/M6250	Sigma Aldrich
Boric acid	6943.3	Carl Roth
Bromophenol blue	A512.1	Carl Roth
Dimethyl sulfoxide (DMSO)	D8418	Sigma Aldrich
Di-sodium hydrogen phosphate (Na_2HPO_4)	P030.2	Carl Roth
Deoxy nucleoside triphosphate (dNTP)	A9823,1000	Applichem
Doxycycline hyclate	D9891-5G	Sigma Aldrich
Ethanol	83813.440	VWR
Ethidium Bromide	A1152,0010	Applichem
Ethylenediaminetetraacetic acid (EDTA)	8043.2	Carl Roth
Giemsa's azur eosin methylene blue	1.09204.0500	Merck
Glycerol	3783.1	Carl Roth
Glycine	3908.3	Carl Roth

Hydrochloric acid	K025.1	Carl Roth
LB-Medium (Luria/Miller)	X968.4	Carl Roth
Lipopolysaccharide (LPS)	L2654	Sigma Aldrich
May-Grünwald's eosin-methylene blue	1.01424.0500	Merck
Methanol	32213-2.5L	Honeywell
Nigericin	N7143-5MG	Sigma Aldrich
Paraformaldehyde (PFA)	sc-281692	Santa Cruz
Phenylmethylsulfonylfluorid (PMSF)	PMSF16-S-50	Alpha Diagnostics
Phorbol 12-myristate 13-acetate (PMA)	ab120297	Abcam
Phosphoric acid (H_3PO_4)	6366.1	Carl Roth
Potassium chloride (KCl)	6781.1	Carl Roth
Potassium dihydrogen phosphate (KH_2PO_4)	P018.2	Carl Roth
Protease inhibitor cocktail (PIC)	P8340	Sigma Aldrich
Roti-Stock 20 % sodium dodecyl sulfate (SDS)	1057.1	Carl Roth
Rotiphorese 30 % Acrylamide	3029.1	Carl Roth
Sodium bicarbonate	S-5761	Sigma Aldrich
Sodium carbonate	1.06398	Merck
Sodium chloride (NaCl)	9265.2	Carl Roth
Sodium hydroxide	P031.2	Carl Roth
Sodium orthovanadate	S6508-10G	Sigma Aldrich
Tetramethylethylenediamine (TEMED)	2367.3	Carl Roth
Tris base	5429.2	Carl Roth
Tris HCl	9090.3	Carl Roth
Triton X-100	T8787	Sigma Aldrich
Tween 20	142312.1611	Applichem
Versene solution	15040066	TFS

Table 16: List of chemicals. TFS, Thermo Fisher Scientific.

3.1.4 Consumables

Product	Order Number	Company
100 mm dish	83.3902.300	Sarstedt
12-well plate	83.3921.300	Sarstedt
12x75 mm tubes with strainer cap	352235	Corning/Falcon
24-well plate	83.3922	Sarstedt
35 mm dish	27150	StemCell
48-well plate	83.3923	Sarstedt
5-alpha Competent E. coli	C2988J	NEB
6-well plate	83.3920	Sarstedt
60 mm Gridded Scoring Dish	100-0085	Stemcell
96-well flat bottom plate	83.3924	Sarstedt
96-well round bottom plate	83.3925.500	Sarstedt

Advanced DMEM/F12	12634-028	TFS
Ampicillin	A9518	Sigma Aldrich
Bambanker	BB01	Niippon Genetics
BlueRay Prestained Protein Marker	PS-103	Jena Bioscience
Bovine Serum Albumin (BSA)	A6588,0100	Applichem
Brilliant stain buffer	563794	BD Biosciences
Cell lysis buffer (10X)	9803S	CST
4-20 % Crit TGX Stain-Free Gel 26W	5678095	BioRad
Cytoslides	311-100	Tharmac
DMEM, high glucose, no glutamine	11960044	TFS
EasySep Human CD14 Positive Selection Kit II	17858	StemCell
Essential 6 medium	A1516401	TFS
Fetal bovine serum (FBS)	10270106	TFS
Ficoll-Paque	17-1440-03	GE Healthcare
Filter cards	305-200	Tharmac
Gentamycin	15750060	TFS
GlutaMax	35050-038	TFS
Growth Factor Reduced Basement Membrane Matrix (Matrigel)	356231	Corning
HEPES	15630056	TFS
IMDM	21980065	TFS
L-Glutamine	25030123	TFS
Lipofectamine2000	11668019	TFS
Lysing Solution 10X Concentrate	349202	BD Biosciences
MaxiSorp Clear Flat-Bottom Immuno Nonsterile 96-Well Plates	439454	TFS
MethoCult H4435 Enriched	H4435	StemCell
Milk powder	T145.3	Carl Roth
mTeSRplus	100-0276 (former: 05825)	StemCell
Nitrocellulose membrane	10600006	GE Healthcare
OptiMEM	11058021	TFS
Phosphate-buffered saline (PBS)	14190-169	TFS
Penicillin/Streptomycin	15140-122	TFS
Polyvinylidene fluoride (PVDF) membrane	10600023	GE Healthcare
Puromycin	A11138-03	TFS
Roti Nanoquant	K880.1	Carl Roth
RPMI 1640 Medium, GlutaMAX Supplement	61870010	TFS
Sodium pyruvate	11360088	TFS
StemPro-34 SFM Complete Medium	10639011	TFS
SuperSignal West Pico Plus Chemiluminescent Substrate	34577	TFS

SuperSignal West Dura Extended Duration Substrate	34076	TFS
Syringe filter (sterile, 0.22 µm)	SLGP033RS	Millipore/Merck
Syringe filter (sterile, 0.45 µm)	514-0063	VWR
T25 flask	83.3910.002	Sarstedt
T75 flask	83.3911.002	Sarstedt
T175 flask	83.3912.002	Sarstedt
TMB Solution (1X)	00-4201-56	TFS
TrypanBlue	15250-061	TFS
Whatman filter paper	WHA10426892	Sigma Aldrich
Wypall X60 sheets	8380	Kimberly Clark

Table 17: List of consumables. CST, Cell Signaling Technologies. TFS, Thermo Fisher Scientific.

3.1.5 Cytokines and Inhibitors

Product	Order Number	Company
Basic fibroblast growth factor (bFGF)	100-18B	Peprotech
bFGF	78003	StemCell
Bone morphogenetic protein (BMP) 4	120-05	Peprotech
BMP4	78211.1	StemCell
CHIR99021	361571	Millipore
CHIR99021	72054	StemCell
Cyclosporine A	30024-25MG	Sigma
Fms like tyrosine kinase 3 (FLT3) Ligand	300-19	Peprotech
Flt3/Flk-2 Ligand	78009.2	StemCell
Granulocyte colony stimulating factor (G-CSF)	300-23	Peprotech
G-CSF	78012	StemCell
GM-CSF	300-03	Peprotech
GM-CSF	78015.3	StemCell
IL-2	AF-200-02	PeproTech
IL-3	200-03	Peprotech
IL-3	78040	StemCell
IL-4	200-04	PeproTech
IL-10	200-10	Peprotech
IL-10	78024.1	StemCell
IL-7	AF-200-07	PeproTech
IL-15	200-15	PeproTech
IL-21	200-21	PeproTech
IFN-γ	300-02	Peprotech
IFN-γ	78020	StemCell
M-CSF	300-25	Peprotech
M-CSF	78057.2	StemCell

RiboLock RNase Inhibitor	EO0381	TFS
Rho kinase inhibitor (Y-27632)	Y-5301-10 mg	Biotrend
Rho kinase inhibitor (Y-27632)	72304	StemCell
S100A9	9254-S9-050	R&D
S100A9	A42590	Invitrogen
SB431542	S1067	Selleckchem
SB431542	72234	StemCell
Stem cell factor (SCF)	300-07	Peprotech
SCF	78062	StemCell
SCR7	74102	StemCell
TGF-β	100-21	Peprotech
TGF-β	78067	StemCell
Thrombopoietin (TPO)	300-18	Peprotech
TPO	78210.1	StemCell
Vascular endothelial growth factor (VEGF)	100-20	Peprotech
VEGF	78073.1	StemCell

Table 18: List of cytokines and inhibitors. TFS, Thermo Fisher Scientific.

3.1.6 Enzymes and accessories

Product	Order Number	Company
Accutase	SCR005	Merck Millipore
Collagenase Type IV	7909	StemCell
FastAP Thermosensitive Alkaline Phosphatase	EF0651	TFS
FastDigest BamHI	FD0054	TFS
FastDigest BpiI	FD1014	TFS
FastDigest EcoRI	FD0275	TFS
FastDigest HindIII	FD0504	TFS
FastDigest XhoI	FD0694	TFS
FAST SYBR Green	4385610	TFS
illustra ExoProStar	GEUS78211	Sigma Aldrich
Neuramidase from C. perfringens (Sialidase)	11585886001	Roche
OneTaq polymerase Mix	M0482L	NEB
PNGase F	P0704S	NEB
PowerUp SYBR Green	A25777	TFS
Protease	19155	Qiagen
Q5 High Fidelity Polymerase	M0491S	NEB
Q5 buffer	B9027S	NEB
T4 ligase	EL0011	TFS
T4 Polynucleotide Kinase	M0201S	NEB
Trypsin-EDTA	T3924-100ML	Sigma Aldrich

Table 19: List of enzymes and accessories. TFS, Thermo Fisher Scientifc.

3.1.7 Instrumentation

Name	Company	Usage
Amaxa Nucleofector II	Lonza	Electroporation
Axioplan 2 Imaging	Zeiss	Microscopy
Cellspin I	Tharmac	Centrifugation
ChemiDoc XRS+	BioRad	Detection of western blots
CoolCell Freezer Container	Corning/Omnilab	Cell cryopreservation
Criterion™ Vertical Electrophoresis Cell	BioRad	SDS-PAGE
FACSARIA III	BD	FACS
GelDoc XR+	BioRad	Detection of agarose gels
Gel tray	BioRad	Casting of agarose gels
Gel caster	BioRad	Casting of agarose gels
LSRFortessa	BD	Flow cytometry
Mini-PROTEAN® Tetra electrophoresis system	BioRad	SDS-PAGE, Wet blotting
Mini-Sub Cell GT Horizontal Electrophoresis System	BioRad	Agarose gel electrophoresis
NanoDrop 2000	TFS	Analysis of DNA/RNA
NextSeq500/550	Illumina	NGS (WES)
StepOnePlus	Applied Biosystems	qPCR
Synergy H1	BioTek	Microplate reader
Trans-Blot® Turbo™ Transfer System	BioRad	Semi-dry blotting

Table 20: List of instrumentation. TFS, Thermo Fisher Scientific.

3.1.8 Kits

Product	Order Number	Company
CloneJET PCR Cloning Kit	K1231	TFS
CytoTox 96 Non-Radioactive Cytotoxicity Assay	G1780	Promega
Gateway LR Clonase II Enzyme Kit	11791020	TFS
High-Capacity cDNA Reverse Transcription Kit	4368813	TFS
Human IL-1 beta/IL-1F2 DuoSet ELISA Kit	DY201	R&D
Human Stem Cell Nucleofector Kit 2	VPH-5022	Lonza
Human TNF ELISA Set	555212	BD Biosciences
PlasmoTest™ - Mycoplasma Detection Kit	rep-pt1	InvivoGen
PureLink RNA Mini Kit	12183018A	TFS
QIAamp DNA blood mini kit	51106	Qiagen
QIAquick Gel Extraction Kit	28706	Qiagen
Qiagen Plasmid *Plus* Maxi Kit	12965	Qiagen
Rneasy Plus Mini Kit	74136	Qiagen
Zymoclean Gel DNA Recovery Kit	D4002	Zymo
Zyppy Plasmid Miniprep Kit	D4020	Zymo

Table 21: List of kits. TFS, Thermo Fisher Scientific.

3.1.9 Plasmids

Name	Usage	Order No.	Company
pSpCas9(BB)-2A-GFP	Delivery of gRNA-Cas9 particles	48138	Addgene
pSpCas9(BB)-2A-RFP	Delivery of gRNA-Cas9 particles	Cloned in the lab	
pENTR1A (w48-1)	Entry vector for gateway cloning	17398	Addgene
PB-TAC-ERP2	Destination vector for gateway cloning with Doxycycline-inducible promoter, mCherry reporter, and puromycin selection cassette	80478	Addgene
pcDNA3.1(+)	Mammalian expression vector	V79020	TFS
pJet1.2	Subcloning vector		TFS

Table 22: List of plasmids. TFS, Thermo Fisher Scientific.

3.1.10 Primer

Primer Name	Target	5’ - 3’ sequence	Usage
DI49_Il2rgexon1fw	*IL2RG*	TACCACCTTACAGCAGCACC	gDNA PCR
DI50_Il2rgexon1rev	*IL2RG*	CCCTTCCCACTCCACTTTTCA	gDNA PCR
DI61_GAPDH_fw	*GAPDH*	TGCTGGGGAGTCCCTGCCACA	qPCR
DI62_GAPDH_rev	*GAPDH*	GGTACATGACAAGGTGCGGCTC	qPCR
DI131_CD33_E2_fw	*CD33*	GAAGCTGCTTCCTCAGACATGC	gDNA PCR
DI132_CD33_E2_rev	*CD33*	CCTAAACCCCTCCCAGTACCAG	gDNA PCR
DI133_CD33_E5_fw	*CD33*	TCACCCCTCTCTACATGCTGGA	gDNA PCR

DI134_CD33_E5_rev	*CD33*	CTACACCAGGTCCATCCTCTTCAC	gDNA PCR
DI163_IL2RG_E1_fw	*IL2RG*	GTTCCTGACACAGACAGACTACACC	qPCR
DI164_IL2RG_E1_rev	*IL2RG*	GGGCAGCTGCAGGAATAAGAGG	qPCR
DI165_IL2RG_E2_fw	*IL2RG*	CCTGACCACTATGCCCACTGACT	qPCR
DI166_IL2RG_E2_rev	*IL2RG*	ATGCAGAGTGAGGTTGGTAGGCT	qPCR
DI167_IL2RG_E5-8_fw	*IL2RG*	CCCAATCCACTGGGGGAGCAAT	qPCR
DI168_IL2RG_E5-8_rev	*IL2RG*	CACCACTCCAGGCCGAAAAGTT	qPCR
DI169_IL2RG_E1-3_fw	*IL2RG*	GAGCAAGCGCCATGTTGAAGC	cDNA PCR
DI170_IL2RG_E1-3_rev1	*IL2RG*	ACCCCAGGGGATCACCAGATT	cDNA PCR
DI171_IL2RG_E1-3_rev2	*IL2RG*	AGATAGTGGCTGCACTTCTGGAC	cDNA PCR
DI180_IL2RG_alt_rev	*IL2RG*	CCCTCCAGTCCCAGATTTCCCA	qPCR
DI181_IL2RG_alt_fw	*IL2RG*	CTGGTGGGAAATCTGGGACTGGA	qPCR
DI210_CD33_qPCR_fw	*CD33M+m*	CCAGCTCAACGTCACCTATGTTCCA	qPCR
DI211_CD33_qPCR_rev	*CD33M+m*	TGAAGAAGATGAGGCAGAGACAAAGAGC	qPCR
DI280_CD33_alt_qPCR_fw	*CD33M*	CAGGAGGAGACTCAGGGCAGATTC	qPCR
DI281_CD33_alt_qPCR_rev	*CD33M*	GGGTTCTAGAGTGCCAGGGATGAG	qPCR
DI284_CD33_T2_qPCR_fw2	*CD33m*	CCCTGCTGTGGGCAGACTTGA	qPCR
DI285_CD33_T2_qPCR_rev2	*CD33m*	GGCAGCTGACAACCAGGAGAAGA	qPCR
DI348_PB_fw	PB	CCATAGAAGACACCGGGACCGAT	Sequencing
DI349_PB_rev	PB	TTCGAGGCCGCGTTTTAGC	Sequencing
DI355_CD33splicereporter_Mut1_fw	*CD33*	TCAGGTGAGGCACAGGCTTCAGAAGTGG	SDM
DI356_CD33splicereporter_Mut1_rev	*CD33*	TGCCTCACCTGACACATGCACAGAGAGC	SDM
DI357_CD33splicereporter_Mut2_fw	*CD33*	TTTCTGCAGGGAAACAAGAGACCAGAGCA	SDM
DI358_CD33splicereporter_Mut2_rev	*CD33*	CCCTGCAGAAAAAAAGATTTGGGGTGAATTC	SDM
DI359_CD33splice_SDM_fw	*CD33*	GATCTTCCGGATGGCTCGAGTTTT	SDM
DI360_CD33splice_SDM_rev	*CD33*	TCCATGGCAGCTGAGAATATTGTAGG	SDM
DI363_CD33_E3_fw	*CD33*	GGGGTAAAGCCTGTCGTGCTTAG	gDNA PCR
DI364_CD33_E3_rev	*CD33*	ACCTGAGCCATCTCCTGGAAAGATAC	gDNA PCR
DI432_CD33_E6-7_q_fw2	*CD33*	GGAATGACACCCACCCTACCACA	qPCR
DI433_CD33_E6-7_q_rev2	*CD33*	TTTCAGTGGGGCCATGTAACTTGGA	qPCR
DI448_CD33_E1-2_fw	*CD33*	TTCCTCAGACATGCCGCTGCT	qPCR
DI449_CD33_E1-2_rev	*CD33*	ACCGTCACTGACTCCTGCACTT	qPCR
DI450_CD33_E2_fw	*CD33*	GCTGCAAGTGCAGGAGTCAGTG	qPCR
DI451_CD33_E2_fw	*CD33*	GAACTGGGGAGTTCTTGTCGTAGTAGG	qPCR
DI466_TREM2_E3_fw	*TREM2*	ATAAGTGGGGAAACTGAGGCTTATGG	gDNA PCR
DI467_TREM2_E3_rev	*TREM2*	GGGAGCTGATATTCAGGAGTCGTAG	gDNA PCR
DI468_CD33_E4skip_fw1	*CD33*	AGCTCAACGTCACCTGGAAACAAGA	qPCR
p-2019-071	*TREM2*	ATAAAGGTTCTCCCGCCAAGGTT	gDNA PCR
p-2019-072	*TREM2*	AGCTGGTGGAGGGGTGTTTAC	gDNA PCR
pENTattL2rev	attL2	ACATCAGAGATTTTGAGACACGGGC	Sequencing
pJet1.2 Seq fw	pJet1.2	CGACTCACTATAGGGAGAGCGGC	Sequencing

pJet1.2 Seq rev	pJet1.2	AAGAACATCGATTTTCCATGGCAG	Sequencing
pLKO1	pLKO1	GACTATCATATGCTTACCGT	Sequencing
T7	T7	TAATACGACTCACTATAGGG	Sequencing
U6	U6	GAGGGCCTATTTCCCATGATTCC	Sequencing

Table 23: List of primer. SDM, site-directed mutagenesis.

3.1.11 Software

Name	Company	Version	Usage
FACSDiva	BD Biosciences	8.0.1	Acquisition of flow cytometry data
FlowJo	FlowJo	10.2	Analysis of flow cytometry data
Gen5	BioTek	1.11.5	Analysis of microplate reader data
ImageLab	BioRad	6.0.1	Acquisition and analysis of agarose gel electrophoresis and western blot data
NanoDrop 2000	TFS	1.6.198	Analysis of DNA/RNA purity
NovaFold	DNASTAR	15	*De novo* prediction of protein structures
Prism	GraphPad	8.4.0	Creation of graphs and statistical analysis
SeqMan Pro	DNASTAR	15 and 17.2.0	Analysis of DNA sequencing data
StepOnePlus	Applied Biosystems	2.3	Analysis of qRT-PCR data
Protean 3D	DNASTAR	15	Alignment and analysis of protein structures
PyMol	Schrödinger	2.4.0	Alignment and analysis of protein structures
Visicam Image Analyser	BEL Engineering	7.1.1.7	Generation and analysis of microscopy pictures

Table 24: List of software. TFS, Thermo Fisher Scientific.

3.2 Methods

3.2.1 Immunophenotyping of human blood cells

Immunophenotyping was performed by the flow cytometry core facility at the Comprehensive Childhood Research Center at the Dr. von Hauner's Childrens Hospital (CCRC Hauner). Human peripheral blood was stained with three different antibody panels (T cells, B cells, Myeloid cells) analogous to section 3.2.10. For each panel, 150 µL peripheral blood was used. Antibody cocktails were prepared in 50 µL brilliant stain buffer (BD Biosciences) and added to the peripheral blood. For single stain controls, 200 µL peripheral blood was mixed with 1 µL of a single antibody conjugated to the same fluorochrome. For staining, mixture was incubated at room temperature

for 15 minutes. Cells were resuspended in 1 mL of a 1X dilution of Lysing Solution 10X Concentrate (BD Biosciences) to lyse erythrocytes and fix immune cells in parallel. After incubation at room temperature for 5 minutes, fixed cells were pelleted at 200 xg for 5 minutes at room temperature and supernatant was removed by aspiration. Cells were washed in 10 mL PBS (Thermo Fisher Scientific (TFS)) and pelleted as before. Cells were resuspended in 200 µL PBS and measured using a LSRFortessa flow cytometer (BD Biosciences). Data were acquired using FACSDiva™ software (BD Biosciences) and analyzed using FlowJo software (TreeStar).

3.2.2 DNA isolation and sequencing

Genomic DNA was isolated from peripheral blood samples in the sequencing facility at CCRC Hauner using QIAamp DNA blood mini kit (Qiagen) according to manufacturer's instructions (see also [255]). Rare sequence variants were identified using next generation sequencing on a NextSeq500 or NextSeq550 machine (Illumina) in the sequencing facility at CCRC Hauner as published before.[226, 255] All identified variants were confirmed by Sanger sequencing and segregation of variants with disease phenotype was analyzed in all available family members. In detail, a polymerase chain reaction (PCR) was prepared according to **Table 25** and was performed as summarized in **Table 26**. Amplified fragments were purified as described in section 3.2.3 and were sent for sequencing at Eurofins Genomics (Ebersberg, Germany) or GENEWIZ (Leipzig, Germany).

Component	Company	Volume [µL]	Mass [ng]
OneTaq 2x Master Mix	NEB	12.5	-
Primer fw		1.25	-
Primer rev		1.25	-
gDNA		-	20-100
DMSO	Sigma	1	-
Nuclease-free H2O		ad 25	-

Table 25: PCR mixture for Sanger sequencing.

Temperature [°C]	Duration	Cycles
Lid at 110	-	-
94	4'	1
94	30''	
56	30''	40
68	1'	
68	10'	1
4	∞	1

Table 26: PCR program for Sanger sequencing.

3.2.3 Enzymatic and electrophoretic purification of DNA

To purify DNA generated using PCR for downstream sequencing applications, enzymatic digestion of primers was performed. In brief, 1 µL illustra ExoProStar (Sigma Aldrich) was added after PCR and mixture was incubated at 37 °C for 18 minutes and at 80 °C for 18 minutes.

For other applications and in case enzymatic digestion cannot be used (e.g., multiple PCR products), DNA was purified using agarose gel electrophoresis. In detail, agarose (Applichem) was mixed with Tris-Borate-EDTA (TBE) buffer (homemade, **Table 14**) in appropriate concentrations for the size of the targeted DNA fragment (e.g., higher agarose concentration for smaller DNA fragments. Standard concentration: 1 %).

The suspension was heated in a microwave until agarose (Applichem) was completely dissolved and the solution was poured into a gel tray (BioRad) placed into a gel caster (BioRad). Ethidium bromide (Applichem) was added to a final concentration of 0.028 % (v/v). After the gel was polymerized, gel was submerged in TBE buffer (homemade, **Table 14**) in a Mini-Sub Cell GT Horizontal Electrophoresis System (BioRad). Samples were mixed with DNA loading buffer (homemade) and loaded onto the gel. DNA fragments were separated based on their size at 120 V for 30 – 60 minutes by electrophoresis and purified using QIAquick gel extraction kit (Qiagen) or Zymoclean Gel DNA recovery kit (Zymo) according to manufacturer's instructions.

3.2.4 Isolation of PBMCs and granulocytes from human blood

Human blood was acquired from patients, family members, and healthy donors to sodium heparin or K_3EDTA tubes by venipuncture. Whole blood was diluted with PBS (TFS) to 35 mL and carefully loaded onto 15 mL Ficoll-Paque (GE Healthcare) solution. Samples were centrifuged at 558 xg

(1600 rpm) for 25 minutes with acceleration set to 2 and deceleration set to 0 to separate plasma, peripheral blood mononuclear cells (PBMCs), and erythrocyte/granulocyte fractions.

The PBMC-containing fraction was transferred to a fresh tube and washed two times with 50 mL PBS (TFS). PBMCs were pelleted at 300 xg and 4 °C for 5 minutes and resuspended in medium for functional assays. Live cells were counted using a Neubauer hemocytometer and Trypan blue (TFS) exclusion staining.

The remaining supernatant of the Ficoll-Paque (GE Healthcare) gradient was removed by aspiration. To remove contaminating erythrocytes, the granulocyte-containing pellet was resuspended in 12 mL dH_2O and incubated for 3 minutes at room temperature. To stop the lysis reaction, 4 mL 0.6 M KCl (Carl Roth) was added. Granulocytes were pelleted at 300 xg for 5 minutes at room temperature and resuspended in medium for functional assays. Live cells were counted using a Neubauer hemocytometer and Trypan blue (TFS) exclusion staining

3.2.5 Generation of EBV-LCLs

To generate Epstein-Barr virus (EBV) supernatant, B95-8 cells (purchased from the German Collection of Microorganisms and Cell Cultures GmbH (DSMZ)) were cultured in complete RPMI (**Table 40**) at 37 °C and 5 % CO_2 in a humidified incubator for 3 days. Cell suspension was harvested and cells were removed by centrifugation for 10 minutes at 300 xg and 4 °C. EBV-containing supernatant was filtered (0.45 µm, VWR) and stored at - 80 °C until usage.

To generate EBV-transformed lymphoblastoid cell lines (EBV-LCLs) from peripheral blood of patients and relatives, 4.0 - 8.0 · 10^6 PBMCs (see section 3.2.4 for isolation) were resuspended in 1.25 mL complete RPMI (**Table 40**) and 1.25 mL EBV supernatant was added. The cell-virus suspension was incubated at 37 °C and 5 % CO_2 in a humidified incubator for 24 h. To remove T cells, 2.5 mL complete RPMI (**Table 40**) and 5 µL of cyclosporine A (0.01 % in the final volume, in this case 5 µL to 5 mL, Sigma) was added. Cell suspension was further incubated at 37 °C and 5 % CO_2 in a humidified incubator for 3 weeks and each week 5 mL complete RPMI was added. Increased cell proliferation and formation of macroscopic clumps indicated successful generation of EBV-LCL.

3.2.6 Cell culture

Adherent cells (HEK293T, purchased from DSMZ) were cultured in sterile cell cultureware (Sarstedt) with complete DMEM medium (**Table 27**) at 37 °C and 5 % CO_2 in a humidified incubator.

Reagent	Manufacturer	Concentration
DMEM, high glucose	TFS	
FBS	TFS	10 %
L-Glutamine (200 mM)	TFS	2 mM
Penicillin-Streptomycin	TFS	1 %
HEPES (1M)	TFS	10 mM
Sodium pyruvate (100 mM)	TFS	1 mM

Table 27: Formulation of complete DMEM. TFS, Thermo Fisher Scientifc

Cells were routinely passaged when reaching 80 % confluency. To harvest adherent cells, medium was removed, and cells were washed once with PBS (TFS). Cells were detached using Trypsin-EDTA (Sigma Aldrich) solution at 37 °C for 5 minutes and the live cell count was determined using a hemocytometer combined with Trypan blue (TFS) exclusion. Cells were pelleted at 300 xg for 5 minutes at 4 °C and supernatant was removed. Cells were re-seeded to cultureware in fresh medium.

Suspension cells (EBV-LCL, section 3.2.5), PBMCs, and granulocytes were cultured in sterile cell cultureware (Sarstedt) with complete RPMI medium (**Table 40**) at 37 °C and 5 % CO_2 in a humidified incubator. To passage suspension cells, cells were harvested, pelleted at 300 xg and 4 °C for 5 minutes and resuspended in fresh medium. Live cell count was determined using a hemocytometer and Trypan blue exclusion. Cells were reseeded to cultureware in fresh medium.

For cryopreservation, cells were pelleted at 300 xg, 4 °C for 5 minutes, resuspended in 10 % DMSO/FBS (Sigma/TFS), and transferred to cryovials. Cell suspension was frozen at - 80 °C using a CoolCell freezing module (Corning/Omnilab) ensuring a constant temperature reduction of - 1 °C/minute. For longterm storage, frozen cells were transferred to liquid nitrogen.

For thawing of cryopreserved cell lines, frozen cells were thawed at 37 °C in a waterbath, mixed with complete medium, and pelleted at 300 xg, 4 °C for 5 minutes. Cells were resuspended in fresh medium and transferred to cell cultureware.

3.2.7 mRNA expression analysis

Total mRNA was isolated from cell lysates using RNeasy Plus Mini Kit (QIAGEN) or PureLink RNA Mini Kit (TFS) according to manufacturer's instructions. RNA concentration was measured using NanoDrop2000 (TFS). Reverse transcription of mRNA to cDNA was performed using High-Capacity cDNA Reverse Transcription Kit (TFS) following manufacturer's instructions. The reverse transcription mix was prepared according to **Table 28** and reaction was performed as in **Table 29**.

Component	Manufacturer	Volume (1X) [µL]
10x RT buffer	TFS	2
25x dNTPs	TFS	0.8
10x Random primers	TFS	2
RiboLock	TFS	1
Reverse Transcriptase	TFS	1
RNA (up to 2 µg)	TFS	x
Nuclease-free water	-	ad 20

Table 28: Reaction mixture for reverse transcription. TFS, Thermo Fisher Scientific

Temperature [°C]	Time [min]
Lid at 110	indefinite
25	10
37	120
85	5
4	indefinite

Table 29: Program for reverse transcription reaction.

Generated cDNA was either analyzed by quantitative real time PCR (qRT-PCR) or by PCR in combination with agarose electrophoresis and Sanger sequencing. For qRT-PCR, the reaction mix was prepared as in **Table 30** (FAST SYBR Green Master Mix or PowerUp SYBR Green Master Mix, both TFS) and was performed on the StepOnePlus Real-Time PCR System (Applied Biosystems) as in **Table 31**. qRT-PCR data were analyzed using StepOnePlus Software (Applied Biosystems) and fold changes were calculated using the $\Delta\Delta C_T$ method.

Component	Manufacturer	Volume [µL]	Mass [ng]
SYBR Green	TFS	3.5	-
Primer fw	-	0.5	-
Primer rev	-	0.5	-
cDNA	-	-	5-20
Nuclease-free water	-	ad 10	-

Table 30: Reaction mixture for qRT-PCR. TFS, Thermo Fisher Scientific

Temperature [°C]	Time [s]	Cycles
Lid at 110	-	-
50	120	1
95	120	1
95	3	40
60	30	
95	15	1
60	60	1
0.3 increments to 95 °C for melting curve		
95	15	1

Table 31: Program for qRT-PCR.

For cDNA sequencing, PCR was performed as described in section 3.2.2. DNA products were purified using agarose electrophoresis (see section 3.2.3) and sequenced at Eurofins Genomics (Ebersberg, Germany) or GENEWIZ (Leipzig, Germany).

3.2.8 Sodium dodecyl sulfate polyacrylamide gel electrophoresis

For generation of cell lysates, cells were resuspended in cell lysis buffer (Cell signaling technologies) containing protease inhibitor cocktail, 1 % PMSF (Alpha Diagnostics), and 2 mM sodium orthovanadate (Sigma Aldrich) and lysed on ice (**Table 3**). All buffers and tubes were pre-chilled on ice to avoid degradation of proteins or loss of phosphorylation. Remaining cell debris was pelleted at 21000 xg and 4 °C for 15 minutes and supernatant was transferred to a fresh, pre-chilled tube. Protein concentration was determined using Roti Nanoquant (Carl Roth) according to manufacturer's instructions. Absorption at 450 and 590 nm was determined using the Synergy H1 Hybrid Multi-Mode Microplate Reader (BioTek) and the Gen5 software (BioTek). In some experiments cell lysates were treated with PNGase F (NEB) for 2 h at 37 °C to deglycosylate proteins according to manufacturer's instructions. 6x Laemmli buffer (homemade,

see **Table 5**) containing β-mercaptoethanol (Sigma Aldrich) was added to the cell lysates and lysates were incubated at 96 °C for 5 minutes. For the Mini-PROTEAN Tetra Vertical Electrophoresis Cell (BioRad) system, polyacrylamide gels with different percentages depending on the size of proteins to be analyzed were prepared according to **Table 32** and **Table 33**. For the Criterion™ Vertical Electrophoresis Cell, 26 well precast gels were bought from BioRad.

Component	Manufacturer	Volume [µL]
1.5 M Tris HCl (pH 8.8)	Carl Roth	2900
10 % SDS	Carl Roth	77.5
Rotiphorese (Acrylamide)	Carl Roth	x
20 % APS	Sigma Aldrich	37.6
TEMED	Carl Roth	5.75
H_2O		5720 - x

Table 32: Formulation of acrylamide separation gels for SDS-PAGE.

Component	Manufacturer	Volume [µL]
0.5 M Tris HCl (pH 6.8)	Carl Roth	360
10 % SDS	Carl Roth	28.75
Rotiphorese (Acrylamide)	Carl Roth	487.5
20 % APS	Sigma Aldrich	18.8
TEMED	Carl Roth	2.87
H_2O		1950

Table 33: Formulation of stacking gels for SDS-PAGE.

Gels were placed into the cell and the chamber was filled with running buffer (**Table 10**). Samples and BlueRay prestained protein marker (JenaBioscience) were loaded on gels. To focus proteins, SDS-PAGE was performed with 80 V until proteins reached the separation gel. Proteins were then separated at 120 V based on their molecular weight.

3.2.9 Western Blot

To detect specific proteins, proteins were transferred from SDS-PAGE gels (see section 3.2.8) to polyvinylidene fluoride (PVDF, GE Healthcare) or nitrocellulose (NC, GE Healthcare) membranes by western blot. PVDF and NC membranes were activated for 1 minute in ethanol or water, respectively. All components were equilibrated in buffer before western blotting.

For wet blotting, one foam pad, three Whatman® filter papers, one SDS-PAGE gel, one blotting membrane, another three Whatman® filter papers, and another foam pad were assembled in transfer buffer (**Table 13**) and placed into a Mini Gel Holder Cassette (BioRad). The loaded cassette and a cooling unit was mounted in a Mini Trans-Blot® cell (Mini-PROTEAN® Tetra electrophoresis system, BioRad). Protein transfer was performed at 100 V for 60 minutes on ice.

For semi-dry blotting, six Wypall X60 sheets (Kimberly Clark), one blotting membrane, one SDS-PAGE gel, and another six Wypall X60 sheets (Kimberly Clark) were assembled in Bjerrum Schafer-Nielsen buffer (**Table 2**) and placed into a Trans-Blot Turbo Cassette (BioRad).

Excess buffer was removed from the loaded cassette and the cassette was placed into the Trans-Blot® Turbo™ Transfer System (BioRad). Protein transfer was performed with the following program: 25 Limit V, 2.5 Const A, 12 minutes.

After transfer, membrane was blocked in 5 % milk powder/PBS (Carl Roth/TFS) or 5 % BSA/PBS (Applichem/TFS, for detection of phosphorylated proteins) for 1 h at room temperature under constant shaking. Primary antibodies were incubated over-night at 4 °C in blocking buffer and horseradish peroxidase (HRP)-coupled secondary antibodies were incubated for 1 h at room temperature under constant shaking. Excess antibody was removed by washing membranes three times for 10 minutes in PBS-T (**Table 9**). In between stainings with different antibodies, remaining antibodies were removed by incubating the membrane for 10 minutes in stripping buffer (**Table 12**) under constant shaking. Chemiluminescence was induced by SuperSignal West Pico Plus Chemiluminescent Substrate (TFS) or SuperSignal West Dura Extended Duration Substrate (TFS) and measured using the ChemiDoc XRS+ System (Bio-Rad).

3.2.10 Flow cytometry

For detection of proteins on the cell surface of living or fixed cells, flow cytometry was performed. Adherent cells (iPSC-derived macrophages, HEK293T) were enzymatically detached as described above. Antibody cocktail for staining was usually prepared in 2 % FBS/PBS (TFS/homemade). If more than one antibody coupled to a brilliant violet dye was used, the antibody cocktail was prepared in a 1:1 mixture of 2 % FBS/PBS (TFS/homemade) and brilliant stain buffer (BD Biosciences). Cells were resuspended in antibody cocktail and incubated at 4 °C for 30 minutes or at room temperature for 20 minutes. Excess antibody was removed by washing

in PBS (homemade) and cells were resuspended in 2 % FBS/PBS (TFS/homemade). Fluorescent signals were detected using an LSRFortessa flow cytometer (BD Biosciences) and the FACSDiva software (BD Biosciences). Data were analyzed using FlowJo Software (TreeStar).

3.2.11 Phospho flow

For quantification of phosphorylation levels of distinct signaling molecules, phospho flow was performed. PBMCs from patients, family members, and healthy donors were isolated as described in section 3.2.4. Procedure was performed as published in [255]. In brief, $1 \cdot 10^6$ PBMCs were serum starved in plain RPMI (TFS) for 15 minutes on ice and then treated with IL-2 (100 ng mL^{-1}), IL-4 (100 ng mL^{-1}), IL-7 (100 ng mL^{-1}), IL-15 (10 ng mL^{-1}), or IL-21 (50 ng mL^{-1}) for 0, 5, 10, or 30 minutes at 37 °C (all cytokines from Peprotech).[255] To allow staining of intracellular signaling molecules, fixation was performed with 4 % PFA/PBS (Santa Cruz) for 3 minutes at room temperature. Permeabilization was conducted using ice-cold methanol (Carl Roth) for 10 minutes on ice.[255] Antibody cocktails were prepared in flow cytometry staining buffer (2 % FBS/PBS, TFS). Different cocktails were added to fixed, permeabilized samples and incubated at room temperature for 30 minutes. Fluorescent signals were measured on a LSRFortessa Flow Cytometer (BD Biosciences) and were analyzed using FlowJo software (TreeStar).[255]

3.2.12 Stimulation of STAT-mediated signaling

To analyze activation of important γ_c signaling pathways, $0.5 \cdot 10^6$ EBV-LCLs or $1.0 \cdot 10^6$ PBMCs were starved for 18 h (EBV-LCLs) or 4 h (PBMCs) at 37 °C and 5 % CO_2 in a humidified incubator. To induce phosphorylation of STAT3 and STAT5, cells were stimulated with 100 ng mL^{-1} IL-2 (Peprotech) or 50 ng mL^{-1} IL-21 (Peprotech) for 0, 10, or 30 minutes at 37 °C and 5 % CO_2 in a humidified incubator. Cold 2 mM sodium orthovanadate solution (Na_3VO_4 in PBS, Sigma Aldrich) was added to stop the reaction, cells were transferred to tubes, and pelleted at 300 xg and 4 °C for 5 minutes. Cell pellets were resuspended in cell lysis buffer (see section 3.2.8) and incubated for 1 h on ice. Proteins were separated by SDS-PAGE and analyzed by immunoblotting (see section 3.2.8 and 3.2.9).

3.2.13 *In silico* modeling of protein structures

As described in [255], *de novo* models of WT and mutated IL-2Rγ were generated with NovaFold and Protean 3D software (DNASTAR). PyMol software (Schrödinger) was used to align the *de novo* structures to published protein structures of different cytokine-receptor-complexes.[593-595]

3.2.14 T cell stimulation

PBMCs were isolated from peripheral blood as described in section 3.2.4 and resuspended in complete RPMI (TFS). Flat-bottom 96-well plates were coated with 2 - 5 µg mL^{-1} anti-CD3 (eBioscience) for 2 h at 37 °C. PBMCs were added to pre-coated plates and mixed with either complete RPMI (anti-CD3 only) or with complete RPMI (TFS) supplemented with 1 µg mL^{-1} anti-CD28 (BioLegend) (anti-CD3+anti-CD28). As negative control, cells were added to uncoated wells without co-stimulation. Cells were incubated for 24 - 96 h at 37 °C and 5 % CO_2 until analysis by flow cytometry (see section 3.2.10).

3.2.15 Generation of vectors for CRISPR/Cas9-mediated genetic engineering

Targets for guide RNA (gRNA) and homologous-directed repair (HDR) templates were chosen using Benchling (www.benchling.com) and Synthego Clustered Regularly Interspaced Short Palindromic Repeats (CRISPR) Design Tool (www.synthego.com/products/bioinformatics/crispr-design-tool). Cloning procedure was performed according to previously published protocols.[596] To linearize PX458 plasmids containing CRISPR-associated 9 (Cas9) from *Streptococcus pyogenes* and a fluorescent selection marker (Green fluorescent protein (GFP) or Red fluorescent protein (RFP)), the following reaction mix was prepared (**Table 34**).

Reagent	Mass/Volume
Empty vector (pSpCas9(BB)-2A-GFP or -RFP)	4 µg
10xFastDigest Buffer	5 µl
FastDigest BpiI	2 µl
FastAP	2 µl
Nuclease-free water	to 50 µl

Table 34: Reaction mixture for linearization of Cas9 plasmids.

The reaction mix was incubated at 37 °C for 30 minutes and the linearized backbone was purified using agarose gel electrophoresis followed by gel extraction (please see section 3.2.3). The DNA concentration was determined using NanoDrop (TFS, please refer to 3.2.17).

For each Cas9 target site, two complementary DNA oligos (Oligo FW and Oligo REV) with gRNA sequences and BpiI restriction site overhang were designed according to [596] and ordered from Integrated DNA Technologies (IDT, 25 nmol single-stranded DNA, Coralville, Iowa, USA). Sequences of ordered oligos are summarized in **Table 35**.

Name	Target	Direction	Usage	Sequence
Guide 1	CD33	Forward	KI1	CACCGGGCTTCAGAAGTGGCCGCAA
Guide 1	CD33	Reverse	KI1	AAACTTGCGGCCACTTCTGAAGCCC
Guide 2	CD33	Forward	KI2	CACCGCAGAGCAGGAGTGGTTCATG
Guide 2	CD33	Reverse	KI2	AAACCATGAACCACTCCTGCTCTGC
Guide E3_KO_1	CD33	Forward	KO	CACCGGGCCGGGTTCTAGAGTGCCA
Guide E3_KO_1	CD33	Reverse	KO	AAACTGGCACTCTAGAACCCGGCCC
Guide E3_KO_2	CD33	Forward	KO	CACCGTCCAGCGAACTTCACCTGAC
Guide E3_KO_2	CD33	Reverse	KO	AAACGTCAGGTGAAGTTCGCTGGAC
Guide 1B	TREM2	Forward	KI, KO	CACCGTGGAGATCTCTGGTTCCCCG
Guide 1B	TREM2	Reverse	KI, KO	AAACCGGGGAACCAGAGATCTCCAC
Guide 2	TREM2	Forward	KO	CACCGGGGTCTTTCCTAAAACCCGT
Guide 2	TREM2	Reverse	KO	AAACACGGGTTTTAGGAAAGACCCC

Table 35: Oligos for cloning of guide sequences into Cas9 plasmids.
BbsI overhang is marked in grey and additional G for U6 promoter efficacy in blue. The residual sequence represents the guide.

To anneal and phosphorylate both complementary oligos the following reaction mixture was prepared (**Table 36**).

Reagent	Volume
Oligo FW (100 µM)	1 µl
Oligo REV (100 µM)	1 µl
10x T4 Ligation buffer	1 µl
T4 PNK	0.5 µl
Nuclease-free water	to 10 µl

Table 36: Reaction mixture for annealing and phosphorylation of gRNA oligos

The reaction mix was incubated at 37 °C for 30 min and at 95 °C for 5 minutes. To allow better annealing, the temperature was reduced slowly to room temperature. The annealed

double-stranded oligo (dsOligo) was diluted 1:250 in nuclease-free water. For ligation of dsOligo and linearized backbone, the following reaction mixture was prepared (**Table 37**).

Reagent	Mass/Volume
Linearized backbone	50 ng
Diluted dsOligo	1 µl
10x T4 Ligation buffer	1 µl
T4 ligase	0.5 µl
Nuclease-free water	to 10 µl

Table 37: Reaction mixture for ligation of Cas9 plasmids and dsOligos.

The mix was incubated at 22 °C for 1 h and transformed into competent bacteria (please refer to section 3.2.16). Integration of dsOligo was confirmed by sequencing using pLKO1 (GACTATCATATGCTTACCGT) or U6 (GAGGGCCTATTTCCCATGATTCC) standard primer from Eurofins Genomics. Sequencing was performed by Eurofins Genomics (Ebersberg, Germany) or GENEWIZ (Leipzig, Germany). Confirmed clones were expanded and plasmids were isolated and purified (please refer to section 3.2.16 and 3.2.17). Final plasmid will be called CRISPR vector in downstream applications (e.g., section 3.2.19)

3.2.16 Transformation of plasmid DNA into competent bacteria

5-alpha Competent Escherichia coli (E. coli) (NEB) were mixed with plasmid DNA and incubated on ice for 20 minutes. Mixture was heat-shocked at 42 °C for 90 s and immediately rescued on ice for 2 minutes. 500 µL plain lysogeny broth (LB) medium (**Table 6**) was added and bacteria were cultured at 37 °C and 200 rpm for at least 1 h. Bacteria were pelleted at 800 xg for 5 minutes at room temperature and 400 µL supernatant was removed. Bacteria were resuspended in remaining supernatant and plated to LB plates containing appropriate antibiotic (homemade, **Table 7**). Plates were cultured inverted at 37 °C over-night. On the next day, colonies were picked and transferred to 4 mL LB medium (**Table 6**) containing appropriate antibiotics. Mini-Prep cultures were grown at 37 °C, 200 rpm over-night and pelleted on the next day at 3200 xg and 4 °C for 15 minutes. Pellets were either frozen at - 20 °C for later DNA isolation or resuspended in 700 µL plain LB medium (**Table 6**). 600 µL bacterial suspension were used for DNA isolation by mini prep (see section 3.2.17) and the remaining 100 µL were stored at 4 °C. After analysis by restriction digest or sequencing, positive mini-preps were selected and stored bacterial

suspensions were used to inoculate 200 mL LB medium (**Table 6**) containing appropriate antibiotics. Alternatively, isolated mini-prep plasmids were used to re-transform bacteria and were used to inoculate 200 mL LB medium (**Table 6**). Maxi-Prep cultures were grown at 37 °C, 200 rpm over-night and pelleted on the next day at 3200 xg and 4 °C for 15 minutes. Plasmid DNA was isolated from pelleted bacteria as described in section 3.2.17.

3.2.17 Isolation of plasmid DNA from bacteria

Plasmid DNA from mini-prep cultures (see section 3.2.16) was isolated using Zippy Miniprep Kit (ZymoResearch) following manufacturer's instructions. DNA from maxi-prep cultures (see section 3.2.16) was isolated using QIAGEN Plasmid Plus Maxi Kit (QIAGEN) according to manufacturer's protocol. DNA concentration and purity were determined using NanoDrop (TFS). In brief, 1 µL of DNA solution was loaded on the NanoDrop (TFS) machine and DNA concentration was determined by measuring absorbance at 260 nm. DNA purity was assessed by determining absorbance at 230 and 280 nm.

3.2.18 Maintenance of iPSC

Human induced pluripotent stem cells (iPSCs) were generated from male foreskin fibroblasts by the iPSC core facility at the German Research Center for Environmental Health (Helmholtz Center Munich). For thin layer coating, extracellular matrix (Matrigel, Corning) was diluted 1:100 in Advanced Dulbecco's Modified Eagle's Medium (DMEM)/F12 (TFS), distributed on cell culture multi-well plates or dishes, and incubated at 37 °C for at least 1 h. After coating, plates/dishes were washed with PBS (TFS), mTeSRplus medium (StemCell) was added, and plates/dishes were pre-warmed at 37 °C. Human iPSC were added, distributed equally by shaking and cultured in a humified incubator at 37 °C and 5 % CO_2. For routine passaging, medium was aspirated and iPSC colonies were washed with PBS (TFS). Collagenase IV (1 mg mL^{-1}, StemCell) solution was added for 45 - 60 minutes at 37 °C and colonies were fragmented by pipetting. To stop the enzymatic reaction, mTeSRplus medium (StemCell) was added and colonies were pelleted at 200 xg for 3 minutes at room temperature. Supernatant was removed by aspiration, colonies were resuspended in mTeSRplus medium (StemCell) and splitted (ratio 1:10 to 1:100) to coated, pre-warmed plates. Medium was changed every day or every two days depending on colony density. For cryopreservation of iPSC, colonies were detached using Collagenase IV (StemCell)

as described above and fragmented by pipetting. Colonies were pelleted at 200 xg for 3 minutes at room temperature and resuspended in Bambanker solution (1 mL per 6-well of iPSC, Nippon Genetics). After aliquoting colonies to cryovials, tubes were frozen at – 80 °C and transferred to liquid nitrogen on the next day for long-term storage. For thawing of cryopreserved iPSC, cell culture plates or dishes were coated and prepared as described above. Frozen cell suspension was thawed in a 37 °C water bath and quickly transferred to Advanced DMEM/F12 (TFS). Colonies were pelleted at 200 xg for 3 minutes at room temperature, resuspended in mTeSRplus (Stemcell), and added to prewarmed, coated plates or dishes. To prevent cell death, 10 µM Y-27632 (Rho kinase inhibitor, Biotrend or StemCell) was added to the medium for one day. iPSC were routinely tested for mycoplasma contamination using PlasmoTest™ - Mycoplasma Detection Kit (InvivoGen).

3.2.19 CRISPR/Cas9-mediated genetic engineering of iPSC

To reduce cytotoxicity, 10 µM Y-27632 (Rho kinase inhibitor, Biotrend or StemCell) was added to the medium for 3 - 24 h before electroporation. Multiwell cell culture plates were coated with Matrigel (Corning) as described in section 3.2.18, mTeSRplus medium (StemCell) containing 10 µM Y-27632 (Rho kinase inhibitor, Biotrend or StemCell) was added, and the plates were prewarmed at 37 °C. To harvest the cells, medium was aspirated, iPSC colonies were washed with PBS (TFS), and colonies were dissociated using Accutase (EMD Millipore) for 10 minutes. Reaction was stopped by addition of mTeSRplus medium (StemCell). To generate single cells, cell clumps were mechanically broken by pipetting. 0.75 - 1.5 · 10^6 single cells were pelleted at 200 xg for 3 minutes at room temperature and supernatant was removed by aspiration. To prepare the nucleofection solution, 18 µL supplement and 82 µL nucleofector solution (both from Human Stem Cell Nucleofector Kit 2, Lonza) were mixed and prewarmed at 37 °C. The cell pellet was resuspended in 100 µL prewarmed nucleofection solution and 5 µg CRISPR vector (see section 3.2.15) was added. For generation of knock-ins (KI), 5-10 µL HDR template (Ultramer DNA oligo ordered from Integrated DNA Technologies, Coralville, Iowa, USA) was also added (**Table 38**).

Name	Target	Mutation	Sequence
Oligo 1	TREM2	c.451G>A	CTCATGGCTCTGCCTCCCATAGACCCCCTGGATCACCGGG ATGCTGGAGATCTCTGGTTCCCCGGCGAGTCTGAGAGCTT CAAGGATGCCCATGTGGAGCACAGCATCTCCAGGTACAGC GATGGGTCTTTCCTAAAACCCGTGGGCAGACTTCCACCCTG CAGAG CCCCACGGGGGTGGGGGCTGGG
Oligo 1	CD33	c.415A>T	GTACCAAATACAGTTACAAATCTCCCCAGCTCTCTGTGCAT GTGTCAGGTGAGGCACAGGCTTCAGAAGTGGCCGCAAGCG AAGTTCATGGGTACTGCAGGGCAGGGCTGGGATGGGACCC TGG TACTGGGAGGGGTTTAGGGGTAAAGC
Oligo 2	CD33	c.746-8delG	TGTTTATCTAGATTAGAATTCACCCCAAATCTTTTTTTCTGCA GGGAAACAAGAGACCAGAGCAGGAGTGGTTCATGGCGCCA TTGGAGGAGCTGGTGTTACAGCCCTGCTCGCTCTTTGTCTC TG CCTCATCTTCTTCATGTGAGCAT

Table 38: Sequences of templates for HDR after Cas9-mediated genetic engineering.In both oligos, targeted mutations are marked red and PAM site mutations (G>C) in blue.

The cell-DNA suspension was transferred to an electroporation cuvette (Lonza) and electroporation was performed using program B-016 using the Nucleofector II device (Lonza, Basel, Switzerland). After nucleofection, cells were transferred to multi-well plates with prewarmed medium and cultured at 37 °C and 5 % CO_2 in a humified incubator. The medium was refreshed on the next day and 10 µM Y-27632 (BioTrend or StemCell) was added. For generation of KIs, the medium was also supplemented with 10 µM SCR7 (StemCell) to inhibit non-homologous end joining. Two days after nucleofection, cells were harvested using accutase (EMDMillipore) as described above and filtered into tubes with strainer cap (Falcon/Corning). Cells were pelleted at 200 xg for 3 minutes at room temperature and resuspended in 250 µL prewarmed mTeSRplus medium (StemCell) containing 10 µM Y-27632 (BioTrend or StemCell). Cells expressing the desired selection marker (GFP, RFP, or GFP+RFP) were sorted into mTeSR plus (StemCell) with 10 µM Y-27632 (BioTrend or StemCell) and 1 % v/v Penicillin-Streptomycin (TFS) using a FACSAria III machine (BD Biosciences) in the Flow Cytometry core facility at the CCRC Hauner (Munich, Germany). Per reaction, a 10 cm cell culture dish was coated with Matrigel as described in section 3.2.18 and prepared with 6 mL of fresh mTeSRplus (StemCell), 4 mL of conditioned medium (0.2 µm filtered supernatant of wild-type iPSC cells), 10 µL of Y-27632 (StemCell) and 1 % v/v Penicillin-Streptomycin. 3000 – 5000 sorted cells were added to the prepared, prewarmed dish and cultivated in a humidified incubator at 37 °C and 5 % CO_2. Residual cells were used for genotyping. Conditioned medium containing Y-27632 (BioTrend or StemCell) and Penicillin-Streptomycin (TFS) was refreshed on day 2 and 3 after sorting. Later, medium was refreshed with fresh mTeSRplus medium (StemCell) every two days. When colonies reached sufficient size, a part of each colony was picked using a pipette and transferred to a coated, prepared 24-well plate (see section 3.2.18 for coating procedure). The remaining colony

was used for DNA isolation and sequencing (see section 3.2.2). Clones with confirmed edits were expanded and cryopreserved as described in section 3.2.18.

3.2.20 Differentiation of iPSC towards macrophages

The procedure for generation of macrophages from iPSC described hereafter is based on previously published protocols[597] and personal communication from the Center for iPS Cell Research and Application (CiRA) at Kyoto University (Kyoto, Japan). Differentiation of iPSC was performed in 6-well cell culture plates, which were coated with Matrigel (Corning) as described in section 3.2.18. After coating, plates were washed with PBS (TFS), mTeSRplus (StemCell) was added, and plates were prewarmed at 37 °C. To harvest iPSC colonies, medium was removed, cells were washed with PBS (TFS), and cells were incubated with Collagenase IV (StemCell) for 45 - 60 minutes (see section 3.2.18). The colonies were detached by pipetting aiming to minimize colony fragmentation. Larger colonies were pelleted at 10 xg for 1 minute at room temperature. If colony yield was too low, centrifugation was repeated at 200 xg for 3 minutes at room temperature. The supernatant was aspirated, and the pellet was resuspended in 0.2 mL of mTeSRplus (StemCell) avoiding excess pipetting, which might generate to small colonies. Number of colonies was determined and 10 – 20 colonies were transferred to each prewarmed 6-well for differentiation. iPSCs were cultured at 37 °C, 5 % CO_2 in a humidified incubator and medium was refreshed every two days until colonies reach a diameter of approx. 1 mm (usually 3-4 days after seeding). To induce hematopoiesis, medium containing different cytokine/inhibitor cocktails was changed on day 0, 2, 4, and 6 according to **Figure 14** and **Table 39**.

On day 6 of differentiation, 6 colonies were selected based on size and differentiation status. Additional colonies were removed by aspiration. After day 6, half medium was removed and refreshed every 3-4 days according to **Figure 14** and **Table 39**. Progress of differentiation was routinely monitored by analyzing CD45, CD34, CD33, and CD14 on floating cells using flow cytometry. Floating cells were harvested between day 18 – 40 every 3-5 days and $CD14^+$ monocytes/macrophages were purified by magnetic cell separation using the EasySep Human CD14 Positive Selection Kit II (StemCell). To generate mature macrophages, purified cells were seeded and cultured for additional 6 - 7 days in complete Roswell Park Memorial Institute (RPMI) medium (**Table 40**) containing M-CSF (Peprotech or StemCell).

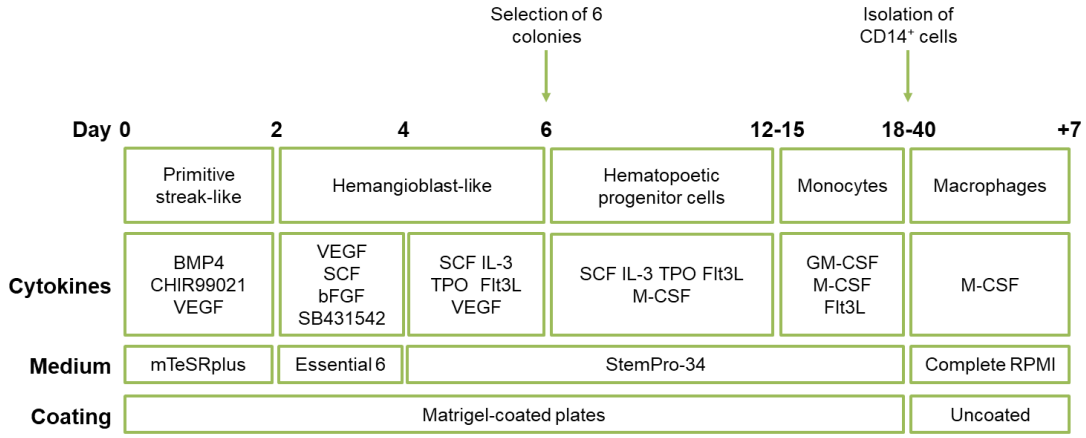

Figure 14: Scheme for differentiation of iPSC towards macrophages.

Day	Reagent	Final Concentration
0-2	BMP4	80 ng mL^{-1}
	CHIR99021	3 µM
	VEGF	80 ng mL^{-1}
2-4	VEGF	80 ng mL^{-1}
	SCF	50 ng mL^{-1}
	bFGF	25 ng mL^{-1}
	SB431542	2 µM
4-6	SCF	50 ng mL^{-1}
	IL-3	50 ng mL^{-1}
	TPO	5 ng mL^{-1}
	FLT3L	50 ng mL^{-1}
	VEGF	50 ng mL^{-1}
6-15	M-CSF	50 ng mL^{-1}
	SCF	50 ng mL^{-1}
	TPO	5 ng mL^{-1}
	IL-3	50 ng mL^{-1}
	FLT3L	50 ng mL^{-1}
15-40	M-CSF	50 ng mL^{-1}
	GM-CSF	25 ng mL^{-1}
	FLT3L	50 ng mL^{-1}
+0 - +7	M-CSF	100 ng mL^{-1}

Table 39: Medium changing routine for macrophage differentiation.

Reagent	Manufacturer	Concentration
RPMI 1640 Medium, GlutaMAX Supplement	TFS	-
FBS	TFS	10 %
Penicillin-Streptomycin	TFS	1 %
HEPES	TFS	10 mM
Sodium pyruvate	TFS	1 mM

Table 40: Formulation of complete RPMI. TFS, Thermo Fisher Scientific

3.2.21 Differentiation of iPSC towards granulocytes

The procedure for generation of granulocytes from iPSC described hereafter was established in the laboratory by Dr. Yoko Mizoguchi and is based on previously published protocols[598] and personal communication from the Center for iPS Cell Research and Application (CiRA) at Kyoto University (Kyoto, Japan). Differentiation of iPSC towards granulocytes was performed analogous to section 3.2.20, but cytokine/inhibitor cocktails were adapted to support granulocyte development. To induce differentiation, medium was changed on day 0, 2, 4, 6, and 8 according to **Figure 15** and **Table 41**.

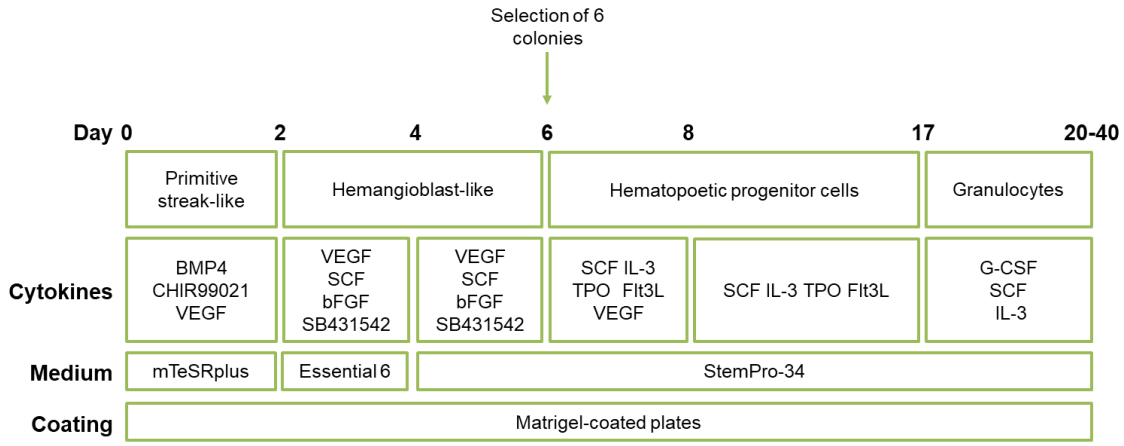

Figure 15: Scheme for differentiation of iPSC towards granulocytes.

Day	Reagent	Final Concentration
0-2	BMP4	80 ngmL^{-1}
	CHIR99021	3 µM
	VEGF	80 ngmL^{-1}
2-6	VEGF	80 ngmL^{-1}
	SCF	50 ngmL^{-1}
	bFGF	25 ngmL^{-1}
	SB431542	2 µM
6-8	SCF	50 ngmL^{-1}
	IL-3	50 ngmL^{-1}
	TPO	5 ngmL^{-1}
	FLT3L	50 ngmL^{-1}
	VEGF	50 ngmL^{-1}
17-40	SCF	50 ngmL^{-1}
	G-CSF	50 ngmL^{-1}
	IL-3	50 ngmL^{-1}

Table 41: Medium changing routine for granulocyte differentiation.

On day 6 of differentiation, 6 colonies were selected based on size and differentiation status. Additional colonies were removed by aspiration. After day 8, half medium was removed and refreshed every 3-4 days. Progress of differentiation was routinely monitored by analyzing CD45, CD34, CD33, and CD14 on floating cells using flow cytometry. Mature, floating granulocytes were harvested between day 20 – 40 every 3-5 days by removing the medium and adding fresh medium.

3.2.22 Cytospin analysis

For cytospin analysis, 30000 to 50000 cells were resuspended in 100 µL 2 % FBS/PBS (TFS). Coated cytoslides (Tharmac) were prepared with filter cards (Tharmac) and funnels. Cell suspension was added to the funnel and slides were centrifuged for 5 minutes at 500 xg in a Cellspin I centrifuge (Tharmac). Cytoslides with cells were air dried over-night at room temperature and stained in May-Grünwald`s eosine-methylene blue solution (Merck) for 2 minutes at room temperature. Slides were washed two times in $dH_2O$ for 2 minutes to remove residual staining solution. Giemsa`s azur eosin methylene blue solution (Merck) was diluted 1:20 in Sørensen buffer (**Table 11**) and was added to the slides for 17 min at room temperature. Slides

were washed two times in dH_2O for 2 minutes to remove residual staining solution and dried over-night at room temperature. Cells were analyzed and counted using an Axioplan 2 microscope (Zeiss) equipped with a VisiCam 3.0 and the Visicam Image Analyser Software (BEL Engineering).

3.2.23 Purification of monocytes from PBMCs

To purify and generate monocytes, PBMCs were pelleted at 300 xg and 4 °C for 5 minutes. The supernatant was removed and PBMCs were resuspended in RPMI plain (TFS) at a concentration of $2.0 \cdot 10^6$ mL^{-1}. PBMCs were seeded to cell culture plates and incubated for 3 h at 37 °C and 5 % CO_2 in a humidified incubator. After adherence of monocytes, medium was removed and cells were washed with warm RPMI plain (TFS). Pre-warmed RPMI complete (TFS, see **Table 40**) was added and cells were incubated over-night at 37 °C and 5 % CO_2 in a humidified incubator. Monocytes were used on the next day for functional experiments.

3.2.24 Molecular cloning

Mutations in CD33 were predicted to affect mRNA splicing. To analyze effects on splicing in heterologous cellular models, a CD33 mini-gene focused on splicing of exon 2 and 5 (**Figure 16**) was designed with the help of Dr. Jens Bohne (MHH Hannover) and was ordered from Integrated DNA Technologies (Coralville, Iowa, USA).

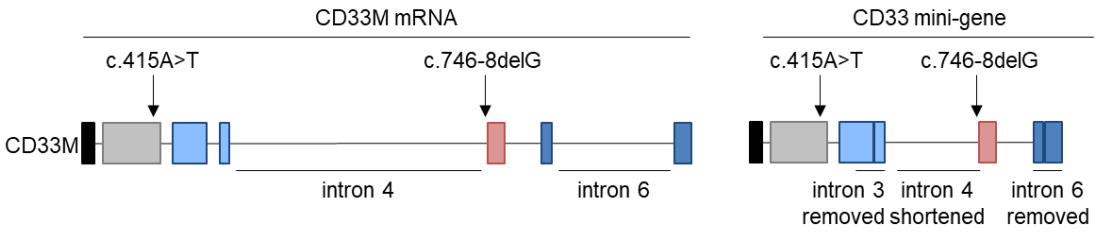

Figure 16: Schematic representation of CD33 mini-gene composition.

CD33 mini-gene oligo (CD33-SPR) was introduced into pJet1.2 vector (TFS) by blunt-end cloning using the CloneJET PCR Cloning Kit (TFS) following manufacturer's instructions and according to **Table 42**.

Reagent	Manufacturer	Volume [µL]	Amount
2X reagent buffer	TFS	10	
Fragment for ligation	Integrated DNA Technologies	x	0.15 pmol ends
pJet1.2/blunt	TFS	1	0.05 pmol ends
T4 ligase	TFS	1	
Nuclease-free water	-	to 20 µL	

Table 42: Reaction mixture for blunt end cloning into pJet1.2. TFS, Thermo Fisher Scientific

Ligation was incubated for 1 h at room temperature and directly transformed into competent bacteria (NEB, for transformation procedure see section 3.2.16) and plated on Ampicillin-containing agar plates (**Table 7**). For clone expansion and plasmid isolation please refer to sections 3.2.16, 3.2.17, and 3.2.3. Clones were analyzed for integration of CD33 mini-gene oligo by digestion with FastDigest (FD, TFS) restriction enzymes. In detail, the following reaction mix was prepared (**Table 43**).

Reagent	Manufacturer	Volume [µL]
Plasmid (pJet1.2-CD33-SPR)		10
FD XhoI	TFS	1
10X FastDigest buffer	TFS	2
Nuclease-free water		7

Table 43: Reaction mixture for XhoI digestion. TFS, Thermo Fisher Scientific

Mixture was incubated at 37 °C for 60 minutes and enzymes were inactivated at 85 °C for 20 minutes. Restriction pattern was analyzed by agarose gel-electrophoresis (see section 3.2.3). Positive clones were sequenced at Eurofins Genomics (Ebersberg, Germany) using the T7 standard primer (5'-TAATACGACTCACTATAGGG-3'). Selected clone was expanded as described in section 3.2.16, isolated as summarized in section 3.2.17, and identity was confirmed by Sanger sequencing at Eurofins Genomics (Ebersberg, Germany) using the pJet1.2 Seq fw (5'-cgactcactatagggagagcggc-3') and pJet seq rev (5'-aagaacatcgattttccatggcag-3') primer.
Site-directed mutagenesis was performed as described in [599]. For introduction of the c.415A>T mutation, the mini-gene was amplified from the 5'-end to the mutation site (Reaction #1) and from the mutation site to the 3'-end (Reaction #2) with primers carrying the targeted point mutation. The reaction mixture, used primer, and the PCR program are summarized in **Table 44**, **Table 45**, and **Table 46**, respectively.

Reagent	Manufacturer	Volume [µL]
Q5 High Fidelity Polymerase	NEB	1
Primer fw	-	1
Primer rev	-	1
pJet-CD33-SPR	-	10 ng
DMSO	Sigma	1
Q5 reaction buffer	NEB	2
dNTPs	Applichem	2
Nuclease-free H_2O	-	to 20

Table 44: Site-directed mutagenesis PCR for introduction of c.415A>T mutation.

Primer Name	Sequence	Reaction #
DI359_CD33splice_SDM_fw	gatcttccggatggctcgagtttt	1
DI356_CD33splicereporter_Mut1_rev	tgcctcacctgAcacatgcacagagagc	1
DI355_CD33splicereporter_Mut1_fw	Tcaggtgaggcacaggcttcagaagtgg	2
DI360_CD33splice_SDM_rev	tccatggcagctgagaatattgtagg	2

Table 45: Site-directed mutagenesis primer for introduction of c.415A>T. Nucleotides with point mutation are capitalized.

Temp. [°C]	Duration	Cycles
Lid at 110	-	-
98	5'	1
98	30''	
68	30''	25
72	2'	
72	10'	1
4	∞	1

Table 46: PCR program for site-directed mutagenesis.

PCR products were separated and purified by agarose gel-electrophoresis as described in section 3.2.3. To ligate the fragments of reaction #1 and #2, a PCR from the 5'- to the 3'-end of the CD33 mini gene was performed (Reaction #3) as summarized in **Table 47**, **Table 48**, and **Table 49**. The first 10 cycles were run without primer.

Reagent	Manufacturer	Volume [µL]
Q5 High Fidelity Polymerase	NEB	1
Fragment of reaction #1	-	10 ng
Fragment of reaction #2	-	10 ng
DMSO	Sigma	1
Q5 reaction buffer	NEB	2
dNTPs	Applichem	2
Nuclease-free H_2O	-	to 18
Primer fw	-	1
Primer rev	-	1

Table 47: PCR mixture for ligation of mutagenized fragments.

Primer Name	Sequence	Reaction #
DI359_CD33splice_SDM_fw	gatcttccggatggctcgagtttt	3
DI360_CD33splice_SDM_rev	tccatggcagctgagaatattgtagg	3

Table 48: Primer for full length amplification of mutated fragments.

Temp. [°C]	Duration	Cycles
Lid at 110	-	-
98	5'	1
98	30''	
50	30''	10
72	2'	
8	Pause	1
98	2'	1
98	30''	
66	30''	30
72	2'	

Table 49: PCR program for full length amplification of mutated fragments.

The final PCR product was purified by agarose gel-electrophoresis as described in section 3.2.3 and blunt-end ligated into pJet1.2 vector (TFS) using the CloneJET PCR Cloning Kit (TFS) following manufacturer's instructions and analogous to **Table 42**. The ligation reaction was incubated at 4 °C over-night and transformed into competent bacteria according to section 3.2.16. For expansion and plasmid isolation, please refer to sections 3.2.16, 3.2.17, and 3.2.3. To analyze incorporation of point mutations, plasmids were sequenced using DI359_CD33splice_SDM_fw (Forward, 5'-gatcttccggatggctcgagtttt-3') or DI132 (Reverse, 5'-CCTAAACCCCTCCCAGTACCAG-3') primer at Eurofins Genomics (Ebersberg, Germany).

For introduction of mutation 2 (c.746-8delG), the mini-gene was amplified from the 5'-end to the mutation site (Reaction #4) and from the mutation site to the 3'-end (Reaction #5) with primers carrying the targeted point mutation. The reaction mixture, used primer, and the PCR program are summarized in **Table 50**, **Table 51**, and **Table 52**, respectively.

Reagent	Manufacturer	Volume [µL]
Q5 High Fidelity Polymerase	NEB	1
Primer fw	-	1
Primer rev	-	1
pJet-CD33-SPR	-	10 ng
DMSO	Sigma	1
Q5 reaction buffer	NEB	2
dNTPs	Applichem	2
Nuclease-free H_2O	-	to 20

Table 50: Site-directed mutagenesis PCR for introduction of c.746-8delG mutation.

Primer Name	Sequence	Reaction #
DI358_CD33splicereporter_Mut2_rev	ccctgcagaAAaaaagatttggggtgaattc	4
DI359_CD33splice_SDM_fw	gatcttccggatggctcgagtttt	4
DI357_CD33splicereporter_Mut2_fw	TTtctgcagggaaacaagagaccagagca	5
DI360_CD33splice_SDM_rev	Tccatggcagctgagaatattgtagg	5

Table 51: Site-directed mutagenesis primer for introduction of c.746-8delG.
Nucleotides surrounding point mutation (deletion) are capitalized.

Temp. [°C]	Duration	Cycles
Lid at 110	-	-
98	5'	1
98	30"	
60/66	30"	25
72	2'	
72	10'	1
4	∞	1

Table 52: PCR program for site-directed mutagenesis.
Reaction #4 was performed at 60 °C and reaction #5 at 66 °C annealing temperature.

PCR products were separated and purified by agarose gel-electrophoresis as described in section 3.2.3. Further procedure was performed analogous to mutation 1 (please see above for details). To analyze incorporation of point mutations, plasmids were sequenced using either DI131_CD33_E2_fw (5'-GAAGCTGCTTCCTCAGACATGC-3') or DI360_CD33splice_SDM_rev

(5'-Tccatggcagctgagaatattgtagg-3') primer at Eurofins Genomics (Ebersberg, Germany). Selected clones were expanded (Maxi-Prep) and isolated as described in section 3.2.16 and 3.2.17, respectively.

For stable, doxycycline-inducible expression in heterologous cellular models, CD33 mini-genes with patient-specific mutations were cloned into the PB-TAC-ERP2 vector (Addgene) using Gateway cloning. To generate entry clones for Gateway cloning, CD33 mini-genes were inserted into pENTR1A vector (Addgene) by restriction digest. pJet1.2-CD33-SPR vectors with patient-specific mutations and pENTR1A vector (Addgene) were digested with XhoI (TFS) at 37 °C for 45 minutes as described above (analogous to **Table 43**). The restriction enzymes were inactivated at 85 °C for 20 minutes and the generated fragments were purified by agarose gel electrophoresis as described in section 3.2.3. Inserts were ligated into digested pENTR1A analogous to previous descriptions **Table 42**. The ligation reaction was transformed into competent bacteria according to section 3.2.16 and plated to Kanamycin-containing agar plates. For clone expansion and plasmid isolation, please refer to sections 3.2.16 and 3.2.17. To test the presence of inserts in entry vectors, plasmids were digested with EcoRI (TFS) as in **Table 53** at 37 °C for 15 minutes and at 85 °C for 5 minutes.

Reagent	Manufacturer	Mass/Volume
Plasmid		500 ng
FD EcoRI	TFS	1 µL
10X FastDigest buffer	TFS	2 µL
Nuclease-free water		to 20 µL

Table 53: Reaction mixture for EcoRI digestion of pENTR1A-CD33-SPR plasmids. TFS, Thermo Fisher Scientific

Restriction pattern was analyzed by agarose gel-electrophoresis as described in section 3.2.3. Positive clones were additionally sequenced at Eurofins Genomics (Ebersberg, Germany) using the pENTattL2rev standard primer (5'-ACATCAGAGATTTTGAGACACGGGC-3'). Selected clones were expanded to Maxi-Preps as described in section 3.2.16 and isolated as summarized in section 3.2.17.

For generation of expression/destination vector, 150 ng entry clone (pENTR1A-CD33-SPR), 150 ng destination vector (PB-TAC-ERP2), 2 µL TE buffer (homemade), and 1 µL of LR Clonase II

enzyme (TFS) were mixed and incubated for 24 h at room temperature. To terminate the reaction, 1 µL Protease solution (Qiagen) was added and proteins were digested at 37 °C for 10 minutes. The reaction was transformed into competent bacteria (NEB) according to section 3.2.16 and plated to ampicillin-containing agar plates. For clone expansion and plasmid isolation, please refer to sections 3.2.16 and 3.2.17. To test presence of inserts in entry vectors, plasmids were digested with BamHI (TFS) as in **Table 54** at 37 °C for 120 minutes and at 85 °C for 10 minutes.

Reagent	Manufacturer	Volume [µL]
Plasmid		5
FD BamHI	TFS	1
10X FastDigest buffer	TFS	2
Nuclease-free water		to 20

Table 54: Reaction mixture for BamHI digestion of pENTR1A-CD33-SPR plasmids. TFS, Thermo Fisher Scientific

Restriction pattern was analyzed by agarose gel-electrophoresis as described in section 3.2.3. For confirmation, positive clones were additionally sequenced at Eurofins Genomics (Ebersberg, Germany) using DI348_PB_fw (Forward, 5'-CCATAGAAGACACCGGGACCGAT-3') and DI349_PB_rev (Reverse, 5'-ttcgaggccgcgttttagc-3') primer. Selected clones were expanded to Maxi-Preps as described in section 3.2.16 and isolated as summarized in section 3.2.17. Identity of plasmids was confirmed by digestion with BamHI (TFS) and sequencing as before.

3.2.25 Generation of HEK293T cells expressing doxycycline-inducible mini-genes

HEK293T (DSMZ) were harvested by removal of medium by aspiration, washing with PBS (TFS), and detachment by addition of Trypsin-EDTA (Sigma-Aldrich) (see also section 3.2.6). Cells were incubated for 5 minutes at 37 °C with Trypsin-EDTA (Sigma-Aldrich) and reaction was stopped with complete medium. 20000 cells were seeded per 24 well and incubated at 37 °C and 5 % CO_2 over-night. To prepare transfection mixes, Opti-MEM medium (TFS) was mixed with Lipofectamine2000 (TFS) and plasmids and incubated for 30 minutes at room temperature. Mix was added to the cells and cells were incubated at 37 °C and 5 % CO_2 over-night. On the next day, medium was removed, and complete DMEM medium (**Table 27**) was added and cells were cultured at 37 °C and 5% CO_2 in a humidified incubator for two days. To select positive cells,

complete DMEM medium (**Table 27**) supplemented with 1 µg mL^{-1} puromycin (TFS) was added, and cells were incubated at 37 °C and 5% CO_2 in a humidified incubator until cells could be used for assays. Cells were maintained in complete growth medium supplemented with 1 µg mL^{-1} puromycin (TFS) at 37 °C and 5 % CO_2 in a humidified incubator. To induce mini-gene expression, 1 µg mL^{-1} doxycycline (Doxycycline hyclate, Sigma Aldrich) dissolved in dH_2O and sterile filtered) was added and cells were cultured at 37 °C and 5 % CO_2 in a humidified incubator until harvest and analysis. Successful induction of mini-gene expression was confirmed by monitoring mCherry expression using a fluorescent microscope.

3.2.26 Analysis of hematopoiesis using CFU assays

To analyze the capacity of iPSC-derived HSPC for proliferation and differentiation, a colony forming unit (CFU) assay was performed using methylcellulose-based semi-solid matrix (MethoCult H4435 Enriched, Stemcell Technologies) according to manufacturer's instructions. In detail, potential HSPCs were harvested at Day 8 or 9 of iPSC differentiation towards granulocytes or macrophages (see 3.2.20 and 3.2.21), pelleted at 300 xg for 5 minutes at 4 °C, and resuspended in IMDM medium (TFS). 10000 cells were mixed with methylcellulose-based semi-solid matrix (MethoCult H4435 Enriched, Stemcell Technologies) and Penicillin-Streptomycin (TFS). After mixing, cell suspension was aliquoted to 35 mm dishes in triplicates. CFU assays were incubated at 37 °C and 5 % CO_2 in a humidified incubator until analysis.

3.2.27 Gentamycin protection assay

Salmonella enterica typhimurium (*S. typhimurium*) were a kind gift from the laboratory of Tobias Schwerd (Dr. von Hauner's Children's Hospital, LMU Klinikum, Munich). Colonies of *S. typhimurium* were used to inoculate LB mini cultures containing ampicillin as selection antibiotic (see 3.2.16 for details) and were cultured at 37 °C and 200 rpm over-night. On the next day, culture was diluted 1:10 and OD600 was determined using the Synergy H1 Hybrid Multi-Mode Microplate Reader (BioTek). Concentration of bacteria was calculated using the formula below:

$$c[\frac{bacteria}{mL}] = OD_{600} * 10 * 10^9$$

Another LB mini culture was inoculated with 10^7 bacteria and incubated at 37 °C and 200 rpm for 3.5 h. OD600 was determined using Synergy H1 Hybrid Multi-Mode Microplate Reader (BioTek). The final concentration of *S. typhimurium* was calculated using the formula below:

$$c[\frac{S.\,typhimurium}{mL}] = OD_{600} * Dilution * 5.06 * 10^8$$

To analyze bacterial uptake and killing of macrophages, cells were detached using versene (TFS) for 15 minutes at 37 °C and 5 % CO_2 in a humidified incubator. Detached cells were pelleted at 300 xg for 5 minutes at 4 °C and cells were resuspended in complete RPMI (without antibiotics) (TFS). 50000 cells were seeded in a 96-well flat bottom plate in triplicates and incubated at 37 °C and 5 % CO_2 in a humidified incubator for 4 to 12 h to ensure adhesion of the cells. After adhesion, 50 µL *S. typhimurium* suspension was added (MOI=10) and the plates were centrifuged at 2000 xg and room temperature for 2 minutes. For infection, plates were incubated at 37 °C and 5 % CO_2 for 1 h in a humidified incubator. Afterwards, cell culture medium was removed, and cells were washed once with PBS (TFS). Complete RPMI medium (TFS) supplemented with 100 µg mL^{-1} gentamycin (TFS) was added and cells were incubated at 37 °C and 5 % CO_2 for 2 h in a humidified incubator to kill extracellular bacteria. Cells were washed two times with PBS and were lysed in 200 µL 1 % Triton-X100 (Sigma Aldrich) diluted in dH_2O. Samples were plated in different dilutions (10 µL volume) on LB plates (**Table 7**) by adding the suspension on top and let it run down the plate. Bacteria were grown over-night at 37 °C and colonies were counted on the next day.

3.2.28 Culture, differentiation, and stimulation of BLaER1 cells

BLaER1 cells were a kind gift of Prof. Dr. Veit Hornung (LMU Munich) and were cultured and differentiated according to previously published protocols.[600, 601] BLaER1 cells were routinely cultured as suspension cells in complete RPMI (**Table 40**) at 37 °C and 5 % CO_2 in a humidified incubator using T25 flasks. To induce trans-differentiation, BLaER1 cells were resuspended in complete RPMI supplemented with 10 ng mL^{-1} IL-3 (Peprotech), 10 ng mL^{-1} M-CSF (Peprotech), and 100 nM β-estradiol (Sigma Aldrich) and 200.000 cells were seeded in 48-well plates (Sarstedt). BLaER1 cells were then differentiated for 6 days at 37 °C and 5 % CO_2 in a humidified incubator and medium was refreshed after 2 and 4 days. Trans-differentiation of cells was verified by analysis of CD14 and CD33 expression by flow cytometry (see section 3.2.10). To analyze

effects of CD33 and Siglecs on inflammasome activation, differentiated BLaER1 cells were pre-stimulated with 10 µg mL^{-1} anti-CD33 (BioRad), 10 µg mL^{-1} IgG (BD Biosciences), or 0.15 U neuraminidase (sialidase, Sigma/Roche) for 48 h at 37 °C and 5 % CO_2 in a humidified incubator. Afterwards, inflammasome expression was primed using 20 ng mL^{-1} LPS (Sigma) for 2.5 hours and inflammasome effectors were activated using 6.5 µM Nigericin (Sigma) for additional 0.5 hours. Inflammasome was analyzed as described in section 3.2.29.

3.2.29 Analysis of inflammasome activation

Inflammasomes are activated by two stimuli, which include a priming signal that upregulates expression of inflammasome effectors and a second signal that activates maturation of inflammasome effectors. Furthermore, priming can be performed with different parameters including timing and dosage of the priming stimulus.

Inflammasome experiments were performed in complete medium containing 10 % FBS (TFS), which was supplemented with 50 - 100 ng mL^{-1} M-CSF (Peprotech or StemCell) for long term stimulation experiments with macrophages. In some experiments, primary monocytes were pre-stimulated with 10 µg mL^{-1} anti-CD33 (BioRad) for 6 h in complete medium. To analyze inflammasome activation, cells were stimulated with priming signal for 3 - 4 h in total for short term experiments and for 19 h for long term experiments. For priming of monocytes/macrophages, LPS (Sigma Aldrich) was used at a concentration of 20 ng mL^{-1} in short term experiments or at a concentration of 200 ng mL^{-1} in long term experiments. For priming of granulocytes, LPS (Sigma Aldrich) was used at a concentration of 250 ng mL^{-1}. S100A9 (R&D/Invitrogen) was used at a concentration of 10 µg mL^{-1} for macrophages and granulocytes. To induce activation of inflammasome components, nigericin (Sigma Aldrich) was used at a final concentration of 6.5 µM for 0.5 - 2 h.

After stimulation, supernatants were harvested to fresh tubes, centrifuged at 300 xg and 4 °C for 5 minutes to remove floating cells, and cleared supernatants were distributed for different assays. 25 – 50 µL supernatant were used for cytotoxicity assays (see section 3.2.31), 30 µL were mixed with 6 µL 6X Laemmli buffer (**Table 5**) and frozen at – 80 °C for immunoblot analysis of supernatants (see section 3.2.8 and 3.2.9), and the remaining supernatant was frozen at – 80 °C for cytokine analysis by ELISA (see section 3.2.30). Stimulated cells were lysed in 30 µL cell lysis

buffer (**Table 3**) and frozen at – 80 °C for immunoblot analysis of cell lysates (see section 3.2.8 and 3.2.9).

3.2.30 Enzyme-linked Immunosorbent Assay

Cytokine concentrations in cell culture supernatants were measured by enzyme-linked immunosorbent assay (ELISA) according to manufacturer's instructions. In detail, MaxiSorp Clear Flat-Bottom Immuno Nonsterile 96-Well Plates (TFS) were coated with coating antibody overnight. IL-1β coating antibody (R&D) was dissolved in PBS (TFS) and TNF-α coating antibody (BD Biosciences) was dissolved in 0.1 M sodium carbonate coating buffer (0.713 g $NaHCO_3$, 0.159 g Na_2CO_3 in 100 mL dH_2O, pH 9.5) Plates were washed four times with PBS-T (**Table 9**). Unspecific binding was blocked with a 0.2 µm filtered solution of 1% BSA/PBS (Applichem/homemade, pH 7.3, „reagent diluent") or 10 % FBS/PBS (TFS/homemade, pH 7.0, "assay diluent") for 1 h at room temperature and the washing step was repeated once. Samples and standard were diluted in reagent or assay diluent and added for 2 h room temperature to the plate. Unspecific cytokines were removed by repeating the washing step four times. A mixture of detection antibody and Streptavidin-HRP in reagent or assay diluent was added to the plate and was incubated at room temperature for 2 h. Plate was washed six times as before. TMB substrate solution (eBioscience) was added and incubated at room temperature for up to 20 minutes. Reaction was stopped with 1 M H_3PO_4 (Carl Roth) and absorption at 450 nm was determined using the Synergy H1 Hybrid Multi-Mode Microplate Reader (BioTek) and the Gen5 software (BioTek).

3.2.31 Cytotoxicity assay

To assess cytotoxicity, lactate dehydrogenase (LDH) concentration in cell culture supernatants was analyzed using CytoTox 96 Non-Radioactive Cytotoxicity Assay (Promega) according to manufacturer's instructions. In detail, cell culture supernatants were mixed at a 1:1 ratio with CytoTox 96 Reagent and incubated for 15 - 30 minutes at room temperature. Lysed cells were used as maximum control. Reaction was stopped by addition of Stop solution (same volume as supernatant/reagent) and absorbance at 490 nm was determined using the Synergy H1 Hybrid Multi-Mode Microplate Reader (BioTek). Background absorbance was subtracted, and cytotoxicity was calculated according to following formula:

$$\text{Cytotoxicity}\,[\%] = 100 \times \frac{\text{Absorption}_{490\,\text{nm}}\,(\text{Sample})}{\text{Absorption}_{490\,\text{nm}}\,(\text{Maximum LDH Release})}$$

3.2.32 Phorbol 12-myristate 13-acetate stimulation

To induce shedding of TREM2, 150.000 macrophages were seeded in 24-well plates in complete RPMI (**Table 40**) supplemented with 100 ng mL^{-1} M-CSF (Peprotech/StemCell) and cultured over-night at 37 °C and 5 % CO_2 in a humidified incubator. On the next day, macrophages were stimulated with 200 nM Phorbol 12-myristate 13-acetate (PMA) (Abcam) in complete RPMI (**Table 40**) for 0, 1, 2, or 3 h at 37 °C and 5 % CO_2 in a humidified incubator. After stimulation, supernatants were harvested to fresh tubes, centrifuged at 300 xg and 4 °C for 5 minutes to remove floating cells, and cleared supernatants were frozen at – 80 °C for further assays. Cells were lysed in 60 µL cell lysis buffer (see section 3.2.8), cell lysates were transferred to a 1.5 mL, and stored on ice. Protein concentration was determined using RotiNanoquant (Carl Roth) according to manufacturer's instructions and samples were diluted with 1X cell lysis buffer to adjust the concentration. Cell lysates were frozen at – 80 °C and analyzed by immunoblotting by our collaboration partner at AG Prof. Christian Haass (DZNE, LMU Munich).

3.2.33 Macrophage polarization

To polarize macrophages towards a pro- (M1) or anti-inflammatory (M2) fate, macrophages were stimulated with complete RPMI (**Table 40**) supplemented with (i) no cytokines (M0), (ii) 50 ng mL^{-1} LPS (Sigma Aldrich) and 20 ng mL^{-1} IFN-γ (M1), or (iii) 20 ng mL^{-1} IL-4, 20 ng mL^{-1} IL-10, and 20 ng mL^{-1} TGF-β (M2) for 24 h at 37 °C and 5 % CO_2 in a humidified incubator. All cytokines were purchased from PeproTech or StemCell. After 24 h, cells were detached using versene (TFS) for 20 minutes at 37 °C and 5 % CO_2 in a humidified incubator. To assess successful polarization, cells were analyzed by flow cytometry (see section 3.2.10).

3.2.34 Statistical analysis

Statistical analysis was conducted using Prism software (GraphPad). Statistical significance was calculated using unpaired t test. Multiple comparisons were corrected using the Holm-Sidak method. $p \leq 0.05$ was defined as limit for statistical significance. P values are shown in figures using asterisks according to the following scheme: * $p < 0.05$, ** $p < 0.01$, *** $p < 0.001$. Error bars represent standard error of the mean (SEM), if not otherwise specified.

3.2.35 Ethics

Patients were treated at the Children's Hospital Zagreb (IL-2Rγ), UZ Leuven (CD33), or Gazi University Hospital (TREM2). Samples of study participants were acquired upon written consent. The studies followed all ethical standards defined by the 1964 Helsinki declaration and its amendments. Furthermore, studies and experiments were approved by the institutional review board at the University Hospital, LMU Munich, and were in agreement with the legal and ethical statutes.

4. Results

4.1 Novel *IL2RG* mutation causes IL-21R deficiency-like phenotype due to alternative splicing

Please note that the results presented in this part of the thesis were previously published in Illig, D. *et al*. 2019.[255] The clinical history and associated data were provided by our collaboration partners from the Children's Hospital Zagreb (Croatia). Previously published figures are reprinted by permission from Springer Nature Customer Service Centre GmbH: Springer Nature, Journal of Clinical Immunology, Alternative Splicing Rescues Loss of Common Gamma Chain Function and Results in IL-21R-like Deficiency, Illig, D. *et al.* 2019, see Apendix A.[255]

4.1.1 *IL2RG* mutation in two patients causes IL-21R deficiency-like phenotype

Two brothers (A.II-1, P1 and A.II-2, P2) from a non-consanguineous family with Romani background were diagnosed with chronic diarrhea (P1: infantile-onset, since 6 months of age; P2: neonatal-onset, since birth) at the Children's Hospital Zagreb (Croatia) (**Figure 17A**). The clinical history and routine immunological analysis of both patients has been provided by our collaboration partners from the Children's Hospital Zagreb (Croatia).[255]

In the first months after birth, P2 developed perianal abscesses that have been treated by surgical drainage. Additionally, both patients suffered from recurrent respiratory tract infections (i.e., otitis media, sinusitis), hepatomegaly (combined with splenomegaly for P2), and dilatation of the bile duct (i.e., ductus choledochus in P1) (**Figure 17B**). Moreover, P1 presented with recurrent viral infections, bacterial pneumonia, as well as failure to thrive and was diagnosed with arthritis of the left elbow and interphalangeal joints in both hands at the age of 4.5 years. At the same age, P1 also developed disseminated, eosinophil-rich skin granulomas associated with necrotic debris in their centers. Histological analysis of liver biopsies from P1 showed cholangitis, chronic inflammatory infiltrates, as well as macro- and microvesicular steatosis (**Figure 17B**). Furthermore, magnetic resonance cholangiography revealed dilatation of hepatic ducts (**Figure 17B**) and imaging indicated infection of the biliary system with *Cryptosporidium*, which was also detected in stool samples of P1.

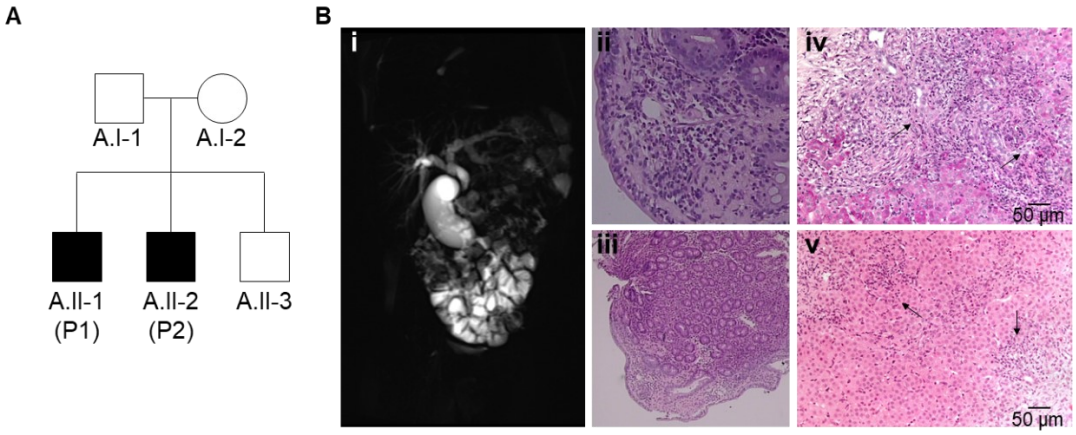

Figure 17: Identification of two patients with IL-21R-like deficiency.
(A) Pedigree of index family with father (A.I-1), mother (A.I-2), index patient (A.II-1, P1), second patient (A.II-2, P2), and healthy brother (A.II-3). (B)(i) Patient 1 (P1) suffered from hepatosplenomegaly with dilatation of the hepatic duct and ductus choledochus as shown by magnetic resonance cholangiography. (ii, iii) Histological assessment of small intestinal biopsies from P1 demonstrated reduced villus length and high frequencies of lymphocytes, plasma cells, eosinophils, and mastocytes. (iv, v) Visualization of chronic inflammatory infiltrates in the portal spaces of the liver of P1 by PAS (iv) and H&E (v) staining. Bile ducts showed proliferation and invasion of mononuclear cells into their walls. Data were generated by collaboration partners at the Children's Hospital Zagreb (Croatia). Figure from [255]. Reprinted by permission from Springer Nature Customer Service Centre GmbH: Springer Nature, Journal of Clinical Immunology, Alternative Splicing Rescues Loss of Common Gamma Chain Function and Results in IL-21R-like Deficiency, Illig, D. *et al.* 2019, see Apendix A.[255]

Routine immunological workup of both patients was performed at the Children's Hospital Zagreb (Croatia) and showed variable effects on different cell populations (**Table 55**). P1 presented with increased numbers of $CD3^+$ T cells and normal numbers of $CD4^+$ T cells, but P2 had normal $CD3^+$, and reduced $CD4^+$ T cell numbers. Whereas P1 showed an absolute and relative increase in eosinophils, P2 had normal absolute numbers, but increased relative frequencies of eosinophils. Common to both patients, $CD8^+$ T cell numbers were increased, which also resulted in an inverted $CD4^+/CD8^+$ T cell ratio (P1: 0.32, P2: 0.125, Normal range: 0.9 – 3.1) for both patients.[255] The numbers of $CD16^+CD56^+$ NK cells and $CD19^+$ B cells were unaffected in both patients.

Population	P1 [$\times 10^9$ L^{-1}]	P2 [$\times 10^9$ L^{-1}]	Normal range [$\times 10^9$ L^{-1}]
$CD3^+$	5.788	2.355	1.32 - 3.3
$CD4^+$	1.482	0.232	0.62 - 2.4
$CD8^+$	3.529	1.853	0.39 - 1.1
$CD16^+CD56^+$	0.353	0.309	0.19 - 0.74
$CD19^+$	0.847	1.081	0.27 - 2.050
Eosinophils	2.54 (13 %)	0.4 (9 %)	< 0.7 (< 6 %)

Table 55: Immune cell numbers in blood of patients during routine workup.
Data were generated by collaboration partners at the Children's Hospital Zagreb (Croatia).[255]

Since inverted T cell ratio might indicate HIV infection, both patients were tested for HIV and were found negative. Functionally, T cells showed mildly reduced proliferation upon stimulation with Phytohemagglutinin (P1: 16, P2: 10, normal: >17) and Concanavalin A (P2: 6, normal: >7). Analysis of B cell function during routine clinical workup at the Children's Hospital Zagreb demonstrated increased levels of IgM and IgA in both patients. In P1, total IgE and IgG levels were also increased, but IgG subtypes were reduced (P1: IgG1 1.77 g L^{-1}, normal range: 3.62 - 12.28 g L^{-1}; IgG2 < 0.34 gL^{-1}, normal range: 0.57 - 2.9 g L^{-1}). Furthermore, vaccination against hepatitis B and morbilli-parotitis-rubella failed to induce antibody responses in both patients indicating a functional defect in the B cell compartment.

In view of unavailable genetic diagnosis, B cell defects in both patients were treated by IVIG substitution (600 mg kg^{-1} per month). To prevent and/or treat recurrent infections, P1 and P2 were given azithromycin (20 mg kg^{-1} per day) and trimethoprim/sulfamethoxazole. Furthermore, medication of both patients included ursodeoxycholic acid, vitamin supplements, and hypercaloric enteral nutrition. After genetic diagnosis (see below), both patients received haploidentical HSCT with the mother as donor. Tragically, both patients died 60 days after HSCT due to GvHD complications (P1) or infections (P2) at the age of 6 and 4 years, respectively.

Since the observed distinct phenotype with diarrhea, chronic respiratory tract infections, cholangitis, and liver pathology associated with *Cryptosporidium* infection was reminiscent of IL-21R-deficient patients, patient samples were sent from the Children's Hospital Zagreb (Croatia) to the Dr. von Hauner's Children's Hospital (Munich, Germany) for genetic and immunological workup.[400, 402] To dissect the immunological status of both patients in detail, multicolor flow cytometry of peripheral blood was performed (**Figure 18**).

In line with defective responses to vaccination and altered levels of Ig levels, both patients showed reduced frequencies of $CD19^+CD20^+CD27^+IgD^+$ marginal-zone and $CD19^+CD20^+CD27^+IgD^-$ class-switched B cells suggesting impaired B cell maturation, which might indicate a common variable immunodeficiency (**Figure 18** lower panel).

Analysis of CD45RO and CCR7 expression in $CD4^+$ and $CD8^+$ T cells demonstrated normal development of T cells in both patients (**Figure 18** upper and middle panel). However, frequencies of $CD45RO^-CCR7^+$ naïve $CD8^+$ cells were reduced in both patients, which might be secondary to chronic infections observed in the patients (**Figure 18** middle panel).

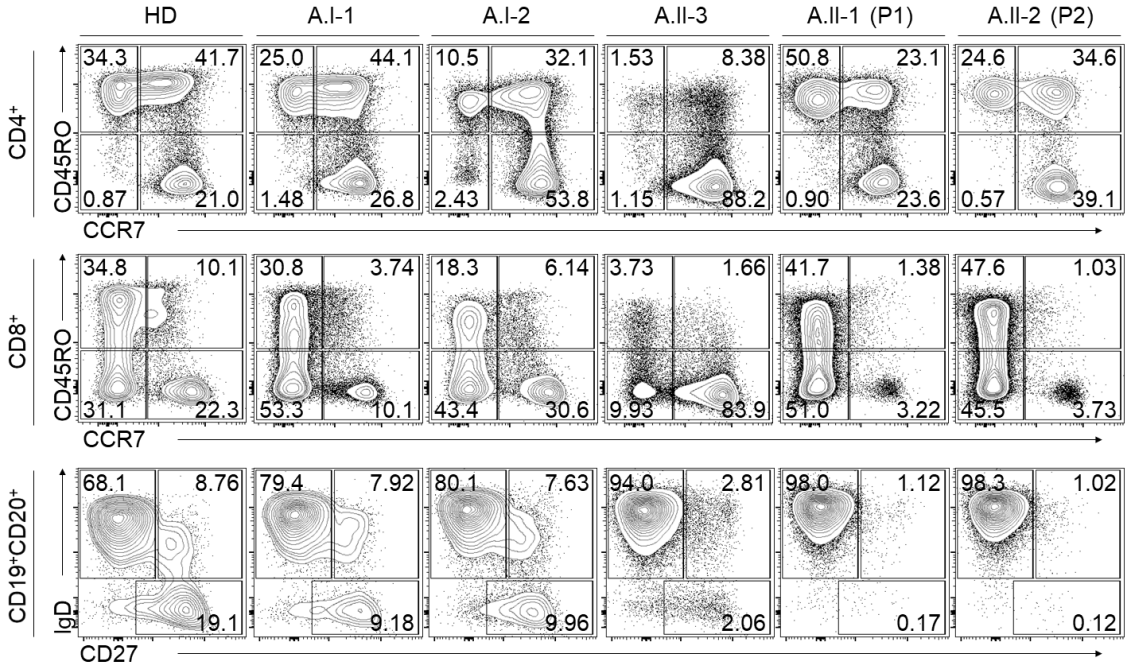

Figure 18: Identification of dysfunctional B cell maturation in both patients.
Representative analysis of peripheral blood $CD3^+CD4^+$ T_H cells, $CD3^+CD8^+$ cytotoxic T cells, and $CD19^+CD20^+$ B cells from a healthy donor (HD), father (A.I-1), mother (A.I-2), brother (A.II-3), patient 1 (A.II-1, P1), and patient 2 (A.II-2, P2). Both patients showed normal T cell development, but reduced frequencies of $CD19^+CD20^+CD27^+IgD^+$ marginal-zone and $CD19^+CD20^+CD27^+IgD^-$ class-switched B cells. Figure from [255]. Reprinted by permission from Springer Nature Customer Service Centre GmbH: Springer Nature, Journal of Clinical Immunology, Alternative Splicing Rescues Loss of Common Gamma Chain Function and Results in IL-21R-like Deficiency, Illig, D. *et al.* 2019, see Apendix A.[255]

Development of $CXCR3^+CCR6^-$ T_H1, $CXCR3^-CCR6^-$ T_H2, and $CXCR3^-CCR6^+$ T_H17 as well as $CD127^-CD25^+$ Tregs was unchanged in the patients (**Figure 19**).

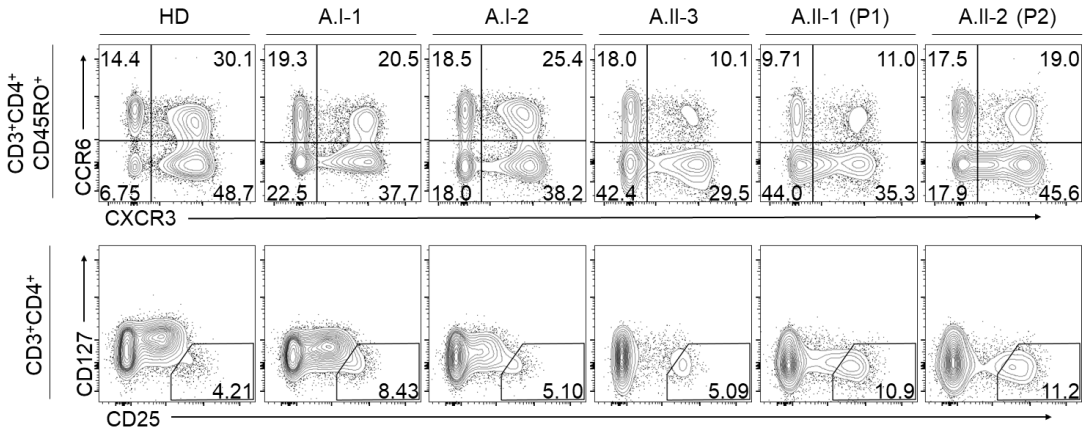

Figure 19: Normal T_H cell polarization and T_{reg} development in both patients.
Representative analysis of peripheral blood $CD3^+CD4^+CD45RO^+$ T_H cells and $CD3^+CD4^+$ T_{reg} cells from a healthy donor (HD), father (A.I-1), mother (A.I-2), brother (A.II-3), patient 1 (A.II-1, P1), and patient 2 (A.II-2, P2). Both patients showed normal polarization of $CXCR3^+CCR6^-$ T_H1 and $CXCR3^-CCR6^+$ T_H17 cells as well as similar development of $CD127^{low}CD25^+$ Treg cells compared to healthy controls.

Since the phenotype was reminiscent of IL-21R deficiency and the infantile onset was suggestive of a monogenetic disorder, WES was performed on genomic DNA isolated from peripheral blood of both patients at the sequencing core facility of the CCRC Hauner. Bioinformatic analysis focusing on rare and deleterious variants revealed a hemizygous mutation in *IL2RG* (ENST00000374202, X:70331302–70331303) deleting a single guanine (c.87delG) in exon 1. On the protein level, the mutation was predicted to cause a frameshift (p.Asn31MetfsTer12), which results in generation of a premature stop codon in exon 2. To confirm segregation of the identified mutation with disease in the affected family, genomic DNA of both patients and all unaffected family members (father, mother, brother) was analyzed by Sanger sequencing (**Figure 20**). As expected, both patients (A.II-1, P1 and A.II-2, P2) carried the hemizygous c.87delG mutation confirming the WES results. In line with an X-linked recessive inheritance, the mutation was found heterozygous in the mother (A.I-2), but all healthy males in the family (father A.I-1 and younger brother A.II-3) were wild-type.

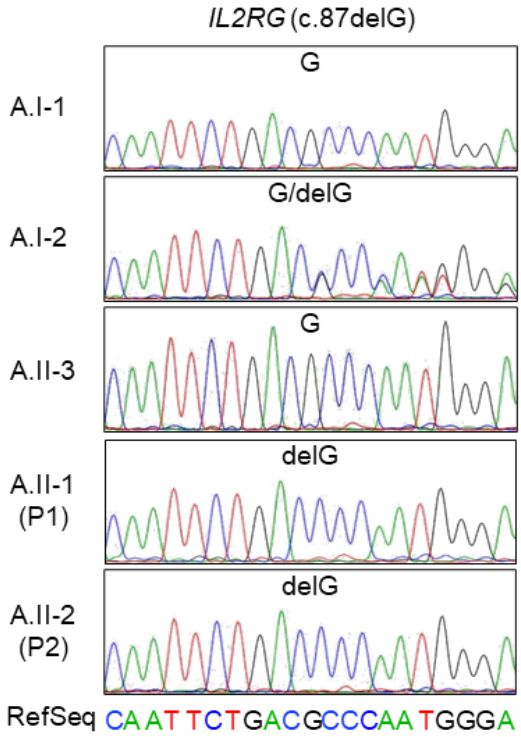

Figure 20: Confirmation of segregation of *IL2RG* mutation by Sanger sequencing. WES identified a c.87delG mutation in the gene *IL2RG* in both patients. Sanger sequencing of DNA from peripheral blood from both patients (A.II-1, P1 and A.II-2, P2) and unaffected relatives (Father: A.I-1, Mother: A.I-2, and healthy brother: A.II-3) demonstrated segregation of the mutation with the disease phenotype. Figure from [255]. Reprinted by permission from Springer Nature Customer Service Centre GmbH: Springer Nature, Journal of Clinical Immunology, Alternative Splicing Rescues Loss of Common Gamma Chain Function and Results in IL-21R-like Deficiency, Illig, D. *et al.* 2019, see Apendix A.[255]

4.1.2 IL-2Rγ expression is rescued by alternative splicing

Since no major developmental defects in T cells could be observed, the immune phenotype of both patients did not correspond to $T^-B^+NK^-$ SCID-X1 suggesting residual function of IL-2Rγ. However, deleterious mutations in *IL2RG*, like in this case, are known to usually cause severe SCID in humans and early premature stop codons increase the probability of mRNA decay, which would result in complete loss of IL-2Rγ. Therefore, expression of *IL2RG* in patient cell-derived EBV-LCLs was analyzed using qRT-PCR, immunoblotting, and flow cytometry (**Figure 21**).

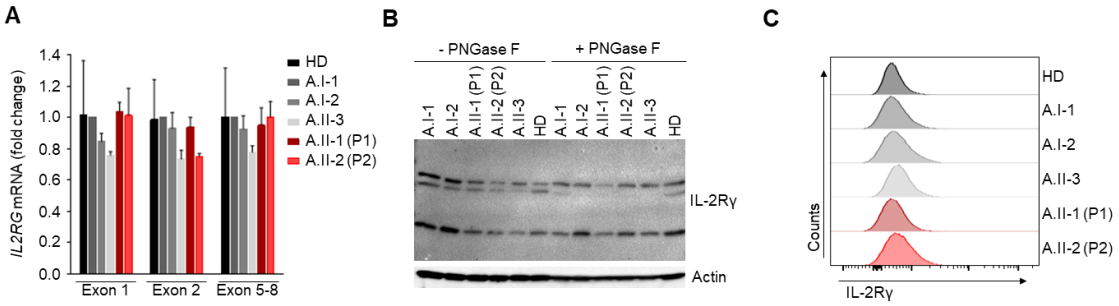

Figure 21: Normal *IL2RG* mRNA and IL-2Rγ protein expression in patient EBV-LCLs.
(A) qRT-PCR-based analysis of *IL2RG* mRNA expression in healthy donor (HD), father (A.I-1), mother (A.I-2), brother (A.II-3), patient 1 (A.II-1, P1), and patient 2 (A.II-2, P2) EBV-LCLs demonstrated comparable expression in all samples (n = 3). (B) Immunoblotting of EBV-LCL lysates showed normal IL-2Rγ protein expression in patients (representative analysis of n = 3 independent experiments). (C) Representative flow cytometry analysis showed normal IL-2Rγ surface expression in EBV-LCLs from all donors (n = 2). Figure from [255]. Reprinted by permission from Springer Nature Customer Service Centre GmbH: Springer Nature, Journal of Clinical Immunology, Alternative Splicing Rescues Loss of Common Gamma Chain Function and Results in IL-21R-like Deficiency, Illig, D. *et al.* 2019, see Apendix A.[255]

Levels of *IL2RG* mRNA were found comparable between healthy donors (HD), healthy family members (A.I-1, A.I-2, A.II-3), and both patients (A.II-1, P1; A.II-2, P2) indicating that mutated IL2RG mRNA is not subject to mRNA decay (**Figure 21A**). Furthermore, immunoblotting showed similar expression of IL-2Rγ in patient EBV-LCLs as compared with healthy controls (**Figure 21B**). To assess presence of IL-2Rγ on the surface of patient cells, EBV-LCLs were analyzed by flow cytometry demonstrating IL-2Rγ surface levels comparable to controls and healthy relatives (**Figure 21C**).

Taken together, expression and surface transport of *IL2RG* seems to be unaffected by the identified frameshift mutation indicative of an unknown mechanism rescuing *IL2RG* expression and function. Since the mutation is located in exon 1 and the potential premature stop codon is located in exon 2, an alternative start site might prevent the inclusion of the mutation or the stop

codon in the mRNA. However, *IL2RG* mRNA lacking exon 1 would probably lose the information encoding the signal peptide necessary for transport of IL-2Rγ to the cell surface, which would also result in loss of IL-2Rγ function and SCID. As the mutation is close to the 5' splice site of intron 1-2, another potential explanation for resolution of the frameshift would be alternative splicing. In fact, the *Ensemble Genome Browser* (https://grch37.ensembl.org/index.html; Human reference genome GRCh37.p13) lists several different transcripts for *IL2RG* mRNA produced by alternative splicing (**Figure 22A**). Interestingly, the transcript *IL2RG-002* uses an alternative 5' splice site of intron 1-2, which is located further downstream of the canonical splice site (**Figure 22A**). In a wild-type setting, the alternative splice site produces a premature stop codon directly with the base triplet at the boundary of exon 2 (**Figure 22B**), which will prevent expression of functional IL-2Rγ. In combination with the identified deletion at c.87, however, the premature stop codon, which is introduced by alternative splicing at the boundary of exon 2, is resolved (**Figure 22B**). Moreover, the combination of c.87delG and alternative splicing also restore the wild-type amino acid sequence starting with exon 2 (**Figure 22B**). The last amino acid of the alternative exon 1 with c.87delG is an alanine, which is also the last amino acid of the canonical exon 1 and increases the overlap between mutant and wild-type IL-2Rγ. Ultimately, c.87delG combined with alternative splicing of exon 1 results in 16 mutant amino acids. However, important motifs before the mutation (e.g., signal peptide) and after the mutation (e.g., transmembrane domain and signaling domain) remain unchanged, which might allow at least partial function (**Figure 22B**).

To test this hypothesis, a fragment of cDNA, which was generated from EBV-LCLs, was amplified using two different primer pairs. Whereas the first pair (reaction 1) was designed to amplify exon 1-3, the second pair (reaction 2) generated a PCR fragment spanning exon 1-4 (**Figure 22C**). Analysis of PCR products from both primer pairs by agarose gel electrophoresis revealed an additional band present only in the patients, but not in the controls (**Figure 22C**). Sequencing of the PCR fragments confirmed deletion of c.87G in cDNA of patient EBV-LCLs and showed additional signals downstream of the canonical splice site. The additional base reads were identical with the *IL2RG* sequence from intron 1 demonstrating inclusion of intronic sequences in the patients, but not in the controls. To quantitatively assess the amount of alternatively spliced *IL2RG* mRNA in the patients, RNA isolated from EBV-LCLs was analyzed by qRT-PCR using two different pair of primers (Reaction 3 and Reaction 4 in **Figure 22**). Both reactions demonstrated significantly increased expression of alternatively spliced *IL2RG* mRNA in EBV-LCLs from both

patients compared to controls. Interestingly, the alternative transcript was also detectable in healthy controls indicating rare usage of the alternative splice site in normal cells.

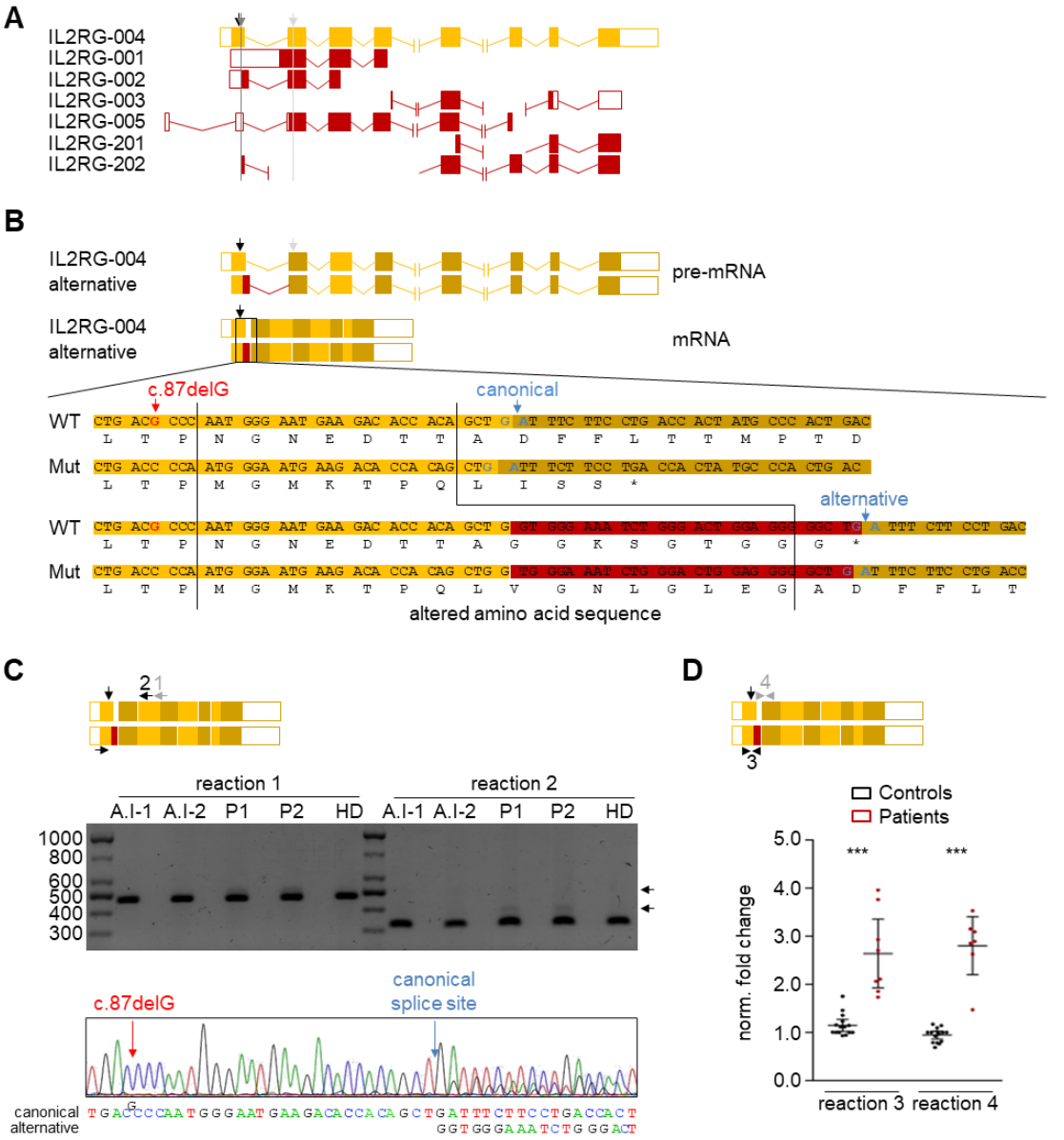

Figure 22: Loss of protein expression is rescued by alternative splicing.
(A) Overview of listed *IL2RG* transcripts in the *Ensemble Genome Browser* (Reference Genome GRCh37.p13). (B) Schematic hypothesis of effects on IL-2Rγ protein sequence by alternative splicing of exon 1 combined with c.87delG. (C) Analysis of cDNA isolated from EBV-LCLs of healthy donor (HD), father (A.I-1), mother (A.I-2), patient 1 (P1), and patient 2 (P2) using PCR reactions with two different sets of primers (reaction 1 and reaction 2). Representative image of agarose gel electrophoresis demonstrated additional bands in patient samples. Representative Sanger sequencing analysis showed additional signature downstream of the canonical splice site. (D) qRT-PCR analysis of alternatively spliced *IL2RG* mRNA using two different primer pairs demonstrated significantly increased expression of novel isoform in both patients (Error bars represent 95 % confidence interval; n = 4). Figure from [255]. Reprinted by permission from Springer Nature Customer Service Centre GmbH: Springer Nature, Journal of Clinical Immunology, Alternative Splicing Rescues Loss of Common Gamma Chain Function and Results in IL-21R-like Deficiency, Illig, D. *et al.* 2019, see Apendix A.[255]

4.1.3 *IL2RG* mutation mimics IL-21R-like deficiency

Since the patients showed normal numbers of T and NK cells, the specific patient phenotype strongly suggested that the mutation of 16 amino acids in the N-terminal domain of IL-2Rγ does not cause complete abrogation of signaling. To assess the effect of the identified mutation on signaling of different γ_c cytokines, phosphorylation of downstream signaling molecules was analyzed in PBMCs using phospho-flow and immunoblotting (**Figure 23**). For phospho-flow, PBMCs were stimulated with IL-2, IL-4, IL-7, IL-15, or IL-21 for 0, 5, 10, or 30 minutes, respectively, and $CD3^-$ and $CD3^+$ cells were analyzed for phosphorylation of STAT5 (pSTAT5, IL-2, IL-7, or IL-15), STAT3 (pSTAT3, IL-21), or STAT6 (pSTAT6, IL-4). STAT5 phosphorylation in response to IL-2 was mostly comparable between healthy controls and both patients, but the patients showed reduced levels of pSTAT5 in $CD3^-$ and $CD3^+$ cells after 30 minutes of IL-2 stimulation indicating enhanced downregulation of the signal.

In contrast IL-7 and IL-15 signaling was unaffected by the mutation, as no significant difference between control and patient samples with respect to STAT5 phosphorylation could be detected. Of note, IL-21-induced phosphorylation of STAT3 was significantly reduced in $CD3^+$ patients' cells after 10 and 30 minutes of stimulation indicating that the patient mutation affects IL-21 signaling. Furthermore, $CD3^-$ patient cells showed also significantly reduced pSTAT3 after 5 minutes of stimulation. In $CD3^-$, pSTAT3 levels were also lower after 10 and 30 minutes, but the difference was not significant.

While a comparable increase in phosphorylation of STAT6 upon IL-4 stimulation for 5 minutes could be observed in $CD3^-$ patient cells, levels of pSTAT6 didn't increase further over time in patient cells in comparison to control samples. Moreover, IL-4 stimulation also resulted in phosphorylation of STAT6 in $CD3^+$ cells of controls but failed to induce STAT6 activation in $CD3^+$ patient cells indicating disturbed IL-2Rγ-mediated IL-4 signaling in patients. To confirm cytokine-specific defects of mutated IL-2Rγ, IL-2 and IL-21-mediated signaling was independently analyzed by immunoblotting. In this experimental setting, healthy donor or patient EBV-LCLs were stimulated for 0, 10, or 30 minutes with IL-2 or IL-21 and phosphorylation of STAT3 and STAT5 was analyzed. In line with phospho-flow data, IL-2 induced phosphorylation of STAT5 in both patients, but levels were lower compared to healthy controls. Furthermore, healthy donor EBV-LCLs demonstrated substantial phosphorylation of STAT3 and STAT5 after IL-21

stimulation, but STAT3 phosphorylation was strongly reduced and STAT5 phosphorylation was not detectable in patient cells. Taken together, functional studies demonstrated that both patients show normal responses to IL-2, IL-7, and IL-15, but defective signaling upon stimulation with IL-4 and IL-21. Whereas IL-2, IL-7, and IL-15 are known to be critical for T and NK cell development, IL-4 and IL-21 are necessary for B cell maturation. In line, the patients showed defective B cell maturation but normal T and NK cell development.

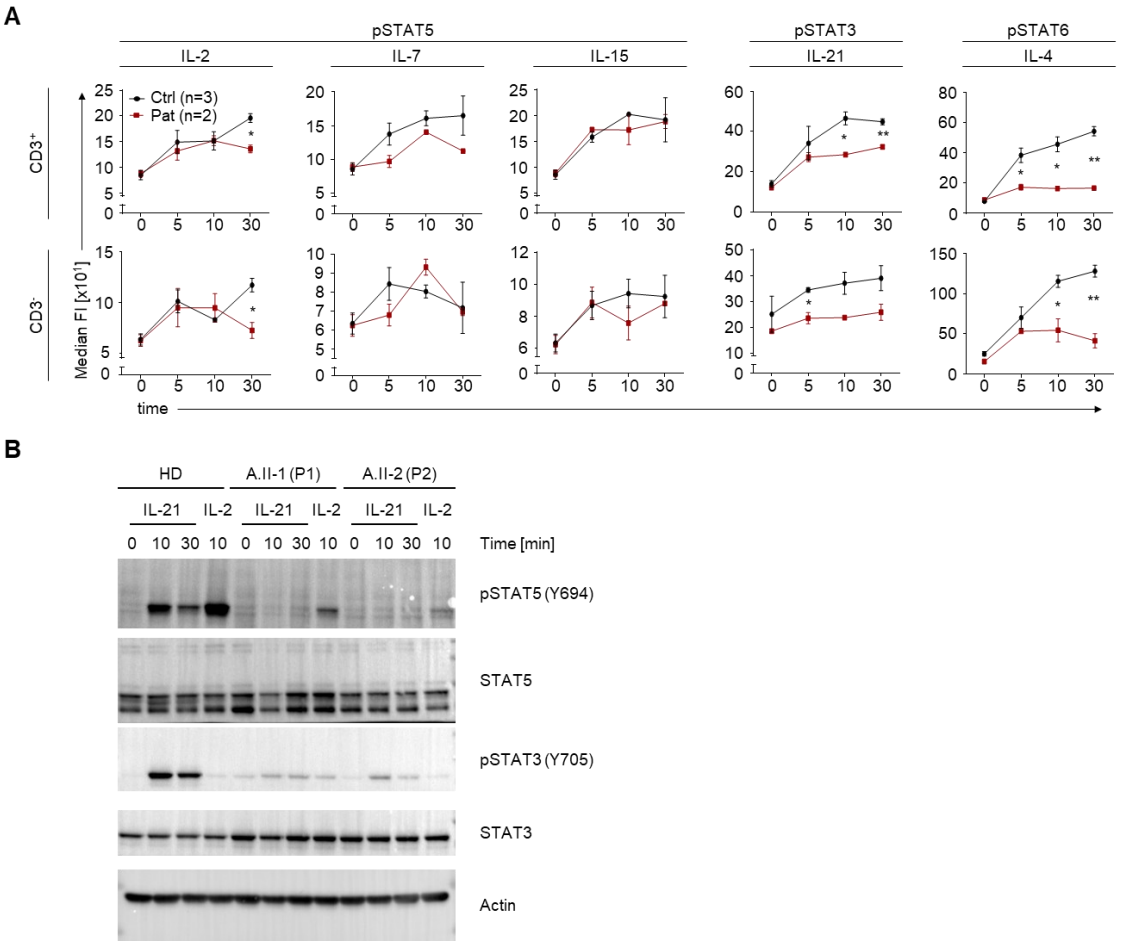

Figure 23: IL2RG mutation functionally mimics IL-21R deficiency.
(A) Representative phospho-flow analysis of STAT3, STAT5, and STAT6 phosphorylation in $CD3^-$ and $CD3^+$ PBMCs isolated from healthy donors (HD) or both patients upon IL-2, IL-4, IL-7, IL-15, or IL-21 stimulation for 0, 5, 10, or 30 minutes (n = 2) (B) Representative immunoblot analysis of STAT3 and STAT5 phosphorylation in EBV-LCLs from a healthy-donor (HD), patient 1 (A.II-1), or patient 2 (A.II-2) upon stimulation with IL-2 or IL-21 for different time points. Figure from [255]. Reprinted by permission from Springer Nature Customer Service Centre GmbH: Springer Nature, Journal of Clinical Immunology, Alternative Splicing Rescues Loss of Common Gamma Chain Function and Results in IL-21R-like Deficiency, Illig, D. *et al.* 2019, see Apendix A.[255]

The mutated 16 amino acids are found at the N-terminus of the protein, so they are closely located to the cytokine binding site of IL-2Rγ, and they might affect differential binding of certain cytokines. Since the protein structures of IL-2Rα, IL-2Rβ, IL-2Rγ, IL-4Rα, and IL-15Rα have been resolved, binding of IL-2, IL-4, and IL-15 to their respective receptor complex (IL-2R (PDB: 2B5I), IL-4R (PDB: 3BPL), and IL-15R (PDB: 4GS7)) can be analyzed using structural analysis.[593-595] However, terminal domains of proteins are often unstructured and/or flexible, which makes them hard to access for crystallization and structural analysis. In line, the N-terminal end of IL-2Rγ is not included in the published protein structures. To compare the N-terminal domains of wild-type and mutant IL-2Rγ, both were modeled *de novo* and were aligned to the published structure of IL-2Rγ in the three complexes (IL-2R, IL-4R, and IL-15; **Figure 24**).

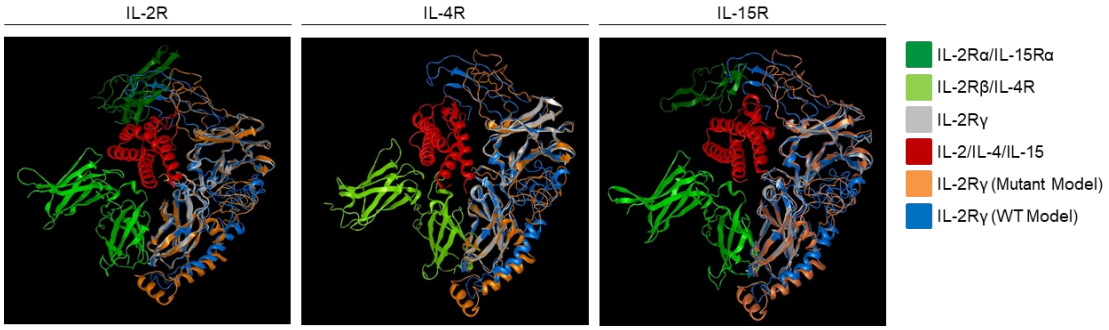

Figure 24: Structure prediction suggested distinct effects of mutant IL-2Rγ on γ_c receptors. Alignment of *de novo* generated protein structures of wild-type (WT) and mutant IL-2Rγ with solved crystal structures of the (IL-2R (PDB: 2B5I), IL-4R (PDB: 3BPL), and IL-15R (PDB: 4GS7).[593-595] Figure from [255]. Reprinted by permission from Springer Nature Customer Service Centre GmbH: Springer Nature, Journal of Clinical Immunology, Alternative Splicing Rescues Loss of Common Gamma Chain Function and Results in IL-21R-like Deficiency, Illig, D. *et al.* 2019, see Apendix A.[255]

In the overlapping parts the predicted structures were largely similar to the published protein structures, indicating that the prediction provides a good model for IL-2Rγ. Whereas wild-type IL-2Rγ shows a largely structured N-terminal domain with two β-sheets, mutant IL-2Rγ is predicted to be more compact and less structured. The compactness of the N-terminal domain might increase the distance of mutant IL-2Rγ to the bound cytokines. Furthermore, the cytokines are less enclosed by the mutant N-terminal domain as compared to the wild-type. The IL-2R and the IL-15R are heterotrimeric and are built by an additional subunit that increases the affinity of the cytokine to the receptor, which might enhance the binding of the cytokine despite reduced stabilization by the ligand binding domain of IL-2Rγ. In line, signaling of heterotrimeric receptors with mutant IL-2Rγ might allow functional IL-2 and IL-15 signaling. However, affinity of cytokines

to receptors without additional subunit might be strongly reduced and cause altered signaling of IL-4 and IL-21.

4.2 Novel mutations affecting expression and function of CD33

4.2.1 Identification of a VEO-IBD patient with biallelic *CD33* mutations

A patient from a non-consanguineous family (**Figure 25A**) presented with severe, refractory VEO-IBD and vasculitis to collaborating physicians at the UZ Leuven (Leuven, Belgium).

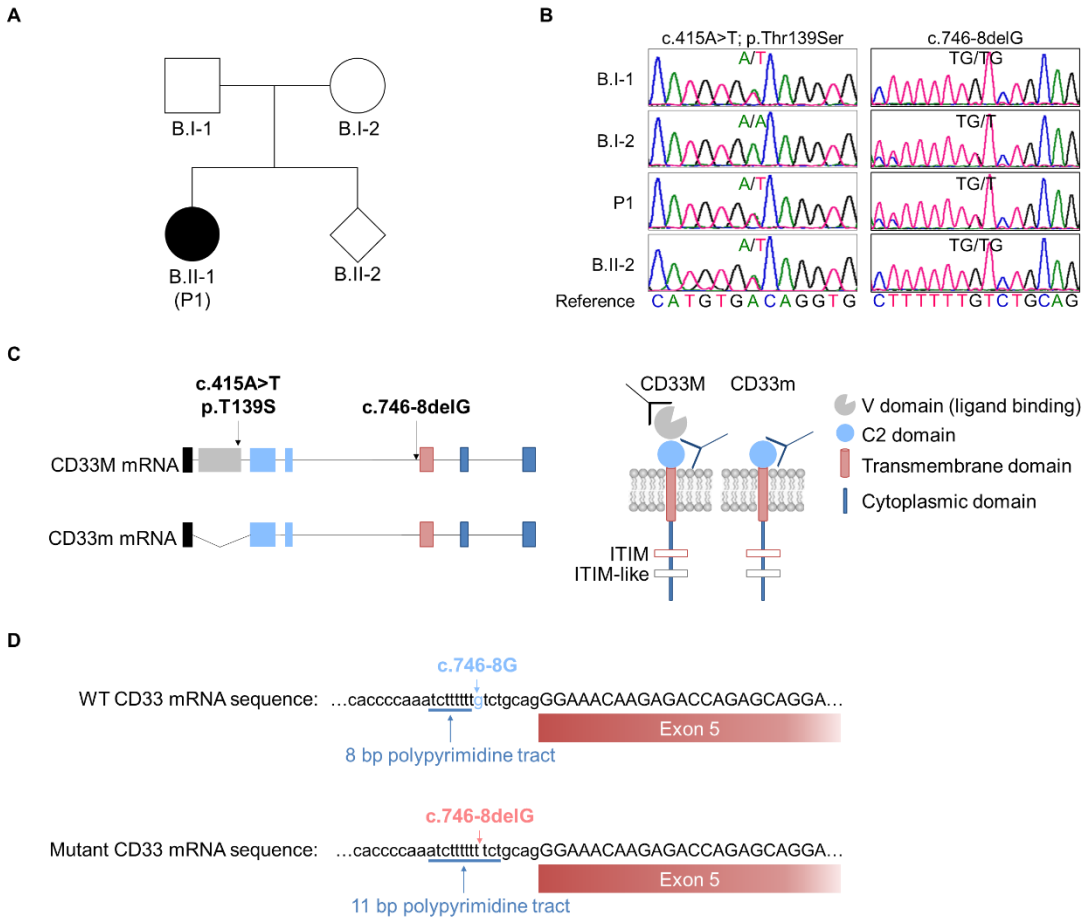

Figure 25: Biallelic CD33 mutations in a VEO-IBD patient.
(A) Pedigree of index family including father (B.I-1), mother (B.I-2), patient (B.II-1, P1), and healthy sibling (B.II-2). (B) Sanger sequencing of gDNA isolated from peripheral blood confirmed segregation of mutations with disease phenotype. (C) Schematic overview of CD33 mRNA and protein structure. CD33 is expressed as two isoforms (CD33M and CD33m), which differ in exon 2 splicing. Index mutations are located in exon 2 (c.415A>T, p.T139S) and in the 3' splice region of intron 4-5 (c.746-8delG). (D) c.746-8delG extends polypyrimidine tract in the 3' splice region of intron 4-5. WT, wild-type.

WES on gDNA isolated from peripheral blood cells revealed compound heterozygous mutations in *CD33* (Mutation 1: 19:51728851, ENST00000262262, c.415A>T, p.Thr139Ser; Mutation 2: 19:51738403, ENST00000262262, c.746-8delG) in the patient. Sanger sequencing confirmed

segregation of the mutations with disease phenotype in samples from healthy relatives (**Figure 25B**). In detail, the father (B.I-1) and the healthy sibling (B.II-2) carried the c.415A>T mutation and the mother (B.I-2) was heterozygous for the c.746-8delG mutation (**Figure 25B**). Mutation 1 is located at the 3' end of exon 2 (fourth from last base pair before the 5' splice site of intron 2-3) and causes a substitution of Threonine139 to Serine (**Figure 25C**). However, bioinformatic analysis predicted that the c.415A>T mutation results in activation of a cryptic splice donor site, creation of an additional exonic splicing silencer (ESS) element, and disruption of a canonical exonic splice enhancer (ESE) motif, which may alter canonical splicing of exon 2. Of note, exon 2 is known to be skipped in the CD33m isoform, which results in a smaller CD33 protein lacking the ligand binding V domain (**Figure 25C**).

Mutation 2 causes a deletion of a guanosine at position c.746-8 in the 3' splice region of intron 4-5 upstream of exon 5, which encodes the transmembrane domain of CD33. 3' splice regions contain a polypyrimidine tract that is an important binding site for splice enhancers and silencers.[602] The length and continuity of the polypyrimidine tract can control the strength of the 3' splice site (i.e., how often the splice site is used for splicing of the pre-mRNA).[602] Of note, the guanine at position c.746-8 is the only purine that disrupts the polypyrimidine tract in the 3' splice site of intron 4-5 (c.746-5 to c.746-16) of *CD33* pre-mRNA (**Figure 25D**). Therefore, deletion of c.746-8G by mutation 2 increases the length of the polypyrimidine tract from 8 bases to 11 bases and might alter the strength of the 3' splice site in intron 4-5 of *CD33* pre-mRNA (**Figure 25D**).

4.2.2 Patient mutations cause aberrant CD33 expression in peripheral blood cells

CD33 is routinely used as marker for myeloid cells. To characterize the effects of the mutations on CD33 surface expression, patient immune cells in the peripheral blood were analyzed by high dimensional immunophenotyping (**Figure 26**).

Immune cells that usually have a high CD33 expression (e.g., $CD14^{+}CD16^{-}$ classical monocytes) showed comparable CD33 levels between the patient and the controls (see panel 1 in **Figure 26A**). However, cells that usually present with low expression of CD33 on the surface including $CD16^{-}$ granulocytes (presumably eosinophils, see panel 2 in **Figure 26A**) and $CD11c^{+}CD123^{-}$ myeloid DCs (see panel 3 in **Figure 26A**) expressed substantially higher CD33 levels in the patient. Of note, analysis of $CD3^{-}CD19^{-}$ myeloid cells in the patient blood further

demonstrated presence of CD33 on cells that usually do not express CD33 (see panel 4 in **Figure 26A**). In detail, CD33 expression could be observed in $CD56^{int}CD16^{int}$ cells in the patient, but not in healthy controls. This population includes $CD56^{+}CD16^{+}$ mature NK cells but might also consist of immature $CD56^{+}$ myeloid cells, which usually cannot be detected in peripheral blood. Furthermore, immunophenotyping revealed lack of $HLA\text{-}DR^{+}CD16^{+}$ monocytes in peripheral blood of the index patient (see panel 1 in **Figure 26B**). Interestingly, HLA-DR and CD16 expression was downregulated in $CD33^{high}$ cells, but normal in $CD33^{-/low}$ patient cells compared to healthy controls (see panel 2 and 3 in **Figure 26B**).

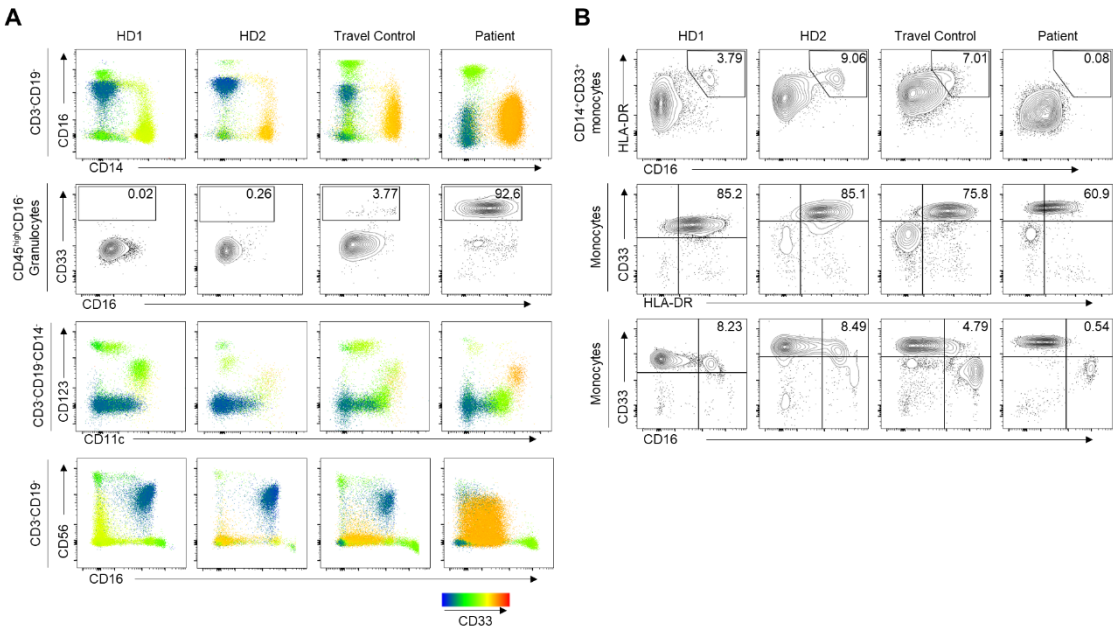

Figure 26: Aberrant CD33 expression in patient peripheral blood cells.
(A) Immunophenotyping of two healthy donors (HD), healthy travel control, or patient peripheral blood cells using multicolor flow cytometry revealed increased CD33 expression in various immune populations. CD33 expression levels are color coded. (n = 2 independent experiments)
(B) Immunophenotyping analysis showed increased CD33 expression and reduced expression of HLA-DR and CD16 in patient monocytes. $CD16^{-}$ granulocytes presented with aberrant CD33 expression and numbers of $CD33^{+}CD16^{+}$ granulocytes were increased in the patient.

Aberrant expression of CD33 in the patient was confirmed in an independent flow cytometric analysis of samples from the patient, healthy controls, and healthy relatives (father, mother, sibling) of the patient using different antibodies recognizing CD33M and CD33M+m (**Figure 27**).

$CD14^{+}$ cells demonstrated only minor differences in CD33 expression levels, but $CD14^{-}$ cells from the patient showed substantial CD33 expression (**Figure 27**). In healthy controls and the father, $CD14^{-}$ cells mostly lacked expression of CD33 indicating aberrant expression of CD33 in the patient (**Figure 27**). Patient $CD14^{-}$ cells all expressed CD33M on their surface since there was

no difference between both tested antibodies. However, CD33m might be co-expressed with CD33M on the surface, which cannot be assessed with available CD33 antibodies. Patient granulocytes had also slightly increased CD33 expression. In contrast to PBMCs, granulocytes isolated from patient blood were only partly positive when using an antibody specific for CD33M but were completely positive for CD33M+m, which indicates that some granulocyte populations express only CD33m (**Figure 27**).

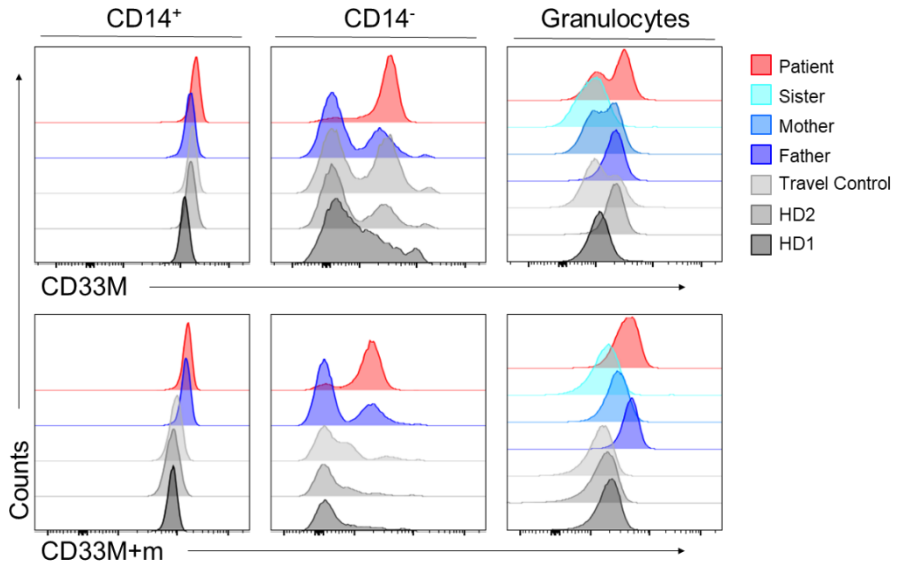

Figure 27: Increased CD33 expression in CD33^{low} cell populations.
Flow cytometry analysis using two CD33-specific antibodies demonstrated increased CD33 expression in patient CD14$^-$ cells and granulocytes, but only slightly increased CD33 expression in CD14$^+$ cells.

Although CD33 is known as myeloid cell marker, it was shown to be also expressed on lymphocyte populations after activation indicating a broader function of CD33 in regulating immune cell activation.[450, 451] Therefore, lymphocyte populations were analyzed by multi-color immunophenotyping and CD33 expression was assessed using flow cytometry (**Figure 28**). Immunophenotyping revealed normal lymphocyte development associated with an increased frequency of CCR6$^+$CXCR3$^-$ T_H17 cells in the peripheral blood of the patient compared to healthy controls (**Figure 28A**). Furthermore, flow cytometry showed increased frequencies of CD33$^+$CD3$^+$CD19$^-$ T cells and CD33$^+$CD3$^-$CD19$^+$ B cells indicating that increased CD33 expression is affecting both lymphocytes and myeloid cells (**Figure 28B**). To further assess expression of CD33 in lymphocytes of the patient, T cells were activated with immobilized anti-CD3 and soluble anti-CD28 and CD33 expression was analyzed over time (**Figure 28C**). In line with data from myeloid subsets, a significantly increased CD33 expression could be detected

on activated CD4⁺ T cells from the patient compared to healthy controls (**Figure 28C**). Whereas CD33 expression on the surface of the cells from the father was indistinguishable from healthy controls, cells isolated from the mother showed intermediate CD33 expression, which was also significantly up-regulated compared to healthy controls indicating an involvment of the c.746-8delG mutation in CD33 up-regulation (**Figure 28C**). Furthermore, no difference in CD33 expression could be observed for activated CD8⁺ T cells suggesting that the observed phenotype might be specific for CD4⁺ T cells (**Figure 28C**).

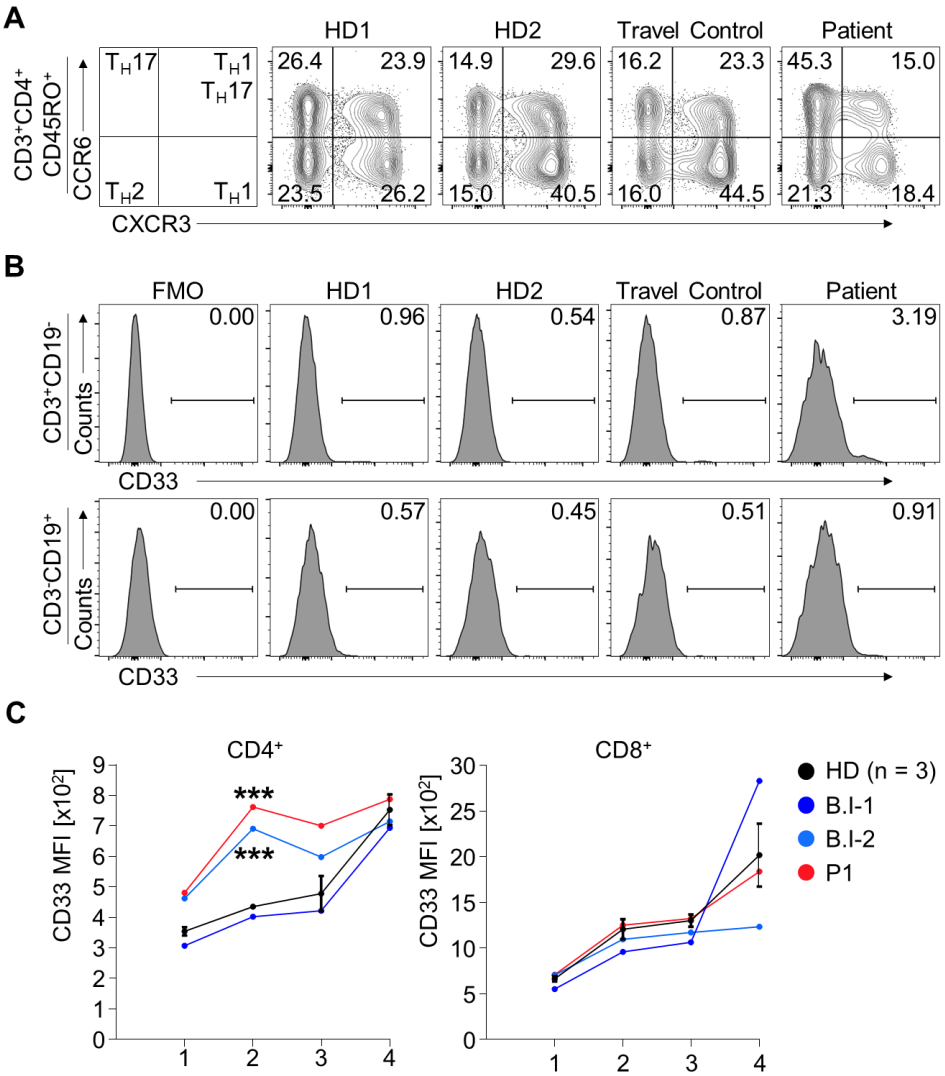

Figure 28: Altered lymphocyte phenotypes in index patient.
(A) Immunophenotyping of two healthy donors (HD), healthy travel control, or patient peripheral blood cells using multicolor flow cytometry revealed increased frequency of CCR6⁺CXCR3⁻ T_H17 cells. (B) Flow cytometry analysis of CD33 expression in CD3⁺CD19⁻ T cells and CD3⁻CD19⁺ B cells demonstrated increased frequencies of CD33⁺ cells in the patient. (C) Representative analysis of CD33 expression in CD4⁺ or CD8⁺ T cells stimulated with anti-CD3/anti-CD28 for 1-4 days revealed significantly increased CD33 levels in patient CD4⁺ T cells (n = 2 independent experiments).

4.2.3 Generation of patient-specific iPSC using CRISPR/Cas9-mediated genetic engineering

The access to primary patient material is limited due to clinical and logistic reasons. However, studies on myeloid cells are critically dependent on fresh blood samples, as they are easily affected by prolonged transport times and/or cryopreservation. iPSC-derived myeloid cells allow characterization of CD33 mutations independent of primary patient material in physiological model systems. Therefore, iPSC with CD33 KO and patient-specific KI were generated using CRISPR/Cas9-mediated genome engineering (**Figure 29**). KO clones with two different deletions (185 and 184 bp deletions) were successfully generated. These deletions cause frameshifts that result in an immediate premature stop codon in exon 3 (184 bp deletion) or in a more downstream stop codon (185 bp deletion) (**Figure 29A**).

Furthermore, homozygous c.415A>T (**Figure 29B**) and c.746-8delG (**Figure 29C**) iPSC clones could be successfully generated by genetic editing allowing modelling of patient specific phenotypes in iPSC-derived myeloid cells.

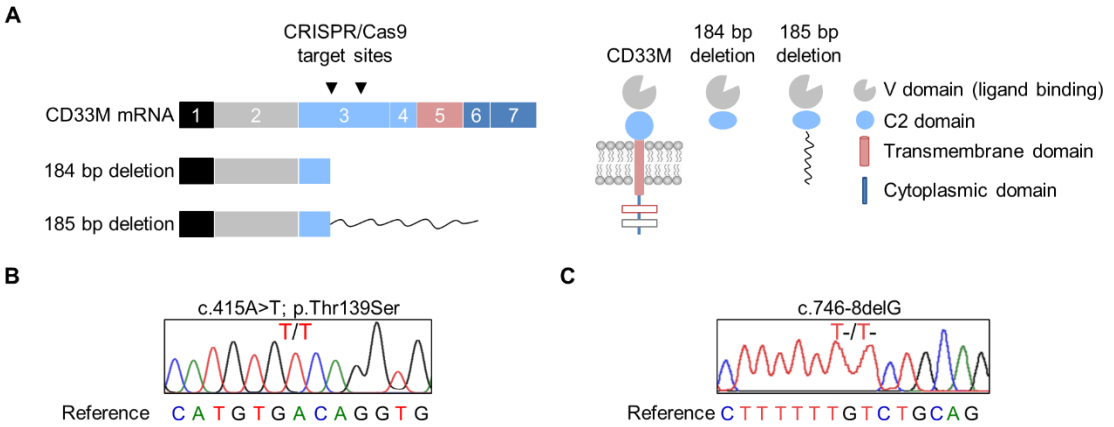

Figure 29: Generation of patient-specific KI and KO iPSC lines by CRISPR/Cas9-mediated genetic engineering.
(A) Schematic overview of strategy and outcome of CRISPR/Cas9-mediated KO of CD33 in iPSC. Cas9 guide RNAs were designed to target two positions in exon 3 of CD33 and to cause a deletion of 185 bp, which results in a frameshift and a premature stop codon. In some clones, 184 bp were deleted, which causes a frameshift, but with an immediate stop codon in exon 3. (B, C) Representative Sanger sequencing analysis demonstrated successful homozygous KI of c.415A>T (B) or c.746-8delG (C) in iPSC lines.

4.2.4 CD33-mutant iPSC-derived cells show altered CD33 surface expression

To characterize both mutations in a physiologically relevant model, a protocol was established to generate CRISPR/Cas9-edited iPSC-derived macrophages carrying CD33 KO or patient-specific KI mutations. Progress and efficiency of macrophage differentiation was evaluated over time using flow cytometry. On day 9, the majority of $CD45^+$ hematopoietic cells differentiated from wild-type iPSC showed expression of the stem cell marker CD34 and myeloid marker CD33 but lacked expression of the monocyte marker CD14 suggesting that these cells have an early myeloid progenitor cell identity (**Figure 30**).

As expected, cells differentiated from CD33 KO iPSC lacked CD33 surface expression proving a successful, homozygous KO generated by CRISPR/Cas9-mediated genetic engineering. In contrast to observations from primary patient material, CD33 expression was also not detectable on the surface of cells homozygous for $CD33^{c.415A>T}$, which might be caused by a dysregulated CD33 isoform balance. $CD33^{c.746\text{-}8delG}$ cells showed normal surface expression of CD33. CD33 KO and CD33 KI cells demonstrated increased frequencies of $CD34^-$ cells suggesting a faster differentiation of CD33-mutated cells (**Figure 30**).

During differentiation, the number of $CD34^+$ stem or progenitor cells decreased, while the number of $CD14^+$ monocytes/macrophages increased in all genotypes over time indicating successful hematopoiesis and efficient generation of iPSC-derived monocytes/macrophages (**Figure 30**). Although numbers of $CD34^+$ cells were rapidly decreasing after day 9, CD33 KO and CD33 KI cell lines showed consistently lower $CD34^+$ cell numbers compared to wild-type samples during differentiation. However, this reduced frequency of progenitor cells was not paralleled by an increased number of $CD14^+$ monocytes/macrophages. Finally, up to 70 % $CD14^+$ monocytes/macrophages could be detected on day 19 of differentiation allowing analysis of CD33 mutants in a relevant physiological model.

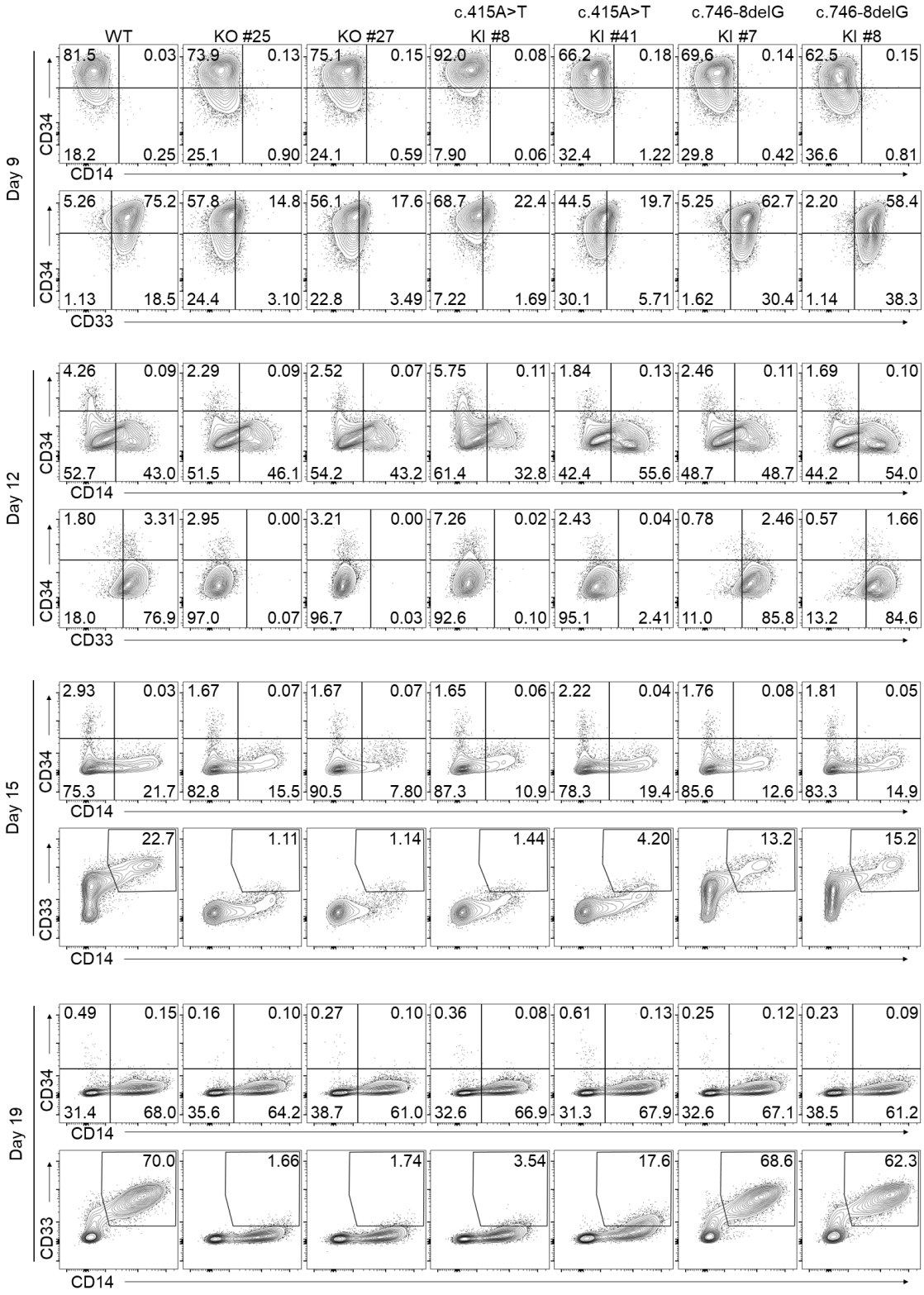

Figure 30: CD33-mutated iPSC-derived macrophages revealed altered CD33 surface expression.

Representative flow cytometry analysis of hematopoietic cell surface markers (CD34, CD33, CD14) during differentiation of macrophages from wild-type (WT), knock-out (KO), and patient-specific knock-in (KI) iPSC over time shows efficient development of $CD45^+$ $CD14^+$ monocytes or macrophages. KO and $CD33^{c.415A>T}$ cells show absent CD33 expression on the cell surface (n = 5 independent experiments).

Successful generation of iPSC-derived monocytes/macrophages was independently confirmed by cytospin analysis demonstrating presence of normal monocytes/macrophages at similar frequencies in samples from all genotypes (**Figure 31**).

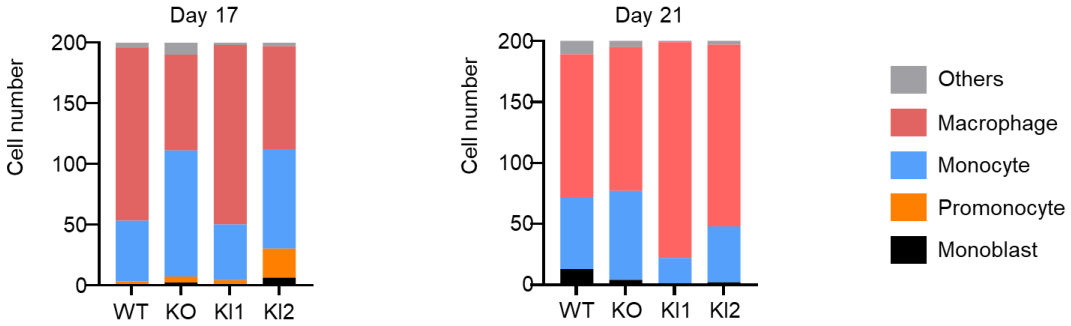

Figure 31: Cytospin analysis revealed similar composition of generated cells.
Representative cytospin analysis of hematopoietic cells generated from CD33 knock-out (KO), CD33$^{c.415A>T}$ (KI1), and CD33$^{c.746\text{-}8delG}$ (KI2) iPSC demonstrates successful generation of monocytes/macrophages.

To allow analysis of CD33 expression and function in non-macrophage cells (i.e., granulocytes), CRISPR/Cas9-edited iPSC carrying CD33 KO or patient-specific KI mutations in CD33 were also differentiated towards granulocytes. Differentiation of granulocytes and development of CD33 expression was analyzed using flow cytometry and cytospin (**Figure 32A,B**). Analogous to observations from macrophage differentiations, CD33 KO and CD33$^{c.415A>T}$ hematopoietic cells displayed no CD33 surface expression at any time of differentiation (**Figure 32A**). As expected, hematopoietic cells did not upregulate CD14 and CD33 surface expression over time indicative of successful generation of neutrophil granulocytes with low monocyte contaminations (**Figure 32A**). In line, cytospin analysis showed presence and maturation of mature neutrophils with increasing frequency over time proving efficient differentiation of granulocytes from iPSC (**Figure 32B**).

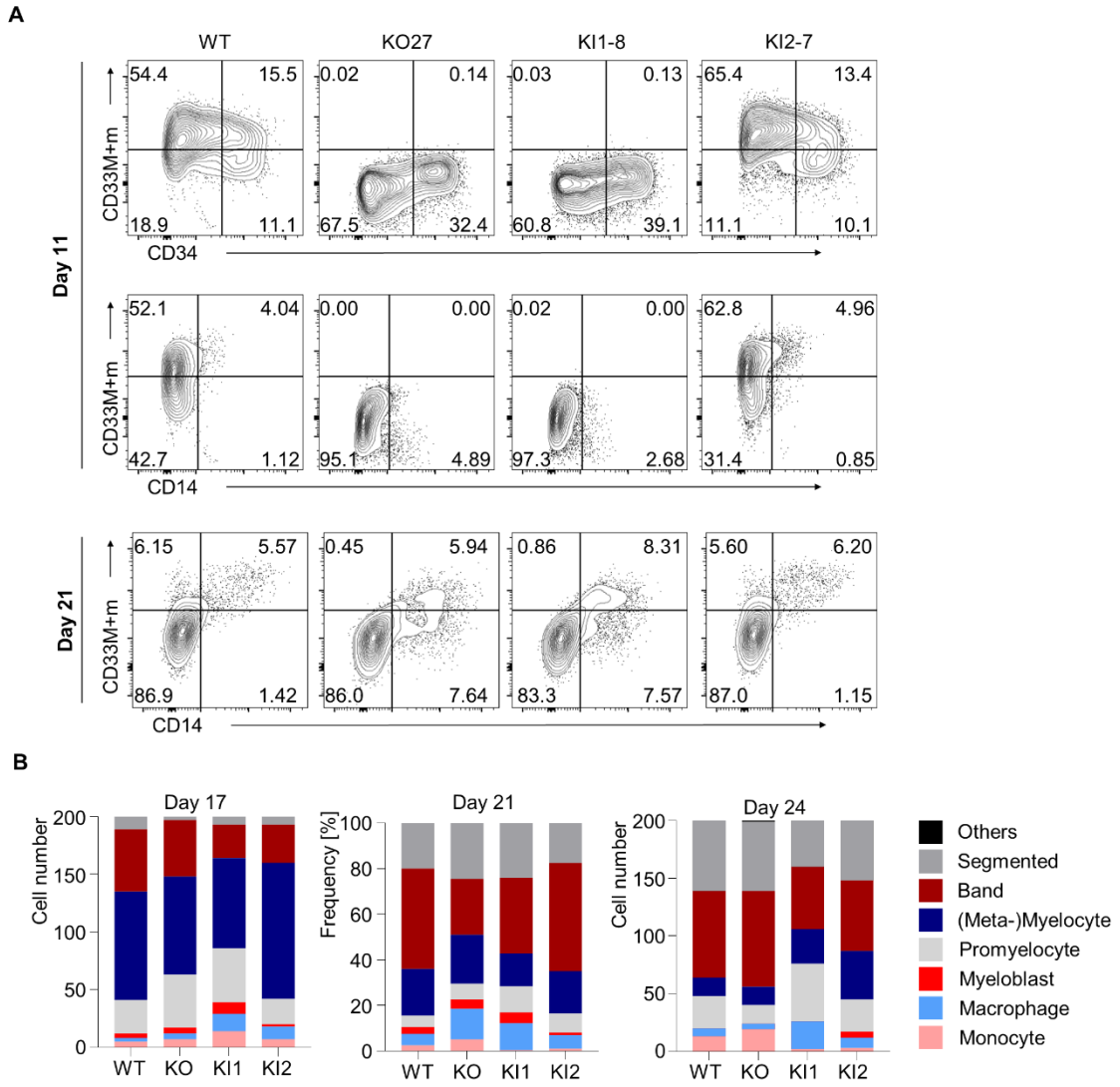

Figure 32: iPSC-derived granulocytes showed altered CD33 isoform expression.
(A) Flow cytometry analysis of hematopoietic cell surface markers during differentiation of granulocytes from wild-type (WT), knock-out (KO), and patient-specific knock-in (KI) iPSC over time showed efficient development of $CD45^{+}CD14^{-}$ granulocytes (n = 3 independent experiments). KO and $CD33^{c.415A>T}$ cells showed absent CD33 expression on the cell surface (B) Representative cytospin analysis of hematopoietic cells generated from CD33 knock-out (KO), $CD33^{c.415A>T}$ (KI1), and $CD33^{c.746\text{-}8delG}$ (KI2) iPSC demonstrated successful generation of neutrophils over time.

4.2.5 CD33 mutations cause dysregulated *CD33* isoform balance

Both mutations were predicted to alter splicing of *CD33* pre-mRNA by bioinformatic analysis and iPSC-derived macrophages demonstrated aberrant surface expression of CD33 indicating a dysregulated isoform balance. Therefore, expression of *CD33* isoforms was analyzed on the mRNA level in peripheral blood monocytes by qRT-PCR (**Figure 33A**).

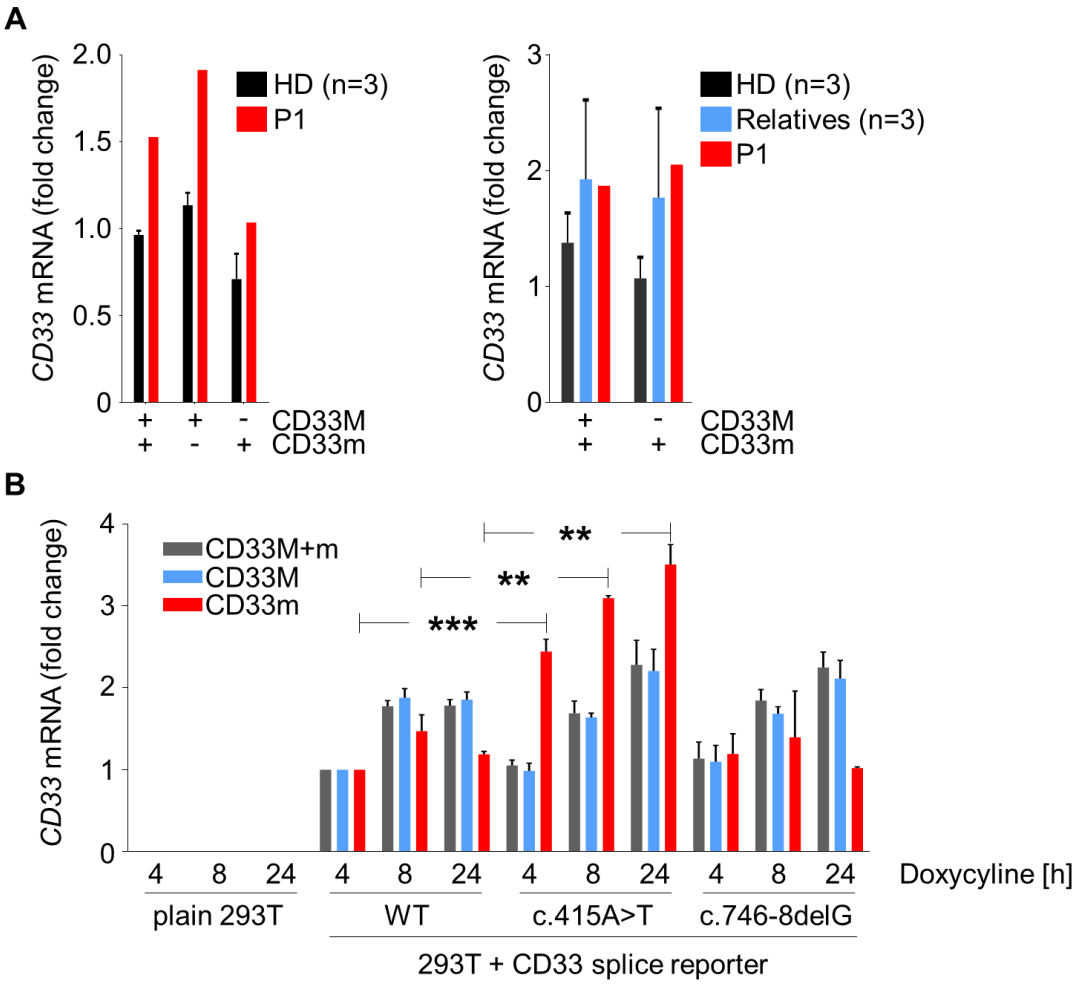

Figure 33: c.415A>T mutation resulted in increased exon 2 skipping.
(A) Analysis of *CD33* mRNA expression in peripheral blood monocytes from healthy donors (HD), healthy relatives, and the index patient (P1) showed slightly increased expression of CD33 in the index family (n = 2 independent experiments). (B) qRT-PCR analysis of *CD33* mRNA expression in HEK293T cells over-expressing CD33 mini-genes with patient-specific mutations revealed significantly increased expression of CD33m isoforms in cells expressing $CD33^{c.415A>T}$ (n = 2 - 4 independent experiments).

In both experiments, slightly increased expression of total *CD33* mRNA (CD33M+m) could be detected in the patient as compared with two healthy controls, which is in line with increased CD33 surface expression detected by flow cytometry (**Figure 33A**). However, in the second experiment healthy relatives also showed increased *CD33* expression comparable to the patient (**Figure 33A**). The overall higher *CD33* mRNA expression was accompanied by an increased expression of both CD33 isoforms. Considering that the largest expression variations of CD33 were detected on non-monocytes in immunophenotyping, larger differences on the mRNA level as well as isoform balance might be masked in monocytes, as they naturally express high CD33 levels. Furthermore, differential effects of the two mutations might be overseen due to a

heterozygous state and might be comparable to healthy relatives but could cause disease in combination.

To further characterize the effects of the identified patient mutations on *CD33* pre-mRNA splicing, doxycycline-inducible CD33 mini-genes carrying patient-specific mutations were stable overexpressed in HEK293T cells and CD33 expression was analyzed by qRT-PCR (**Figure 33B**). In line with bioinformatic predictions, the first mutation (c.415A>T) altered splicing of exon 2 and resulted in significantly increased expression of the small CD33m isoform compared to wild-type (**Figure 33B**). For the second mutation (c.746-8delG) no difference could be observed in this setting, which might be due to differences in splicing machineries in different cell types or the design of the mini-gene.

Lack of CD33 surface expression in CD33$^{c.415A>T}$ iPSC-derived cells (**Figure 30**) and the observed increase in the CD33m/CD33M ratio in CD33 mini-gene experiments indicate a severe change in *CD33* mRNA expression. Therefore, *CD33* mRNA expression and isoform balance was also analyzed in greater detail in iPSC-derived macrophages by qRT-PCR detecting exonic fragments specific for distinct isoforms (**Figure 34**).

Interestingly, CD33 KO macrophages with different deletions (185 bp in KO25 and 184 bp in KO27) showed distinct effects on expression of *CD33* mRNA (**Figure 34A**). Whereas *CD33* mRNA expression was unaffected in KO25 clones, it was strongly reduced in KO27 clones (**Figure 34A**). Since the 184 bp deletion causes an earlier premature stop codon (in exon 3) and the 185 bp deletion results in a longer frameshift and a later premature stop codon, the difference is probably explained by nonsense-mediated mRNA decay of *CD33* mRNA in the KO27 clone. Both deletions cause loss of binding sites for Exon Δ2 and Exon 2-3 primer pairs, which cannot be detected in both KO clones confirming homozygous deletions in the *CD33* gene (**Figure 34A**). Of note, CD33$^{c.415A>T}$ clones showed substantially reduced expression of the CD33M isoform (detected by Exon 2, Exon 2-3) paralleled by a higher expression of the CD33m isoform (detected by Exon Δ2) (**Figure 34A**). Overall, a shifted isoform ratio towards the CD33m isoform CD33$^{c.415A>T}$ clones (**Figure 34B**) and a higher overall frequency of CD33m (**Figure 34C**) could be detected in CD33$^{c.415A>T}$ clones.

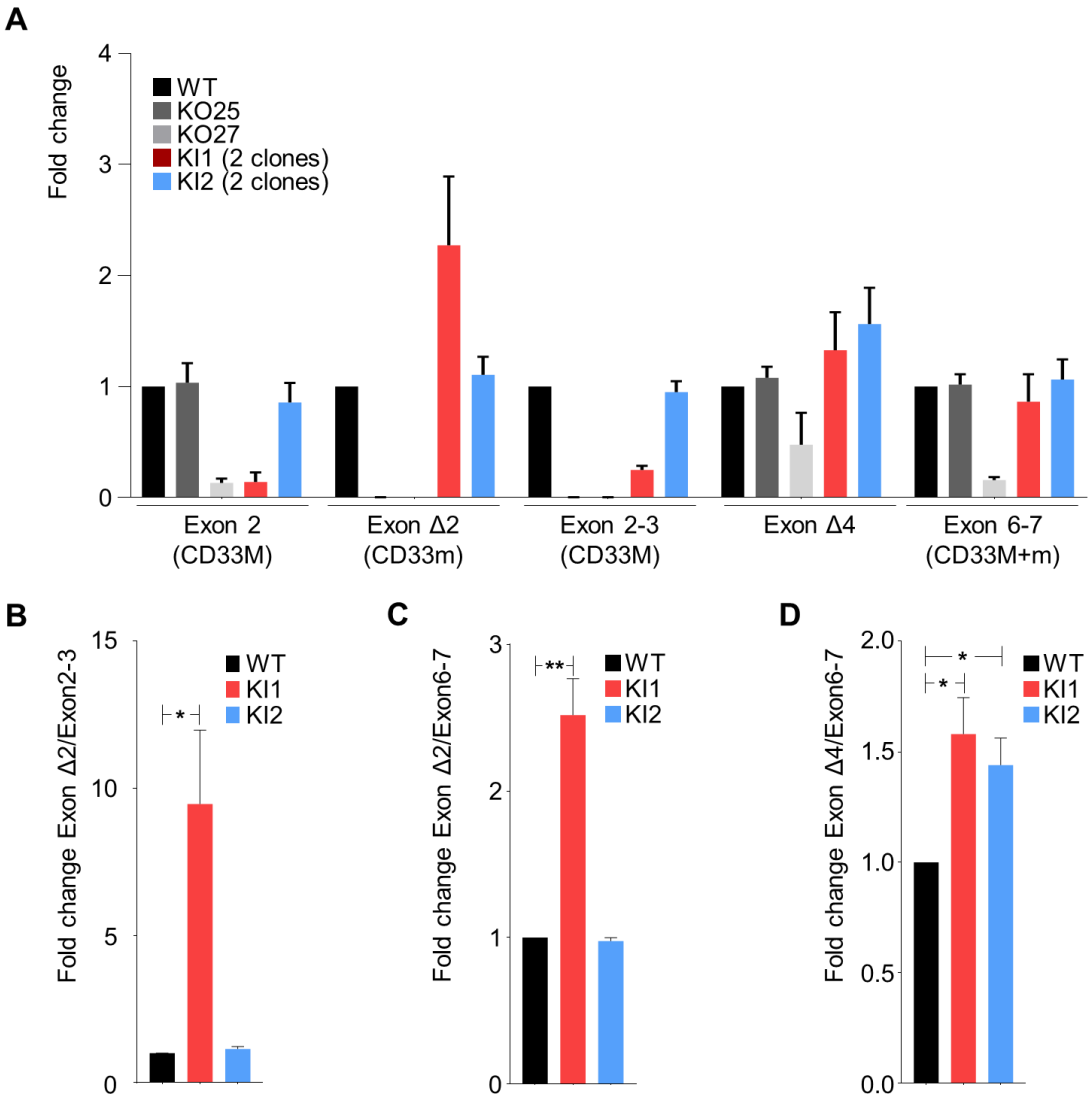

Figure 34: Altered mRNA expression in CD33 mutant iPSC-derived macrophages.
(A) Representative qRT-PCR analysis of *CD33* mRNA expression in macrophages differentiated from wild-type (WT), CD33 knock-out (KO), CD33$^{c.415A>T}$ (KI1), or CD33$^{c.746\text{-}8delG}$ (KI2) iPSC clones revealed increased expression of CD33m (Exon Δ2) and novel Exon Δ4 isoforms in CD33-mutated cells (n = 2 - 5 independent experiments). CD33 KO macrophages with deletion of 185 bp (KO25) and 184 bp (KO27) showed different CD33 mRNA expression indicative of nonsense-mediated mRNA decay in KO27 macrophages with earlier premature stop codon (**Figure 29**). (B) Quantification of CD33m (Exon Δ2) isoform expression relative to CD33M (Exon 2-3) revealed aberrant isoform balance (n = 2 - 5 independent experiments, mean of 2 clones for each KI). (C) Quantification of CD33m (Exon Δ2) isoform expression relative to total CD33 (CD33M+m, Exon 6-7) revealed increased expression of the CD33m isoform (n = 2 - 4 independent experiments, mean of 2 clones for each KI). (D) Quantification of Exon Δ4 isoform expression relative to total CD33 expression showed increased abundance of the Exon Δ4 isoform in CD33 mutated macrophages (n = 2 - 4 independent experiments, mean of 2 clones for each KI).

As exon 4 is built by only 48 basepairs and represents the smallest exon in *CD33* mRNA, exon 4 might be prone to exon skipping and might be also affected by alternative splicing. Therefore,

exon 4 skipping was analyzed by qRT-PCR with primers specific for the exon 3-5 boundary. Interestingly, exon Δ4 *CD33* mRNA could be detected in all genotypes indicating that the size of exon 4 indeed increases the probability of skipping of this exon, which was not described before. Furthermore, macrophages with homozygous KIs of both mutations showed an increased frequency of exon Δ4 *CD33* mRNA when normalized to the total *CD33* mRNA expression (Exon 6-7) indicating that both mutations might increase the probability of exon 4 skipping (**Figure 34D**). Since c.746-8delG alters the 3' splice site of intron 4-5, it is plausible that this might change inclusion of exon 4 in mature CD33 mRNA. However, the effects of exon 4 skipping on protein function have still to be elucidated and more detailed studies using new generation of mini-genes have been initiated.

CD33 mRNA expression was also analyzed in iPSC-derived granulocytes by qRT-PCR (**Figure 35**). Analogous to macrophages, the homozygous CD33$^{c.415A>T}$ mutation caused reduced expression of the CD33M isoform (Exon 1-2, Exon 2, Exon 2-3) and increased expression of the CD33m (Exon Δ2) isoform proving the strong effect of this variant on exon 2 skipping (**Figure 35**). In fact, reduction of CD33M expression was similar to KO of CD33 indicating nearly complete absence of the ligand-binding CD33M isoform in CD33$^{c.415A>T}$ cells (**Figure 35**).

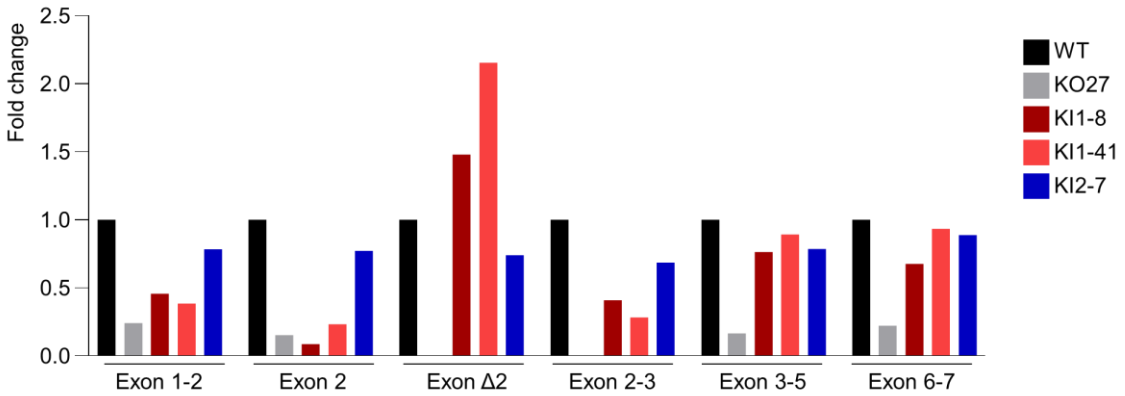

Figure 35: Altered CD33 isoform balance in iPSC-derived granulocytes.
Representative qRT-PCR analysis of *CD33* mRNA expression in granulocytes differentiated from wild-type (WT), CD33 knock-out (KO), CD33$^{c.415A>T}$ (KI1), or CD33$^{c.746-8delG}$ (KI2) iPSC clones revealed increased expression of CD33m (Exon Δ2) and reduced CD33M (Exon 1-2, Exon 2, Exon 2-3) isoforms in CD33-mutated cells (n = 1 independent experiment).

4.2.6 Altered hematopoiesis of CD33-mutated iPSC-derived hematopoietic progenitor cells

CD33 expression is upregulated early during hematopoiesis and is a marker for myeloid progenitor cells, but its function in hematopoietic progenitor cells is still not clear.

CRISPR/Cas9-edited iPSC lines allow to study the role of CD33 during hematopoiesis *in vitro*. Here, the hematopoietic differentiation potential of iPSC-derived CD33 KO and KI HSPCs was analyzed using a CFU assay in semi-solid methylcellulose medium (**Figure 36**).

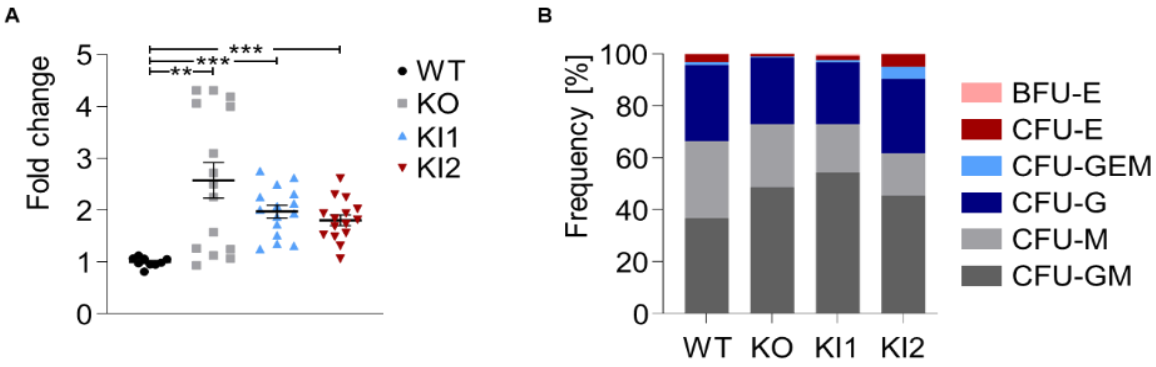

Figure 36: CD33 mutants showed altered myelopoiesis.
(A) Cells from CD33 knock-out (KO), CD33$^{c.415A>T}$ (KI1), and CD33$^{c.746\text{-}8delG}$ (KI2) generated significantly increased colony numbers in a CFU assay in semi-solid methylcellulose compared to wild-type (WT) (n = 3 independent experiments). (B) Representative analysis of colony type revealed similar composition in all samples. BFU: Burst-forming unit. CFU: Colony-forming unit. E: Erythrocyte. G: Granulocyte. M: Macrophage.

Interestingly, CD33 KO cells, CD33$^{c.415A>T}$ (KI1), and CD33$^{c.746\text{-}8delG}$ (KI2) generated significantly higher numbers of colonies compared to WT cells indicating increased proliferation and/or faster differentiation kinetics in CD33-mutated cells (**Figure 36A**). Of note, increased number of colonies was not associated with changes in colony composition, as similar frequencies of different erythrocyte and myeloid colony types could be observed in all genotypes (**Figure 36B**). In line, CD33 KO and CD33 KI cells demonstrated increased frequencies of CD34^{-} cells during macrophage differentiation suggesting a faster differentiation of CD33-mutated cells (**Figure 30**).

4.2.7 Mutant CD33 alters bacterial killing of macrophages

In the CNS CD33 was shown to regulate phagocytosis of microglia.[455, 481] In fact, SNPs changing the CD33M/CD33m isoform balance were shown to have pathogenic or beneficial effects on AD pathogenesis by inhibiting or activating microglial phagocytosis, respectively.[481] Therefore, phagocytosis and bacterial killing of CD33-mutated iPSC-derived macrophages was analyzed using gentamycin protection assays upon challenge with *S. typhimurium*, which is a pathogen relevant for intestinal pathology (**Figure 37**).

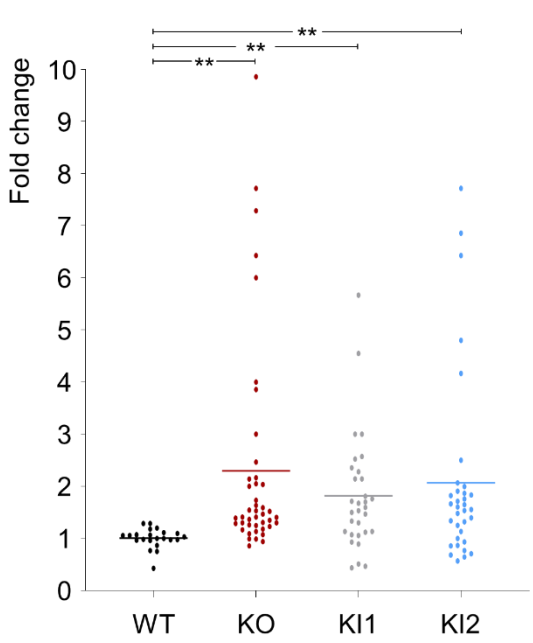

Figure 37: Reduced bacterial killing in CD33-mutated cells.
Quantification of *S. typhimurium* colonies in a gentamycin protection assay showed higher number of surviving bacteria in CD33 knock-out (KO), CD33$^{c.415A>T}$ (KI1), or CD33$^{c.746\text{-}8delG}$ (KI2) iPSC-derived macrophages compared to wild-type (WT) macrophages (n = 5 - 8 independent experiments, mean of 2 different clones for KO, KI1, KI2). A higher number of intracellular surviving bacteria is a proxy for dysfunctional bacterial killing of CD33-mutated macrophages. Independent experiments were normalized to the colony number of WT samples to correct for differences in total colonies between experiments.

Compared to wild-type iPSC-derived macrophages, CD33 KO as well as patient-specific KI cells showed increased numbers of surviving intracellular *S. typhimurium* bacteria (**Figure 37**). Since loss of CD33 function or expression of the small CD33m isoform caused increased phagocytosis by microglia, this observation might be explained by increased uptake of *S. typhimurium* bacteria in CD33-mutated cells and might indicate that both mutations represent loss-of-function alleles. However, this result would be also in line with defective bacterial killing of CD33-mutated cells. Further studies are required to assess whether CD33 mutations affect uptake and/or killing of bacteria by macrophages and if phagocytosis (e.g., cell debris) of other targets is defective.

4.2.8 CD33 mutations alter inflammasome activity in macrophages

Inflammasomes play a central role in IBD pathogenesis (see also section 1.1.6 and **Figure 3**) and dysregulation of inflammasome activity can cause increased IL-1β production and hyperinflammatory conditions. Interestingly, blocking of CD33 as well as removal of sialic acids from the cell surface by sialidase was shown to result in IL-1β release independent of other activating stimuli indicating an inhibitory role of CD33 for inflammasome activation.[456]

CD33 controls cell death in macrophage-like BLaER1 cells

The role of CD33 on inflammasome activation was evaluated in BLaER1 cells, which can be trans-differentiated towards CD14$^+$ monocyte-like cells using IL-3, M-CSF, and β-estradiol (**Figure 38A**).[600, 601] Of note, trans-differentiated BLaER1 cells also express CD33 on their surface

making them a suitable model to test CD33 function (**Figure 38A**). Since there is no specific CD33 ligand available, CD33 was targeted using an anti-CD33 antibody that was shown to induce IL-1β release similar to CD33 KD in previous studies.[456] As expected, IL-1β release was only detected in BLaER1 cells primed with LPS and activated with Nigericin, but not in cells stimulated with LPS alone (**Figure 38B**). While cells pre-treated with anti-CD33 for 48 h showed no production of IL-1β, substantially higher release of LDH independent of inflammasome activation could be detected indicating cell death in response to anti-CD33 treatment (**Figure 38B**). In line, release of CASP1 could be detected by immunoblotting in supernatants from cells treated with anti-CD33. Since CASP1 and especially pro-CASP1 is usually retained in cells, presence in cell supernatants is a marker for cell membrane disintegrity and release of cytosolic proteins during cell death (**Figure 38C**). Immunoblotting of cell lysates confirmed reduced production of pro-IL-1β (**Figure 38C**).

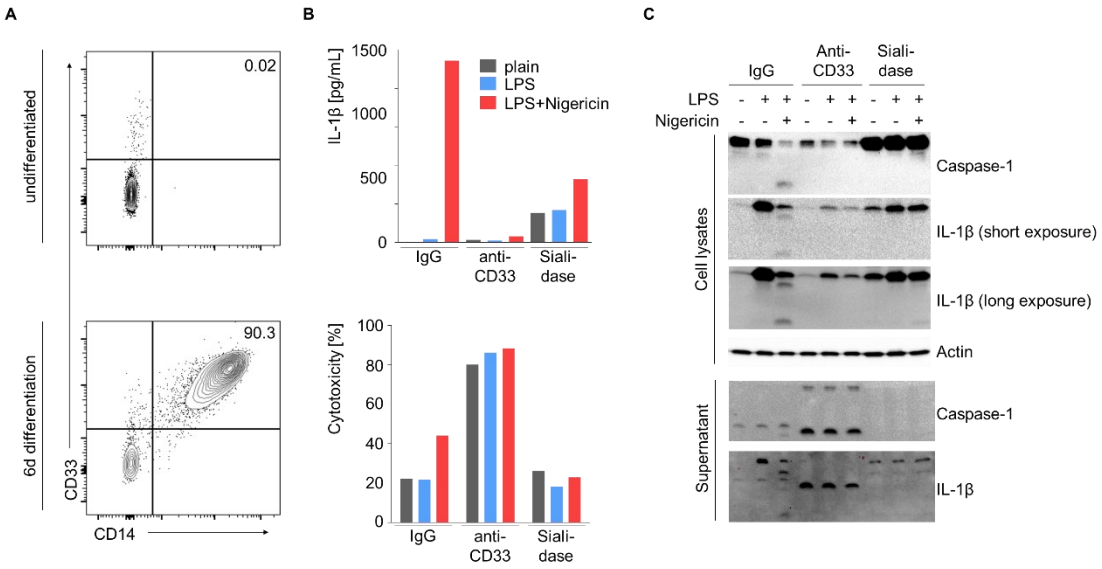

Figure 38: CD33 activity affected inflammasome and cell death in BLaER1 cells.
(A) Representative flow cytometry analysis of BLaER1 differentiation demonstrated successful generation of $CD33^{+}CD14^{+}$ monocyte-like cells. (B) Representative analysis of inflammasome activity by ELISA and LDH release assay in trans-differentiated BLaER1 cells after pre-stimulation with IgG, anti-CD33, or Sialidase for 48 h indicated reduced inflammasome activation and increased cell death in cells treated with anti-CD33 (n = 3 independent experiments). (C) Representative immunoblot analysis of Caspase-1, IL-1β, and actin in trans-differentiated BLaER1 cells after pre-stimulation with IgG, anti-CD33, or Sialidase for 48 h confirmed reduced inflammasome activation and increased cell death in cells treated with anti-CD33 (n = 3 independent experiments).

Of note, removal of sialic acids by sialidase resulted in IL-1β secretion without addition of LPS and Nigericin indicating pre-mature activation (**Figure 38B**). However, IL-1β production by sialidase-treated cells was reduced after stimulation with LPS and nigericin, which might indicate

disturbed inflammasome activation (**Figure 38B**). In line, immunoblotting of cell lysates from inflammasome experiments showed increased expression of pro-IL-1β in sialidase treated cells, but no cleavage of IL-1β could be detected indicating that sialidase treatment causes expression of pro-IL-1β and disturbs inflammasome activation (**Figure 38C**). Pre-mature IL-1β secretion detected by ELISA might be caused by release of pro-IL-1β in the supernatant, which also indicates cell death.

Primary monocytes of the index family show hyperinflammatory signature

The phenotypes of IBD and vasculitis observed in the index patient are suggestive of an inborn error of immunity associated with increased pro-inflammatory cytokine secretion. In this regard, CD33 was shown to influence TLR4 signaling, which can trigger pro-inflammatory cytokine release and inflammasome activation.[442, 456] Therefore, inflammasome activation was analyzed in primary monocytes derived from peripheral blood in two independent experiments (**Figure 39**). In the first experiment, patient monocytes showed an IL-1β hypersecretion upon stimulation with LPS and nigericin as compared with healthy donors (**Figure 39A**). Of note, patient monocytes secreted more IL-1β after LPS priming indicating premature activation of these cells (**Figure 39A**). In a second experiment, an increased IL-1β secretion could be observed in all individuals of the index family (mother, father, patient) compared to healthy controls and a travel control indicating a pro-inflammatory genetic signature in the family (**Figure 39B**).

Interestingly, pre-treatment of primary monocytes with anti-CD33 for 6 h resulted in higher IL-1β levels in healthy donor samples but did not increase IL-1β production in cells from the affected family members, which might indicate CD33-dependent inflammasome activation in the index family (**Figure 39C**). Furthermore, anti-CD33 treatment induced IL-1β release independent of LPS/Nigericin-mediated inflammasome activation in line with previous publications.[456]

Unlike ELISA analysis, immunoblotting of supernatants from cells, which were not treated with anti-CD33 suggested increased levels of mature IL-1β in patient samples compared to the parents (**Figure 39D** left panel). Interestingly, S100A9 could be detected in supernatants of monocytes isolated from the mother and the patient whereas no expression could be observed in supernatants from healthy controls nor the father (**Figure 39D**).

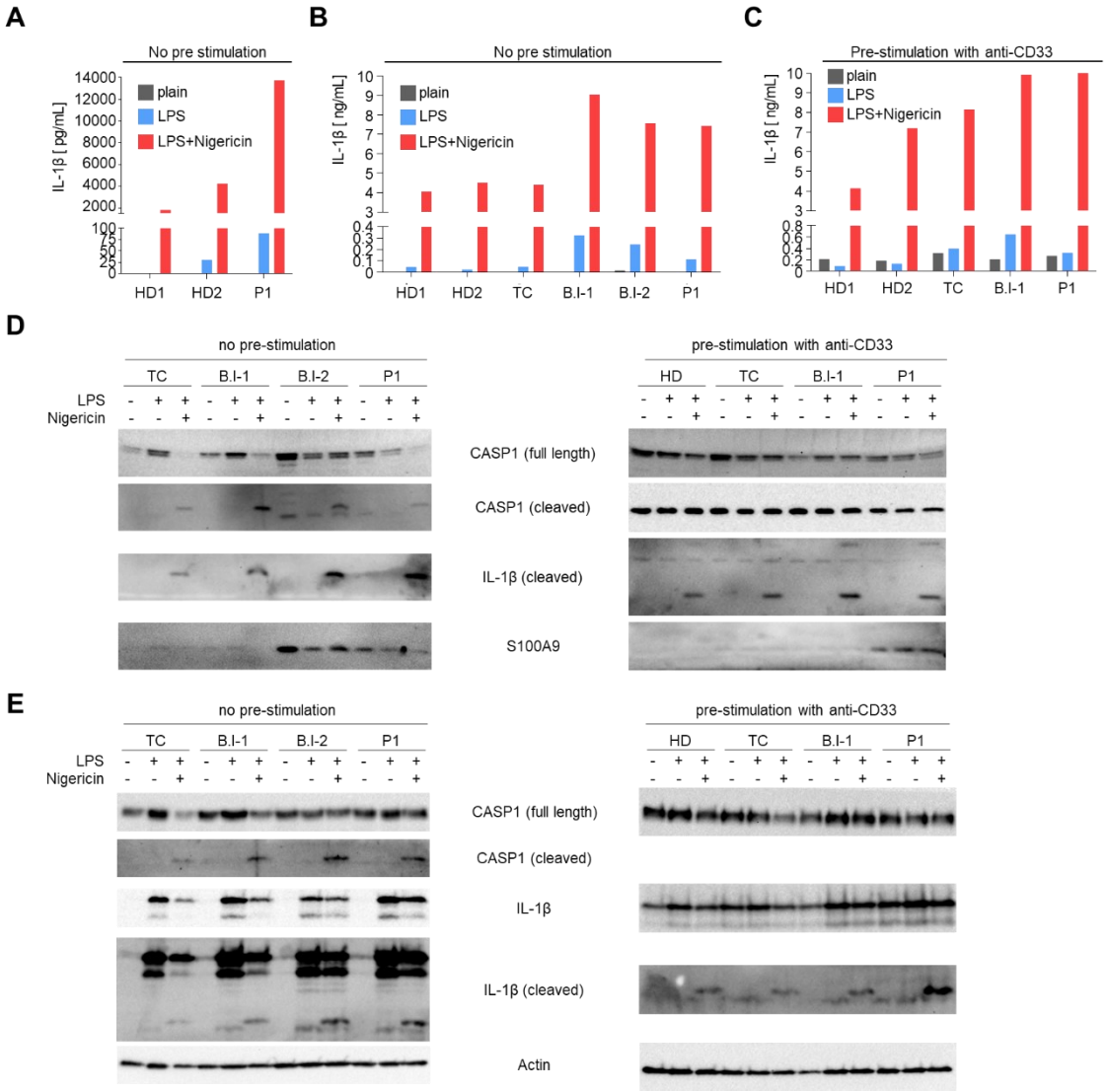

Figure 39: Increased inflammasome activity in monocytes of the index family.
(A) First analysis of IL-1β secretion by peripheral blood monocytes from two healthy donors (HD) and the index patient (P1) by ELISA indicated increased IL-1β secretion by cells from the index patient. (B) Repetition of (A) with additional family members (Father: B.I-1, Mother: B.I-2) and a travel control (TC) revealed increased IL-1β secretion by cells from the complete index family. (C) Analysis of LPS/Nigericin-mediated inflammasome activation after pre-incubation with anti-CD33 for 6 h demonstrated influence of CD33 on increased IL-1β secretion. (D) Immunoblot analysis of cell supernatants generated in (C) and (B) confirmed increased inflammasome activation in the index family without pre-stimulation and show higher S100A9 production in B.I-2 and P1. Anti-CD33-treated cells of HD showed similar IL-1β secretion compared to index family. (E) Immunoblot analysis of cell lysates with (C) or without (B) anti-CD33 pre-treatment indicated increased inflammasome activation in the index family. Of note, P1 shows highest IL-1β production after pre-incubation with anti-CD33.

In line with observations in the ELISA, supernatants from anti-CD33-treated cells showed similar IL-1β levels in all samples indicating a regulatory function of CD33 in inflammasome activation (**Figure 39D** right panel).

Intracellular activation of inflammasomes in monocytes was analyzed by immunoblotting of cell lysates (**Figure 39E**). Corresponding to the ELISA data, the index family showed increased IL-1β production compared to the travel control without anti-CD33 treatment (**Figure 39E** left panel). However, immunoblotting suggested increased pro-IL-1β levels in the patient indicating higher activation of NF-κB signaling in patient cells (**Figure 39E** left panel).

Anti-CD33 stimulated expression of pro-IL-1β independent of LPS in all samples indicating induction of NF-κB signaling and cellular activation upon modulation of CD33 (**Figure 39E** right panel). After pre-treatment with anti-CD33, patient cells showed substantially increased levels of mature IL-1β upon inflammasome activation (**Figure 39E** right panel). Of note, more intracellularly retained mature IL-1β might explain why there was no difference detectable by ELISA between healthy family members and the patient.

CD33 mutations cause increased inflammasome activation in iPSC-derived macrophages

To shed light on the role of CD33 on inflammasome activation and to assess the effect of patient-specific mutations on inflammatory functions of macrophages, classical inflammasome activation by LPS and Nigericin was analyzed in iPSC-derived macrophages (**Figure 40**).

As expected, substantial IL-1β secretion could be only detected in iPSC-derived macrophages activated with LPS and Nigericin demonstrating the relevance of this advanced disease model system (**Figure 40**). In contrast to primary monocytes, no detectable difference in IL-1β expression, maturation, or secretion could be observed for any genotype by ELISA or immunoblotting indicating that CD33 might not directly regulate LPS-mediated inflammasome activation in this setting (**Figure 40**). The observed discrepancy between primary and iPSC-derived model systems might be caused by (i) different cell types, (ii) genetic background, and (iii) pre-activation of primary cells.

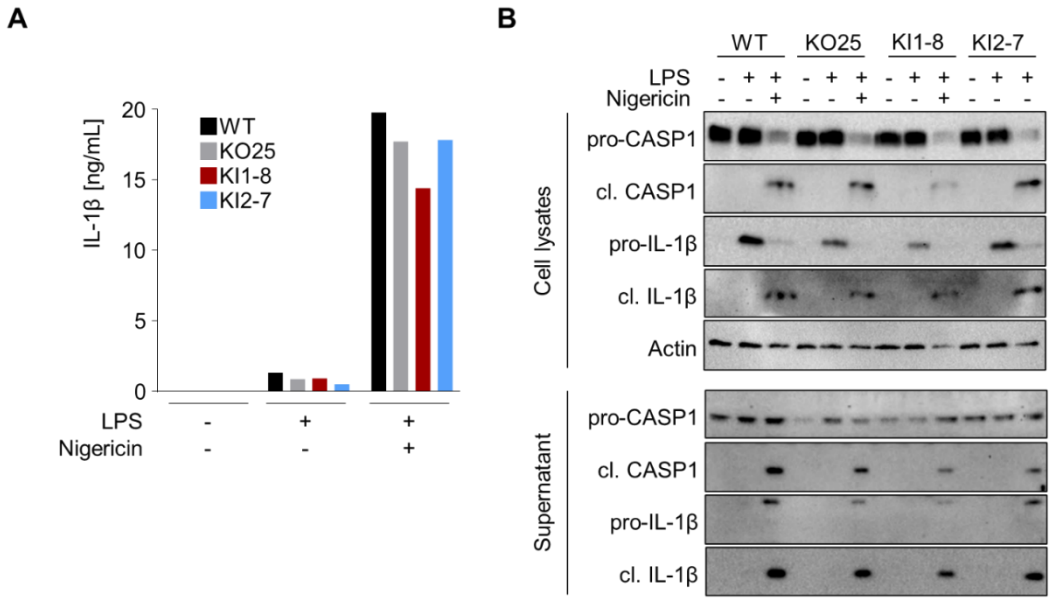

Figure 40: LPS-induced inflammasome is not altered by CD33 mutations.
(A) Representative analysis of IL-1β secretion from macrophages differentiated from wild-type (WT), CD33 knock-out (KO), CD33$^{c.415A>T}$ (KI1), or CD33$^{c.746\text{-}8delG}$ (KI2) iPSC clones by ELISA indicated normal LPS/Nigericin-mediated inflammasome activation (short term, n = 4 independent experiments, 2 different clones for KO, KI1, KI2 used in experiments). (B) Representative immunoblot analysis of cell lysates and supernatants from (A) confirmed normal inflammasome activation (n = 3 independent experiments, 2 different clones for KO, KI1, KI2 used).

Since CD33 was shown to influence S100A9-mediated cellular activation and an increased S100A9 secretion could be observed in monocytes from the patient and mother, S100A9-mediated inflammasome activation was analyzed (**Figure 41**). Similar to experiments using LPS for priming of inflammasome, secretion of mature IL-1β was only detected upon co-stimulation of S100A9 in combination with the second trigger Nigericin (**Figure 41A**). However, in contrast to LPS-stimulated macrophages, inflammasome activation by S100A9 induced higher levels of IL-1β in macrophages carrying the homozygous, patient-specific mutations indicating an increased response after S100A9 stimulation (**Figure 41A**).

In parallel, S100A9 stimulation caused substantially increased cell death in macrophages with KI of patient mutations indicating dysregulated inflammasome responses in these cells (**Figure 41B**). Immunoblotting of cell lysates confirmed increased levels of mature IL-1β in CD33-mutated cells but did not show any difference in pro-IL-1β expression (**Figure 41C**). Similarly, immunoblotting of cell culture supernatants showed increased mature IL-1β levels in macrophages with CD33 KO or KI of patient-specific mutations in CD33 (**Figure 41D**). Furthermore, increased cell death could be detected in CD33-mutated cells confirming previous observations (**Figure 41D**). Of note, detection of pro-IL-1β in the supernatant without addition of

Nigericin indicates that S100A9 alone might induce death in CD33-mutant cells independent of inflammasome activation, which might indicate dysregulated cell death and/or inflammatory responses (**Figure 41D**).

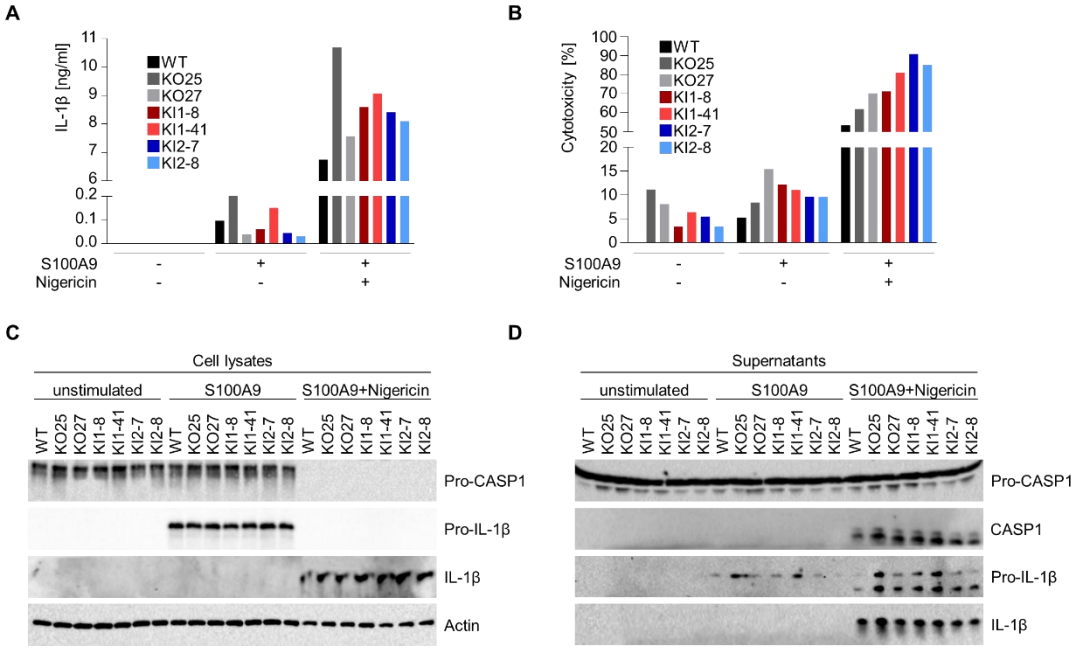

Figure 41: CD33 mutants cause increased S100A9-mediated inflammasome activity.
(A) Representative ELISA of IL-1β secretion from macrophages differentiated from wild-type (WT), CD33 knock-out (KO), CD33$^{c.415A>T}$ (KI1), or CD33$^{c.746\text{-}8delG}$ (KI2) iPSC clones indicated increased S100A9/Nigericin-mediated inflammasome activation (n = 4 independent experiments). (B) Analysis of LDH release from macrophages differentiated from wild-type (WT), CD33 knock-out (KO), CD33$^{c.415A>T}$ (KI1), or CD33$^{c.746\text{-}8delG}$ (KI2) iPSC clones showed increased cytotoxicity for CD33-mutated cells after S100A9 and S100A9/Nigericin stimulation (n = 3 independent experiments). (C) Immunoblotting of cell lysates (C) and supernatants (D) from (A) confirmed efficient inflammasome activation and increased IL-1β cleavage and secretion (n = 1 independent experiments).

4.2.9 CD33-mutant granulocytes show altered inflammatory function

In addition to primary macrophages, inflammasome activity was also assessed in primary granulocytes isolated in the second experiment. In line with monocyte data, granulocytes from the index family (except for the mother) showed increased IL-1β production compared to healthy controls confirming the hyperinflammatory signature in the index family (**Figure 42**).

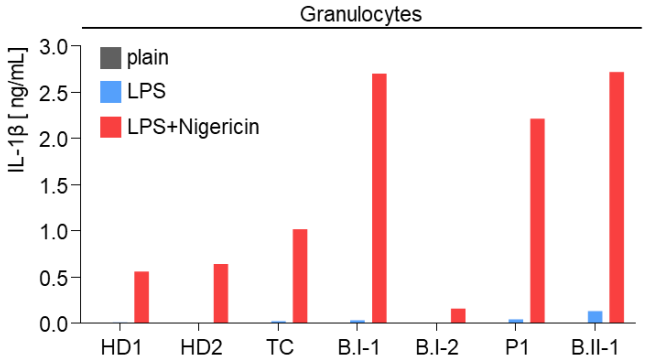

Figure 42: Increased inflammasome activity in granulocytes of the index family.
Analysis of inflammasome activation by LPS and nigericin in granulocytes from two healthy donors (HD), a travel control (TC), father (B.I-1), mother (B.I-2), patient (P1), and sibling (B.II-2) showed increased IL-1β secretion by cells of the index family.

Furthermore, CD33-mutated iPSC-derived granulocytes were assessed for their inflammatory responses. Analogous to macrophages, inflammasome activation in response to LPS/Nigericin or S100A9/Nigericin was analyzed (**Figure 43**). Similar to macrophages, a comparable release of IL-1β could be observed from granulocytes with different genotypes upon stimulation with LPS and Nigericin suggesting normal TLR4-mediated inflammasome activation in CD33-mutated granulocytes (**Figure 43A**). There was similar LDH release from wild-type and mutant iPSC-derived granulocytes upon LPS or LPS/Nigericin stimulation (**Figure 43B**). Analogous to macrophages S100A9-mediated inflammasome activation was tested in iPSC-derived granulocytes. In line with observations in macrophages, CD33$^{c.746\text{-}8delG}$ granulocytes also produced higher amounts of IL-1β upon co-stimulation of S100A9 and Nigericin (**Figure 43C**). Furthermore, S100A9 alone also induced IL-1β secretion in CD33$^{c.746\text{-}8delG}$ granulocytes (**Figure 43C**). However, no difference could be observed for CD33 KO and CD33$^{c.415A>T}$ granulocytes compared to wild-type, which is different to iPSC-derived macrophages. Whereas S100A9 induced increased LDH release indicative of higher cytotoxicity in CD33-mutant macrophages, no difference could be observed for iPSC-derived granulocytes suggesting differential responses or kinetics in different cell types.

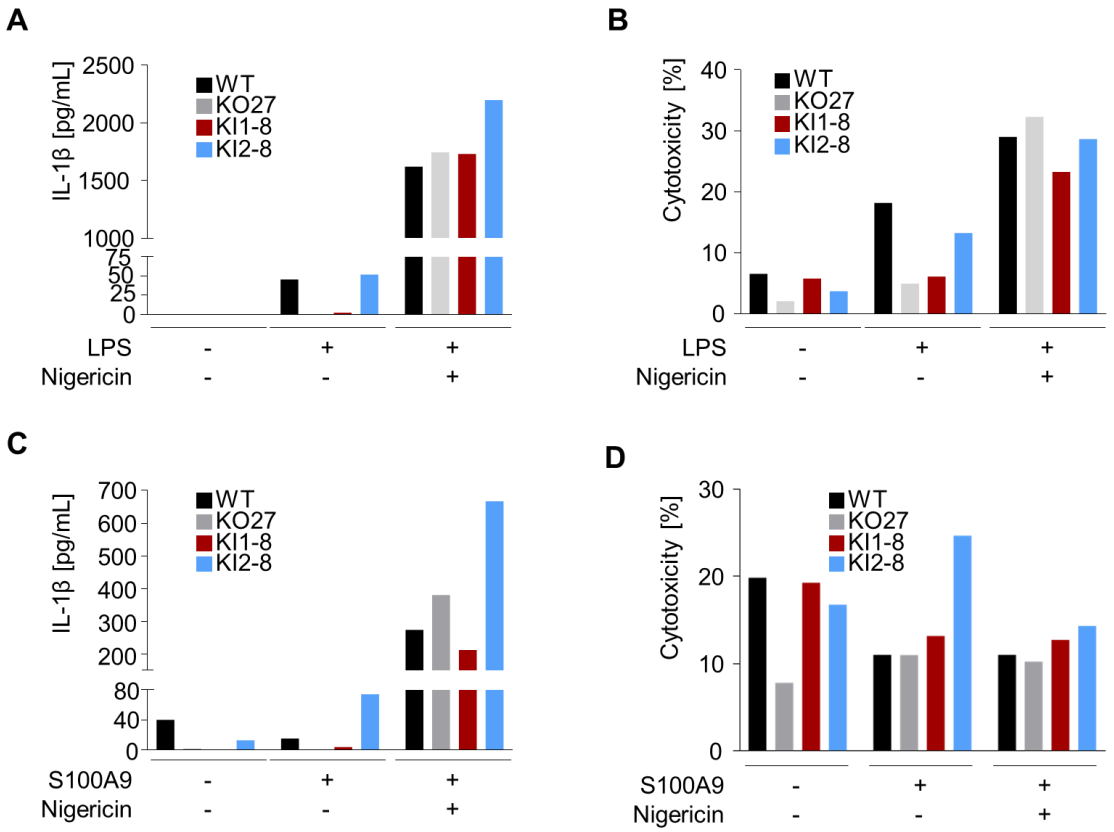

Figure 43: Increased inflammasome activation in CD33-mutated iPSC-derived granulocytes. (A) Representative analysis of IL-1β secretion from granulocytes differentiated from wild-type (WT), CD33 knock-out (KO), $CD33^{c.415A>T}$ (KI1), or $CD33^{c.746\text{-}8delG}$ (KI2) iPSC clones by ELISA indicated normal LPS/Nigericin-mediated inflammasome activation (n = 4 independent experiments). (B) Representative analysis of LDH release from granulocytes differentiated from wild-type (WT), CD33 knock-out (KO), $CD33^{c.415A>T}$ (KI1), or $CD33^{c.746\text{-}8delG}$ (KI2) iPSC clones showed comparable cytotoxicity (n = 3 independent experiments). (C) Representative ELISA results of IL-1β secretion from granulocytes differentiated from wild-type (WT), CD33 knock-out (KO), $CD33^{c.415A>T}$ (KI1), or $CD33^{c.746\text{-}8delG}$ (KI2) iPSC clones indicated increased S100A9/Nigericin-mediated inflammasome activation in granulocytes expressing $CD33^{c.746\text{-}8delG}$ (n = 2 independent experiments). (D) Representative analysis of LDH release from granulocytes differentiated from wild-type (WT), CD33 knock-out (KO), $CD33^{c.415A>T}$ (KI1), or $CD33^{c.746\text{-}8delG}$ (KI2) iPSC clones showed comparable cytotoxicity for all tested genotypes (n = 1 independent experiments).

4.3 TREM2 deficiency as a novel genetic entity causing VEO-IBD

4.3.1 Identification of a patient with homozygous TREM2 mutation

A male patient born to non-consanguineous parents with Turkish descent presented with severe, infantile-onset IBD and neuromuscular developmental disorders at Gazi University Hospital (Ankara, Turkey) (**Figure 44A**).

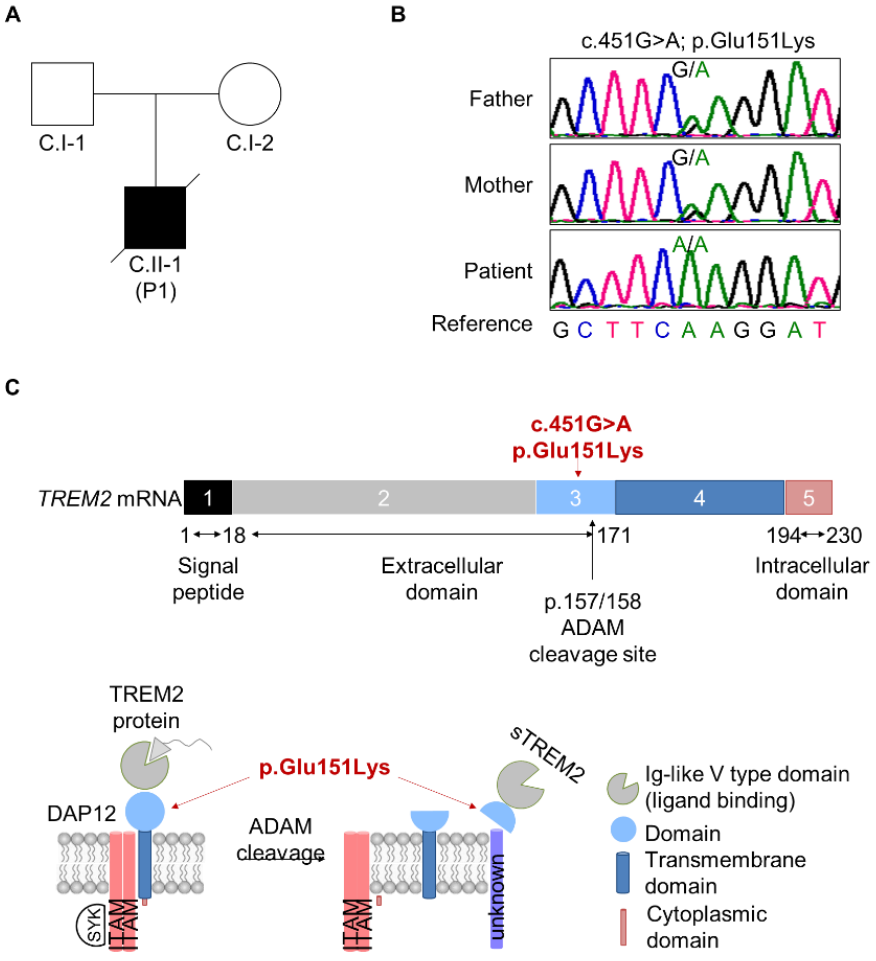

Figure 44: Identification of a patient with homozygous missense mutation in *TREM2*.
(A) Pedigree of index family with father (C.I-1), mother (C.I-2), and index patient (C.II-1, P1). (B) Sanger sequencing confirmed homozygous presence and segregation of c.451G>A mutation in the index family. (C) Schematic overview of TREM2 mRNA and protein structure. The index mutation (c.451G>A; p.Glu151Lys) is located close to the TREM2 shedding site.

Since the infantile onset suggested a monogenetic cause of the disease, genomic DNA was isolated from peripheral blood samples and subjected to WES at the sequencing core facility of the CCRC Hauner. Using bioinformatic analysis filtering for rare, deleterious variants, we identified a homozygous missense mutation in *TREM2* (6:41127561, ENST00000373113; c.451G>A; p.Glu151Lys). Sanger sequencing confirmed the presence of the homozygous c.451G>A mutation in the patient and showed that both parents were heterozygous carriers proving segregation of the mutation with the disease phenotype in the family (**Figure 44B**).

The identified c.451G>A is located in exon 3 and results in exchange of the negatively charged Glutamine 151 with a positively charged Lysine (p.Glu151Lys, E151K, **Figure 44C**). Of note, Glu151 is located only 6 amino acids upstream of the ADAM cleavage site, which can be found between position 157 and 158 and is important for shutdown of TREM2 signaling. Since Glu151 is upstream of the cleavage site, it is one of the most C-terminal amino acids in sTREM2 after shedding from the cell surface (**Figure 44C**).

4.3.2 Generation of patient-specific iPSC using CRISPR/Cas9-mediated genetic engineering

TREM2 is involved in controlling the homeostasis in the CNS and gut by regulating responses of microglial or macrophages to DAMPs and PAMPs. Therefore, TREM2 represents an interesting candidate for causing IBD as well as neurological disorders, which both are observed in the index patient. Unfortunately, the patient succumbed at 8 months of age. Since there is no access to primary biospecimens due to the early death of the patient, the functional effects of the mutation could only be studied using cellular model systems. iPSC-derived macrophages represent a suitable model since they express TREM2 in high levels, show (near-)physiological responses, and can be generated in a large scale. Furthermore, usage of isogenic iPSC lines allows exploration of functional defects by distinct patient mutations in a genetically defined setting.

iPSC clones carrying the c.451G>A mutation identified in the patient were genetically engineered using CRISPR/Cas9-mediated genome editing. Homozygosity of the engineered mutation was confirmed by Sanger sequencing (**Figure 45A**). Furthermore, TREM2 KO iPSC were generated by inducing a homozygous deletion of a 79 bp large fragment in exon 3 of the TREM2 gene (**Figure 45B**).

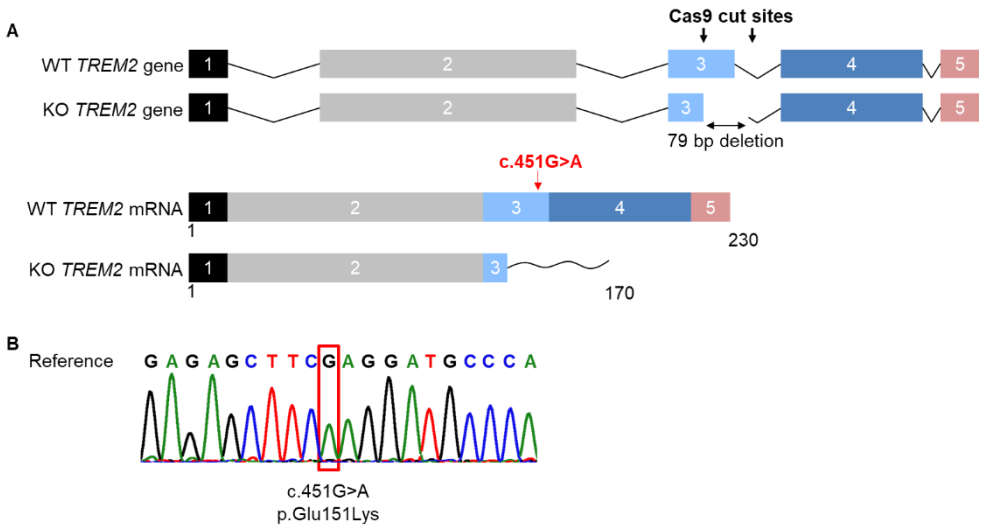

Figure 45: Successful genetic engineering of patient-specific iPSC lines.
(A) Schematic overview for the generation of *TREM2* KO iPSC. CRISPR/Cas9-mediated genome engineering resulted in deletion of 79 bp in exon 3 and intron 3 of *TREM2*. 52 bp were deleted in exon 3 of mature TREM2 mRNA, which causes a frameshift and premature stop. (B) Representative Sanger sequencing chromatogram confirmed successful introduction of c.451G>A mutation in iPSC clones.

4.3.3 TREM2 deficiency alters myelopoiesis

TREM2 mutations in patients with NHD were shown to disturb osteoclast differentiation. To assess if TREM2 mutations affect differentiation of monocytes, hematopoiesis of patient-specific iPSC-derived hematopoietic progenitor cells was analyzed using a CFU assay in semi-solid methylcellulose medium (**Figure 46**).

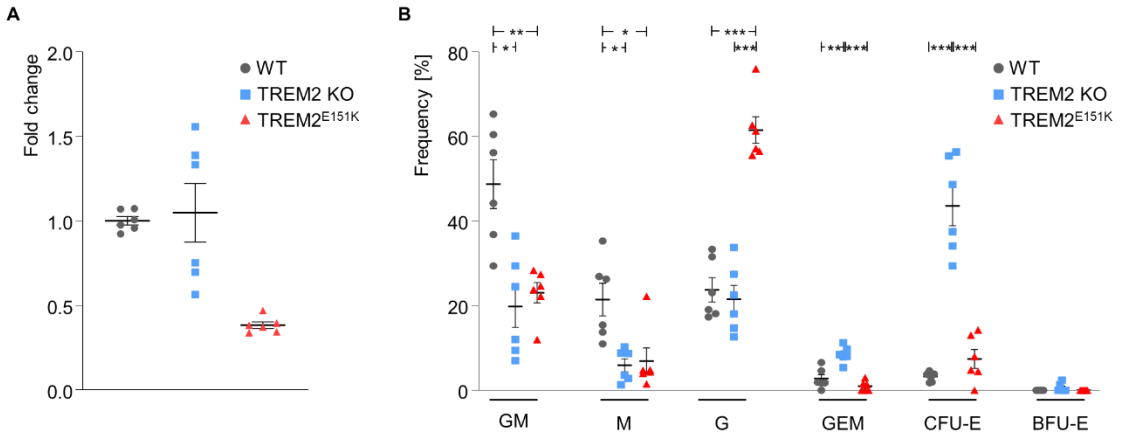

Figure 46: Altered myelopoiesis in TREM2-deficient iPSC-derived HSPCs.
(A) Cells from TREM2^{E151K} (KI) iPSC generated decreased numbers of colonies in a CFU assay in semi-solid methylcellulose compared to wild-type (WT) (n = 2 independent experiments).
(B) Analysis of colony type revealed reduced frequencies of granulocyte-macrophage (GM) and macrophage (M) colonies in TREM2 knock-out (KO) and TREM2^{E151K} (KI) cells compared to wild-type (WT). In parallel, TREM2 KO showed increased frequencies of Erythrocyte (E) colonies TREM2^{E151K} cells showed higher frequencies of granulocyte (G) colonies (n = 2 independent experiments). BFU: Burst-forming unit. CFU: Colony-forming unit.

Cells derived from TREM2^{E151K} iPSC demonstrated a reduced number of colonies compared to WT cells indicating a reduced capacity of TREM2-mutant hematopoietic progenitor cells to generate mature myeloid/erythrocyte cells (**Figure 46A**)**.** Of note, analysis of CFU assays revealed quantitative differences during hematopoiesis. In detail, TREM2 KO and TREM2^{E151K} caused increased generation of erythrocyte and granulocyte colonies, respectively (**Figure 46B**). In parallel, TREM2-deficient cells showed reduced frequencies of macrophage colonies suggesting a dysbalanced myelopoiesis with block of macrophage development In TREM2-deficient cells.

To functionally characterize the identified *TREM2* variant, patient-specific iPSCs were differentiated towards monocytes. Flow cytometry showed comparable frequency of CD45$^+$CD14$^+$ cells in TREM2 WT, KO, and KI cells (**Figure 47A**).

Interestingly, TREM2 KO and TREM2^{E151K} cells showed reduced numbers of dead cells and increased numbers of CD45$^+$ hematopoietic cells at day 15 - 18 of the differentiation during all performed experiments (n = 3 for KI, n = 2 for KO), which might suggest a survival or proliferation advantage of TREM2-deficient cells compared to WT cells (**Figure 47A**). Of note, TREM2^{E151K} cells showed a similar phenotype to TREM2 KO cells indicating that TREM2^{E151K} might represent a loss-of-function allele. TREM2 KO and TREM2^{E151K} iPSC-derived CD45$^+$ hematopoietic cells demonstrated an increased level of CD14 expression at day 15 - 18 of the differentiation confirming the similarity between TREM2 KO and TREM2^{E151K} cells (**Figure 47B**). It is known that CD14 expression increases during macrophage differentiation but might be also induced by PAMP-mediated macrophage activation and associated with a pro-inflammatory macrophage fate. Thus, higher CD14 levels in TREM2-deficient monocytes might be explained by faster differentiation or by an altered activation state.

iPSC-derived monocytes were matured to macrophages and their purity was analyzed by flow cytometry (**Figure 47C**). Independent of the genotype, CD45$^+$CD14$^+$CD33$^+$ could be successfully generated with high purity (≥ 94.5 %, **Figure 47C**). In murine *Trem2*$^{-/-}$ microglia expression of CD11c (Integrin αX, encoded by the gene *ITGAX*), which is an important integrin for adhesion and extravasation of monocytes, was shown to be downregulated.[549, 584] Interestingly, CD11c expression was reduced in human iPSC-derived TREM2 KO macrophages, but not in

TREM2^{E151K} cells indicating that this phenotype is not affected by the patient mutation (**Figure 47D**).

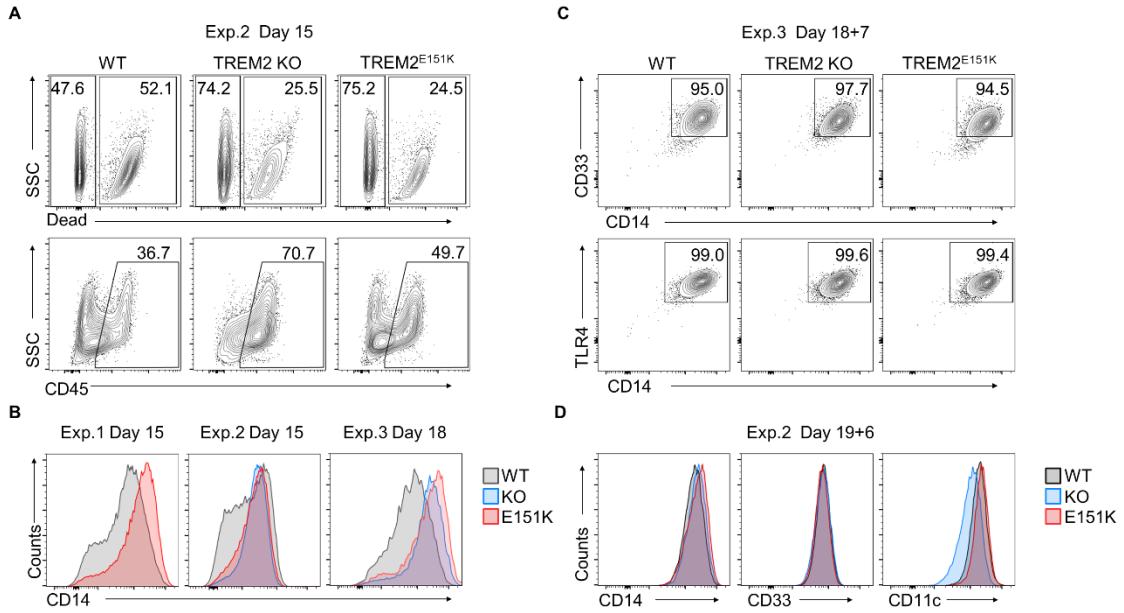

Figure 47: TREM2-deficient iPSC-derived monocytes showed higher CD14 expression.
(A) Representative flow cytometry analysis of floating cells after 15 days of differentiation from wild-type (WT), TREM2 knock-out (KO), TREM2 knock-in (TREM2^{E151K}) iPSC demonstrated successful generation of CD45^{+} hematopoietic cells. TREM2 KO and TREM2^{E151K} cells showed reduced frequencies of dead cells and higher frequencies of CD45^{+} cells (n=3 experiments for KI, n = 2 experiments for KO). (B) CD14^{+} monocytes could be successfully generated from iPSC as indicated by flow cytometry. Increased CD14 expression could be observed in TREM2 KO and TREM2^{E151K} after 15-18 days of differentiation (monocyte stage) in three independent experiments. (C) Flow cytometry of macrophages matured from iPSC-derived monocytes revealed successful generation of highly pure populations of CD45^{+}CD14^{+}CD33^{+} macrophages in all genotypes (WT, TREM2 KO, and TREM2^{E151K}). (D) WT, TREM2 KO, and TREM2^{E151K} macrophages showed similar expression levels of CD14, CD33, and TLR4 as indicated by flow cytometry analysis. Reduced CD11c expression could be observed in TREM2 KO iPSC-derived macrophages.

TREM2 shedding is induced upon activation of macrophages by different signals and can be successfully stimulated by PMA treatment.[603] Since the index mutation is located in close proximity to the ADAM cleavage site, TREM2 shedding upon PMA treatment was analyzed by immunoblotting (**Figure 48**). As expected, mature TREM2 levels were strongly reduced after 1 h of PMA treatment in wild-type macrophages (**Figure 48A,B**). In parallel, levels of cleaved TREM2 C-terminal fragments were increasing indicating effective shedding (**Figure 48A**). In cell lysates from TREM2 KO macrophages no expression of TREM2 could be detected using two different antibodies binding to C-terminal (**Figure 48A**) or N-terminal (**Figure 48B**) epitopes of TREM2 confirming efficient modification by CRISPR/Cas9-mediated genome engineering. TREM2^{E151K} macrophages demonstrated normal shedding of mature TREM2 upon PMA stimulation, but

substantially increased levels of mature TREM2 could be observed in unstimulated conditions using a C-terminal antibody (**Figure 48A**). Interestingly, TREM2^{E151K} showed a reduced molecular weight compared to WT samples, which might be caused by altered post-translational modification of mutant TREM2 (**Figure 48A,B**).

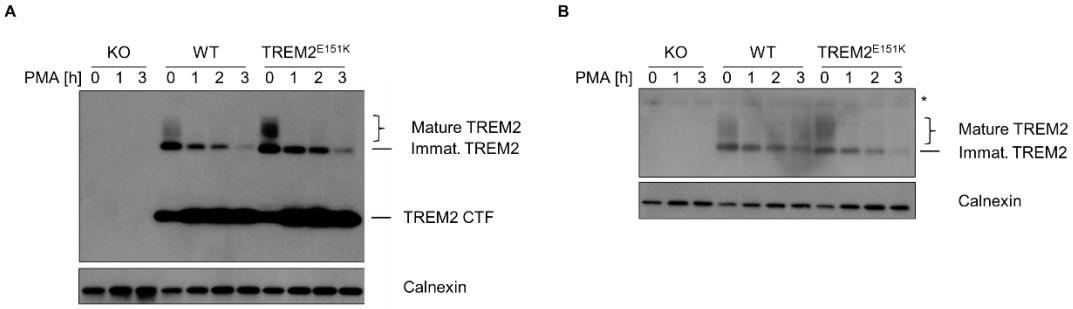

Figure 48: Mutant TREM2 shows aberrant molecular weight.
Immunoblotting for both blots was performed by the laboratory of Prof. Dr. Christian Haass (DZNE, LMU Munich). (A) Usage of a C-terminal epitope-specific antibody demonstrated efficient knock-out (KO) of TREM2 and effective shedding of TREM2 in wild-type (WT) and patient-specific knock-in (TREM2^{E151K}) samples upon PMA stimulation. Reduced molecular weight could be observed for the TREM2^{E151K} mutant. (B) Detection of TREM2 using an antibody specific for a N-terminal TREM2 epitope confirms deletion of TREM2 in KO samples and efficient shedding of TREM2 upon PMA stimulation. In line with the C-terminal antibody, reduced molecular weight could be observed for the TREM2^{E151K} mutant. Calnexin was used as loading control. Immat. = Immature, CTF= C-terminal fragment.

4.3.4 TREM2 deficiency affects inflammatory responses of macrophages

TREM2 was shown to induce phagocytosis of microglia and contribute to clearance of apoptotic neurons and protein aggregates by microglia in the CNS.[525, 527, 540] Similarly, macrophages in the gut are critical to phagocytose and clear pathogens and other danger signals in the intestinal LP allowing surveillance of this important compartment. Therefore, iPSC-derived macrophages were analyzed for their ability to handle *S. typhimurium* in a gentamycin protection assay (**Figure 49**). Overall, uptake and/or killing of *S. typhimurium* was not affected by loss of TREM2. However, *S. typhimurium* might not be binding to TREM2 and/or induce other types of phagocytosis (i.e., macropinocytosis). Therefore, effects of TREM2^{E151K} on phagocytosis of other bacterial species and substrates are currently investigated.

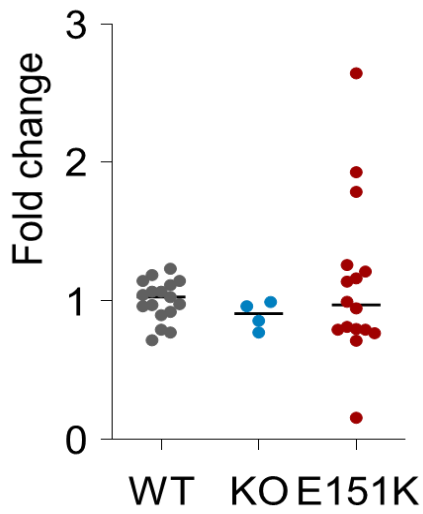

Figure 49: Killing of *S. typhimurium* is not affected by TREM2 mutation.
Killing of *S. typhimurium* by iPSC-derived macrophages from wild-type (WT), TREM2 knock-out (KO), and patient-specific TREM2 knock-in (E151K) was assessed using gentamycin protection assays (n = 3 independent experiments for WT, E151K, n = 2 for KO). Experiments were normalized to the mean number of colonies in WT for each experiment. Number of surviving colonies was similar in all assessed genotypes, but E151K samples showed increased numbers of surviving bacteria in some experiments.

In mouse experiments, loss of *Trem2* in intestinal macrophages caused increased expression of genes characteristic for pro-inflammatory M1 macrophages and reduced levels of genes relevant for anti-inflammatory M2 macrophages indicating an altered polarization of intestinal *Trem2*$^{-/-}$ macrophages.[582] Interestingly, attenuated healing of the intestinal mucosa in *Trem2*$^{-/-}$ mice was shown to be caused by reduced M2 macrophage-derived IL-4 and IL-13.[582] Therefore, polarization of TREM2 KO or TREM2^{E151K} iPSC-derived macrophages towards pro-inflammatory M1 and anti-inflammatory M2 macrophages was analyzed by flow cytometry upon challenge with LPS and IFN-γ or IL-4, IL-10, and TGF-β, respectively (**Figure 50**).

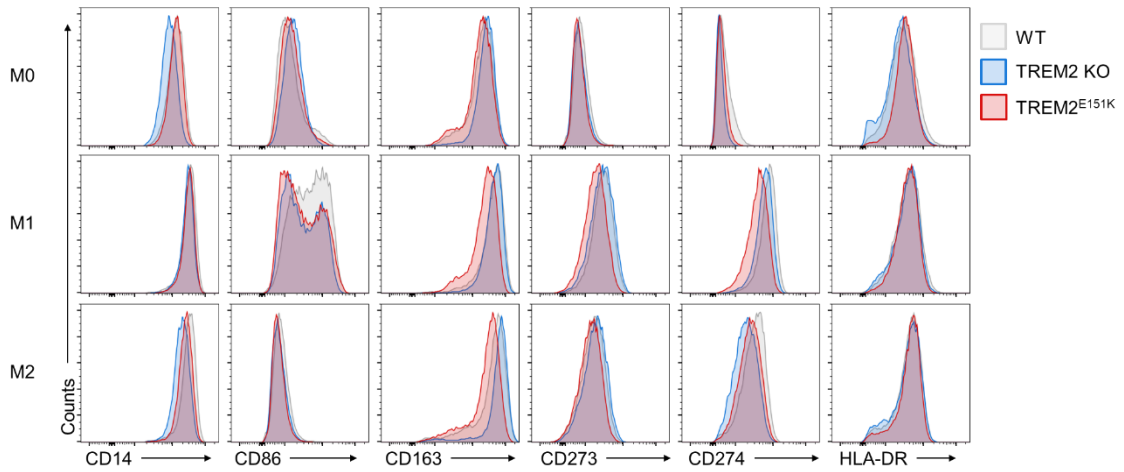

Figure 50: Mutant TREM2 causes reduced expression of pro-inflammatory macrophage associated markers after polarization.
Representative flow cytometry analysis of wild-type (WT), TREM2 knock-out (KO), and patient specific TREM2 knock-in (TREM2^{E151K}) macrophages after polarization towards a M0, pro inflammatory M1, or anti-inflammatory M2 fate. TREM2 KO and TREM2^{E151K} showed defective development of M1 macrophages as shown by reduced expression of CD86 and CD274 (n = 5 independent experiments).

Up-regulation of pro-inflammatory markers (CD86, CD274, HLA-DR) on the cell surface demonstrated that wild-type macrophages could be successfully polarized towards a M1 fate. On the other hand, M2 polarization conditions effectively induced (i) high expression of CD163 and CD273 (PD-L2), (ii) intermediate expression of CD274 (PD-L1), and (iii) reduced expression of CD86.[604] Unpolarized TREM2 KO and TREM2^{E151K} macrophages did not showed substantially different phenotypes compared to wild-type cells (M0, **Figure 50**, upper panel). However, both TREM2 KO and TREM2^{E151K} caused reduced expression of CD274 and up-regulation of CD86 upon induction of M1 polarization. Additionally, TREM2-mutated macrophages also failed to increase expression of HLA-DR in some experiments, but this effect was variable. Taken together, TREM2 KO and TREM2^{E151K} macrophages that were treated with M1 stimulants demonstrated a surface phenotype reminiscent of M2 macrophages suggesting an impaired development of pro-inflammatory macrophages upon loss of TREM2 in humans. Unlike TREM2 KO cells, TREM2^{E151K} also showed reduced expression of CD163 after stimulation of M1 or M2 polarization indicating that the patient mutation might has some additional effect on macrophage polarization.

TREM2 was shown to regulate expression of pro-inflammatory cytokines and can have an activating or inhibitory role depending on the avidity of its ligand. To further characterize the effect of the identified TREM2^{E151K} mutation on inflammatory responses and function of macrophages, activation of important inflammatory pathways was analyzed. In a long-term stimulation assay, iPSC-derived macrophages were first primed with LPS and then NLRP3 inflammasomes were activated using Nigericin to induce K^+ efflux. To determine inflammasome activity, IL-1β secretion into the supernatant was measured by ELISA and expression as well as activation of inflammasome effectors was analyzed by immunoblotting of cell lysates and supernatants (**Figure 51**).

As expected, substantial release of IL-1β by wild-type cells was only detected after full activation of the inflammasome with both stimuli. Interestingly, both TREM2 KO and TREM2^{E151K} secreted reduced levels of IL-1β indicating reduced activation of the NLRP3 inflammasome (**Figure 51A**). Reduced IL-1β concentrations in the supernatant can be a result of reduced expression of pro-IL-1β, impaired cleavage of IL-1β, or defective release of IL-1β via gasdermin pores. Analysis of pro-IL-1β expression in cell lysates by immunoblotting revealed reduced expression levels of pro-IL-1β in TREM2 KO and TREM2^{E151K} macrophages (**Figure 51B**). Since expression of IL-1β in this experimental setting depends on LPS-induced signaling, reduced pro-IL-1β levels indicate

defects in priming of macrophages rather than inflammasome activation. In line with reduced IL-1β secretion measured by ELISA, immunoblotting of cell supernatants also demonstrated reduced levels of mature IL-1β in TREM2 KO and TREM2^{E151K} macrophages (**Figure 51C**).

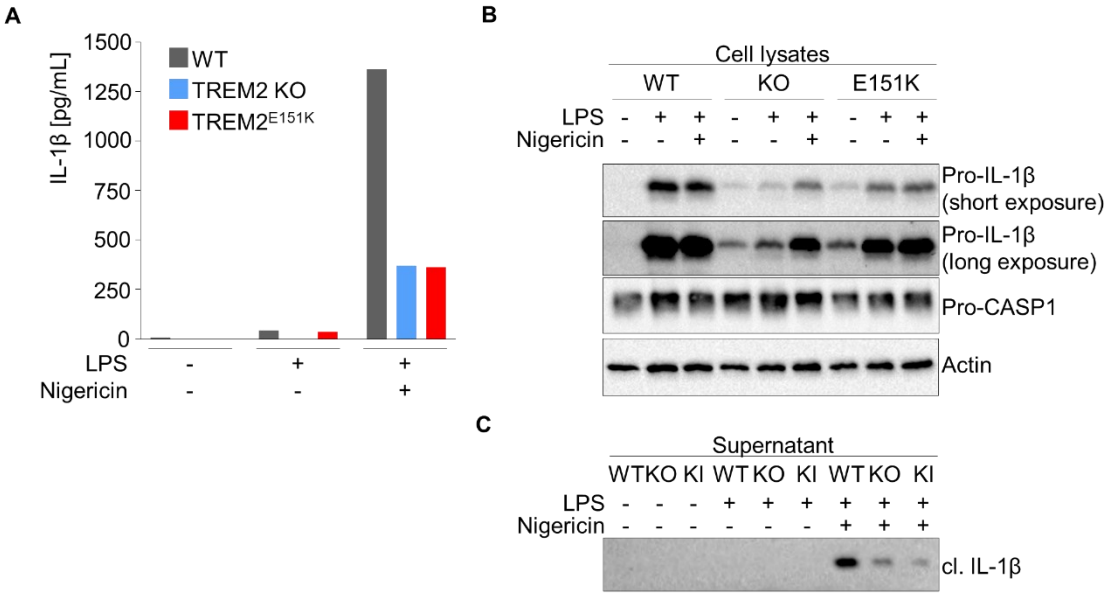

Figure 51: Mutant TREM2 disturbs IL-1β production by macrophages.
(A) Representative ELISA analysis of IL-1β concentration in supernatants from wild-type (WT), TREM2 knock-out (KO), and patient-specific TREM2 knock-in (TREM2^{E151K}) macrophages primed with LPS for 17 h (long-term) and stimulated with nigericin for additional 2 h revealed reduced IL-1β secretion from TREM2 KO and TREM2^{E151K} cells (n = 3 independent experiments for WT, KI, n = 1 for KO). (B) Representative immunoblot analysis of cell lysates from WT, TREM2 KO, and TREM2^{E151K} cells showed reduced expression of pro-IL-1β after LPS stimulation. Notably, pro-IL-1β could be detected in TREM2 KO and TREM2^{E151K} macrophages show expression of pro-IL-1β (n = 3 independent experiments for WT, KI, n = 1 for KO). (C) Representative immunoblot analysis of supernatants from WT, TREM2 KO, and TREM2^{E151K} cells confirmed reduced secretion of mature IL-1β after inflammasome activation (n = 3 independent experiments for WT, KI, n = 1 for KO).

To further substantiate these findings, inflammasome activation was also assessed using short term and low dose LPS priming conditions. In line with long term stimulation, TREM2 KO and TREM2^{E151K} macrophages also showed reduced IL-1β secretion after short term stimulation with LPS (**Figure 52A**). However, the difference was not as pronounced as compared to long term stimulation and TREM2^{E151K} macrophages showed an intermediate phenotype between TREM2 KO and wild-type cells. Analogous to long term stimulation experiments, but less pronounced, reduced pro and mature IL-1β levels could be also confirmed by immunoblotting confirming different regulation of LPS mediated signaling (**Figure 52B**).

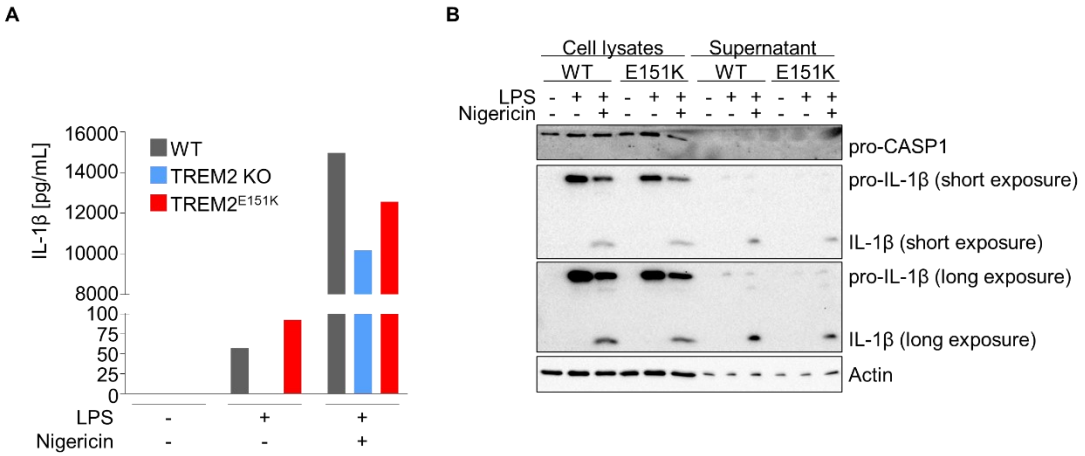

Figure 52: Analysis of short term inflammasome activation in mutant TREM2 macrophages. (A) Representative ELISA analysis of IL-1β concentration in supernatants from wild-type (WT), TREM2 knock-out (KO), and patient-specific TREM2 knock-in (TREM2^{E151K}) macrophages primed with LPS for 2.5 h (short-term) and stimulated with nigericin for additional 0.5 h reveals reduced IL-1β secretion from TREM2 KO and TREM2^{E151K} cells (n = 2 independent experiments for WT, KI; n = 1 for KO). (B) Representative immunoblot analysis of cell lysates and supernatants from WT, TREM2 KO, and TREM2^{E151K} cells confirms reduced expression of pro- and mature IL-1β after LPS stimulation and inflammasome activation (n = 1 independent experiment).

LPS-mediated signaling via TLR4 induces expression of IL-1β, but also leads to production of other inflammasome-independent pro-inflammatory cytokines. To assess, if the reduced expression of cytokines upon LPS stimulation in TREM2-mutated cells is inflammasome-specific or also affects other cytokines, secretion of TNF-α was analyzed (**Figure 53**). ELISA revealed reduced TNF-α secretion upon LPS stimulation in TREM2 KO and TREM2^{E151K} macrophages indicating that the TREM2 mutant disturbs not specifically inflammasome activation, but rather LPS-mediated signaling in general (**Figure 53**).

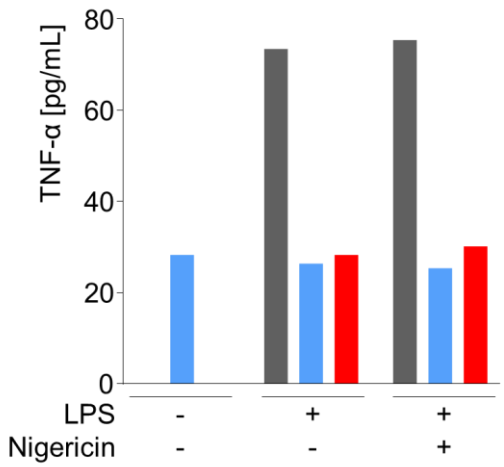

Figure 53: Mutant TREM2 disturbs TNF-α production by macrophages.
Representative ELISA analysis of TNF-α concentration in supernatants from WT, TREM2 KO, and TREM2^{E151K} macrophages primed with LPS for 18 h (long-term) revealed reduced TNF-α secretion from TREM2 KO and TREM2^{E151K} cells. (n = 3 independent experiments for WT, KI, n = 1 for KO).

Taken together, TREM2^{E151K} macrophages largely resembled TREM2 KO macrophages and demonstrated defective inflammatory responses. Interestingly, TREM2 deficiency impairs TLR4-mediated activation of macrophages causing reduced production of pro-inflammatory

markers as well as cytokines, which might prevent efficacy of macrophage functions and altered responses to infections/dangers. TREM2 deficiency might represent a novel genetic entity causing VEO-IBD associated with defective macrophage functions.

5. Discussion

5.1 Novel *IL2RG* mutation causing atypical SCID due to alternative splicing

SCID is a devastating disease, which causes loss of adaptive immunity and impairs defense strategies that nature has developed to protect the human body from pathogens. Consequently, SCID patients suffer from severe infections and usually die in the first year of life without treatment.[250-253] Besides severe infections, SCID patients often present with chronic gastrointestinal inflammation, which is probably caused by lack of tolerance to intestinal microbiota and demonstrates the importance of a healthy immune system for intestinal homeostasis.[250, 251, 253, 254] Mostly due to the lack of attention for rare diseases from the pharmaceutical industry, the only available curative treatment option for SCID-X1 is HSCT. To avoid severe side effects and transplant-related complications, early genetic diagnosis is critical for the successful treatment of SCID-X1 by HSCT.[605] Therefore, newborn screening approaches, which help to identify patients with SCID mutations early in life, are necessary, but are not even performed in all countries in Europe.[606] However, screening approaches might fail to detect atypical SCID, as it might present with different immune phenotypes. To allow efficient diagnosis of atypical SCID, novel causative mutations need to be identified and new pathomechanisms have to be elucidated providing the knowledge for rationale-based treatment decisions.

5.1.1 IL-21R deficiency-like phenotype in a patient with *IL2RG* mutation

I have identified a novel deleterious mutation in *IL2RG* as cause for atypical SCID in two brothers. The mutation has been predicted to cause an early deleterious frameshift in exon 1 of *IL2RG*. Unexpectedly, both patients did not present with typical SCID symptoms, but with a phenotype reminiscent of IL-21R-like deficiency including cryptosporidiosis, chronic diarrhea, recurrent respiratory tract infections, hepatomegaly, and dilatation of the bile duct.[400, 402] Furthermore, both patients showed normal T and NK cell development, which are usually impaired in typical SCID patients.[258] Since the IL2RG mutation was undoubtedly detected in peripheral blood of both patients, somatic mosaicism and maternal engraftment of T cells could be excluded as reasons for the presence of T cells. In line with IL-21R deficiency, class-switched B cells were nearly

absent in both patients indicating defective B cell maturation. Both patients showed severe disease courses and treatment (i.e., HSCT) decision was depending on a precise genetic diagnosis. However, the discrepancy between genotype and phenotype did not allow an unequivocal genetic diagnosis and warranted mechanistic studies on the molecular pathomechanisms of the mutation.

5.1.2 Novel intronic splice site rescues IL-2Rγ expression

A frameshift starting in exon 1 of a mRNA usually causes nonsense-mediated decay resulting in complete loss of mRNA and protein expression. However, I could detect normal *IL2RG* mRNA and IL-2Rγ protein expression in patient EBV-LCLs, corresponding to a normal T and NK cell development. The strong discrepancy between the genotype with a deleterious *IL2RG* mutation and the normal IL-2Rγ expression indicated an unknown molecular mechanism resolving the frameshift and a partial rescue of γ_c signaling. Therefore, I have tested whether the consequences of the deletion might be cleared by alternative start sites or alternative splicing of mRNA. Since exon 1 contains the signal peptide of IL-2Rγ and the identified mutation is located at the end of exon 1, an alternative start site downstream of exon 1 would have to precede a complete novel exon with a similar sequence. Genetic duplication during evolution might result in near-identical genetic sequences, but it is rather unlikely that genetic duplication leads to a position of the sequence that serves as alternative start exon. In contrast, cryptic splice sites are numerous in the human genome and can be activated by changes in the conditions of the splicing reaction. Alternative splicing could either remove the codon carrying the deletion, which would be possible with an exonic cryptic splice site, or by incorporation of additional bases to resolve the frameshift, which can be achieved by intronic cryptic splice sites. Here, I could show that an intronic cryptic splice site exists in intron 1-2 of *IL2RG,* that is rarely used in healthy individuals, as it leads to a non-sense transcript. However, in combination with the identified patient mutation the cryptic splice site results in a productive *IL2RG* transcript, which is partially functionally. This remarkable coincidence of increased usage of an intronic cryptic splice site thus rescued IL-2Rγ expression and contributed to the atypical IL-21R deficiency-like phenotype observed in both patients.

5.1.3 Mutant IL-2Rγ causes IL-21R-like deficiency

The novel isoform generated by a combinatorial effect of the patient mutation and alternative splicing results in a mutant protein with 16 inserted amino acids in the N-terminal domain of IL-2Rγ. My functional studies showed that mutant IL-2Rγ did not cause substantial defects in IL-2, IL-7, and IL-15 signaling, corresponding to the atypical SCID phenotype with normal numbers of T and NK cells. In contrast, I could observe significantly reduced signaling in response to IL-4 and IL-21, which is in line with a phenotype reminiscent of IL-21R deficiency.[400, 402] Since both cytokines are important for B cell development, this finding explains abrogated B cell maturation in both patients. However, due to limited access to patient material I could not address, if defective B cell development is a consequence of missing signals in B cells or a result of dysfunctional T_{FH} cells, which are a major source of IL-21 and their functions are critically dependent on IL-21 signaling.[258] Presumably, lack of IL-21 signaling disturbs both B and T_{FH} cell functions causing the near-complete absence of class-switched B cells in the patients.

Previously, it was shown that IL-2Rγ-deficient B cells are still responsive to IL-4, which might be a result of signaling by type II IL-4R complexes built by IL-4Rα and IL-13Rα in B cells.[318, 607, 608] In contrast, our patients showed abrogated IL-4 responses indicating that IL-4 signaling cannot be rescued by type II IL-4R complexes. Since mutant IL-2Rγ is still expressed on the surface of patient cells, loss of IL-4-mediated signaling might be a result of a dominant-negative effect of mutant IL-2Rγ. Accordingly, mutant IL-2Rγ might form a complex with IL-4 and IL-4Rα, which does not induce an intracellular signal, but prevents formation of type II IL-4R complexes by sequestering IL-4Rα from IL-13Rα. Further studies are required to assess if mutant IL-2Rγ can interact with IL-4Rα and how the mutation might impair signaling by type II IL-4R complexes.

IL-21 is important but not essential for the development of T_H17 cells, as they can still be produced in $Il21r^{-/-}$ mice.[318, 384] In line, I could not observe any difference in the frequencies of T_H cell subsets in the peripheral blood of both patients. On the other hand, IL-4 signaling is important for many different immune subtypes including T_H2 cells, granulocytes, and macrophages, but limited access to patient material did not allow further studies on IL-4 signaling in other cell types.

To analyze the differential effect of the mutation on different γ_c cytokines, I generated a model for mutant IL-2Rγ using *de novo* structural prediction and aligned it to known protein structures of different γ_c complexes.[593-595] Interestingly, the model indicated a more unstructured N-terminal

domain of the mutant protein, which increased the distance between the IL-2Rγ cytokines and the mutant IL-2Rγ. Furthermore, the cytokines were less enclosed by mutant IL-2Rγ indicating reduced interaction strength. Ultimately, changes in the N-terminal domain of IL-2Rγ might cause reduced cytokine binding. Of note, IL-4 and IL-21 use similar binding sites on IL-2Rγ, which might explain that both are affected by the mutation. In contrast, IL-7 was shown to use distinct binding sites on IL-2Rγ compared to other γ_c cytokines, which might be less affected by the identified mutation and allow normal IL-7 function.[609] Lastly, in the heterotrimeric IL-2 and IL-15 receptor complexes, the additional third subunit, which increases the affinity of receptor and cytokine, might create sufficient interaction strength between the cytokine and receptor allowing normal IL-2- and IL-15-mediated signaling observed in patient cells.

5.1.4 Implications for diagnosis and treatment of atypical SCID

Early genetic diagnosis is critical for the treatment of typical and atypical SCID. Cost-effective availability of next-generation sequencing as well as newborn screening approaches have significantly improved diagnosis rates of SCID.[260, 610-613] However, both techniques show inherent limitations in identifying mutations with complicated or unusual pathomechanisms. Most genetic analysis focus on exonic mutations, as the effects of changes in non-coding regions of the human genome are still difficult to predict. On the other hand, exonic mutations might not necessarily cause a phenotype due to a change in the amino acid sequence of the protein, but also cause effects for mRNA expression, splicing, and maturation. Of note, this is especially true for synonymous mutations. Furthermore, effects of mutation in non-coding regions might affect not necessarily the closest gene, but also causes changes in expression of more distant genes, which further complicates the analysis. In this study, I demonstrated that an unusual phenotype is caused by a severe mutation in *IL2RG* that was partially rescued by a novel splicing mechanism, which shows that a functional workup is critical to understand unusual pathomechanisms of novel variants. I am convinced that elucidation of atypical genetic disease mechanisms like the one studied here will provide the knowledge to better understand basic biological and immunological mechanisms; thereby improving rates and speed of genetic diagnosis. Consequently, these insights allow early treatment decisions and will ultimately save many future lives.

5.2 A biallelic CD33 mutation as potential novel cause for inflammatory phenotypes

Since CD33 is a routine marker for myeloid cells and known to modulate different immune-related pathologies, it represents an attractive target in different diseases.[614] Despite this important role, there are still many open questions about the function of CD33, making it difficult to predict the full spectrum of efficacy or unwanted side effects of anti-CD33 therapies. Therefore, deciphering the role of CD33 can increase our knowledge on the development and function of myeloid cells and help to improve therapies for various diseases including inflammatory, neurological, and hematological disorders. However, studies on CD33 are hindered by species differences between mouse and humans, as murine CD33 shows a different expression pattern and has an activating function.[416] Furthermore, increasing evidence suggests that different CD33 isoforms have distinct functions, which is complicating the role of CD33 in humans.[444, 452-455] Rare mutations affecting genes important for immune cell function can help us to improve our understanding of the basic mechanism controlling the immune system. In line, CD33 SNPs were shown to modulate the function of microglia in the CNS resulting in an altered clearance of neurotoxins, which influences the risk of developing LOAD.[481] Analogously, I hypothesize that rare mutations in CD33 might affect the functions of immune cells outside of the CNS and shed light on the general function of CD33 in humans.

5.2.1 Identification of a patient with a biallelic germline CD33 mutation

In this thesis, I have identified a biallelic mutation in the *CD33* gene in a patient suffering from severe VEO-IBD accompanied by vasculitis refractory to conventional state-of-the-art treatment. Manifestation of inflammation in the gut and vascular system strongly indicated an underlying immune defect, since both compartments are built by different cell types (i.e., epithelial vs. endothelial cells), but share the presence of immune cells in high abundancy. In comparison to the intestine, the vascular system rarely encounters external toxins or pathogens and vasculitis might be suggestive of an immune defect that causes over-activation or dysfunction of immune cells.

The identified mutations are found close to splice sites of the *CD33* pre-mRNA and were predicted to influence splicing efficacy. Of note, the mutation c.415A>T is located at the end of exon 2,

which encodes the ligand-binding domain of CD33 and is differentially spliced in CD33M and CD33m isoforms. The function and localization of CD33m are still controversial and different studies came to contrary conclusions.[444, 452-455] Whereas some studies propose the CD33m represents a loss-of-function isoform due to a missing capability to bind sialic acids, others suggested that CD33m might be a gain-of-function isoform that is constitutively active.[454, 455] In some studies, CD33m was found to be located intracellularly (i.e., in peroxisomes), but other reports have detected CD33m also on the cell surface.[444, 452, 453] These contrary observations might be caused by the usage of different antibodies, over-expression vs. primary cellular models, and cell type-specific differences. Further studies are needed to address the exact role of different CD33 isoforms.

5.2.2 CD33 mutations cause altered mRNA and protein expression in immune cells

Since both mutations were predicted to alter splicing of *CD33* pre-mRNA, I analyzed *CD33* expression by qRT-PCR in primary cells and could observe increased levels of CD33 in the patient but also in the healthy relatives. However, the identified compound heterozygosity might mask pronounced effects in the index patient, as the mutations might not have a cumulative or even contrary effect. Therefore, I generated doxycycline-inducible *CD33* mini-genes and over-expressed them in HEK293T cells. Of note, I could observe a significantly increased expression of small CD33m isoforms in cells expressing the c.415A>T mutation. Since c.415A>T is located at the 3'-end of exon 2, it is likely that this mutation affects the 5' splice site of intron 2-3 and causes increased skipping of exon 2, which alters the isoform balance of CD33. As the function of the small CD33m isoform remains controversial, we will continue to evaluate the functional consequences in relevant physiological models. In contrast, I could not observe any difference for the c.746-8delG mutation in this experimental setting. However, splicing might be subject to other regulatory mechanisms in different cell types and immune cells might show different isoform expression. As I removed or shortened introns to reduce the size of the mini-gene, the role of the c.746-8delG mutation might be also masked by the design of the CD33 mini-gene. In particular removal of intron 3 and fusing of exon 3-4 might prevent skipping of exon 4, which was observed in experiments with iPSC-derived macrophages. Therefore, I will design and over-express a novel generation of mini-genes containing intron 3 and analyze CD33

expression in subsequent experiments. Furthermore, we will tag the CD33 mini-gene to analyze protein expression and localization of different CD33 isoforms by immunoblotting and immunofluorescence microscopy.

To analyze CD33 expression in a physiological disease model, I generated iPSC lines with KO of CD33 and patient-specific KIs of CD33 using CRISPR/Cas9-mediated genetic engineering in order to differentiate iPSC-derived macrophages and granulocytes. Of note, $CD33^{c.415A>T}$ cells showed a strongly reduced or absent CD33 surface expression in the hematopoietic stages during differentiation. Mini-gene studies demonstrated that cells expressing c.415A>T have a significantly increased expression of the small CD33m isoform, which might be localized mostly intracellularly based on published literature.[452] Therefore, absent CD33 surface expression might be due to an increased CD33m/CD33M ratio in $CD33^{c.415A>T}$ hematopoietic cells. Indeed, RNA expression analysis in $CD33^{c.415A>T}$ macrophages and granulocytes demonstrated an inverted CD33 isoform ratio accompanied by a strong reduction of CD33M expression indicating that the c.415A>T mutation strongly augments skipping of exon 2 during *CD33* pre-mRNA maturation. Of note, CD33M expression levels in $CD33^{c.415A>T}$ cells were comparable to CD33 KO cells indicating a nearly complete loss of CD33M expression. In mini-gene over-expression models I could not observe such a profound loss of CD33M expression confirming the necessity to analyze pathomechanisms in more physiological-relevant disease models.

Moreover, mRNA expression analysis in iPSC-derived myeloid cells also revealed a previously undescribed splicing mechanism in CD33, which results in skipping of exon 4. Interestingly, both patient mutations caused an increased expression of CD33 mRNA lacking exon 4, which encodes the C-terminal end of the extracellular domain in front of the transmembrane domain. The role of exon 4 remains unclear, as there are no specific descriptions or structural data available. However, loss of exon 4 will reduce the distance of the V-set and the C2-set domain from the cell membrane, which might prevent mutant CD33 to bind certain ligands that are found more far away from the surface. Since the cell membrane is crowded with membrane proteins and is electrostatically charged, proximity of the extracellular domain to the cell surface might cause structural problems by steric hindrance or electrostatic repulsion, which might change the activity of mutant CD33.

On a protein level, peripheral blood cells showed increased or altered expression of CD33 on the surface of various immune cell populations, which is in line with mRNA expression data from primary cells but might sound contrary to the observed reduction in iPSC-derived model systems. However, the patient carries a compound heterozygous mutation and thus distinct effects on splicing of both mutations might affect the phenotype differentially than the homozygous model systems. Since my data in heterologous cellular models suggest that the c.415A>T mutant results in a loss of CD33M expression, the aberrant surface expression pattern might be reflected solely by the effects of the c.746-8delG mutation.

Detailed immunophenotyping of peripheral blood cells showed that populations characterized by high CD33 expression levels in healthy donors showed only mild upregulation of CD33 in the patient whereas cell populations with absent or low expression of CD33 in healthy individuals showed a strong up-regulation of CD33. For example, eosinophils usually down-regulate CD33 expression during differentiation and mature eosinophils demonstrate only low levels of CD33 on the surface.[615] In contrast, more than 90 % of $CD45^{high}CD16^{-}$ eosinophil-like cells from the patient showed high CD33 expression levels, which might be due to defective eosinophil maturation or aberrant expression of CD33 in mature eosinophils. The detection of eosinophil and granulocyte progenitors might indicate a hematological disorder, which could not be observed in the patient. Furthermore, CD33 expression was also strongly increased in $CD3^{-}CD19^{-}CD56^{+}$ cells, which weren't positive for CD33 in healthy donor samples. Although this population includes $CD56^{+}CD16^{+}$ NK cells, CD33 expression was also seen in $CD16^{-}$ populations. Similar to granulocytes, $CD33^{+}CD56^{+}$ cells might represent immature NK cells precursors or mature NK cells that aberrantly express CD33 in the periphery.[616, 617] Taken together, the immunophenotypical characterization suggested that patient peripheral blood cells showed an altered regulation of CD33 expression or that immature $CD33^{+}$ cells are enriched in the periphery due to defective hematopoiesis. Immature cell populations might react very differently to external stimuli and might cause immune defects and/or inflammatory syndromes.

In addition, detailed immunophenotyping revealed reduced expression of the activation markers HLA-DR and CD16 in patient $CD33^{+}$ peripheral blood cells (i.e., monocytes). Remarkably, the difference in expression was most pronounced for $CD33^{+}$ patient monocytes, which may indicate a role of CD33 in monocyte activation.

Furthermore, I could detect altered distribution of T helper cells accompanied by increased frequencies of $CXCR3^{-}CCR6^{+}$ T_H17-like cells and decreased frequencies of $CXCR3^{+}$ T_H1-like cells in the patient compared to healthy controls. Since T_H17 cell development can be driven by IL-1β, increased frequencies of T_H17 cells might be caused by premature activation of $CD33^{+}$ cells and release of pro-inflammatory cytokines. However, numbers of T_H17 cells are increased in many IBD patients and might be not a specific symptom but represent rather a sign of severe inflammation. Although CD33 is used as marker for myeloid cells, it was shown that CD33 can be also expressed on lymphocytes upon activation. Therefore, I also analyzed CD33 expression on lymphocytes and found that higher proportions of patient lymphocytes were positive for CD33 on the cell surface. Furthermore, patient $CD4^{+}$ T cells showed significantly stronger up-regulation of CD33 mean fluorescence intensity after *ex vivo* stimulation, which is in line with our observation that cell with lower expression of CD33 have a stronger CD33 expression in the patient. Interestingly, cells from the father were indistinguishable from healthy donor samples but cells isolated from the blood of the mother demonstrated an intermediate phenotype. Since the mother is a heterozygous carrier of the c.746-8delG mutation, this observation is in line with the hypothesis of that the expression pattern in the patient might be primarily caused by the c.746-8delG mutation. In detail, if the c.746-8delG mutation is responsible for the observed aberrant expression pattern, I would expect an intermediate or masked phenotype in heterozygous carriers (i.e., the mother), as they still have a wild-type copy of the gene. In homozygous or homozygous-like carriers (i.e., the patient when considering the loss of expression by c.415A>T) I would expect a strong upregulation, as seen in the patient. In summary, I hypothesize that the c.746-8delG mutation causes an altered splicing of intron 4-5 and/or exon 4, which leads to aberrant expression of CD33 on the cell surface. In the patient the combination of both mutations results in a homozygous-like state of the second mutation, which may result in the observed expression differences. However, the role of CD33 in lymphocytes remains unclear and needs to be analyzed in further studies. Lack of primary patient material limited the studies on CD33 mutated T cells. Therefore, I will generate humanized mouse models that will be reconstituted by CRISPR/Cas9-engineered iPSC-derived HSPCs allowing more detailed analysis of human T cell development and function *in vivo*.

5.2.3 CD33 mutations affect hematopoiesis

Immunophenotyping of peripheral immune cells demonstrated increased expression of CD33 in various immune cell lineages, which might be caused by aberrant expression of CD33 in mature immune cells or by presence of $CD33^{+}$ immature immune cell types in the periphery. CD33 is known to be expressed early in hematopoiesis and thus might have an inhibitory role on immune cell development. Therefore, I analyzed the effect of CD33 mutations on hematopoiesis of iPSC-derived HSPCs using an CFU assay in semi-solid medium. Interestingly, I could observe a significantly increased colony formation of CD33 KO, $CD33^{c.415A>T}$, and $CD33^{c.746\text{-}8delG}$ cells indicating an enhanced proliferation and/or differentiation potential of mutant CD33 HSPCs. In contrast to published studies, I could observe a regulatory effect of CD33 on hematopoiesis. Thus these studies warrant caution for available treatments using CD33 as target, since altered HSPC biology and differentiation might also result in malignant or exhausted immune phenotypes.

5.2.4 CD33 modulates inflammatory responses of myeloid cells

CD33 is known to influence phagocytosis and it was shown that reduced CD33M or higher CD33m expression is a critical determinant of microglial ability to clear neurotoxins like Aβ plaques in LOAD.[455, 481] Since I could demonstrate a shift in isoform homeostasis and an aberrant CD33 expression caused by the identified compound heterozygous mutation, I analyzed the ability of iPSC-derived macrophages to phagocytose and kill bacteria. Although with variable intensity across individual experiments, I could observe an increased number of surviving intracellular *S. typhimurium* in CD33 KO and KI macrophages. This observation can be explained by increased uptake of the bacteria or by defective intracellular killing of the bacteria. Since *S. typhimurium* induces macropinocytosis to enter cells, it is more likely that the increased number of surviving bacteria represents a defect in bacterial killing then increased phagocytosis. Confirming experiments with other bacterial species are currently established. The variability of the experiments might be caused by differences in number and replication phase of bacteria, which is hard to adjust perfectly. Although no substantial differences in surface marker expression could be detected in iPSC-derived macrophages, variable outcomes of the experiments could be also caused by different states of polarization at different time points. To further assess the effect of both mutations on phagocytosis, phagocytic capacity needs to be assessed directly (e.g., uptake measurements by flow cytometry) and with different stimuli.

Besides inhibition of phagocytosis, CD33 was also shown to inhibit cellular activation in a steady-state and targeting of CD33 using antibodies, KD of CD33, or removal of CD33 cis-ligands resulted in increased pro-inflammatory cytokine release (i.e., IL-1β, IL-8, and TNF-α) indicating a central role of CD33 in controlling myeloid cell homeostasis.[456] To confirm this role, I treated trans-differentiated $CD14^{+}CD33^{+}$ macrophage-like BLaER1 cells with anti-CD33 and sialidase and analyzed inflammasome activation.[600, 601] In line with published data, removal of cis ligands by sialidase induced release of IL-1β.[456] Interestingly, I could show that stimulation with anti-CD33 impaired production of IL-1β. In parallel, anti-CD33 induced strong release of LDH into the supernatant indicating increased cell death of anti-CD33-treated cells. LDH might be released into the supernatant after rupture of the cell membrane during necrosis or via gasdermin pores inserted into the cell membrane during pyroptosis, which is executed after inflammasome activation. In contrast to apoptosis, necrosis and pyroptosis are inflammatory forms of cell death causing immune cell activation and amplification of inflammation. Dysregulated cell death mechanisms can cause severe inflammation and, in line, our group recently demonstrated that disturbed cell death responses can cause inflammatory syndromes presenting with VEO-IBD.[112, 113] Cell death might be induced by various cellular pathways, but the strong response to anti-CD33 indicates an important role of CD33 in controlling survival and activation of cells in steady state. Although molecular mechanisms of anti-CD33 antibodies are still controversial, the similarity between the effects of CD33 KD and anti-CD33 suggests that the CD33-targeting antibody has a blocking effect on CD33 function. Taken together, the BLaER1 cell model suggested that loss of CD33 function results in inflammatory cell death in macrophages and that removal of sialic acids causes pre-mature activation of macrophages. CD33-mediated inflammatory cell death might explain the observed autoinflammatory phenotype in the patient, which needs to be confirmed in primary patient material and more sophisticated model systems.

In a first experiment with primary patient material, I could observe an increased IL-1β production after activation of the NLRP3 inflammasome by LPS and Nigericin in patient monocyte-derived macrophages. When analyzing the complete index family in a second experiment, I observed similarly high IL-1β production in monocyte-derived macrophages and granulocytes of healthy family members. IL-1β production of all family members measured by ELISA was still strongly increased compared to unrelated controls indicating rather a genetic predisposition towards an increased inflammatory response of the complete family. Notably, substantial release of IL-1β

could be detected in samples from the index family after LPS priming without inflammasome activation indicating a pre-mature activation of the cells or presence of other second stimuli in these cells.

On the other hand, immunoblot analysis of cell supernatants revealed highest production of mature IL-1β in patient cells and intermediate production in cells from the father and the mother. Although tested with high dilution, differences between ELISA and immunoblotting might be caused by an upper detection limit of the ELISA, which might prevent detection of very high IL-1β concentrations in the patient. Furthermore, the ELISA might cross-react with immature IL-1β masking differences of active IL-1β. Immunoblotting of cell lysates confirmed increased expression of pro- and mature IL-1β in the index family, but differences between the patient and the healthy family members were less pronounced.

Interestingly, anti-CD33 treatment caused an increased IL-1β secretion in healthy donor monocytes but did not affect IL-1β production by cells from the index family suggesting that cells from the index family are either not responsive to anti-CD33 stimulation or reached a maximum IL-1β production. Stimulation with anti-CD33 also caused release of IL-1β without LPS/Nigericin-mediated inflammasome activation confirming the role of CD33 in controlling cellular activation in steady-state in a primary cell model. In line, immunoblot analysis revealed IL-1β expression in cell lysates pre-treated with anti-CD33 without LPS/Nigericin stimulation. Furthermore, anti-CD33 stimulation resulted in cleavage of CASP1 and release of mature CASP1 into the supernatant independent of inflammasome activity, which may be a sign of pyroptosis and confirmed the observation of increased cell death in response to anti-CD33 in BLaER1 cells. Differences in the outcome of cell death responses might be also due to variations in the experimental conditions between BLaER1 cells and macrophages.

Furthermore, immunoblotting of cell supernatants revealed increased secretion of S100A9 by macrophages from the mother and the patient, but not in samples from the father or healthy donors. S100A9 production was independent of LPS/Nigericin stimulation or even reduced upon inflammasome activation in both samples. Since S100A9 was shown to interact with CD33 increased S100A9 expression and/or secretion might be linked to altered CD33 expression and function in both samples, but at the moment it is not clear how mutant CD33 might regulate S100A9 expression or secretion.

To shed light on the role of the two CD33 mutations on inflammasome activation, I generated iPSC-derived macrophages and granulocytes and tested inflammasome responses after different stimuli (i.e., priming with LPS or S100A9). Interestingly, I could not observe a consistently increased IL-1β production upon priming with LPS in both cell models (i.e., macrophages and granulocytes), but after priming with S100A9 in macrophages. Increased IL-1β production was accompanied by higher LDH release indicative of enhanced pyroptosis in macrophages upon stimulation with S100A9. In granulocytes, only $CD33^{c.746\text{-}8delG}$ cells demonstrated increased IL-1β production and LDH release in response to S100A9. As hypothesized before, $CD33^{c.746\text{-}8delG}$ might cause altered CD33 expression in cells expressing low levels of CD33 (e.g., granulocytes) and, as CD33 might bind S100A9, increased CD33 expression caused by c.746-8delG might alter the response to S100A9. This might be also in line with increased production of S100A9 in carriers of the c.746-8delG allele (i.e., mother and patient).

5.2.5 Studies on CD33 help to understand pathomechanisms in different diseases

In summary, I could identify a germline compound heterozygous mutation in CD33 that changes the expression of CD33 on mRNA and protein level in various immune cell populations. Altered CD33 expression was associated with increased proliferation/differentiation of HSPCs, reduced bacterial killing, and increased inflammasome activation in macrophages and granulocytes. Of note, enhanced IL-1β secretion could be the driver of the inflammatory phenotype in our index patient resulting in IBD and vasculitis, which was observed in the patient. Furthermore, an IL-1β-mediated inflammation in the patient might explain failure of treatment with routine biologics targeting TNF-α. Higher IL-1β levels would be also in line with increased frequencies of T_H17 cells detected in immunophenotyping. Therefore, our study provides important arguments to test therapies targeting IL-1β (e.g., Anakinra), which are currently not routinely used in VEO-IBD patients.

CD33 mutations were shown to modulate the risk of LOAD development by changing the phagocytic activity of microglia.[481] Here, I identified novel variants affecting the splicing of CD33. In fact, $CD33^{c.415A>T}$ causes a near-complete loss of CD33M expression and a substantial increase in CD33m expression. Therefore, the identified mutations can help us to increase the understanding of mechanisms regulating CD33 expression and function. However, identification

of additional patients with germline CD33 mutations will be necessary to shed light on the enigmatic role of CD33. Since higher CD33m expression was shown to be protective for LOAD, our study might help to develop novel strategies to change CD33 isoform balance and treat LOAD in future.[481, 498, 500] However, our study also cautions that alteration of CD33 expression might have pathogenic effects in other organs that need to be considered before using CD33-based treatments.

In addition, our study raises questions regarding the usage of CD33-targeted therapies in various other disease settings. Gemtuzumab-Ozogamicin (GO) is an CD33-directed monoclonal antibody and is approved for the treatment of AML but showed substantial side effects.[484, 486, 487] Of note, the epitope of GO is located in the V-set domain of CD33 encoded by exon 2. Increasing evidence on the expression of CD33m in various immune cells suggests that GO might not affect cells that express CD33m and thus might not target all malignant cells.[484] Especially humans with SNPs in CD33 that change the isoform balance of CD33 might not be fully responsive to GO treatment.[484] Although cell death is desired for cancer cells, CD33 antibodies also target normal hematopoietic cells and early progenitor cells, which might affect the balance of hematopoiesis and cause prolonged cytopenia after treatment.[487] More importantly our studies demonstrated that anti-CD33 antibodies that bind in the same domain result in strong induction of inflammatory cell death in myeloid cells and this inflammation might cause severe side effects.

5.3 TREM2 deficiency affects TLR4-mediated inflammatory responses

TREM2 is a cell surface receptor predominantly expressed on different myeloid cells that binds negatively charged proteins and lipids.[492, 525] TREM2 has no intracellular signaling domain but relies on DAP12 to transduce its signal inside the cell.[528, 529, 532, 533] TREM2-DAP12 signaling and its functional consequences are diverse and can be activating or inhibiting depending on the context, cell type, and tissue.[528, 529] Therefore, the effect of TREM2-DAP12 signaling in mice and humans is still actively investigated. The important role of TREM2 is exemplified by TREM2 mutations in patients with NHD that suffer from neurodegeneration, osteoporosis, and bone cysts.[569] In NHD, TREM2 deficiency results in phagocytic defects and pro-inflammatory phenotypes of macrophage-like cells (i.e., microglia and osteoclasts), which ultimately leads to

tissue inflammation and destruction.[569, 571, 572, 575] In line, murine models demonstrated a protective role for TREM2 in development of experimental autoimmune encephalomyelitis.[581, 618, 619]

Besides regulation of myeloid cells in the CNS and the bones, TREM2 has been also shown to regulate the function of intestinal myeloid cells (i.e., DCs and macrophages).[580, 581] $TREM2^{+}$ cells are enriched in the LP of IBD patients and experimental mouse models of colitis.[580, 581] In contrast to CNS and bones, TREM2 is considered to have a pro-inflammatory effect in intestinal myeloid cells, as loss of TREM2 ameliorated chemically-induced colitis in an experimental model.[580] However, the role of TREM2 in intestinal homeostasis is still discussed controversial, as TREM2 KO caused impaired wound healing in another model.[582] These conflicting results might be caused by differences in the experimental study design or might reflect the dual role of TREM2 in regulating intracellular signaling.[529]

Identification of rare mutations and elucidation of their pathomechanisms in NHD and FTD critically contributed to an improved understanding of TREM2 function and regulation.[569, 571, 572, 575] Similarly, rare TREM2 mutations might cause intestinal inflammation and thus also help to expand the knowledge on the role of TREM2 in intestinal myeloid cells and intestinal homeostasis.

5.3.1 TREM2 mutation changes molecular properties of TREM2 protein and alter myelopoiesis

Here, I identified a homozygous mutation (p.E151K) in TREM2 in a patient with severe VEO-IBD and neuromuscular development disorder. Interestingly, the mutation has been previously associated with an increased risk for AD.[620] Structural analysis suggested that the mutation is located in the extracellular domain close to the shedding site of TREM2. Other mutations at the shedding site were reported to have detrimental effects on the function of TREM2 and to increase the risk of AD.[537] Unfortunately, the index patient succumbed to his disease at an age of 8 months, which prevented detailed studies on primary patient material, but indicates a severe form of VEO-IBD. To study the effects of the identified mutation on TREM2 function, I generated iPSC cells with KO of TREM2 and KI of the patient-specific mutation using CRISPR/Cas9 engineering. Immunoblotting demonstrated successful KO of *TREM2* and revealed a reduced molecular weight of the $TREM2^{E151K}$ mutant as compared with WT TREM2. Preliminary experiments by our collaboration partner (AG Haass, DZNE, LMU Munich) showed that this shift is not caused by an altered glycosylation pattern of mutant TREM2, which might indicate that other post-translational

modifications are affected by the TREM2 mutation or that the mutation changes the electrostatic properties of the peptide.

Although iPSC-derived macrophages could be successfully generated, TREM2 KO and KI cells showed reduced cell death and increased frequencies of $CD45^+$ cells during differentiation. Cell death is a normal phenomenon during *in vitro* differentiation, as cells that mature into different immune subsets (e.g., lymphocytes) miss the correct survival cues and undergo apoptosis. Reduced cell death in TREM2-deficient cells may indicate either a changed potential to differentiate towards myeloid subsets or a faster progression towards myelopoiesis.

In line, CFU assays with iPSC-derived HSPCs showed quantitative and qualitative differences in differentiation of TREM2-mutant cells compared to wild-type cells. TREM2 KO and $TREM2^{E151K}$ cells both showed a reduced potential to generate colonies containing macrophages, which was associated with an increased frequency of erythrocyte-containing (KO) or granulocyte-containing ($TREM2^{E151K}$) colonies indicating that TREM2 deficiency disturbs differentiation of macrophages. Since TREM2 is not expressed in erythrocytes and granulocytes, the simultaneous increase in other colony types suggests that TREM2 might be involved in lineage determination during myelopoiesis. In line, TREM2 mutations identified in NHD patients disturb differentiation of macrophage-like osteoclasts and TREM2/DAP12 were shown to influence survival of macrophages and microglia by regulating CSF-1R and mTOR signaling.[550, 571, 621-625] Furthermore, TREM2 was recently shown to interact with CSF-1R indicating a regulatory role of TREM2 for M-CSF-mediated signaling in macrophages.[626] High concentration of supplemented M-CSF during macrophage differentiation might rescue survival disadvantages of TREM2-deficient cells and might explain succesfull generation of iPSC-derived macrophages.[626]

Interestingly, $CD45^+$ hematopoietic cells during the monocyte differentiation stage expressed higher levels of CD14, which is a sign of a pro-inflammatory and/or activated state in monocytes. However, it might be also caused by faster differentiation of monocytes towards macrophages, as no different immunophenotype could be observed in mature macrophages.

5.3.2 TREM2 deficiency is associated with impaired pro-inflammatory functions of human macrophages

TREM2 and DAP12 were shown to have dual effects on intracellular signaling.[528, 529] This dichotomy might explain differential results in various studies showing that TREM2 deficiency can result in increased or reduced pro-inflammatory cytokine release.[530, 548, 552, 580, 627, 628] To test the effects of the identified mutation on macrophage functions, I analyzed inflammasome activation and macrophage polarization. Interestingly, I could observe decreased pro-inflammatory cytokine production (e.g., IL-1β, TNF-α) by TREM2 KO and KI cells upon LPS stimulation indicating an activating effect of wild-type TREM2 in TLR4-mediated signaling of macrophages. Of note, similarities between TREM2 KO and KI indicated that the $TREM2^{E151K}$ variant is a loss-of-function allele. Different outcomes of experiments might be caused by different experimental settings (e.g., concentration of stimuli, duration of stimulation), but might also reflect differences between mouse and human. To clarify these differences, further experiments to assess different stimuli and kinetics will be performed.

TREM2 was also shown to inhibit polarization of M1 macrophages in mice.[582] In contrast, our studies showed that TREM2-deficient macrophages failed to up-regulate important M1 markers like the co-stimulatory molecule CD86 in response to LPS and IFN-γ stimulation. For other M1 surface markers like CD274 (PD-L1) I could observe only minor differences in the expression pattern. Smaller effects for some markers (e.g., CD274) might be explained by stronger effects of IFN-γ-mediated signaling independent of LPS.[604]

Reduced pro-inflammatory cytokine secretion and reduced CD86 expression in response to LPS stimulation can both be explained by an impaired or inhibited TLR4-mediated signaling in TREM2-deficient cells. TREM2-mediated effects on other surface molecules during macrophage polarization might be masked by efficient IFN-γ-induced signals. Therefore, macrophage polarization needs to be further assessed upon stimulation with LPS ± IFN-γ in the future in order to study whether TREM2 deficiency causes inhibition of TLR4 signaling. Furthermore, effects of TREM2 deficiency on macrophage development and polarization needs to be analyzed in different model systems. Ultimately, effects of altered macrophage polarization on T cell polarization needs to be assessed further.

The identified mutation is located in the extracellular domain and thus is also present in sTREM2 after shedding. In detail, the E151K variant is located at the C-terminal end of sTREM2 and thus might influence binding of sTREM2 to its receptor, which has not been identified yet. Furthermore, the mutation might change the cleavage site of TREM2, which would result in the production of an altered sTREM2. Despite similarity between TREM2 KO and KI, an influence of sTREM2 cannot be excluded. Therefore, in prospective experiments, purified sTREM2^{E151K} will be used to stimulate cells in order to exclude effects of the mutation in sTREM2.

5.4 Role of immune cells in IBD pathogenesis

In this thesis, I identified novel mutations in three different genes (i.e., *IL2RG, CD33*, and *TREM2*), which all encode cell surface receptors expressed on different immune cell populations. The described patients suffered from a broad spectrum of phenotypes affecting various organs (e.g., liver, skin, nervous system), but all shared chronic intestinal inflammation as their primary diagnosis demonstrating the importance of the immune systems for intestinal homeostasis. Whereas the mutations in *IL2RG* predominantly affected lymphocytes, my studies suggested that *CD33* and *TREM2* mutations cause primarily defects in myeloid cell subsets. However, my studies also illustrate the connectivity between innate and adaptive immunity in maintaining intestinal homeostasis. First, the atypical SCID-X1 phenotype caused by the mutation in *IL2RG* is characterized by defective B cell proliferation and impaired IL-4 and IL-21 signaling. However, IL-4 also induces polarization of M2 macrophages, which control intestinal wound healing and are thus critical for repairing damages of the intestinal mucosa. On the other hand, *CD33* and *TREM2* mutations caused altered secretion of pro-inflammatory cytokines by myeloid cells, which are important cues for differentiation and polarization of T cells. *CD33* and *TREM2* mutations also resulted in a changed expression of co-stimulatory surface molecules (e.g., HLA-DR, CD86), which might indicate a disturbed antigen presentation by MNPs to T cells in the index patients. Furthermore, increased CD33 expression in T cells of the index patient with a compound heterozygous mutation demonstrated that myeloid receptors can also be expressed on lymphocytes and might also alter their function evidencing the complex network between various immune cells.

5.5 Unusual pathomechanisms in genetic diseases

VEO-IBD and primary immunodeficiencies are often caused by rare, monogenic mutations that have severe consequences on protein function.[38, 245, 246] In the beginning non-coding mutations were largely ignored in the analysis of genetic data, as their role could not be assessed or explained. However, advances in the understanding of human cellular biology and sequencing technologies questioned the DNA-RNA-Protein dogma and resulted in the identification of a growing number of mutations with unexpected pathomechanisms. Here, I found two examples how alterations in splicing can dramatically change the function of proteins and/or the development of disease. Alternative splicing of *CD33* pre-mRNA resulted in an altered expression of isoforms and changed the phenotype and functions of various immune cell subsets, which may lead to inflammatory phenotypes. Interestingly, the c.415A>T mutation in *CD33* is an exonic mutation that was first identified as a missense mutation. However, without a detailed functional workup the strong effect on splicing might have been overseen and would have resulted in a wrong interpretation of the genetic data. On the other hand, I could show that a cryptic intronic splice site rescued the expression of a deleterious *IL2RG* mutation and partially reverted the loss of γ_c function resulting in an atypical SCID phenotype. These findings advocate that genetic analysis pipelines and screening approaches need to consider molecular pathomechanisms outside of the dogma of coding mutations in order to identify more complex genetic diseases, which will ultimately help to cure more patients with severe disorders.

5.6 Rare diseases help to understand human biology

Dysfunction of innate and adaptive immune cells results in defective recognition and clearance of pathogens, overreactive immune responses, and impaired regulation of inflammatory processes, which ultimately causes chronic inflammation and the severe phenotypes observed in the described patients. Genetic diagnosis is key to understand the disease of these patients, provide appropriate treatments, and find curative approaches. However, our studies showed that many pathomechanisms might be not straightforward and need to be clarified by a detailed functional workup. Following this approach, I could provide definitive diagnosis to the two *IL2RG*-deficient patients and initiate HSCT as a curative approach. Unfortunately, both patients died due to complications, which will be a memorial for us to identify novel mutations and provide fast genetic

diagnosis. The gained insights, however, will help future patients with similar diseases, so that they can be cured in an efficient timeframe. Furthermore, findings from the studied genes will shed light on fundamental biological mechanisms in immunity, define novel therapeutic targets, evaluate established treatment options, and might help to better understand pathomechanisms in other diseases.

References

1. Sartor RB. Mechanisms of disease: pathogenesis of Crohn's disease and ulcerative colitis. Nat Clin Pract Gastroenterol Hepatol. 2006;3(7):390-407.

2. Xavier RJ, Podolsky DK. Unravelling the pathogenesis of inflammatory bowel disease. Nature. 2007;448(7152):427-34.

3. Abraham C, Cho JH. Inflammatory bowel disease. N Engl J Med. 2009;361(21):2066-78.

4. Podolsky DK. Inflammatory bowel disease. N Engl J Med. 2002;347(6):417-29.

5. Carter MJ, Lobo AJ, Travis SP, Ibd Section BSoG. Guidelines for the management of inflammatory bowel disease in adults. Gut. 2004;53 Suppl 5:V1-16.

6. Jairath V, Feagan BG. Global burden of inflammatory bowel disease. Lancet Gastroenterol Hepatol. 2020;5(1):2-3.

7. Collaborators GBDIBD. The global, regional, and national burden of inflammatory bowel disease in 195 countries and territories, 1990-2017: a systematic analysis for the Global Burden of Disease Study 2017. Lancet Gastroenterol Hepatol. 2020;5(1):17-30.

8. Engel MA, Neurath MF. New pathophysiological insights and modern treatment of IBD. J Gastroenterol. 2010;45(6):571-83.

9. Molodecky NA, Soon IS, Rabi DM, Ghali WA, Ferris M, Chernoff G, et al. Increasing incidence and prevalence of the inflammatory bowel diseases with time, based on systematic review. Gastroenterology. 2012;142(1):46-54 e42; quiz e30.

10. Nikolaus S, Schreiber S. Diagnostics of inflammatory bowel disease. Gastroenterology. 2007;133(5):1670-89.

11. Graham DB, Xavier RJ. Pathway paradigms revealed from the genetics of inflammatory bowel disease. Nature. 2020;578(7796):527-39.

12. Nambu R, Muise AM. Advanced Understanding of Monogenic Inflammatory Bowel Disease. Front Pediatr. 2020;8:618918.

13. Levine A, Koletzko S, Turner D, Escher JC, Cucchiara S, de Ridder L, et al. ESPGHAN revised porto criteria for the diagnosis of inflammatory bowel disease in children and adolescents. J Pediatr Gastroenterol Nutr. 2014;58(6):795-806.

14. Shivananda S, Lennard-Jones J, Logan R, Fear N, Price A, Carpenter L, et al. Incidence of inflammatory bowel disease across Europe: is there a difference between north and south? Results of the European Collaborative Study on Inflammatory Bowel Disease (EC-IBD). Gut. 1996;39(5):690-7.

15. Munkholm P, Langholz E, Davidsen M, Binder V. Intestinal cancer risk and mortality in patients with Crohn's disease. Gastroenterology. 1993;105(6):1716-23.

16. Rutgeerts P, Vermeire S, Van Assche G. Biological therapies for inflammatory bowel diseases. Gastroenterology. 2009;136(4):1182-97.

17. Torres J, Bonovas S, Doherty G, Kucharzik T, Gisbert JP, Raine T, et al. ECCO Guidelines on Therapeutics in Crohn's Disease: Medical Treatment. J Crohns Colitis. 2020;14(1):4-22.

18. Kennedy NA, Heap GA, Green HD, Hamilton B, Bewshea C, Walker GJ, et al. Predictors of anti-TNF treatment failure in anti-TNF-naive patients with active luminal Crohn's disease: a prospective, multicentre, cohort study. Lancet Gastroenterol Hepatol. 2019;4(5):341-53.

19. Cosnes J, Cattan S, Blain A, Beaugerie L, Carbonnel F, Parc R, et al. Long-term evolution of disease behavior of Crohn's disease. Inflamm Bowel Dis. 2002;8(4):244-50.

20. Peyrin-Biroulet L, Loftus EV, Jr., Colombel JF, Sandborn WJ. The natural history of adult Crohn's disease in population-based cohorts. Am J Gastroenterol. 2010;105(2):289-97.

21. Peterson LW, Artis D. Intestinal epithelial cells: regulators of barrier function and immune homeostasis. Nat Rev Immunol. 2014;14(3):141-53.

22. Coates M, Lee MJ, Norton D, MacLeod AS. The Skin and Intestinal Microbiota and Their Specific Innate Immune Systems. Front Immunol. 2019;10:2950.

23. de Lange KM, Moutsianas L, Lee JC, Lamb CA, Luo Y, Kennedy NA, et al. Genome-wide association study implicates immune activation of multiple integrin genes in inflammatory bowel disease. Nat Genet. 2017;49(2):256-61.

24. Orholm M, Munkholm P, Langholz E, Nielsen OH, Sorensen TI, Binder V. Familial occurrence of inflammatory bowel disease. N Engl J Med. 1991;324(2):84-8.

25. Tysk C, Lindberg E, Jarnerot G, Floderus-Myrhed B. Ulcerative colitis and Crohn's disease in an unselected population of monozygotic and dizygotic twins. A study of heritability and the influence of smoking. Gut. 1988;29(7):990-6.

26. Halfvarson J, Bodin L, Tysk C, Lindberg E, Jarnerot G. Inflammatory bowel disease in a Swedish twin cohort: a long-term follow-up of concordance and clinical characteristics. Gastroenterology. 2003;124(7):1767-73.

27. Duerr RH. The genetics of inflammatory bowel disease. Gastroenterol Clin North Am. 2002;31(1):63-76.

28. Cho JH, Weaver CT. The genetics of inflammatory bowel disease. Gastroenterology. 2007;133(4):1327-39.

29. Elson CO, Cong Y, McCracken VJ, Dimmitt RA, Lorenz RG, Weaver CT. Experimental models of inflammatory bowel disease reveal innate, adaptive, and regulatory mechanisms of host dialogue with the microbiota. Immunol Rev. 2005;206:260-76.

30. Hugot JP, Chamaillard M, Zouali H, Lesage S, Cezard JP, Belaiche J, et al. Association of NOD2 leucine-rich repeat variants with susceptibility to Crohn's disease. Nature. 2001;411(6837):599-603.

31. Ogura Y, Bonen DK, Inohara N, Nicolae DL, Chen FF, Ramos R, et al. A frameshift mutation in NOD2 associated with susceptibility to Crohn's disease. Nature. 2001;411(6837):603-6.

32. Stokkers PC, Reitsma PH, Tytgat GN, van Deventer SJ. HLA-DR and -DQ phenotypes in inflammatory bowel disease: a meta-analysis. Gut. 1999;45(3):395-401.

33. Hugot JP, Laurent-Puig P, Gower-Rousseau C, Olson JM, Lee JC, Beaugerie L, et al. Mapping of a susceptibility locus for Crohn's disease on chromosome 16. Nature. 1996;379(6568):821-3.

34. Rioux JD, Daly MJ, Silverberg MS, Lindblad K, Steinhart H, Cohen Z, et al. Genetic variation in the 5q31 cytokine gene cluster confers susceptibility to Crohn disease. Nat Genet. 2001;29(2):223-8.

35. Inohara N, Ogura Y, Fontalba A, Gutierrez O, Pons F, Crespo J, et al. Host recognition of bacterial muramyl dipeptide mediated through NOD2. Implications for Crohn's disease. J Biol Chem. 2003;278(8):5509-12.

36. Girardin SE, Boneca IG, Viala J, Chamaillard M, Labigne A, Thomas G, et al. Nod2 is a general sensor of peptidoglycan through muramyl dipeptide (MDP) detection. J Biol Chem. 2003;278(11):8869-72.

37. Cario E. Bacterial interactions with cells of the intestinal mucosa: Toll-like receptors and NOD2. Gut. 2005;54(8):1182-93.

38. McGovern DP, Kugathasan S, Cho JH. Genetics of Inflammatory Bowel Diseases. Gastroenterology. 2015;149(5):1163-76 e2.

39. Yamazaki K, McGovern D, Ragoussis J, Paolucci M, Butler H, Jewell D, et al. Single nucleotide polymorphisms in TNFSF15 confer susceptibility to Crohn's disease. Hum Mol Genet. 2005;14(22):3499-506.

40. Loos RJF. 15 years of genome-wide association studies and no signs of slowing down. Nat Commun. 2020;11(1):5900.

41. Huang H, Fang M, Jostins L, Umicevic Mirkov M, Boucher G, Anderson CA, et al. Fine-mapping inflammatory bowel disease loci to single-variant resolution. Nature. 2017;547(7662):173-8.

42. Jostins L, Ripke S, Weersma RK, Duerr RH, McGovern DP, Hui KY, et al. Host-microbe interactions have shaped the genetic architecture of inflammatory bowel disease. Nature. 2012;491(7422):119-24.

43. Duerr RH, Taylor KD, Brant SR, Rioux JD, Silverberg MS, Daly MJ, et al. A genome-wide association study identifies IL23R as an inflammatory bowel disease gene. Science. 2006;314(5804):1461-3.

44. Sarin R, Wu X, Abraham C. Inflammatory disease protective R381Q IL23 receptor polymorphism results in decreased primary CD4+ and CD8+ human T-cell functional responses. Proc Natl Acad Sci U S A. 2011;108(23):9560-5.

45. Di Meglio P, Di Cesare A, Laggner U, Chu CC, Napolitano L, Villanova F, et al. The IL23R R381Q gene variant protects against immune-mediated diseases by impairing IL-23-induced Th17 effector response in humans. PLoS One. 2011;6(2):e17160.

46. Pidasheva S, Trifari S, Phillips A, Hackney JA, Ma Y, Smith A, et al. Functional studies on the IBD susceptibility gene IL23R implicate reduced receptor function in the protective genetic variant R381Q. PLoS One. 2011;6(10):e25038.

47. Feagan BG, Sandborn WJ, Gasink C, Jacobstein D, Lang Y, Friedman JR, et al. Ustekinumab as Induction and Maintenance Therapy for Crohn's Disease. N Engl J Med. 2016;375(20):1946-60.

48. Sands BE, Sandborn WJ, Panaccione R, O'Brien CD, Zhang H, Johanns J, et al. Ustekinumab as Induction and Maintenance Therapy for Ulcerative Colitis. N Engl J Med. 2019;381(13):1201-14.

49. Beaudoin M, Goyette P, Boucher G, Lo KS, Rivas MA, Stevens C, et al. Deep resequencing of GWAS loci identifies rare variants in CARD9, IL23R and RNF186 that are associated with ulcerative colitis. PLoS Genet. 2013;9(9):e1003723.

50. Choi M, Scholl UI, Ji W, Liu T, Tikhonova IR, Zumbo P, et al. Genetic diagnosis by whole exome capture and massively parallel DNA sequencing. Proc Natl Acad Sci U S A. 2009;106(45):19096-101.

51. Pigneur B, Seksik P, Viola S, Viala J, Beaugerie L, Girardet JP, et al. Natural history of Crohn's disease: comparison between childhood- and adult-onset disease. Inflamm Bowel Dis. 2010;16(6):953-61.

52. Ruemmele FM, Veres G, Kolho KL, Griffiths A, Levine A, Escher JC, et al. Consensus guidelines of ECCO/ESPGHAN on the medical management of pediatric Crohn's disease. J Crohns Colitis. 2014;8(10):1179-207.

53. Uhlig HH, Schwerd T, Koletzko S, Shah N, Kammermeier J, Elkadri A, et al. The diagnostic approach to monogenic very early onset inflammatory bowel disease. Gastroenterology. 2014;147(5):990-1007 e3.

54. Prenzel F, Uhlig HH. Frequency of indeterminate colitis in children and adults with IBD - a metaanalysis. J Crohns Colitis. 2009;3(4):277-81.

55. De Benedetti F, Alonzi T, Moretta A, Lazzaro D, Costa P, Poli V, et al. Interleukin 6 causes growth impairment in transgenic mice through a decrease in insulin-like growth factor-I. A model for stunted growth in children with chronic inflammation. J Clin Invest. 1997;99(4):643-50.

56. Kirschner BS, Klich JR, Kalman SS, deFavaro MV, Rosenberg IH. Reversal of growth retardation in Crohn's disease with therapy emphasizing oral nutritional restitution. Gastroenterology. 1981;80(1):10-5.

57. Martensson K, Chrysis D, Savendahl L. Interleukin-1beta and TNF-alpha act in synergy to inhibit longitudinal growth in fetal rat metatarsal bones. J Bone Miner Res. 2004;19(11):1805-12.

58. Walters TD, Griffiths AM. Mechanisms of growth impairment in pediatric Crohn's disease. Nat Rev Gastroenterol Hepatol. 2009;6(9):513-23.

59. Crowley E, Warner N, Pan J, Khalouei S, Elkadri A, Fiedler K, et al. Prevalence and Clinical Features of Inflammatory Bowel Diseases Associated With Monogenic Variants, Identified by Whole-Exome Sequencing in 1000 Children at a Single Center. Gastroenterology. 2020;158(8):2208-20.

60. Glocker EO, Kotlarz D, Boztug K, Gertz EM, Schaffer AA, Noyan F, et al. Inflammatory bowel disease and mutations affecting the interleukin-10 receptor. N Engl J Med. 2009;361(21):2033-45.

61. Uhlig HH. Monogenic diseases associated with intestinal inflammation: implications for the understanding of inflammatory bowel disease. Gut. 2013;62(12):1795-805.

62. Uhlig HH, Schwerd T. From Genes to Mechanisms: The Expanding Spectrum of Monogenic Disorders Associated with Inflammatory Bowel Disease. Inflamm Bowel Dis. 2016;22(1):202-12.

63. Nambu R, Warner N, Mulder DJ, Kotlarz D, McGovern DPB, Cho J, et al. A Systematic Review of Monogenic Inflammatory Bowel Disease. Clin Gastroenterol Hepatol. 2021.

64. Uhlig HH, Charbit-Henrion F, Kotlarz D, Shouval DS, Schwerd T, Strisciuglio C, et al. Clinical Genomics for the Diagnosis of Monogenic Forms of Inflammatory Bowel Disease: A Position Paper From the Paediatric IBD Porto Group of European Society of Paediatric Gastroenterology, Hepatology and Nutrition. J Pediatr Gastroenterol Nutr. 2021;72(3):456-73.

65. Kotlarz D, Beier R, Murugan D, Diestelhorst J, Jensen O, Boztug K, et al. Loss of interleukin-10 signaling and infantile inflammatory bowel disease: implications for diagnosis and therapy. Gastroenterology. 2012;143(2):347-55.

66. Ananthakrishnan AN, Bernstein CN, Iliopoulos D, Macpherson A, Neurath MF, Ali RAR, et al. Environmental triggers in IBD: a review of progress and evidence. Nat Rev Gastroenterol Hepatol. 2018;15(1):39-49.

67. Ho SM, Lewis JD, Mayer EA, Plevy SE, Chuang E, Rappaport SM, et al. Challenges in IBD Research: Environmental Triggers. Inflamm Bowel Dis. 2019;25(Suppl 2):S13-S23.

68. Choung RS, Princen F, Stockfisch TP, Torres J, Maue AC, Porter CK, et al. Serologic microbial associated markers can predict Crohn's disease behaviour years before disease diagnosis. Aliment Pharmacol Ther. 2016;43(12):1300-10.

69. Falony G, Joossens M, Vieira-Silva S, Wang J, Darzi Y, Faust K, et al. Population-level analysis of gut microbiome variation. Science. 2016;352(6285):560-4.

70. Zhernakova A, Kurilshikov A, Bonder MJ, Tigchelaar EF, Schirmer M, Vatanen T, et al. Population-based metagenomics analysis reveals markers for gut microbiome composition and diversity. Science. 2016;352(6285):565-9.

71. Lynch SV, Pedersen O. The Human Intestinal Microbiome in Health and Disease. N Engl J Med. 2016;375(24):2369-79.

72. Forbes JD, Van Domselaar G, Bernstein CN. Microbiome Survey of the Inflamed and Noninflamed Gut at Different Compartments Within the Gastrointestinal Tract of Inflammatory Bowel Disease Patients. Inflamm Bowel Dis. 2016;22(4):817-25.

73. Gevers D, Kugathasan S, Denson LA, Vazquez-Baeza Y, Van Treuren W, Ren B, et al. The treatment-naive microbiome in new-onset Crohn's disease. Cell Host Microbe. 2014;15(3):382-92.

74. Kostic AD, Xavier RJ, Gevers D. The microbiome in inflammatory bowel disease: current status and the future ahead. Gastroenterology. 2014;146(6):1489-99.

75. Ng SC, Tang W, Ching JY, Wong M, Chow CM, Hui AJ, et al. Incidence and phenotype of inflammatory bowel disease based on results from the Asia-pacific Crohn's and colitis epidemiology study. Gastroenterology. 2013;145(1):158-65 e2.

76. Loftus EV, Jr. Clinical epidemiology of inflammatory bowel disease: Incidence, prevalence, and environmental influences. Gastroenterology. 2004;126(6):1504-17.

77. Benchimol EI, Kaplan GG, Otley AR, Nguyen GC, Underwood FE, Guttmann A, et al. Rural and Urban Residence During Early Life is Associated with Risk of Inflammatory Bowel Disease: A Population-Based Inception and Birth Cohort Study. Am J Gastroenterol. 2017;112(9):1412-22.

78. Shaw SY, Blanchard JF, Bernstein CN. Association between the use of antibiotics in the first year of life and pediatric inflammatory bowel disease. Am J Gastroenterol. 2010;105(12):2687-92.

79. Kronman MP, Zaoutis TE, Haynes K, Feng R, Coffin SE. Antibiotic exposure and IBD development among children: a population-based cohort study. Pediatrics. 2012;130(4):e794-803.

80. Shaw SY, Blanchard JF, Bernstein CN. Association between early childhood otitis media and pediatric inflammatory bowel disease: an exploratory population-based analysis. J Pediatr. 2013;162(3):510-4.

81. Dethlefsen L, Huse S, Sogin ML, Relman DA. The pervasive effects of an antibiotic on the human gut microbiota, as revealed by deep 16S rRNA sequencing. PLoS Biol. 2008;6(11):e280.

82. Dethlefsen L, Relman DA. Incomplete recovery and individualized responses of the human distal gut microbiota to repeated antibiotic perturbation. Proc Natl Acad Sci U S A. 2011;108 Suppl 1:4554-61.

83. Devkota S, Wang Y, Musch MW, Leone V, Fehlner-Peach H, Nadimpalli A, et al. Dietary-fat-induced taurocholic acid promotes pathobiont expansion and colitis in Il10-/- mice. Nature. 2012;487(7405):104-8.

84. Chassaing B, Koren O, Goodrich JK, Poole AC, Srinivasan S, Ley RE, et al. Dietary emulsifiers impact the mouse gut microbiota promoting colitis and metabolic syndrome. Nature. 2015;519(7541):92-6.

85. Zimmer J, Lange B, Frick JS, Sauer H, Zimmermann K, Schwiertz A, et al. A vegan or vegetarian diet substantially alters the human colonic faecal microbiota. Eur J Clin Nutr. 2012;66(1):53-60.

86. Brown K, DeCoffe D, Molcan E, Gibson DL. Diet-induced dysbiosis of the intestinal microbiota and the effects on immunity and disease. Nutrients. 2012;4(8):1095-119.

87. Heuschkel RB, Menache CC, Megerian JT, Baird AE. Enteral nutrition and corticosteroids in the treatment of acute Crohn's disease in children. J Pediatr Gastroenterol Nutr. 2000;31(1):8-15.

88. Dziechciarz P, Horvath A, Shamir R, Szajewska H. Meta-analysis: enteral nutrition in active Crohn's disease in children. Aliment Pharmacol Ther. 2007;26(6):795-806.

89. Turner D, Levine A, Escher JC, Griffiths AM, Russell RK, Dignass A, et al. Management of pediatric ulcerative colitis: joint ECCO and ESPGHAN evidence-based consensus guidelines. J Pediatr Gastroenterol Nutr. 2012;55(3):340-61.

90. Rhee SH, Pothoulakis C, Mayer EA. Principles and clinical implications of the brain-gut-enteric microbiota axis. Nat Rev Gastroenterol Hepatol. 2009;6(5):306-14.

91. Levenstein S, Prantera C, Varvo V, Scribano ML, Andreoli A, Luzi C, et al. Stress and exacerbation in ulcerative colitis: a prospective study of patients enrolled in remission. Am J Gastroenterol. 2000;95(5):1213-20.

92. Wintjens DSJ, de Jong MJ, van der Meulen-de Jong AE, Romberg-Camps MJ, Becx MC, Maljaars JP, et al. Novel Perceived Stress and Life Events Precede Flares of Inflammatory Bowel Disease: A Prospective 12-Month Follow-Up Study. J Crohns Colitis. 2019;13(4):410-6.

93. Coleman OI, Haller D. Bacterial Signaling at the Intestinal Epithelial Interface in Inflammation and Cancer. Front Immunol. 2017;8:1927.

94. Turner JR. Intestinal mucosal barrier function in health and disease. Nat Rev Immunol. 2009;9(11):799-809.

95. Pastorelli L, De Salvo C, Mercado JR, Vecchi M, Pizarro TT. Central role of the gut epithelial barrier in the pathogenesis of chronic intestinal inflammation: lessons learned from animal models and human genetics. Front Immunol. 2013;4:280.

96. Lopez-Posadas R, Sturzl M, Atreya I, Neurath MF, Britzen-Laurent N. Interplay of GTPases and Cytoskeleton in Cellular Barrier Defects during Gut Inflammation. Front Immunol. 2017;8:1240.

97. Hollander D, Vadheim CM, Brettholz E, Petersen GM, Delahunty T, Rotter JI. Increased intestinal permeability in patients with Crohn's disease and their relatives. A possible etiologic factor. Ann Intern Med. 1986;105(6):883-5.

98. Madsen KL, Malfair D, Gray D, Doyle JS, Jewell LD, Fedorak RN. Interleukin-10 gene-deficient mice develop a primary intestinal permeability defect in response to enteric microflora. Inflamm Bowel Dis. 1999;5(4):262-70.

99. Musch MW, Clarke LL, Mamah D, Gawenis LR, Zhang Z, Ellsworth W, et al. T cell activation causes diarrhea by increasing intestinal permeability and inhibiting epithelial Na+/K+-ATPase. J Clin Invest. 2002;110(11):1739-47.

100. Schmitz H, Barmeyer C, Fromm M, Runkel N, Foss HD, Bentzel CJ, et al. Altered tight junction structure contributes to the impaired epithelial barrier function in ulcerative colitis. Gastroenterology. 1999;116(2):301-9.

101. Ukabam SO, Clamp JR, Cooper BT. Abnormal small intestinal permeability to sugars in patients with Crohn's disease of the terminal ileum and colon. Digestion. 1983;27(2):70-4.

102. Bruewer M, Luegering A, Kucharzik T, Parkos CA, Madara JL, Hopkins AM, et al. Proinflammatory cytokines disrupt epithelial barrier function by apoptosis-independent mechanisms. J Immunol. 2003;171(11):6164-72.

103. Johansson ME, Phillipson M, Petersson J, Velcich A, Holm L, Hansson GC. The inner of the two Muc2 mucin-dependent mucus layers in colon is devoid of bacteria. Proc Natl Acad Sci U S A. 2008;105(39):15064-9.

104. Ayabe T, Satchell DP, Wilson CL, Parks WC, Selsted ME, Ouellette AJ. Secretion of microbicidal alpha-defensins by intestinal Paneth cells in response to bacteria. Nat Immunol. 2000;1(2):113-8.

105. Ganz T. Defensins: antimicrobial peptides of innate immunity. Nat Rev Immunol. 2003;3(9):710-20.

106. Avitzur Y, Guo C, Mastropaolo LA, Bahrami E, Chen H, Zhao Z, et al. Mutations in tetratricopeptide repeat domain 7A result in a severe form of very early onset inflammatory bowel disease. Gastroenterology. 2014;146(4):1028-39.

107. Chen R, Giliani S, Lanzi G, Mias GI, Lonardi S, Dobbs K, et al. Whole-exome sequencing identifies tetratricopeptide repeat domain 7A (TTC7A) mutations for combined immunodeficiency with intestinal atresias. J Allergy Clin Immunol. 2013;132(3):656-64 e17.

108. Lemoine R, Pachlopnik-Schmid J, Farin HF, Bigorgne A, Debre M, Sepulveda F, et al. Immune deficiency-related enteropathy-lymphocytopenia-alopecia syndrome results from tetratricopeptide repeat domain 7A deficiency. J Allergy Clin Immunol. 2014;134(6):1354-64 e6.

109. Samuels ME, Majewski J, Alirezaie N, Fernandez I, Casals F, Patey N, et al. Exome sequencing identifies mutations in the gene TTC7A in French-Canadian cases with hereditary multiple intestinal atresia. J Med Genet. 2013;50(5):324-9.

110. Jardine S, Dhingani N, Muise AM. TTC7A: Steward of Intestinal Health. Cell Mol Gastroenterol Hepatol. 2019;7(3):555-70.

111. Kammermeier J, Lucchini G, Pai SY, Worth A, Rampling D, Amrolia P, et al. Stem cell transplantation for tetratricopeptide repeat domain 7A deficiency: long-term follow-up. Blood. 2016;128(9):1306-8.

112. Lehle AS, Farin HF, Marquardt B, Michels BE, Magg T, Li Y, et al. Intestinal Inflammation and Dysregulated Immunity in Patients With Inherited Caspase-8 Deficiency. Gastroenterology. 2019;156(1):275-8.

113. Li Y, Fuhrer M, Bahrami E, Socha P, Klaudel-Dreszler M, Bouzidi A, et al. Human RIPK1 deficiency causes combined immunodeficiency and inflammatory bowel diseases. Proc Natl Acad Sci U S A. 2019;116(3):970-5.

114. Cuchet-Lourenco D, Eletto D, Wu C, Plagnol V, Papapietro O, Curtis J, et al. Biallelic RIPK1 mutations in humans cause severe immunodeficiency, arthritis, and intestinal inflammation. Science. 2018;361(6404):810-3.

115. Neurath MF. Cytokines in inflammatory bowel disease. Nat Rev Immunol. 2014;14(5):329-42.

116. Chassaing B, Kumar M, Baker MT, Singh V, Vijay-Kumar M. Mammalian gut immunity. Biomed J. 2014;37(5):246-58.

117. Bain CC, Mowat AM. Macrophages in intestinal homeostasis and inflammation. Immunol Rev. 2014;260(1):102-17.

118. Ruder B, Becker C. At the Forefront of the Mucosal Barrier: The Role of Macrophages in the Intestine. Cells. 2020;9(10).

119. Caer C, Wick MJ. Human Intestinal Mononuclear Phagocytes in Health and Inflammatory Bowel Disease. Front Immunol. 2020;11:410.

120. Li Q, Lee CH, Peters LA, Mastropaolo LA, Thoeni C, Elkadri A, et al. Variants in TRIM22 That Affect NOD2 Signaling Are Associated With Very-Early-Onset Inflammatory Bowel Disease. Gastroenterology. 2016;150(5):1196-207.

121. Zammit NW, Siggs OM, Gray PE, Horikawa K, Langley DB, Walters SN, et al. Denisovan, modern human and mouse TNFAIP3 alleles tune A20 phosphorylation and immunity. Nat Immunol. 2019;20(10):1299-310.

122. Patel AA, Zhang Y, Fullerton JN, Boelen L, Rongvaux A, Maini AA, et al. The fate and lifespan of human monocyte subsets in steady state and systemic inflammation. J Exp Med. 2017;214(7):1913-23.

123. Ziegler-Heitbrock L, Ancuta P, Crowe S, Dalod M, Grau V, Hart DN, et al. Nomenclature of monocytes and dendritic cells in blood. Blood. 2010;116(16):e74-80.

124. Corces MR, Buenrostro JD, Wu B, Greenside PG, Chan SM, Koenig JL, et al. Lineage-specific and single-cell chromatin accessibility charts human hematopoiesis and leukemia evolution. Nat Genet. 2016;48(10):1193-203.

125. Bao EL, Cheng AN, Sankaran VG. The genetics of human hematopoiesis and its disruption in disease. EMBO Mol Med. 2019;11(8):e10316.

126. Jakubzick CV, Randolph GJ, Henson PM. Monocyte differentiation and antigen-presenting functions. Nat Rev Immunol. 2017;17(6):349-62.

127. Mosser DM, Edwards JP. Exploring the full spectrum of macrophage activation. Nat Rev Immunol. 2008;8(12):958-69.

128. Takeda K, Clausen BE, Kaisho T, Tsujimura T, Terada N, Forster I, et al. Enhanced Th1 activity and development of chronic enterocolitis in mice devoid of Stat3 in macrophages and neutrophils. Immunity. 1999;10(1):39-49.

129. Kamada N, Hisamatsu T, Okamoto S, Sato T, Matsuoka K, Arai K, et al. Abnormally differentiated subsets of intestinal macrophage play a key role in Th1-dominant chronic colitis through excess production of IL-12 and IL-23 in response to bacteria. J Immunol. 2005;175(10):6900-8.

130. Bujko A, Atlasy N, Landsverk OJB, Richter L, Yaqub S, Horneland R, et al. Transcriptional and functional profiling defines human small intestinal macrophage subsets. J Exp Med. 2018;215(2):441-58.

131. Bajpai G, Schneider C, Wong N, Bredemeyer A, Hulsmans M, Nahrendorf M, et al. The human heart contains distinct macrophage subsets with divergent origins and functions. Nat Med. 2018;24(8):1234-45.

132. Hashimoto D, Chow A, Noizat C, Teo P, Beasley MB, Leboeuf M, et al. Tissue-resident macrophages self-maintain locally throughout adult life with minimal contribution from circulating monocytes. Immunity. 2013;38(4):792-804.

133. Schulz C, Gomez Perdiguero E, Chorro L, Szabo-Rogers H, Cagnard N, Kierdorf K, et al. A lineage of myeloid cells independent of Myb and hematopoietic stem cells. Science. 2012;336(6077):86-90.

134. Stremmel C, Schuchert R, Wagner F, Thaler R, Weinberger T, Pick R, et al. Yolk sac macrophage progenitors traffic to the embryo during defined stages of development. Nat Commun. 2018;9(1):75.

135. Yona S, Kim KW, Wolf Y, Mildner A, Varol D, Breker M, et al. Fate mapping reveals origins and dynamics of monocytes and tissue macrophages under homeostasis. Immunity. 2013;38(1):79-91.

136. Schenk M, Bouchon A, Birrer S, Colonna M, Mueller C. Macrophages expressing triggering receptor expressed on myeloid cells-1 are underrepresented in the human intestine. J Immunol. 2005;174(1):517-24.

137. Schenk M, Bouchon A, Seibold F, Mueller C. TREM-1--expressing intestinal macrophages crucially amplify chronic inflammation in experimental colitis and inflammatory bowel diseases. J Clin Invest. 2007;117(10):3097-106.

138. Kamada N, Hisamatsu T, Okamoto S, Chinen H, Kobayashi T, Sato T, et al. Unique CD14 intestinal macrophages contribute to the pathogenesis of Crohn disease via IL-23/IFN-gamma axis. J Clin Invest. 2008;118(6):2269-80.

139. Bernardo D, Marin AC, Fernandez-Tome S, Montalban-Arques A, Carrasco A, Tristan E, et al. Human intestinal pro-inflammatory CD11c(high)CCR2(+)CX3CR1(+) macrophages, but not their tolerogenic CD11c(-)CCR2(-)CX3CR1(-) counterparts, are expanded in inflammatory bowel disease. Mucosal Immunol. 2018;11(4):1114-26.

140. Smythies LE, Maheshwari A, Clements R, Eckhoff D, Novak L, Vu HL, et al. Mucosal IL-8 and TGF-beta recruit blood monocytes: evidence for cross-talk between the lamina propria stroma and myeloid cells. J Leukoc Biol. 2006;80(3):492-9.

141. Thiesen S, Janciauskiene S, Uronen-Hansson H, Agace W, Hogerkorp CM, Spee P, et al. CD14(hi)HLA-DR(dim) macrophages, with a resemblance to classical blood monocytes, dominate inflamed mucosa in Crohn's disease. J Leukoc Biol. 2014;95(3):531-41.

142. Dige A, Magnusson MK, Ohman L, Hvas CL, Kelsen J, Wick MJ, et al. Reduced numbers of mucosal DR(int) macrophages and increased numbers of CD103(+) dendritic cells during anti-TNF-alpha treatment in patients with Crohn's disease. Scand J Gastroenterol. 2016;51(6):692-9.

143. Vos AC, Wildenberg ME, Arijs I, Duijvestein M, Verhaar AP, de Hertogh G, et al. Regulatory macrophages induced by infliximab are involved in healing in vivo and in vitro. Inflamm Bowel Dis. 2012;18(3):401-8.

144. Zeissig S, Rosati E, Dowds CM, Aden K, Bethge J, Schulte B, et al. Vedolizumab is associated with changes in innate rather than adaptive immunity in patients with inflammatory bowel disease. Gut. 2019;68(1):25-39.

145. Black RA, Rauch CT, Kozlosky CJ, Peschon JJ, Slack JL, Wolfson MF, et al. A metalloproteinase disintegrin that releases tumour-necrosis factor-alpha from cells. Nature. 1997;385(6618):729-33.

146. Moss ML, Jin SL, Milla ME, Bickett DM, Burkhart W, Carter HL, et al. Cloning of a disintegrin metalloproteinase that processes precursor tumour-necrosis factor-alpha. Nature. 1997;385(6618):733-6.

147. Breese EJ, Michie CA, Nicholls SW, Murch SH, Williams CB, Domizio P, et al. Tumor necrosis factor alpha-producing cells in the intestinal mucosa of children with inflammatory bowel disease. Gastroenterology. 1994;106(6):1455-66.

148. Atreya R, Zimmer M, Bartsch B, Waldner MJ, Atreya I, Neumann H, et al. Antibodies against tumor necrosis factor (TNF) induce T-cell apoptosis in patients with inflammatory bowel diseases via TNF receptor 2 and intestinal CD14(+) macrophages. Gastroenterology. 2011;141(6):2026-38.

149. Gunther C, Martini E, Wittkopf N, Amann K, Weigmann B, Neumann H, et al. Caspase-8 regulates TNF-alpha-induced epithelial necroptosis and terminal ileitis. Nature. 2011;477(7364):335-9.

150. Su L, Nalle SC, Shen L, Turner ES, Singh G, Breskin LA, et al. TNFR2 activates MLCK-dependent tight junction dysregulation to cause apoptosis-mediated barrier loss and experimental colitis. Gastroenterology. 2013;145(2):407-15.

151. Baud V, Karin M. Signal transduction by tumor necrosis factor and its relatives. Trends Cell Biol. 2001;11(9):372-7.

152. Perrier C, de Hertogh G, Cremer J, Vermeire S, Rutgeerts P, Van Assche G, et al. Neutralization of membrane TNF, but not soluble TNF, is crucial for the treatment of experimental colitis. Inflamm Bowel Dis. 2013;19(2):246-53.

153. Van den Brande JM, Braat H, van den Brink GR, Versteeg HH, Bauer CA, Hoedemaeker I, et al. Infliximab but not etanercept induces apoptosis in lamina propria T-lymphocytes from patients with Crohn's disease. Gastroenterology. 2003;124(7):1774-85.

154. Mao L, Kitani A, Strober W, Fuss IJ. The Role of NLRP3 and IL-1beta in the Pathogenesis of Inflammatory Bowel Disease. Front Immunol. 2018;9:2566.

155. Zhen Y, Zhang H. NLRP3 Inflammasome and Inflammatory Bowel Disease. Front Immunol. 2019;10:276.

156. Coccia M, Harrison OJ, Schiering C, Asquith MJ, Becher B, Powrie F, et al. IL-1beta mediates chronic intestinal inflammation by promoting the accumulation of IL-17A secreting innate lymphoid cells and CD4(+) Th17 cells. J Exp Med. 2012;209(9):1595-609.

157. Ligumsky M, Simon PL, Karmeli F, Rachmilewitz D. Role of interleukin 1 in inflammatory bowel disease--enhanced production during active disease. Gut. 1990;31(6):686-9.

158. McAlindon ME, Hawkey CJ, Mahida YR. Expression of interleukin 1 beta and interleukin 1 beta converting enzyme by intestinal macrophages in health and inflammatory bowel disease. Gut. 1998;42(2):214-9.

159. Casini-Raggi V, Kam L, Chong YJ, Fiocchi C, Pizarro TT, Cominelli F. Mucosal imbalance of IL-1 and IL-1 receptor antagonist in inflammatory bowel disease. A novel mechanism of chronic intestinal inflammation. J Immunol. 1995;154(5):2434-40.

160. Ludwiczek O, Vannier E, Borggraefe I, Kaser A, Siegmund B, Dinarello CA, et al. Imbalance between interleukin-1 agonists and antagonists: relationship to severity of inflammatory bowel disease. Clin Exp Immunol. 2004;138(2):323-9.

161. Schroder K, Tschopp J. The inflammasomes. Cell. 2010;140(6):821-32.

162. Chan AH, Schroder K. Inflammasome signaling and regulation of interleukin-1 family cytokines. J Exp Med. 2020;217(1).

163. Bauer C, Duewell P, Mayer C, Lehr HA, Fitzgerald KA, Dauer M, et al. Colitis induced in mice with dextran sulfate sodium (DSS) is mediated by the NLRP3 inflammasome. Gut. 2010;59(9):1192-9.

164. Mao L, Kitani A, Similuk M, Oler AJ, Albenberg L, Kelsen J, et al. Loss-of-function CARD8 mutation causes NLRP3 inflammasome activation and Crohn's disease. J Clin Invest. 2018;128(5):1793-806.

165. Neudecker V, Haneklaus M, Jensen O, Khailova L, Masterson JC, Tye H, et al. Myeloid-derived miR-223 regulates intestinal inflammation via repression of the NLRP3 inflammasome. J Exp Med. 2017;214(6):1737-52.

166. Villani AC, Lemire M, Fortin G, Louis E, Silverberg MS, Collette C, et al. Common variants in the NLRP3 region contribute to Crohn's disease susceptibility. Nat Genet. 2009;41(1):71-6.

167. Zaki MH, Boyd KL, Vogel P, Kastan MB, Lamkanfi M, Kanneganti TD. The NLRP3 inflammasome protects against loss of epithelial integrity and mortality during experimental colitis. Immunity. 2010;32(3):379-91.

168. Shouval DS, Biswas A, Kang YH, Griffith AE, Konnikova L, Mascanfroni ID, et al. Interleukin 1beta Mediates Intestinal Inflammation in Mice and Patients With Interleukin 10 Receptor Deficiency. Gastroenterology. 2016;151(6):1100-4.

169. Bauer C, Duewell P, Lehr HA, Endres S, Schnurr M. Protective and aggravating effects of Nlrp3 inflammasome activation in IBD models: influence of genetic and environmental factors. Dig Dis. 2012;30 Suppl 1:82-90.

170. Mariathasan S, Newton K, Monack DM, Vucic D, French DM, Lee WP, et al. Differential activation of the inflammasome by caspase-1 adaptors ASC and Ipaf. Nature. 2004;430(6996):213-8.

171. Thornberry NA, Bull HG, Calaycay JR, Chapman KT, Howard AD, Kostura MJ, et al. A novel heterodimeric cysteine protease is required for interleukin-1 beta processing in monocytes. Nature. 1992;356(6372):768-74.

172. Akita K, Ohtsuki T, Nukada Y, Tanimoto T, Namba M, Okura T, et al. Involvement of caspase-1 and caspase-3 in the production and processing of mature human interleukin 18 in monocytic THP.1 cells. J Biol Chem. 1997;272(42):26595-603.

173. Shi J, Zhao Y, Wang K, Shi X, Wang Y, Huang H, et al. Cleavage of GSDMD by inflammatory caspases determines pyroptotic cell death. Nature. 2015;526(7575):660-5.

174. Huang Y, Xu W, Zhou R. NLRP3 inflammasome activation and cell death. Cell Mol Immunol. 2021.

175. Ding J, Wang K, Liu W, She Y, Sun Q, Shi J, et al. Pore-forming activity and structural autoinhibition of the gasdermin family. Nature. 2016;535(7610):111-6.

176. He WT, Wan H, Hu L, Chen P, Wang X, Huang Z, et al. Gasdermin D is an executor of pyroptosis and required for interleukin-1beta secretion. Cell Res. 2015;25(12):1285-98.

177. Liu X, Zhang Z, Ruan J, Pan Y, Magupalli VG, Wu H, et al. Inflammasome-activated gasdermin D causes pyroptosis by forming membrane pores. Nature. 2016;535(7610):153-8.

178. de Luca A, Smeekens SP, Casagrande A, Iannitti R, Conway KL, Gresnigt MS, et al. IL-1 receptor blockade restores autophagy and reduces inflammation in chronic granulomatous disease in mice and in humans. Proc Natl Acad Sci U S A. 2014;111(9):3526-31.

179. Revu S, Wu J, Henkel M, Rittenhouse N, Menk A, Delgoffe GM, et al. IL-23 and IL-1beta Drive Human Th17 Cell Differentiation and Metabolic Reprogramming in Absence of CD28 Costimulation. Cell Rep. 2018;22(10):2642-53.

180. Stritesky GL, Yeh N, Kaplan MH. IL-23 promotes maintenance but not commitment to the Th17 lineage. J Immunol. 2008;181(9):5948-55.

181. Zhou L, Ivanov, II, Spolski R, Min R, Shenderov K, Egawa T, et al. IL-6 programs T(H)-17 cell differentiation by promoting sequential engagement of the IL-21 and IL-23 pathways. Nat Immunol. 2007;8(9):967-74.

182. Athie-Morales V, Smits HH, Cantrell DA, Hilkens CM. Sustained IL-12 signaling is required for Th1 development. J Immunol. 2004;172(1):61-9.

183. Hsieh CS, Macatonia SE, Tripp CS, Wolf SF, O'Garra A, Murphy KM. Development of TH1 CD4+ T cells through IL-12 produced by Listeria-induced macrophages. Science. 1993;260(5107):547-9.

184. Manetti R, Parronchi P, Giudizi MG, Piccinni MP, Maggi E, Trinchieri G, et al. Natural killer cell stimulatory factor (interleukin 12 [IL-12]) induces T helper type 1 (Th1)-specific immune responses and inhibits the development of IL-4-producing Th cells. J Exp Med. 1993;177(4):1199-204.

185. Barrett JC, Hansoul S, Nicolae DL, Cho JH, Duerr RH, Rioux JD, et al. Genome-wide association defines more than 30 distinct susceptibility loci for Crohn's disease. Nat Genet. 2008;40(8):955-62.

186. Monteleone G, Biancone L, Marasco R, Morrone G, Marasco O, Luzza F, et al. Interleukin 12 is expressed and actively released by Crohn's disease intestinal lamina propria mononuclear cells. Gastroenterology. 1997;112(4):1169-78.

187. Wang K, Zhang H, Kugathasan S, Annese V, Bradfield JP, Russell RK, et al. Diverse genome-wide association studies associate the IL12/IL23 pathway with Crohn Disease. Am J Hum Genet. 2009;84(3):399-405.

188. Liu Z, Yadav PK, Xu X, Su J, Chen C, Tang M, et al. The increased expression of IL-23 in inflammatory bowel disease promotes intraepithelial and lamina propria lymphocyte inflammatory responses and cytotoxicity. J Leukoc Biol. 2011;89(4):597-606.

189. Goyette P, Boucher G, Mallon D, Ellinghaus E, Jostins L, Huang H, et al. High-density mapping of the MHC identifies a shared role for HLA-DRB1*01:03 in inflammatory bowel diseases and heterozygous advantage in ulcerative colitis. Nat Genet. 2015;47(2):172-9.

190. Imam T, Park S, Kaplan MH, Olson MR. Effector T Helper Cell Subsets in Inflammatory Bowel Diseases. Front Immunol. 2018;9:1212.

191. Fais S, Capobianchi MR, Pallone F, Di Marco P, Boirivant M, Dianzani F, et al. Spontaneous release of interferon gamma by intestinal lamina propria lymphocytes in Crohn's disease. Kinetics of in vitro response to interferon gamma inducers. Gut. 1991;32(4):403-7.

192. Fuss IJ, Neurath M, Boirivant M, Klein JS, de la Motte C, Strong SA, et al. Disparate CD4+ lamina propria (LP) lymphokine secretion profiles in inflammatory bowel disease. Crohn's disease LP cells manifest increased secretion of IFN-gamma, whereas ulcerative colitis LP cells manifest increased secretion of IL-5. J Immunol. 1996;157(3):1261-70.

193. Fuss IJ, Strober W. The role of IL-13 and NK T cells in experimental and human ulcerative colitis. Mucosal Immunol. 2008;1 Suppl 1:S31-3.

194. Heller F, Florian P, Bojarski C, Richter J, Christ M, Hillenbrand B, et al. Interleukin-13 is the key effector Th2 cytokine in ulcerative colitis that affects epithelial tight junctions, apoptosis, and cell restitution. Gastroenterology. 2005;129(2):550-64.

195. Schmitt N, Ueno H. Regulation of human helper T cell subset differentiation by cytokines. Curr Opin Immunol. 2015;34:130-6.

196. Sallusto F. Heterogeneity of Human CD4(+) T Cells Against Microbes. Annu Rev Immunol. 2016;34:317-34.

197. Szabo SJ, Sullivan BM, Peng SL, Glimcher LH. Molecular mechanisms regulating Th1 immune responses. Annu Rev Immunol. 2003;21:713-58.

198. Bustamante J, Boisson-Dupuis S, Abel L, Casanova JL. Mendelian susceptibility to mycobacterial disease: genetic, immunological, and clinical features of inborn errors of IFN-gamma immunity. Semin Immunol. 2014;26(6):454-70.

199. Doffinger R, Jouanguy E, Altare F, Wood P, Shirakawa T, Novelli F, et al. Inheritable defects in interleukin-12- and interferon-gamma-mediated immunity and the TH1/TH2 paradigm in man. Allergy. 1999;54(5):409-12.

200. Chan SH, Perussia B, Gupta JW, Kobayashi M, Pospisil M, Young HA, et al. Induction of interferon gamma production by natural killer cell stimulatory factor: characterization of the responder cells and synergy with other inducers. J Exp Med. 1991;173(4):869-79.

201. Morris SC, Madden KB, Adamovicz JJ, Gause WC, Hubbard BR, Gately MK, et al. Effects of IL-12 on in vivo cytokine gene expression and Ig isotype selection. J Immunol. 1994;152(3):1047-56.

202. Afkarian M, Sedy JR, Yang J, Jacobson NG, Cereb N, Yang SY, et al. T-bet is a STAT1-induced regulator of IL-12R expression in naive CD4+ T cells. Nat Immunol. 2002;3(6):549-57.

203. Lighvani AA, Frucht DM, Jankovic D, Yamane H, Aliberti J, Hissong BD, et al. T-bet is rapidly induced by interferon-gamma in lymphoid and myeloid cells. Proc Natl Acad Sci U S A. 2001;98(26):15137-42.

204. Palm NW, Rosenstein RK, Medzhitov R. Allergic host defences. Nature. 2012;484(7395):465-72.

205. Jenner RG, Townsend MJ, Jackson I, Sun K, Bouwman RD, Young RA, et al. The transcription factors T-bet and GATA-3 control alternative pathways of T-cell differentiation through a shared set of target genes. Proc Natl Acad Sci U S A. 2009;106(42):17876-81.

206. Kishikawa H, Sun J, Choi A, Miaw SC, Ho IC. The cell type-specific expression of the murine IL-13 gene is regulated by GATA-3. J Immunol. 2001;167(8):4414-20.

207. Lee GR, Fields PE, Flavell RA. Regulation of IL-4 gene expression by distal regulatory elements and GATA-3 at the chromatin level. Immunity. 2001;14(4):447-59.

208. Zhang DH, Cohn L, Ray P, Bottomly K, Ray A. Transcription factor GATA-3 is differentially expressed in murine Th1 and Th2 cells and controls Th2-specific expression of the interleukin-5 gene. J Biol Chem. 1997;272(34):21597-603.

209. Kaplan MH, Schindler U, Smiley ST, Grusby MJ. Stat6 is required for mediating responses to IL-4 and for development of Th2 cells. Immunity. 1996;4(3):313-9.

210. Murphy KM, Reiner SL. The lineage decisions of helper T cells. Nat Rev Immunol. 2002;2(12):933-44.

211. Ouyang W, Ranganath SH, Weindel K, Bhattacharya D, Murphy TL, Sha WC, et al. Inhibition of Th1 development mediated by GATA-3 through an IL-4-independent mechanism. Immunity. 1998;9(5):745-55.

212. Swain SL, Weinberg AD, English M, Huston G. IL-4 directs the development of Th2-like helper effectors. J Immunol. 1990;145(11):3796-806.

213. Zheng W, Flavell RA. The transcription factor GATA-3 is necessary and sufficient for Th2 cytokine gene expression in CD4 T cells. Cell. 1997;89(4):587-96.

214. Gratchev A, Kzhyshkowska J, Utikal J, Goerdt S. Interleukin-4 and dexamethasone counterregulate extracellular matrix remodelling and phagocytosis in type-2 macrophages. Scand J Immunol. 2005;61(1):10-7.

215. Hesse M, Modolell M, La Flamme AC, Schito M, Fuentes JM, Cheever AW, et al. Differential regulation of nitric oxide synthase-2 and arginase-1 by type 1/type 2 cytokines in vivo: granulomatous pathology is shaped by the pattern of L-arginine metabolism. J Immunol. 2001;167(11):6533-44.

216. Kreider T, Anthony RM, Urban JF, Jr., Gause WC. Alternatively activated macrophages in helminth infections. Curr Opin Immunol. 2007;19(4):448-53.

217. Bamias G, Cominelli F. Role of type 2 immunity in intestinal inflammation. Curr Opin Gastroenterol. 2015;31(6):471-6.

218. Cheever AW, Williams ME, Wynn TA, Finkelman FD, Seder RA, Cox TM, et al. Anti-IL-4 treatment of Schistosoma mansoni-infected mice inhibits development of T cells and non-B, non-T cells expressing Th2 cytokines while decreasing egg-induced hepatic fibrosis. J Immunol. 1994;153(2):753-9.

219. Cerboni S, Gehrmann U, Preite S, Mitra S. Cytokine-regulated Th17 plasticity in human health and diseases. Immunology. 2021;163(1):3-18.

220. Ivanov, II, McKenzie BS, Zhou L, Tadokoro CE, Lepelley A, Lafaille JJ, et al. The orphan nuclear receptor RORgammat directs the differentiation program of proinflammatory IL-17+ T helper cells. Cell. 2006;126(6):1121-33.

221. Mangan PR, Harrington LE, O'Quinn DB, Helms WS, Bullard DC, Elson CO, et al. Transforming growth factor-beta induces development of the T(H)17 lineage. Nature. 2006;441(7090):231-4.

222. Veldhoen M, Hocking RJ, Atkins CJ, Locksley RM, Stockinger B. TGFbeta in the context of an inflammatory cytokine milieu supports de novo differentiation of IL-17-producing T cells. Immunity. 2006;24(2):179-89.

223. Yang XO, Pappu BP, Nurieva R, Akimzhanov A, Kang HS, Chung Y, et al. T helper 17 lineage differentiation is programmed by orphan nuclear receptors ROR alpha and ROR gamma. Immunity. 2008;28(1):29-39.

224. Kobayashi T, Okamoto S, Hisamatsu T, Kamada N, Chinen H, Saito R, et al. IL23 differentially regulates the Th1/Th17 balance in ulcerative colitis and Crohn's disease. Gut. 2008;57(12):1682-9.

225. Rovedatti L, Kudo T, Biancheri P, Sarra M, Knowles CH, Rampton DS, et al. Differential regulation of interleukin 17 and interferon gamma production in inflammatory bowel disease. Gut. 2009;58(12):1629-36.

226. Kotlarz D, Marquardt B, Baroy T, Lee WS, Konnikova L, Hollizeck S, et al. Human TGF-beta1 deficiency causes severe inflammatory bowel disease and encephalopathy. Nat Genet. 2018;50(3):344-8.

227. Harrington LE, Hatton RD, Mangan PR, Turner H, Murphy TL, Murphy KM, et al. Interleukin 17-producing CD4+ effector T cells develop via a lineage distinct from the T helper type 1 and 2 lineages. Nat Immunol. 2005;6(11):1123-32.

228. Laurence A, Tato CM, Davidson TS, Kanno Y, Chen Z, Yao Z, et al. Interleukin-2 signaling via STAT5 constrains T helper 17 cell generation. Immunity. 2007;26(3):371-81.

229. Jovanovic DV, Di Battista JA, Martel-Pelletier J, Jolicoeur FC, He Y, Zhang M, et al. IL-17 stimulates the production and expression of proinflammatory cytokines, IL-beta and TNF-alpha, by human macrophages. J Immunol. 1998;160(7):3513-21.

230. Liang SC, Tan XY, Luxenberg DP, Karim R, Dunussi-Joannopoulos K, Collins M, et al. Interleukin (IL)-22 and IL-17 are coexpressed by Th17 cells and cooperatively enhance expression of antimicrobial peptides. J Exp Med. 2006;203(10):2271-9.

231. Onishi RM, Gaffen SL. Interleukin-17 and its target genes: mechanisms of interleukin-17 function in disease. Immunology. 2010;129(3):311-21.

232. Peric M, Koglin S, Kim SM, Morizane S, Besch R, Prinz JC, et al. IL-17A enhances vitamin D3-induced expression of cathelicidin antimicrobial peptide in human keratinocytes. J Immunol. 2008;181(12):8504-12.

233. Tanoue T, Atarashi K, Honda K. Development and maintenance of intestinal regulatory T cells. Nat Rev Immunol. 2016;16(5):295-309.

234. Cosovanu C, Neumann C. The Many Functions of Foxp3(+) Regulatory T Cells in the Intestine. Front Immunol. 2020;11:600973.

235. Atarashi K, Tanoue T, Shima T, Imaoka A, Kuwahara T, Momose Y, et al. Induction of colonic regulatory T cells by indigenous Clostridium species. Science. 2011;331(6015):337-41.

236. Fontenot JD, Gavin MA, Rudensky AY. Foxp3 programs the development and function of CD4+CD25+ regulatory T cells. Nat Immunol. 2003;4(4):330-6.

237. Hori S, Nomura T, Sakaguchi S. Control of regulatory T cell development by the transcription factor Foxp3. Science. 2003;299(5609):1057-61.

238. Li MO, Wan YY, Flavell RA. T cell-produced transforming growth factor-beta1 controls T cell tolerance and regulates Th1- and Th17-cell differentiation. Immunity. 2007;26(5):579-91.

239. Rubtsov YP, Rasmussen JP, Chi EY, Fontenot J, Castelli L, Ye X, et al. Regulatory T cell-derived interleukin-10 limits inflammation at environmental interfaces. Immunity. 2008;28(4):546-58.

240. Wing K, Onishi Y, Prieto-Martin P, Yamaguchi T, Miyara M, Fehervari Z, et al. CTLA-4 control over Foxp3+ regulatory T cell function. Science. 2008;322(5899):271-5.

241. Kuehn HS, Ouyang W, Lo B, Deenick EK, Niemela JE, Avery DT, et al. Immune dysregulation in human subjects with heterozygous germline mutations in CTLA4. Science. 2014;345(6204):1623-7.

242. Schubert D, Bode C, Kenefeck R, Hou TZ, Wing JB, Kennedy A, et al. Autosomal dominant immune dysregulation syndrome in humans with CTLA4 mutations. Nat Med. 2014;20(12):1410-6.

243. Kim KS, Hong SW, Han D, Yi J, Jung J, Yang BG, et al. Dietary antigens limit mucosal immunity by inducing regulatory T cells in the small intestine. Science. 2016;351(6275):858-63.

244. Round JL, Mazmanian SK. Inducible Foxp3+ regulatory T-cell development by a commensal bacterium of the intestinal microbiota. Proc Natl Acad Sci U S A. 2010;107(27):12204-9.

245. Tangye SG, Al-Herz W, Bousfiha A, Chatila T, Cunningham-Rundles C, Etzioni A, et al. Human Inborn Errors of Immunity: 2019 Update on the Classification from the International Union of Immunological Societies Expert Committee. J Clin Immunol. 2020;40(1):24-64.

246. Tangye SG, Al-Herz W, Bousfiha A, Cunningham-Rundles C, Franco JL, Holland SM, et al. The Ever-Increasing Array of Novel Inborn Errors of Immunity: an Interim Update by the IUIS Committee. J Clin Immunol. 2021;41(3):666-79.

247. Hartono S, Ippoliti MR, Mastroianni M, Torres R, Rider NL. Gastrointestinal Disorders Associated with Primary Immunodeficiency Diseases. Clin Rev Allergy Immunol. 2019;57(2):145-65.

248. Fischer A, Notarangelo LD, Neven B, Cavazzana M, Puck JM. Severe combined immunodeficiencies and related disorders. Nat Rev Dis Primers. 2015;1:15061.

249. Buckley RH. Molecular defects in human severe combined immunodeficiency and approaches to immune reconstitution. Annu Rev Immunol. 2004;22:625-55.

250. Buckley RH, Schiff RI, Schiff SE, Markert ML, Williams LW, Harville TO, et al. Human severe combined immunodeficiency: genetic, phenotypic, and functional diversity in one hundred eight infants. J Pediatr. 1997;130(3):378-87.

251. Kalman L, Lindegren ML, Kobrynski L, Vogt R, Hannon H, Howard JT, et al. Mutations in genes required for T-cell development: IL7R, CD45, IL2RG, JAK3, RAG1, RAG2, ARTEMIS, and ADA and severe combined immunodeficiency: HuGE review. Genet Med. 2004;6(1):16-26.

252. Felgentreff K, Perez-Becker R, Speckmann C, Schwarz K, Kalwak K, Markelj G, et al. Clinical and immunological manifestations of patients with atypical severe combined immunodeficiency. Clin Immunol. 2011;141(1):73-82.

253. Stephan JL, Vlekova V, Le Deist F, Blanche S, Donadieu J, De Saint-Basile G, et al. Severe combined immunodeficiency: a retrospective single-center study of clinical presentation and outcome in 117 patients. J Pediatr. 1993;123(4):564-72.

254. Conley ME, Notarangelo LD, Etzioni A. Diagnostic criteria for primary immunodeficiencies. Representing PAGID (Pan-American Group for Immunodeficiency) and ESID (European Society for Immunodeficiencies). Clin Immunol. 1999;93(3):190-7.

255. Illig D, Navratil M, Kelecic J, Conca R, Hojsak I, Jadresin O, et al. Alternative Splicing Rescues Loss of Common Gamma Chain Function and Results in IL-21R-like Deficiency. J Clin Immunol. 2019;39(2):207-15.

256. Kumrah R, Vignesh P, Patra P, Singh A, Anjani G, Saini P, et al. Genetics of severe combined immunodeficiency. Genes Dis. 2020;7(1):52-61.

257. Blanco E, Izotova N, Booth C, Thrasher AJ. Immune Reconstitution After Gene Therapy Approaches in Patients With X-Linked Severe Combined Immunodeficiency Disease. Front Immunol. 2020;11:608653.

258. Leonard WJ, Lin JX, O'Shea JJ. The gammac Family of Cytokines: Basic Biology to Therapeutic Ramifications. Immunity. 2019;50(4):832-50.

259. Dvorak CC, Haddad E, Buckley RH, Cowan MJ, Logan B, Griffith LM, et al. The genetic landscape of severe combined immunodeficiency in the United States and Canada in the current era (2010-2018). J Allergy Clin Immunol. 2019;143(1):405-7.

260. Puck JM. Newborn screening for severe combined immunodeficiency and T-cell lymphopenia. Immunol Rev. 2019;287(1):241-52.

261. Lim CK, Abolhassani H, Appelberg SK, Sundin M, Hammarstrom L. IL2RG hypomorphic mutation: identification of a novel pathogenic mutation in exon 8 and a review of the literature. Allergy Asthma Clin Immunol. 2019;15:2.

262. Noguchi M, Yi H, Rosenblatt HM, Filipovich AH, Adelstein S, Modi WS, et al. Interleukin-2 receptor gamma chain mutation results in X-linked severe combined immunodeficiency in humans. Cell. 1993;73(1):147-57.

263. Puck JM, Deschenes SM, Porter JC, Dutra AS, Brown CJ, Willard HF, et al. The interleukin-2 receptor gamma chain maps to Xq13.1 and is mutated in X-linked severe combined immunodeficiency, SCIDX1. Hum Mol Genet. 1993;2(8):1099-104.

264. Spolski R, Li P, Leonard WJ. Biology and regulation of IL-2: from molecular mechanisms to human therapy. Nat Rev Immunol. 2018;18(10):648-59.

265. Abd Hamid IJ, Slatter MA, McKendrick F, Pearce MS, Gennery AR. Long-term outcome of hematopoietic stem cell transplantation for IL2RG/JAK3 SCID: a cohort report. Blood. 2017;129(15):2198-201.

266. Gatti RA, Meuwissen HJ, Allen HD, Hong R, Good RA. Immunological reconstitution of sex-linked lymphopenic immunological deficiency. Lancet. 1968;2(7583):1366-9.

267. Pai SY, Logan BR, Griffith LM, Buckley RH, Parrott RE, Dvorak CC, et al. Transplantation outcomes for severe combined immunodeficiency, 2000-2009. N Engl J Med. 2014;371(5):434-46.

268. Asao H, Okuyama C, Kumaki S, Ishii N, Tsuchiya S, Foster D, et al. Cutting edge: the common gamma-chain is an indispensable subunit of the IL-21 receptor complex. J Immunol. 2001;167(1):1-5.

269. Giri JG, Ahdieh M, Eisenman J, Shanebeck K, Grabstein K, Kumaki S, et al. Utilization of the beta and gamma chains of the IL-2 receptor by the novel cytokine IL-15. EMBO J. 1994;13(12):2822-30.

270. Kennedy MK, Glaccum M, Brown SN, Butz EA, Viney JL, Embers M, et al. Reversible defects in natural killer and memory CD8 T cell lineages in interleukin 15-deficient mice. J Exp Med. 2000;191(5):771-80.

271. Kimura Y, Takeshita T, Kondo M, Ishii N, Nakamura M, Van Snick J, et al. Sharing of the IL-2 receptor gamma chain with the functional IL-9 receptor complex. Int Immunol. 1995;7(1):115-20.

272. Noguchi M, Nakamura Y, Russell SM, Ziegler SF, Tsang M, Cao X, et al. Interleukin-2 receptor gamma chain: a functional component of the interleukin-7 receptor. Science. 1993;262(5141):1877-80.

273. Russell SM, Keegan AD, Harada N, Nakamura Y, Noguchi M, Leland P, et al. Interleukin-2 receptor gamma chain: a functional component of the interleukin-4 receptor. Science. 1993;262(5141):1880-3.

274. Takeshita T, Asao H, Ohtani K, Ishii N, Kumaki S, Tanaka N, et al. Cloning of the gamma chain of the human IL-2 receptor. Science. 1992;257(5068):379-82.

275. Miyazaki T, Kawahara A, Fujii H, Nakagawa Y, Minami Y, Liu ZJ, et al. Functional activation of Jak1 and Jak3 by selective association with IL-2 receptor subunits. Science. 1994;266(5187):1045-7.

276. Russell SM, Johnston JA, Noguchi M, Kawamura M, Bacon CM, Friedmann M, et al. Interaction of IL-2R beta and gamma c chains with Jak1 and Jak3: implications for XSCID and XCID. Science. 1994;266(5187):1042-5.

277. Witthuhn BA, Silvennoinen O, Miura O, Lai KS, Cwik C, Liu ET, et al. Involvement of the Jak-3 Janus kinase in signalling by interleukins 2 and 4 in lymphoid and myeloid cells. Nature. 1994;370(6485):153-7.

278. Macchi P, Villa A, Giliani S, Sacco MG, Frattini A, Porta F, et al. Mutations of Jak-3 gene in patients with autosomal severe combined immune deficiency (SCID). Nature. 1995;377(6544):65-8.

279. Russell SM, Tayebi N, Nakajima H, Riedy MC, Roberts JL, Aman MJ, et al. Mutation of Jak3 in a patient with SCID: essential role of Jak3 in lymphoid development. Science. 1995;270(5237):797-800.

280. Morgan DA, Ruscetti FW, Gallo R. Selective in vitro growth of T lymphocytes from normal human bone marrows. Science. 1976;193(4257):1007-8.

281. Nakamura Y, Russell SM, Mess SA, Friedmann M, Erdos M, Francois C, et al. Heterodimerization of the IL-2 receptor beta- and gamma-chain cytoplasmic domains is required for signalling. Nature. 1994;369(6478):330-3.

282. Nakamura M, Asao H, Takeshita T, Sugamura K. Interleukin-2 receptor heterotrimer complex and intracellular signaling. Semin Immunol. 1993;5(5):309-17.

283. Cote-Sierra J, Foucras G, Guo L, Chiodetti L, Young HA, Hu-Li J, et al. Interleukin 2 plays a central role in Th2 differentiation. Proc Natl Acad Sci U S A. 2004;101(11):3880-5.

284. Liao W, Lin JX, Wang L, Li P, Leonard WJ. Modulation of cytokine receptors by IL-2 broadly regulates differentiation into helper T cell lineages. Nat Immunol. 2011;12(6):551-9.

285. Malek TR, Yu A, Vincek V, Scibelli P, Kong L. CD4 regulatory T cells prevent lethal autoimmunity in IL-2Rbeta-deficient mice. Implications for the nonredundant function of IL-2. Immunity. 2002;17(2):167-78.

286. Schmitt E, Germann T, Goedert S, Hoehn P, Huels C, Koelsch S, et al. IL-9 production of naive CD4+ T cells depends on IL-2, is synergistically enhanced by a combination of TGF-beta and IL-4, and is inhibited by IFN-gamma. J Immunol. 1994;153(9):3989-96.

287. Klatzmann D, Abbas AK. The promise of low-dose interleukin-2 therapy for autoimmune and inflammatory diseases. Nat Rev Immunol. 2015;15(5):283-94.

288. Depper JM, Leonard WJ, Kronke M, Noguchi PD, Cunningham RE, Waldmann TA, et al. Regulation of interleukin 2 receptor expression: effects of phorbol diester, phospholipase C, and reexposure to lectin or antigen. J Immunol. 1984;133(6):3054-61.

289. John S, Robbins CM, Leonard WJ. An IL-2 response element in the human IL-2 receptor alpha chain promoter is a composite element that binds Stat5, Elf-1, HMG-I(Y) and a GATA family protein. EMBO J. 1996;15(20):5627-35.

290. Kim HP, Kelly J, Leonard WJ. The basis for IL-2-induced IL-2 receptor alpha chain gene regulation: importance of two widely separated IL-2 response elements. Immunity. 2001;15(1):159-72.

291. Leonard WJ, Kronke M, Peffer NJ, Depper JM, Greene WC. Interleukin 2 receptor gene expression in normal human T lymphocytes. Proc Natl Acad Sci U S A. 1985;82(18):6281-5.

292. Sakaguchi S, Sakaguchi N, Asano M, Itoh M, Toda M. Immunologic self-tolerance maintained by activated T cells expressing IL-2 receptor alpha-chains (CD25). Breakdown of a single mechanism of self-tolerance causes various autoimmune diseases. J Immunol. 1995;155(3):1151-64.

293. Yu A, Snowhite I, Vendrame F, Rosenzwajg M, Klatzmann D, Pugliese A, et al. Selective IL-2 responsiveness of regulatory T cells through multiple intrinsic mechanisms supports the use of low-dose IL-2 therapy in type 1 diabetes. Diabetes. 2015;64(6):2172-83.

294. Yu A, Zhu L, Altman NH, Malek TR. A low interleukin-2 receptor signaling threshold supports the development and homeostasis of T regulatory cells. Immunity. 2009;30(2):204-17.

295. Suzuki H, Kundig TM, Furlonger C, Wakeham A, Timms E, Matsuyama T, et al. Deregulated T cell activation and autoimmunity in mice lacking interleukin-2 receptor beta. Science. 1995;268(5216):1472-6.

296. Sadlack B, Merz H, Schorle H, Schimpl A, Feller AC, Horak I. Ulcerative colitis-like disease in mice with a disrupted interleukin-2 gene. Cell. 1993;75(2):253-61.

297. Goettel JA, Kotlarz D, Emani R, Canavan JB, Konnikova L, Illig D, et al. Low-Dose Interleukin-2 Ameliorates Colitis in a Preclinical Humanized Mouse Model. Cell Mol Gastroenterol Hepatol. 2019;8(2):193-5.

298. Howard M, Farrar J, Hilfiker M, Johnson B, Takatsu K, Hamaoka T, et al. Identification of a T cell-derived b cell growth factor distinct from interleukin 2. J Exp Med. 1982;155(3):914-23.

299. Isakson PC, Pure E, Vitetta ES, Krammer PH. T cell-derived B cell differentiation factor(s). Effect on the isotype switch of murine B cells. J Exp Med. 1982;155(3):734-48.

300. Vitetta ES, Ohara J, Myers CD, Layton JE, Krammer PH, Paul WE. Serological, biochemical, and functional identity of B cell-stimulatory factor 1 and B cell differentiation factor for IgG1. J Exp Med. 1985;162(5):1726-31.

301. Le Gros G, Ben-Sasson SZ, Seder R, Finkelman FD, Paul WE. Generation of interleukin 4 (IL-4)-producing cells in vivo and in vitro: IL-2 and IL-4 are required for in vitro generation of IL-4-producing cells. J Exp Med. 1990;172(3):921-9.

302. Stein M, Keshav S, Harris N, Gordon S. Interleukin 4 potently enhances murine macrophage mannose receptor activity: a marker of alternative immunologic macrophage activation. J Exp Med. 1992;176(1):287-92.

303. Junttila IS. Tuning the Cytokine Responses: An Update on Interleukin (IL)-4 and IL-13 Receptor Complexes. Front Immunol. 2018;9:888.

304. Abbas AK, Murphy KM, Sher A. Functional diversity of helper T lymphocytes. Nature. 1996;383(6603):787-93.

305. Ansel KM, Djuretic I, Tanasa B, Rao A. Regulation of Th2 differentiation and Il4 locus accessibility. Annu Rev Immunol. 2006;24:607-56.

306. Brown MA, Pierce JH, Watson CJ, Falco J, Ihle JN, Paul WE. B cell stimulatory factor-1/interleukin-4 mRNA is expressed by normal and transformed mast cells. Cell. 1987;50(5):809-18.

307. Mosmann TR, Cherwinski H, Bond MW, Giedlin MA, Coffman RL. Two types of murine helper T cell clone. I. Definition according to profiles of lymphokine activities and secreted proteins. J Immunol. 1986;136(7):2348-57.

308. Nonaka M, Nonaka R, Woolley K, Adelroth E, Miura K, Okhawara Y, et al. Distinct immunohistochemical localization of IL-4 in human inflamed airway tissues. IL-4 is localized to eosinophils in vivo and is released by peripheral blood eosinophils. J Immunol. 1995;155(6):3234-44.

309. Seder RA, Paul WE, Dvorak AM, Sharkis SJ, Kagey-Sobotka A, Niv Y, et al. Mouse splenic and bone marrow cell populations that express high-affinity Fc epsilon receptors and produce interleukin 4 are highly enriched in basophils. Proc Natl Acad Sci U S A. 1991;88(7):2835-9.

310. Yoshimoto T, Paul WE. CD4pos, NK1.1pos T cells promptly produce interleukin 4 in response to in vivo challenge with anti-CD3. J Exp Med. 1994;179(4):1285-95.

311. Aman MJ, Tayebi N, Obiri NI, Puri RK, Modi WS, Leonard WJ. cDNA cloning and characterization of the human interleukin 13 receptor alpha chain. J Biol Chem. 1996;271(46):29265-70.

312. Hilton DJ, Zhang JG, Metcalf D, Alexander WS, Nicola NA, Willson TA. Cloning and characterization of a binding subunit of the interleukin 13 receptor that is also a component of the interleukin 4 receptor. Proc Natl Acad Sci U S A. 1996;93(1):497-501.

313. Miloux B, Laurent P, Bonnin O, Lupker J, Caput D, Vita N, et al. Cloning of the human IL-13R alpha1 chain and reconstitution with the IL4R alpha of a functional IL-4/IL-13 receptor complex. FEBS Lett. 1997;401(2-3):163-6.

314. Kondo M, Takeshita T, Ishii N, Nakamura M, Watanabe S, Arai K, et al. Sharing of the interleukin-2 (IL-2) receptor gamma chain between receptors for IL-2 and IL-4. Science. 1993;262(5141):1874-7.

315. McKenzie AN, Culpepper JA, de Waal Malefyt R, Briere F, Punnonen J, Aversa G, et al. Interleukin 13, a T-cell-derived cytokine that regulates human monocyte and B-cell function. Proc Natl Acad Sci U S A. 1993;90(8):3735-9.

316. Defrance T, Carayon P, Billian G, Guillemot JC, Minty A, Caput D, et al. Interleukin 13 is a B cell stimulating factor. J Exp Med. 1994;179(1):135-43.

317. Recher M, Berglund LJ, Avery DT, Cowan MJ, Gennery AR, Smart J, et al. IL-21 is the primary common gamma chain-binding cytokine required for human B-cell differentiation in vivo. Blood. 2011;118(26):6824-35.

318. Spolski R, Leonard WJ. Interleukin-21: a double-edged sword with therapeutic potential. Nat Rev Drug Discov. 2014;13(5):379-95.

319. Ozaki K, Spolski R, Feng CG, Qi CF, Cheng J, Sher A, et al. A critical role for IL-21 in regulating immunoglobulin production. Science. 2002;298(5598):1630-4.

320. Mackall CL, Fry TJ, Gress RE. Harnessing the biology of IL-7 for therapeutic application. Nat Rev Immunol. 2011;11(5):330-42.

321. Puel A, Ziegler SF, Buckley RH, Leonard WJ. Defective IL7R expression in T(-)B(+)NK(+) severe combined immunodeficiency. Nat Genet. 1998;20(4):394-7.

322. Goodwin RG, Friend D, Ziegler SF, Jerzy R, Falk BA, Gimpel S, et al. Cloning of the human and murine interleukin-7 receptors: demonstration of a soluble form and homology to a new receptor superfamily. Cell. 1990;60(6):941-51.

323. Boesteanu A, Silva AD, Nakajima H, Leonard WJ, Peschon JJ, Joyce S. Distinct roles for signals relayed through the common cytokine receptor gamma chain and interleukin 7 receptor alpha chain in natural T cell development. J Exp Med. 1997;186(2):331-6.

324. Hassan J, Reen DJ. Human recent thymic emigrants--identification, expansion, and survival characteristics. J Immunol. 2001;167(4):1970-6.

325. Mazzucchelli R, Durum SK. Interleukin-7 receptor expression: intelligent design. Nat Rev Immunol. 2007;7(2):144-54.

326. Miller JP, Izon D, DeMuth W, Gerstein R, Bhandoola A, Allman D. The earliest step in B lineage differentiation from common lymphoid progenitors is critically dependent upon interleukin 7. J Exp Med. 2002;196(5):705-11.

327. Munitic I, Williams JA, Yang Y, Dong B, Lucas PJ, El Kassar N, et al. Dynamic regulation of IL-7 receptor expression is required for normal thymopoiesis. Blood. 2004;104(13):4165-72.

328. Park JH, Yu Q, Erman B, Appelbaum JS, Montoya-Durango D, Grimes HL, et al. Suppression of IL7Ralpha transcription by IL-7 and other prosurvival cytokines: a novel mechanism for maximizing IL-7-dependent T cell survival. Immunity. 2004;21(2):289-302.

329. Van De Wiele CJ, Marino JH, Murray BW, Vo SS, Whetsell ME, Teague TK. Thymocytes between the beta-selection and positive selection checkpoints are nonresponsive to IL-7 as assessed by STAT-5 phosphorylation. J Immunol. 2004;172(7):4235-44.

330. Webb LM, Foxwell BM, Feldmann M. Putative role for interleukin-7 in the maintenance of the recirculating naive CD4+ T-cell pool. Immunology. 1999;98(3):400-5.

331. Johnson SE, Shah N, Bajer AA, LeBien TW. IL-7 activates the phosphatidylinositol 3-kinase/AKT pathway in normal human thymocytes but not normal human B cell precursors. J Immunol. 2008;180(12):8109-17.

332. Kim K, Lee CK, Sayers TJ, Muegge K, Durum SK. The trophic action of IL-7 on pro-T cells: inhibition of apoptosis of pro-T1, -T2, and -T3 cells correlates with Bcl-2 and Bax levels and is independent of Fas and p53 pathways. J Immunol. 1998;160(12):5735-41.

333. Li WQ, Jiang Q, Khaled AR, Keller JR, Durum SK. Interleukin-7 inactivates the pro-apoptotic protein Bad promoting T cell survival. J Biol Chem. 2004;279(28):29160-6.

334. Maraskovsky E, O'Reilly LA, Teepe M, Corcoran LM, Peschon JJ, Strasser A. Bcl-2 can rescue T lymphocyte development in interleukin-7 receptor-deficient mice but not in mutant rag-1-/- mice. Cell. 1997;89(7):1011-9.

335. Pallard C, Stegmann AP, van Kleffens T, Smart F, Venkitaraman A, Spits H. Distinct roles of the phosphatidylinositol 3-kinase and STAT5 pathways in IL-7-mediated development of human thymocyte precursors. Immunity. 1999;10(5):525-35.

336. Li WQ, Jiang Q, Aleem E, Kaldis P, Khaled AR, Durum SK. IL-7 promotes T cell proliferation through destabilization of p27Kip1. J Exp Med. 2006;203(3):573-82.

337. Angkasekwinai P, Dong C. IL-9-producing T cells: potential players in allergy and cancer. Nat Rev Immunol. 2021;21(1):37-48.

338. Chen CY, Lee JB, Liu B, Ohta S, Wang PY, Kartashov AV, et al. Induction of Interleukin-9-Producing Mucosal Mast Cells Promotes Susceptibility to IgE-Mediated Experimental Food Allergy. Immunity. 2015;43(4):788-802.

339. Dardalhon V, Awasthi A, Kwon H, Galileos G, Gao W, Sobel RA, et al. IL-4 inhibits TGF-beta-induced Foxp3+ T cells and, together with TGF-beta, generates IL-9+ IL-10+ Foxp3(-) effector T cells. Nat Immunol. 2008;9(12):1347-55.

340. Eller K, Wolf D, Huber JM, Metz M, Mayer G, McKenzie AN, et al. IL-9 production by regulatory T cells recruits mast cells that are essential for regulatory T cell-induced immune suppression. J Immunol. 2011;186(1):83-91.

341. Turner JE, Morrison PJ, Wilhelm C, Wilson M, Ahlfors H, Renauld JC, et al. IL-9-mediated survival of type 2 innate lymphoid cells promotes damage control in helminth-induced lung inflammation. J Exp Med. 2013;210(13):2951-65.

342. Veldhoen M, Uyttenhove C, van Snick J, Helmby H, Westendorf A, Buer J, et al. Transforming growth factor-beta 'reprograms' the differentiation of T helper 2 cells and promotes an interleukin 9-producing subset. Nat Immunol. 2008;9(12):1341-6.

343. Wang Y, Shi J, Yan J, Xiao Z, Hou X, Lu P, et al. Germinal-center development of memory B cells driven by IL-9 from follicular helper T cells. Nat Immunol. 2017;18(8):921-30.

344. Behnke JM, Wahid FN, Grencis RK, Else KJ, Ben-Smith AW, Goyal PK. Immunological relationships during primary infection with Heligmosomoides polygyrus (Nematospiroides dubius): downregulation of specific cytokine secretion (IL-9 and IL-10) correlates with poor mastocytosis and chronic survival of adult worms. Parasite Immunol. 1993;15(7):415-21.

345. Hultner L, Druez C, Moeller J, Uyttenhove C, Schmitt E, Rude E, et al. Mast cell growth-enhancing activity (MEA) is structurally related and functionally identical to the novel mouse T cell growth factor P40/TCGFIII (interleukin 9). Eur J Immunol. 1990;20(6):1413-6.

346. Townsend JM, Fallon GP, Matthews JD, Smith P, Jolin EH, McKenzie NA. IL-9-deficient mice establish fundamental roles for IL-9 in pulmonary mastocytosis and goblet cell hyperplasia but not T cell development. Immunity. 2000;13(4):573-83.

347. Gounni AS, Hamid Q, Rahman SM, Hoeck J, Yang J, Shan L. IL-9-mediated induction of eotaxin1/CCL11 in human airway smooth muscle cells. J Immunol. 2004;173(4):2771-9.

348. Longphre M, Li D, Gallup M, Drori E, Ordonez CL, Redman T, et al. Allergen-induced IL-9 directly stimulates mucin transcription in respiratory epithelial cells. J Clin Invest. 1999;104(10):1375-82.

349. Lu Y, Hong S, Li H, Park J, Hong B, Wang L, et al. Th9 cells promote antitumor immune responses in vivo. J Clin Invest. 2012;122(11):4160-71.

350. Purwar R, Schlapbach C, Xiao S, Kang HS, Elyaman W, Jiang X, et al. Robust tumor immunity to melanoma mediated by interleukin-9-producing T cells. Nat Med. 2012;18(8):1248-53.

351. Xiao X, Fan Y, Li J, Zhang X, Lou X, Dou Y, et al. Guidance of super-enhancers in regulation of IL-9 induction and airway inflammation. J Exp Med. 2018;215(2):559-74.

352. Gerlach K, Hwang Y, Nikolaev A, Atreya R, Dornhoff H, Steiner S, et al. TH9 cells that express the transcription factor PU.1 drive T cell-mediated colitis via IL-9 receptor signaling in intestinal epithelial cells. Nat Immunol. 2014;15(7):676-86.

353. Nalleweg N, Chiriac MT, Podstawa E, Lehmann C, Rau TT, Atreya R, et al. IL-9 and its receptor are predominantly involved in the pathogenesis of UC. Gut. 2015;64(5):743-55.

354. Abadie V, Jabri B. IL-15: a central regulator of celiac disease immunopathology. Immunol Rev. 2014;260(1):221-34.

355. Blauvelt A, Asada H, Klaus-Kovtun V, Altman DJ, Lucey DR, Katz SI. Interleukin-15 mRNA is expressed by human keratinocytes Langerhans cells, and blood-derived dendritic cells and is downregulated by ultraviolet B radiation. J Invest Dermatol. 1996;106(5):1047-52.

356. Carson WE, Ross ME, Baiocchi RA, Marien MJ, Boiani N, Grabstein K, et al. Endogenous production of interleukin 15 by activated human monocytes is critical for optimal production of interferon-gamma by natural killer cells in vitro. J Clin Invest. 1995;96(6):2578-82.

357. Doherty TM, Seder RA, Sher A. Induction and regulation of IL-15 expression in murine macrophages. J Immunol. 1996;156(2):735-41.

358. Fehniger TA, Caligiuri MA. Interleukin 15: biology and relevance to human disease. Blood. 2001;97(1):14-32.

359. Grabstein KH, Eisenman J, Shanebeck K, Rauch C, Srinivasan S, Fung V, et al. Cloning of a T cell growth factor that interacts with the beta chain of the interleukin-2 receptor. Science. 1994;264(5161):965-8.

360. Jonuleit H, Wiedemann K, Muller G, Degwert J, Hoppe U, Knop J, et al. Induction of IL-15 messenger RNA and protein in human blood-derived dendritic cells: a role for IL-15 in attraction of T cells. J Immunol. 1997;158(6):2610-5.

361. Lee YB, Satoh J, Walker DG, Kim SU. Interleukin-15 gene expression in human astrocytes and microglia in culture. Neuroreport. 1996;7(5):1062-6.

362. Reinecker HC, MacDermott RP, Mirau S, Dignass A, Podolsky DK. Intestinal epithelial cells both express and respond to interleukin 15. Gastroenterology. 1996;111(6):1706-13.

363. Waldmann TA. The biology of interleukin-2 and interleukin-15: implications for cancer therapy and vaccine design. Nat Rev Immunol. 2006;6(8):595-601.

364. Fehniger TA. Mystery Solved: IL-15. J Immunol. 2019;202(11):3125-6.

365. Lorenzen I, Dingley AJ, Jacques Y, Grotzinger J. The structure of the interleukin-15 alpha receptor and its implications for ligand binding. J Biol Chem. 2006;281(10):6642-7.

366. Rickert M, Wang X, Boulanger MJ, Goriatcheva N, Garcia KC. The structure of interleukin-2 complexed with its alpha receptor. Science. 2005;308(5727):1477-80.

367. Burkett PR, Koka R, Chien M, Chai S, Boone DL, Ma A. Coordinate expression and trans presentation of interleukin (IL)-15Ralpha and IL-15 supports natural killer cell and memory CD8+ T cell homeostasis. J Exp Med. 2004;200(7):825-34.

368. Dubois S, Mariner J, Waldmann TA, Tagaya Y. IL-15Ralpha recycles and presents IL-15 In trans to neighboring cells. Immunity. 2002;17(5):537-47.

369. Carson WE, Fehniger TA, Haldar S, Eckhert K, Lindemann MJ, Lai CF, et al. A potential role for interleukin-15 in the regulation of human natural killer cell survival. J Clin Invest. 1997;99(5):937-43.

370. Gordy LE, Bezbradica JS, Flyak AI, Spencer CT, Dunkle A, Sun J, et al. IL-15 regulates homeostasis and terminal maturation of NKT cells. J Immunol. 2011;187(12):6335-45.

371. Johnston JA, Bacon CM, Finbloom DS, Rees RC, Kaplan D, Shibuya K, et al. Tyrosine phosphorylation and activation of STAT5, STAT3, and Janus kinases by interleukins 2 and 15. Proc Natl Acad Sci U S A. 1995;92(19):8705-9.

372. Ku CC, Murakami M, Sakamoto A, Kappler J, Marrack P. Control of homeostasis of CD8+ memory T cells by opposing cytokines. Science. 2000;288(5466):675-8.

373. Schluns KS, Williams K, Ma A, Zheng XX, Lefrancois L. Cutting edge: requirement for IL-15 in the generation of primary and memory antigen-specific CD8 T cells. J Immunol. 2002;168(10):4827-31.

374. Zhang C, Zhang J, Niu J, Zhang J, Tian Z. Interleukin-15 improves cytotoxicity of natural killer cells via up-regulating NKG2D and cytotoxic effector molecule expression as well as STAT1 and ERK1/2 phosphorylation. Cytokine. 2008;42(1):128-36.

375. Lodolce JP, Boone DL, Chai S, Swain RE, Dassopoulos T, Trettin S, et al. IL-15 receptor maintains lymphoid homeostasis by supporting lymphocyte homing and proliferation. Immunity. 1998;9(5):669-76.

376. Chtanova T, Tangye SG, Newton R, Frank N, Hodge MR, Rolph MS, et al. T follicular helper cells express a distinctive transcriptional profile, reflecting their role as non-Th1/Th2 effector cells that provide help for B cells. J Immunol. 2004;173(1):68-78.

377. Coquet JM, Kyparissoudis K, Pellicci DG, Besra G, Berzins SP, Smyth MJ, et al. IL-21 is produced by NKT cells and modulates NKT cell activation and cytokine production. J Immunol. 2007;178(5):2827-34.

378. Parrish-Novak J, Dillon SR, Nelson A, Hammond A, Sprecher C, Gross JA, et al. Interleukin 21 and its receptor are involved in NK cell expansion and regulation of lymphocyte function. Nature. 2000;408(6808):57-63.

379. Spolski R, Leonard WJ. Interleukin-21: basic biology and implications for cancer and autoimmunity. Annu Rev Immunol. 2008;26:57-79.

380. Wei L, Laurence A, Elias KM, O'Shea JJ. IL-21 is produced by Th17 cells and drives IL-17 production in a STAT3-dependent manner. J Biol Chem. 2007;282(48):34605-10.

381. Ozaki K, Kikly K, Michalovich D, Young PR, Leonard WJ. Cloning of a type I cytokine receptor most related to the IL-2 receptor beta chain. Proc Natl Acad Sci U S A. 2000;97(21):11439-44.

382. Konforte D, Paige CJ. Identification of cellular intermediates and molecular pathways induced by IL-21 in human B cells. J Immunol. 2006;177(12):8381-92.

383. Zeng R, Spolski R, Casas E, Zhu W, Levy DE, Leonard WJ. The molecular basis of IL-21-mediated proliferation. Blood. 2007;109(10):4135-42.

384. Korn T, Bettelli E, Gao W, Awasthi A, Jager A, Strom TB, et al. IL-21 initiates an alternative pathway to induce proinflammatory T(H)17 cells. Nature. 2007;448(7152):484-7.

385. Attridge K, Wang CJ, Wardzinski L, Kenefeck R, Chamberlain JL, Manzotti C, et al. IL-21 inhibits T cell IL-2 production and impairs Treg homeostasis. Blood. 2012;119(20):4656-64.

386. Bauquet AT, Jin H, Paterson AM, Mitsdoerffer M, Ho IC, Sharpe AH, et al. The costimulatory molecule ICOS regulates the expression of c-Maf and IL-21 in the development of follicular T helper cells and TH-17 cells. Nat Immunol. 2009;10(2):167-75.

387. Eto D, Lao C, DiToro D, Barnett B, Escobar TC, Kageyama R, et al. IL-21 and IL-6 are critical for different aspects of B cell immunity and redundantly induce optimal follicular helper CD4 T cell (Tfh) differentiation. PLoS One. 2011;6(3):e17739.

388. Liao W, Spolski R, Li P, Du N, West EE, Ren M, et al. Opposing actions of IL-2 and IL-21 on Th9 differentiation correlate with their differential regulation of BCL6 expression. Proc Natl Acad Sci U S A. 2014;111(9):3508-13.

389. Nurieva R, Yang XO, Martinez G, Zhang Y, Panopoulos AD, Ma L, et al. Essential autocrine regulation by IL-21 in the generation of inflammatory T cells. Nature. 2007;448(7152):480-3.

390. Nurieva RI, Chung Y, Hwang D, Yang XO, Kang HS, Ma L, et al. Generation of T follicular helper cells is mediated by interleukin-21 but independent of T helper 1, 2, or 17 cell lineages. Immunity. 2008;29(1):138-49.

391. Pallikkuth S, Rogers K, Villinger F, Dosterii M, Vaccari M, Franchini G, et al. Interleukin-21 administration to rhesus macaques chronically infected with simian immunodeficiency virus increases cytotoxic effector molecules in T cells and NK cells and enhances B cell function without increasing immune activation or viral replication. Vaccine. 2011;29(49):9229-38.

392. Roda JM, Parihar R, Lehman A, Mani A, Tridandapani S, Carson WE, 3rd. Interleukin-21 enhances NK cell activation in response to antibody-coated targets. J Immunol. 2006;177(1):120-9.

393. Schmitz I, Schneider C, Frohlich A, Frebel H, Christ D, Leonard WJ, et al. IL-21 restricts virus-driven Treg cell expansion in chronic LCMV infection. PLoS Pathog. 2013;9(5):e1003362.

394. Zeng R, Spolski R, Finkelstein SE, Oh S, Kovanen PE, Hinrichs CS, et al. Synergy of IL-21 and IL-15 in regulating CD8+ T cell expansion and function. J Exp Med. 2005;201(1):139-48.

395. Tamagawa-Mineoka R, Kishida T, Mazda O, Katoh N. IL-21 reduces immediate hypersensitivity reactions in mouse skin by suppressing mast cell activation or IgE production. J Invest Dermatol. 2011;131(7):1513-20.

396. Wan CK, Oh J, Li P, West EE, Wong EA, Andraski AB, et al. The cytokines IL-21 and GM-CSF have opposing regulatory roles in the apoptosis of conventional dendritic cells. Immunity. 2013;38(3):514-27.

397. Fantini MC, Monteleone G, MacDonald TT. IL-21 comes of age as a regulator of effector T cells in the gut. Mucosal Immunol. 2008;1(2):110-5.

398. Fina D, Sarra M, Fantini MC, Rizzo A, Caruso R, Caprioli F, et al. Regulation of gut inflammation and th17 cell response by interleukin-21. Gastroenterology. 2008;134(4):1038-48.

399. Monteleone G, Monteleone I, Fina D, Vavassori P, Del Vecchio Blanco G, Caruso R, et al. Interleukin-21 enhances T-helper cell type I signaling and interferon-gamma production in Crohn's disease. Gastroenterology. 2005;128(3):687-94.

400. Kotlarz D, Zietara N, Uzel G, Weidemann T, Braun CJ, Diestelhorst J, et al. Loss-of-function mutations in the IL-21 receptor gene cause a primary immunodeficiency syndrome. J Exp Med. 2013;210(3):433-43.

401. Marquez A, Orozco G, Martinez A, Palomino-Morales R, Fernandez-Arquero M, Mendoza JL, et al. Novel association of the interleukin 2-interleukin 21 region with inflammatory bowel disease. Am J Gastroenterol. 2009;104(8):1968-75.

402. Kotlarz D, Zietara N, Milner JD, Klein C. Human IL-21 and IL-21R deficiencies: two novel entities of primary immunodeficiency. Curr Opin Pediatr. 2014;26(6):704-12.

403. Hirschhorn R, Yang DR, Israni A, Huie ML, Ownby DR. Somatic mosaicism for a newly identified splice-site mutation in a patient with adenosine deaminase-deficient immunodeficiency and spontaneous clinical recovery. Am J Hum Genet. 1994;55(1):59-68.

404. Hirschhorn R, Yang DR, Puck JM, Huie ML, Jiang CK, Kurlandsky LE. Spontaneous in vivo reversion to normal of an inherited mutation in a patient with adenosine deaminase deficiency. Nat Genet. 1996;13(3):290-5.

405. Stephan V, Wahn V, Le Deist F, Dirksen U, Broker B, Muller-Fleckenstein I, et al. Atypical X-linked severe combined immunodeficiency due to possible spontaneous reversion of the genetic defect in T cells. N Engl J Med. 1996;335(21):1563-7.

406. Kotas ME, Medzhitov R. Homeostasis, inflammation, and disease susceptibility. Cell. 2015;160(5):816-27.

407. Rumpret M, Drylewicz J, Ackermans LJE, Borghans JAM, Medzhitov R, Meyaard L. Functional categories of immune inhibitory receptors. Nat Rev Immunol. 2020;20(12):771-80.

408. Amigorena S, Bonnerot C, Drake JR, Choquet D, Hunziker W, Guillet JG, et al. Cytoplasmic domain heterogeneity and functions of IgG Fc receptors in B lymphocytes. Science. 1992;256(5065):1808-12.

409. D'Ambrosio D, Hippen KL, Minskoff SA, Mellman I, Pani G, Siminovitch KA, et al. Recruitment and activation of PTP1C in negative regulation of antigen receptor signaling by Fc gamma RIIB1. Science. 1995;268(5208):293-7.

410. Daeron M, Latour S, Malbec O, Espinosa E, Pina P, Pasmans S, et al. The same tyrosine-based inhibition motif, in the intracytoplasmic domain of Fc gamma RIIB, regulates negatively BCR-, TCR-, and FcR-dependent cell activation. Immunity. 1995;3(5):635-46.

411. Gergely J, Pecht I, Sarmay G. Immunoreceptor tyrosine-based inhibition motif-bearing receptors regulate the immunoreceptor tyrosine-based activation motif-induced activation of immune competent cells. Immunol Lett. 1999;68(1):3-15.

412. Olcese L, Lang P, Vely F, Cambiaggi A, Marguet D, Blery M, et al. Human and mouse killer-cell inhibitory receptors recruit PTP1C and PTP1D protein tyrosine phosphatases. J Immunol. 1996;156(12):4531-4.

413. Ono M, Bolland S, Tempst P, Ravetch JV. Role of the inositol phosphatase SHIP in negative regulation of the immune system by the receptor Fc(gamma)RIIB. Nature. 1996;383(6597):263-6.

414. Vely F, Olivero S, Olcese L, Moretta A, Damen JE, Liu L, et al. Differential association of phosphatases with hematopoietic co-receptors bearing immunoreceptor tyrosine-based inhibition motifs. Eur J Immunol. 1997;27(8):1994-2000.

415. Vivier E, Daeron M. Immunoreceptor tyrosine-based inhibition motifs. Immunol Today. 1997;18(6):286-91.

416. Crocker PR, Paulson JC, Varki A. Siglecs and their roles in the immune system. Nat Rev Immunol. 2007;7(4):255-66.

417. Macauley MS, Crocker PR, Paulson JC. Siglec-mediated regulation of immune cell function in disease. Nat Rev Immunol. 2014;14(10):653-66.

418. Schwarzkopf M, Knobeloch KP, Rohde E, Hinderlich S, Wiechens N, Lucka L, et al. Sialylation is essential for early development in mice. Proc Natl Acad Sci U S A. 2002;99(8):5267-70.

419. Rawal P, Zhao L. Sialometabolism in Brain Health and Alzheimer's Disease. Front Neurosci. 2021;15:648617.

420. Sprenger N, Duncan PI. Sialic acid utilization. Adv Nutr. 2012;3(3):392S-7S.

421. Lubbers J, Rodriguez E, van Kooyk Y. Modulation of Immune Tolerance via Siglec-Sialic Acid Interactions. Front Immunol. 2018;9:2807.

422. Chou HH, Takematsu H, Diaz S, Iber J, Nickerson E, Wright KL, et al. A mutation in human CMP-sialic acid hydroxylase occurred after the Homo-Pan divergence. Proc Natl Acad Sci U S A. 1998;95(20):11751-6.

423. Irie A, Koyama S, Kozutsumi Y, Kawasaki T, Suzuki A. The molecular basis for the absence of N-glycolylneuraminic acid in humans. J Biol Chem. 1998;273(25):15866-71.

424. Varki A. N-glycolylneuraminic acid deficiency in humans. Biochimie. 2001;83(7):615-22.

425. Warren L, Blacklow RS. The biosynthesis of cytidine 5'-monophospho-n-acetylneuraminic acid by an enzyme from Neisseria meningitidis. J Biol Chem. 1962;237:3527-34.

426. Eckhardt M, Muhlenhoff M, Bethe A, Gerardy-Schahn R. Expression cloning of the Golgi CMP-sialic acid transporter. Proc Natl Acad Sci U S A. 1996;93(15):7572-6.

427. Martinez-Duncker I, Dupre T, Piller V, Piller F, Candelier JJ, Trichet C, et al. Genetic complementation reveals a novel human congenital disorder of glycosylation of type II, due to inactivation of the Golgi CMP-sialic acid transporter. Blood. 2005;105(7):2671-6.

428. Freeze HH, Hart GW, Schnaar RL. Glycosylation Precursors. In: rd, Varki A, Cummings RD, Esko JD, Stanley P, Hart GW, et al., editors. Essentials of Glycobiology. Cold Spring Harbor (NY)2015. p. 51-63.

429. Varki A, Schnaar RL, Schauer R. Sialic Acids and Other Nonulosonic Acids. In: rd, Varki A, Cummings RD, Esko JD, Stanley P, Hart GW, et al., editors. Essentials of Glycobiology. Cold Spring Harbor (NY)2015. p. 179-95.

430. Freeze HH, Schachter H, Kinoshita T. Genetic Disorders of Glycosylation. In: rd, Varki A, Cummings RD, Esko JD, Stanley P, Hart GW, et al., editors. Essentials of Glycobiology. Cold Spring Harbor (NY)2015. p. 569-82.

431. Hennet T, Chui D, Paulson JC, Marth JD. Immune regulation by the ST6Gal sialyltransferase. Proc Natl Acad Sci U S A. 1998;95(8):4504-9.

432. Doring Y, Noels H, Mandl M, Kramp B, Neideck C, Lievens D, et al. Deficiency of the sialyltransferase St3Gal4 reduces Ccl5-mediated myeloid cell recruitment and arrest: short communication. Circ Res. 2014;114(6):976-81.

433. Angata T, Margulies EH, Green ED, Varki A. Large-scale sequencing of the CD33-related Siglec gene cluster in five mammalian species reveals rapid evolution by multiple mechanisms. Proc Natl Acad Sci U S A. 2004;101(36):13251-6.

434. Collins BE, Blixt O, DeSieno AR, Bovin N, Marth JD, Paulson JC. Masking of CD22 by cis ligands does not prevent redistribution of CD22 to sites of cell contact. Proc Natl Acad Sci U S A. 2004;101(16):6104-9.

435. Crocker PR, Mucklow S, Bouckson V, McWilliam A, Willis AC, Gordon S, et al. Sialoadhesin, a macrophage sialic acid binding receptor for haemopoietic cells with 17 immunoglobulin-like domains. EMBO J. 1994;13(19):4490-503.

436. Varki A. Since there are PAMPs and DAMPs, there must be SAMPs? Glycan "self-associated molecular patterns" dampen innate immunity, but pathogens can mimic them. Glycobiology. 2011;21(9):1121-4.

437. Avril T, Floyd H, Lopez F, Vivier E, Crocker PR. The membrane-proximal immunoreceptor tyrosine-based inhibitory motif is critical for the inhibitory signaling mediated by Siglecs-7 and -9, CD33-related Siglecs expressed on human monocytes and NK cells. J Immunol. 2004;173(11):6841-9.

438. Paul SP, Taylor LS, Stansbury EK, McVicar DW. Myeloid specific human CD33 is an inhibitory receptor with differential ITIM function in recruiting the phosphatases SHP-1 and SHP-2. Blood. 2000;96(2):483-90.

439. Ulyanova T, Shah DD, Thomas ML. Molecular cloning of MIS, a myeloid inhibitory siglec, that binds protein-tyrosine phosphatases SHP-1 and SHP-2. J Biol Chem. 2001;276(17):14451-8.

440. Ulyanova T, Blasioli J, Woodford-Thomas TA, Thomas ML. The sialoadhesin CD33 is a myeloid-specific inhibitory receptor. Eur J Immunol. 1999;29(11):3440-9.

441. Taylor VC, Buckley CD, Douglas M, Cody AJ, Simmons DL, Freeman SD. The myeloid-specific sialic acid-binding receptor, CD33, associates with the protein-tyrosine phosphatases, SHP-1 and SHP-2. J Biol Chem. 1999;274(17):11505-12.

442. Ishida A, Akita K, Mori Y, Tanida S, Toda M, Inoue M, et al. Negative regulation of Toll-like receptor-4 signaling through the binding of glycosylphosphatidylinositol-anchored glycoprotein, CD14, with the sialic acid-binding lectin, CD33. J Biol Chem. 2014;289(36):25341-50.

443. Freeman SD, Kelm S, Barber EK, Crocker PR. Characterization of CD33 as a new member of the sialoadhesin family of cellular interaction molecules. Blood. 1995;85(8):2005-12.

444. Estus S, Shaw BC, Devanney N, Katsumata Y, Press EE, Fardo DW. Evaluation of CD33 as a genetic risk factor for Alzheimer's disease. Acta Neuropathol. 2019;138(2):187-99.

445. Lock K, Zhang J, Lu J, Lee SH, Crocker PR. Expression of CD33-related siglecs on human mononuclear phagocytes, monocyte-derived dendritic cells and plasmacytoid dendritic cells. Immunobiology. 2004;209(1-2):199-207.

446. Vitale C, Romagnani C, Falco M, Ponte M, Vitale M, Moretta A, et al. Engagement of p75/AIRM1 or CD33 inhibits the proliferation of normal or leukemic myeloid cells. Proc Natl Acad Sci U S A. 1999;96(26):15091-6.

447. Ferlazzo G, Spaggiari GM, Semino C, Melioli G, Moretta L. Engagement of CD33 surface molecules prevents the generation of dendritic cells from both monocytes and CD34+ myeloid precursors. Eur J Immunol. 2000;30(3):827-33.

448. Vitale C, Romagnani C, Puccetti A, Olive D, Costello R, Chiossone L, et al. Surface expression and function of p75/AIRM-1 or CD33 in acute myeloid leukemias: engagement of CD33 induces apoptosis of leukemic cells. Proc Natl Acad Sci U S A. 2001;98(10):5764-9.

449. Nguyen DH, Ball ED, Varki A. Myeloid precursors and acute myeloid leukemia cells express multiple CD33-related Siglecs. Exp Hematol. 2006;34(6):728-35.

450. Hernandez-Caselles T, Martinez-Esparza M, Perez-Oliva AB, Quintanilla-Cecconi AM, Garcia-Alonso A, Alvarez-Lopez DM, et al. A study of CD33 (SIGLEC-3) antigen expression and function on activated human T and NK cells: two isoforms of CD33 are generated by alternative splicing. J Leukoc Biol. 2006;79(1):46-58.

451. Perez-Oliva AB, Martinez-Esparza M, Vicente-Fernandez JJ, Corral-San Miguel R, Garcia-Penarrubia P, Hernandez-Caselles T. Epitope mapping, expression and post-translational modifications of two isoforms of CD33 (CD33M and CD33m) on lymphoid and myeloid human cells. Glycobiology. 2011;21(6):757-70.

452. Siddiqui SS, Springer SA, Verhagen A, Sundaramurthy V, Alisson-Silva F, Jiang W, et al. The Alzheimer's disease-protective CD33 splice variant mediates adaptive loss of function via diversion to an intracellular pool. J Biol Chem. 2017;292(37):15312-20.

453. Saha S, Siddiqui SS, Khan N, Verhagen A, Jiang W, Springer S, et al. Controversies about the subcellular localization and mechanisms of action of the Alzheimer's disease-protective CD33 splice variant. Acta Neuropathol. 2019;138(4):671-2.

454. Bhattacherjee A, Jung J, Zia S, Ho M, Eskandari-Sedighi G, St Laurent CD, et al. The CD33 short isoform is a gain-of-function variant that enhances Abeta1-42 phagocytosis in microglia. Mol Neurodegener. 2021;16(1):19.

455. Ann Butler C, Thornton P, Charles Brown G. CD33M inhibits microglial phagocytosis, migration and proliferation, but the Alzheimer's disease-protective variant CD33m stimulates phagocytosis and proliferation, and inhibits adhesion. J Neurochem. 2021;158(2):297-310.

456. Lajaunias F, Dayer JM, Chizzolini C. Constitutive repressor activity of CD33 on human monocytes requires sialic acid recognition and phosphoinositide 3-kinase-mediated intracellular signaling. Eur J Immunol. 2005;35(1):243-51.

457. Orr SJ, Morgan NM, Elliott J, Burrows JF, Scott CJ, McVicar DW, et al. CD33 responses are blocked by SOCS3 through accelerated proteasomal-mediated turnover. Blood. 2007;109(3):1061-8.

458. Walter RB, Raden BW, Zeng R, Hausermann P, Bernstein ID, Cooper JA. ITIM-dependent endocytosis of CD33-related Siglecs: role of intracellular domain, tyrosine phosphorylation, and the tyrosine phosphatases, Shp1 and Shp2. J Leukoc Biol. 2008;83(1):200-11.

459. Walter RB, Hausermann P, Raden BW, Teckchandani AM, Kamikura DM, Bernstein ID, et al. Phosphorylated ITIMs enable ubiquitylation of an inhibitory cell surface receptor. Traffic. 2008;9(2):267-79.

460. Suzuki A, Hanada T, Mitsuyama K, Yoshida T, Kamizono S, Hoshino T, et al. CIS3/SOCS3/SSI3 plays a negative regulatory role in STAT3 activation and intestinal inflammation. J Exp Med. 2001;193(4):471-81.

461. Wong PK, Egan PJ, Croker BA, O'Donnell K, Sims NA, Drake S, et al. SOCS-3 negatively regulates innate and adaptive immune mechanisms in acute IL-1-dependent inflammatory arthritis. J Clin Invest. 2006;116(6):1571-81.

462. Born GV, Palinski W. Unusually high concentrations of sialic acids on the surface of vascular endothelia. Br J Exp Pathol. 1985;66(5):543-9.

463. Groux-Degroote S, Krzewinski-Recchi MA, Cazet A, Vincent A, Lehoux S, Lafitte JJ, et al. IL-6 and IL-8 increase the expression of glycosyltransferases and sulfotransferases involved in the biosynthesis of sialylated and/or sulfated Lewisx epitopes in the human bronchial mucosa. Biochem J. 2008;410(1):213-23.

464. Huet G, Kim I, de Bolos C, Lo-Guidice JM, Moreau O, Hemon B, et al. Characterization of mucins and proteoglycans synthesized by a mucin-secreting HT-29 cell subpopulation. J Cell Sci. 1995;108 (Pt 3):1275-85.

465. Lievin-Le Moal V, Servin AL, Coconnier-Polter MH. The increase in mucin exocytosis and the upregulation of MUC genes encoding for membrane-bound mucins induced by the thiol-activated exotoxin listeriolysin O is a host cell defence response that inhibits the cell-entry of Listeria monocytogenes. Cell Microbiol. 2005;7(7):1035-48.

466. Ogasawara Y, Namai T, Yoshino F, Lee MC, Ishii K. Sialic acid is an essential moiety of mucin as a hydroxyl radical scavenger. FEBS Lett. 2007;581(13):2473-7.

467. Huang YL, Chassard C, Hausmann M, von Itzstein M, Hennet T. Sialic acid catabolism drives intestinal inflammation and microbial dysbiosis in mice. Nat Commun. 2015;6:8141.

468. Fuhrer A, Sprenger N, Kurakevich E, Borsig L, Chassard C, Hennet T. Milk sialyllactose influences colitis in mice through selective intestinal bacterial colonization. J Exp Med. 2010;207(13):2843-54.

469. Kurakevich E, Hennet T, Hausmann M, Rogler G, Borsig L. Milk oligosaccharide sialyl(alpha2,3)lactose activates intestinal CD11c+ cells through TLR4. Proc Natl Acad Sci U S A. 2013;110(43):17444-9.

470. Ha SH, Kwak CH, Park JY, Abekura F, Lee YC, Kim JS, et al. 3'-sialyllactose targets cell surface protein, SIGLEC-3, and induces megakaryocyte differentiation and apoptosis by lipid raft-dependent endocytosis. Glycoconj J. 2020;37(2):187-200.

471. Chang YC, Nizet V. The interplay between Siglecs and sialylated pathogens. Glycobiology. 2014;24(9):818-25.

472. Avril T, Wagner ER, Willison HJ, Crocker PR. Sialic acid-binding immunoglobulin-like lectin 7 mediates selective recognition of sialylated glycans expressed on Campylobacter jejuni lipooligosaccharides. Infect Immun. 2006;74(7):4133-41.

473. Jones C, Virji M, Crocker PR. Recognition of sialylated meningococcal lipopolysaccharide by siglecs expressed on myeloid cells leads to enhanced bacterial uptake. Mol Microbiol. 2003;49(5):1213-25.

474. Khatua B, Ghoshal A, Bhattacharya K, Mandal C, Saha B, Crocker PR, et al. Sialic acids acquired by Pseudomonas aeruginosa are involved in reduced complement deposition and siglec mediated host-cell recognition. FEBS Lett. 2010;584(3):555-61.

475. Vogel U, Hammerschmidt S, Frosch M. Sialic acids of both the capsule and the sialylated lipooligosaccharide of Neisseria meningitis serogroup B are prerequisites for virulence of meningococci in the infant rat. Med Microbiol Immunol. 1996;185(2):81-7.

476. Carlin AF, Uchiyama S, Chang YC, Lewis AL, Nizet V, Varki A. Molecular mimicry of host sialylated glycans allows a bacterial pathogen to engage neutrophil Siglec-9 and dampen the innate immune response. Blood. 2009;113(14):3333-6.

477. Chang YC, Olson J, Beasley FC, Tung C, Zhang J, Crocker PR, et al. Group B Streptococcus engages an inhibitory Siglec through sialic acid mimicry to blunt innate immune and inflammatory responses in vivo. PLoS Pathog. 2014;10(1):e1003846.

478. Rodrigues E, Macauley MS. Hypersialylation in Cancer: Modulation of Inflammation and Therapeutic Opportunities. Cancers (Basel). 2018;10(6).

479. Heneka MT, Carson MJ, El Khoury J, Landreth GE, Brosseron F, Feinstein DL, et al. Neuroinflammation in Alzheimer's disease. Lancet Neurol. 2015;14(4):388-405.

480. Heneka MT, Kummer MP, Latz E. Innate immune activation in neurodegenerative disease. Nat Rev Immunol. 2014;14(7):463-77.

481. Griciuc A, Serrano-Pozo A, Parrado AR, Lesinski AN, Asselin CN, Mullin K, et al. Alzheimer's disease risk gene CD33 inhibits microglial uptake of amyloid beta. Neuron. 2013;78(4):631-43.

482. Duan S, Koziol-White CJ, Jester WF, Jr., Smith SA, Nycholat CM, Macauley MS, et al. CD33 recruitment inhibits IgE-mediated anaphylaxis and desensitizes mast cells to allergen. J Clin Invest. 2019;129(3):1387-401.

483. Chen X, Eksioglu EA, Zhou J, Zhang L, Djeu J, Fortenbery N, et al. Induction of myelodysplasia by myeloid-derived suppressor cells. J Clin Invest. 2013;123(11):4595-611.

484. Laszlo GS, Harrington KH, Gudgeon CJ, Beddoe ME, Fitzgibbon MP, Ries RE, et al. Expression and functional characterization of CD33 transcript variants in human acute myeloid leukemia. Oncotarget. 2016;7(28):43281-94.

485. Bross PF, Beitz J, Chen G, Chen XH, Duffy E, Kieffer L, et al. Approval summary: gemtuzumab ozogamicin in relapsed acute myeloid leukemia. Clin Cancer Res. 2001;7(6):1490-6.

486. Larson RA, Boogaerts M, Estey E, Karanes C, Stadtmauer EA, Sievers EL, et al. Antibody-targeted chemotherapy of older patients with acute myeloid leukemia in first relapse using Mylotarg (gemtuzumab ozogamicin). Leukemia. 2002;16(9):1627-36.

487. Taussig DC, Pearce DJ, Simpson C, Rohatiner AZ, Lister TA, Kelly G, et al. Hematopoietic stem cells express multiple myeloid markers: implications for the origin and targeted therapy of acute myeloid leukemia. Blood. 2005;106(13):4086-92.

488. Long JM, Holtzman DM. Alzheimer Disease: An Update on Pathobiology and Treatment Strategies. Cell. 2019;179(2):312-39.

489. Bertram L, Lange C, Mullin K, Parkinson M, Hsiao M, Hogan MF, et al. Genome-wide association analysis reveals putative Alzheimer's disease susceptibility loci in addition to APOE. Am J Hum Genet. 2008;83(5):623-32.

490. Naj AC, Jun G, Beecham GW, Wang LS, Vardarajan BN, Buros J, et al. Common variants at MS4A4/MS4A6E, CD2AP, CD33 and EPHA1 are associated with late-onset Alzheimer's disease. Nat Genet. 2011;43(5):436-41.

491. Hollingworth P, Harold D, Sims R, Gerrish A, Lambert JC, Carrasquillo MM, et al. Common variants at ABCA7, MS4A6A/MS4A4E, EPHA1, CD33 and CD2AP are associated with Alzheimer's disease. Nat Genet. 2011;43(5):429-35.

492. Griciuc A, Tanzi RE. The role of innate immune genes in Alzheimer's disease. Curr Opin Neurol. 2021;34(2):228-36.

493. Halle A, Hornung V, Petzold GC, Stewart CR, Monks BG, Reinheckel T, et al. The NALP3 inflammasome is involved in the innate immune response to amyloid-beta. Nat Immunol. 2008;9(8):857-65.

494. Heneka MT, Kummer MP, Stutz A, Delekate A, Schwartz S, Vieira-Saecker A, et al. NLRP3 is activated in Alzheimer's disease and contributes to pathology in APP/PS1 mice. Nature. 2013;493(7434):674-8.

495. Wissfeld J, Nozaki I, Mathews M, Raschka T, Ebeling C, Hornung V, et al. Deletion of Alzheimer's disease-associated CD33 results in an inflammatory human microglia phenotype. Glia. 2021;69(6):1393-412.

496. Aguzzi A, Barres BA, Bennett ML. Microglia: scapegoat, saboteur, or something else? Science. 2013;339(6116):156-61.

497. Raj T, Ryan KJ, Replogle JM, Chibnik LB, Rosenkrantz L, Tang A, et al. CD33: increased inclusion of exon 2 implicates the Ig V-set domain in Alzheimer's disease susceptibility. Hum Mol Genet. 2014;23(10):2729-36.

498. Malik M, Simpson JF, Parikh I, Wilfred BR, Fardo DW, Nelson PT, et al. CD33 Alzheimer's risk-altering polymorphism, CD33 expression, and exon 2 splicing. J Neurosci. 2013;33(33):13320-5.

499. Papageorgiou I, Loken MR, Brodersen LE, Gbadamosi M, Uy GL, Meshinchi S, et al. CCGG deletion (rs201074739) in CD33 results in premature termination codon and complete loss

of CD33 expression: another key variant with potential impact on response to CD33-directed agents. Leuk Lymphoma. 2019;60(9):2287-90.

500. Griciuc A, Federico AN, Natasan J, Forte AM, McGinty D, Nguyen H, et al. Gene therapy for Alzheimer's disease targeting CD33 reduces amyloid beta accumulation and neuroinflammation. Hum Mol Genet. 2020;29(17):2920-35.

501. Holgate ST, Polosa R. Treatment strategies for allergy and asthma. Nat Rev Immunol. 2008;8(3):218-30.

502. Shade KC, Conroy ME, Washburn N, Kitaoka M, Huynh DJ, Laprise E, et al. Sialylation of immunoglobulin E is a determinant of allergic pathogenicity. Nature. 2020;582(7811):265-70.

503. Nimer SD. Myelodysplastic syndromes. Blood. 2008;111(10):4841-51.

504. Tefferi A, Vardiman JW. Myelodysplastic syndromes. N Engl J Med. 2009;361(19):1872-85.

505. Rollison DE, Howlader N, Smith MT, Strom SS, Merritt WD, Ries LA, et al. Epidemiology of myelodysplastic syndromes and chronic myeloproliferative disorders in the United States, 2001-2004, using data from the NAACCR and SEER programs. Blood. 2008;112(1):45-52.

506. Veglia F, Sanseviero E, Gabrilovich DI. Myeloid-derived suppressor cells in the era of increasing myeloid cell diversity. Nat Rev Immunol. 2021;21(8):485-98.

507. Kontaki E, Boumpas DT, Tzardi M, Mouzas IA, Papadakis KA, Verginis P. Aberrant function of myeloid-derived suppressor cells (MDSCs) in experimental colitis and in inflammatory bowel disease (IBD) immune responses. Autoimmunity. 2017;50(3):170-81.

508. Wang S, Song R, Wang Z, Jing Z, Wang S, Ma J. S100A8/A9 in Inflammation. Front Immunol. 2018;9:1298.

509. Edgeworth J, Gorman M, Bennett R, Freemont P, Hogg N. Identification of p8,14 as a highly abundant heterodimeric calcium binding protein complex of myeloid cells. J Biol Chem. 1991;266(12):7706-13.

510. Roseth AG, Schmidt PN, Fagerhol MK. Correlation between faecal excretion of indium-111-labelled granulocytes and calprotectin, a granulocyte marker protein, in patients with inflammatory bowel disease. Scand J Gastroenterol. 1999;34(1):50-4.

511. Tibble J, Teahon K, Thjodleifsson B, Roseth A, Sigthorsson G, Bridger S, et al. A simple method for assessing intestinal inflammation in Crohn's disease. Gut. 2000;47(4):506-13.

512. Kummer MP, Vogl T, Axt D, Griep A, Vieira-Saecker A, Jessen F, et al. Mrp14 deficiency ameliorates amyloid beta burden by increasing microglial phagocytosis and modulation of amyloid precursor protein processing. J Neurosci. 2012;32(49):17824-9.

513. Shepherd CE, Goyette J, Utter V, Rahimi F, Yang Z, Geczy CL, et al. Inflammatory S100A9 and S100A12 proteins in Alzheimer's disease. Neurobiol Aging. 2006;27(11):1554-63.

514. Benedyk M, Sopalla C, Nacken W, Bode G, Melkonyan H, Banfi B, et al. HaCaT keratinocytes overexpressing the S100 proteins S100A8 and S100A9 show increased NADPH oxidase and NF-kappaB activities. J Invest Dermatol. 2007;127(8):2001-11.

515. Roth J, Burwinkel F, van den Bos C, Goebeler M, Vollmer E, Sorg C. MRP8 and MRP14, S-100-like proteins associated with myeloid differentiation, are translocated to plasma membrane and intermediate filaments in a calcium-dependent manner. Blood. 1993;82(6):1875-83.

516. Vogl T, Ludwig S, Goebeler M, Strey A, Thorey IS, Reichelt R, et al. MRP8 and MRP14 control microtubule reorganization during transendothelial migration of phagocytes. Blood. 2004;104(13):4260-8.

517. Ghavami S, Rashedi I, Dattilo BM, Eshraghi M, Chazin WJ, Hashemi M, et al. S100A8/A9 at low concentration promotes tumor cell growth via RAGE ligation and MAP kinase-dependent pathway. J Leukoc Biol. 2008;83(6):1484-92.

518. Lackmann M, Rajasekariah P, Iismaa SE, Jones G, Cornish CJ, Hu S, et al. Identification of a chemotactic domain of the pro-inflammatory S100 protein CP-10. J Immunol. 1993;150(7):2981-91.

519. Laouedj M, Tardif MR, Gil L, Raquil MA, Lachhab A, Pelletier M, et al. S100A9 induces differentiation of acute myeloid leukemia cells through TLR4. Blood. 2017;129(14):1980-90.

520. Low D, Subramaniam R, Lin L, Aomatsu T, Mizoguchi A, Ng A, et al. Chitinase 3-like 1 induces survival and proliferation of intestinal epithelial cells during chronic inflammation and colitis-associated cancer by regulating S100A9. Oncotarget. 2015;6(34):36535-50.

521. Ma L, Sun P, Zhang JC, Zhang Q, Yao SL. Proinflammatory effects of S100A8/A9 via TLR4 and RAGE signaling pathways in BV-2 microglial cells. Int J Mol Med. 2017;40(1):31-8.

522. Simard JC, Noel C, Tessier PA, Girard D. Human S100A9 potentiates IL-8 production in response to GM-CSF or fMLP via activation of a different set of transcription factors in neutrophils. FEBS Lett. 2014;588(13):2141-6.

523. Yui S, Mikami M, Tsurumaki K, Yamazaki M. Growth-inhibitory and apoptosis-inducing activities of calprotectin derived from inflammatory exudate cells on normal fibroblasts: regulation by metal ions. J Leukoc Biol. 1997;61(1):50-7.

524. Basiorka AA, McGraw KL, Eksioglu EA, Chen X, Johnson J, Zhang L, et al. The NLRP3 inflammasome functions as a driver of the myelodysplastic syndrome phenotype. Blood. 2016;128(25):2960-75.

525. Zhao Y, Wu X, Li X, Jiang LL, Gui X, Liu Y, et al. TREM2 Is a Receptor for beta-Amyloid that Mediates Microglial Function. Neuron. 2018;97(5):1023-31 e7.

526. N'Diaye EN, Branda CS, Branda SS, Nevarez L, Colonna M, Lowell C, et al. TREM-2 (triggering receptor expressed on myeloid cells 2) is a phagocytic receptor for bacteria. J Cell Biol. 2009;184(2):215-23.

527. Filipello F, Morini R, Corradini I, Zerbi V, Canzi A, Michalski B, et al. The Microglial Innate Immune Receptor TREM2 Is Required for Synapse Elimination and Normal Brain Connectivity. Immunity. 2018;48(5):979-91 e8.

528. Turnbull IR, Colonna M. Activating and inhibitory functions of DAP12. Nat Rev Immunol. 2007;7(2):155-61.

529. Konishi H, Kiyama H. Microglial TREM2/DAP12 Signaling: A Double-Edged Sword in Neural Diseases. Front Cell Neurosci. 2018;12:206.

530. Turnbull IR, Gilfillan S, Cella M, Aoshi T, Miller M, Piccio L, et al. Cutting edge: TREM-2 attenuates macrophage activation. J Immunol. 2006;177(6):3520-4.

531. Li JT, Zhang Y. TREM2 regulates innate immunity in Alzheimer's disease. J Neuroinflammation. 2018;15(1):107.

532. Bouchon A, Dietrich J, Colonna M. Cutting edge: inflammatory responses can be triggered by TREM-1, a novel receptor expressed on neutrophils and monocytes. J Immunol. 2000;164(10):4991-5.

533. Bouchon A, Hernandez-Munain C, Cella M, Colonna M. A DAP12-mediated pathway regulates expression of CC chemokine receptor 7 and maturation of human dendritic cells. J Exp Med. 2001;194(8):1111-22.

534. Lanier LL, Corliss BC, Wu J, Leong C, Phillips JH. Immunoreceptor DAP12 bearing a tyrosine-based activation motif is involved in activating NK cells. Nature. 1998;391(6668):703-7.

535. Feng J, Call ME, Wucherpfennig KW. The assembly of diverse immune receptors is focused on a polar membrane-embedded interaction site. PLoS Biol. 2006;4(5):e142.

536. Angata T, Hayakawa T, Yamanaka M, Varki A, Nakamura M. Discovery of Siglec-14, a novel sialic acid receptor undergoing concerted evolution with Siglec-5 in primates. FASEB J. 2006;20(12):1964-73.

537. Schlepckow K, Kleinberger G, Fukumori A, Feederle R, Lichtenthaler SF, Steiner H, et al. An Alzheimer-associated TREM2 variant occurs at the ADAM cleavage site and affects shedding and phagocytic function. EMBO Mol Med. 2017;9(10):1356-65.

538. Mocsai A, Humphrey MB, Van Ziffle JA, Hu Y, Burghardt A, Spusta SC, et al. The immunomodulatory adapter proteins DAP12 and Fc receptor gamma-chain (FcRgamma) regulate development of functional osteoclasts through the Syk tyrosine kinase. Proc Natl Acad Sci U S A. 2004;101(16):6158-63.

539. Peng Q, Malhotra S, Torchia JA, Kerr WG, Coggeshall KM, Humphrey MB. TREM2- and DAP12-dependent activation of PI3K requires DAP10 and is inhibited by SHIP1. Sci Signal. 2010;3(122):ra38.

540. Takahashi K, Rochford CD, Neumann H. Clearance of apoptotic neurons without inflammation by microglial triggering receptor expressed on myeloid cells-2. J Exp Med. 2005;201(4):647-57.

541. Zou W, Reeve JL, Liu Y, Teitelbaum SL, Ross FP. DAP12 couples c-Fms activation to the osteoclast cytoskeleton by recruitment of Syk. Mol Cell. 2008;31(3):422-31.

542. Zhang W, Trible RP, Zhu M, Liu SK, McGlade CJ, Samelson LE. Association of Grb2, Gads, and phospholipase C-gamma 1 with phosphorylated LAT tyrosine residues. Effect of LAT tyrosine mutations on T cell angigen receptor-mediated signaling. J Biol Chem. 2000;275(30):23355-61.

543. Jiang K, Zhong B, Gilvary DL, Corliss BC, Vivier E, Hong-Geller E, et al. Syk regulation of phosphoinositide 3-kinase-dependent NK cell function. J Immunol. 2002;168(7):3155-64.

544. Paz PE, Wang S, Clarke H, Lu X, Stokoe D, Abo A. Mapping the Zap-70 phosphorylation sites on LAT (linker for activation of T cells) required for recruitment and activation of signalling proteins in T cells. Biochem J. 2001;356(Pt 2):461-71.

545. Shim EK, Jung SH, Lee JR. Role of two adaptor molecules SLP-76 and LAT in the PI3K signaling pathway in activated T cells. J Immunol. 2011;186(5):2926-35.

546. Bilal MY, Houtman JC. GRB2 Nucleates T Cell Receptor-Mediated LAT Clusters That Control PLC-gamma1 Activation and Cytokine Production. Front Immunol. 2015;6:141.

547. Fischer KD, Kong YY, Nishina H, Tedford K, Marengere LE, Kozieradzki I, et al. Vav is a regulator of cytoskeletal reorganization mediated by the T-cell receptor. Curr Biol. 1998;8(10):554-62.

548. Jay TR, Miller CM, Cheng PJ, Graham LC, Bemiller S, Broihier ML, et al. TREM2 deficiency eliminates TREM2+ inflammatory macrophages and ameliorates pathology in Alzheimer's disease mouse models. J Exp Med. 2015;212(3):287-95.

549. Mazaheri F, Snaidero N, Kleinberger G, Madore C, Daria A, Werner G, et al. TREM2 deficiency impairs chemotaxis and microglial responses to neuronal injury. EMBO Rep. 2017;18(7):1186-98.

550. Otero K, Turnbull IR, Poliani PL, Vermi W, Cerutti E, Aoshi T, et al. Macrophage colony-stimulating factor induces the proliferation and survival of macrophages via a pathway involving DAP12 and beta-catenin. Nat Immunol. 2009;10(7):734-43.

551. Kagan JC, Medzhitov R. Phosphoinositide-mediated adaptor recruitment controls Toll-like receptor signaling. Cell. 2006;125(5):943-55.

552. Hamerman JA, Jarjoura JR, Humphrey MB, Nakamura MC, Seaman WE, Lanier LL. Cutting edge: inhibition of TLR and FcR responses in macrophages by triggering receptor expressed on myeloid cells (TREM)-2 and DAP12. J Immunol. 2006;177(4):2051-5.

553. Feuerbach D, Schindler P, Barske C, Joller S, Beng-Louka E, Worringer KA, et al. ADAM17 is the main sheddase for the generation of human triggering receptor expressed in myeloid cells (hTREM2) ectodomain and cleaves TREM2 after Histidine 157. Neurosci Lett. 2017;660:109-14.

554. Zhong L, Chen XF, Wang T, Wang Z, Liao C, Wang Z, et al. Soluble TREM2 induces inflammatory responses and enhances microglial survival. J Exp Med. 2017;214(3):597-607.

555. Wunderlich P, Glebov K, Kemmerling N, Tien NT, Neumann H, Walter J. Sequential proteolytic processing of the triggering receptor expressed on myeloid cells-2 (TREM2) protein by ectodomain shedding and gamma-secretase-dependent intramembranous cleavage. J Biol Chem. 2013;288(46):33027-36.

556. Piccio L, Deming Y, Del-Aguila JL, Ghezzi L, Holtzman DM, Fagan AM, et al. Cerebrospinal fluid soluble TREM2 is higher in Alzheimer disease and associated with mutation status. Acta Neuropathol. 2016;131(6):925-33.

557. Henjum K, Almdahl IS, Arskog V, Minthon L, Hansson O, Fladby T, et al. Cerebrospinal fluid soluble TREM2 in aging and Alzheimer's disease. Alzheimers Res Ther. 2016;8(1):17.

558. Suarez-Calvet M, Kleinberger G, Araque Caballero MA, Brendel M, Rominger A, Alcolea D, et al. sTREM2 cerebrospinal fluid levels are a potential biomarker for microglia activity in early-stage Alzheimer's disease and associate with neuronal injury markers. EMBO Mol Med. 2016;8(5):466-76.

559. Kleinberger G, Brendel M, Mracsko E, Wefers B, Groeneweg L, Xiang X, et al. The FTD-like syndrome causing TREM2 T66M mutation impairs microglia function, brain perfusion, and glucose metabolism. EMBO J. 2017;36(13):1837-53.

560. Lawson LJ, Perry VH, Gordon S. Turnover of resident microglia in the normal adult mouse brain. Neuroscience. 1992;48(2):405-15.

561. Fellner L, Irschick R, Schanda K, Reindl M, Klimaschewski L, Poewe W, et al. Toll-like receptor 4 is required for alpha-synuclein dependent activation of microglia and astroglia. Glia. 2013;61(3):349-60.

562. Jin JJ, Kim HD, Maxwell JA, Li L, Fukuchi K. Toll-like receptor 4-dependent upregulation of cytokines in a transgenic mouse model of Alzheimer's disease. J Neuroinflammation. 2008;5:23.

563. Udan ML, Ajit D, Crouse NR, Nichols MR. Toll-like receptors 2 and 4 mediate Abeta(1-42) activation of the innate immune response in a human monocytic cell line. J Neurochem. 2008;104(2):524-33.

564. Vom Berg J, Prokop S, Miller KR, Obst J, Kalin RE, Lopategui-Cabezas I, et al. Inhibition of IL-12/IL-23 signaling reduces Alzheimer's disease-like pathology and cognitive decline. Nat Med. 2012;18(12):1812-9.

565. Liu Y, Walter S, Stagi M, Cherny D, Letiembre M, Schulz-Schaeffer W, et al. LPS receptor (CD14): a receptor for phagocytosis of Alzheimer's amyloid peptide. Brain. 2005;128(Pt 8):1778-89.

566. Paresce DM, Ghosh RN, Maxfield FR. Microglial cells internalize aggregates of the Alzheimer's disease amyloid beta-protein via a scavenger receptor. Neuron. 1996;17(3):553-65.

567. Mawuenyega KG, Sigurdson W, Ovod V, Munsell L, Kasten T, Morris JC, et al. Decreased clearance of CNS beta-amyloid in Alzheimer's disease. Science. 2010;330(6012):1774.

568. Paloneva J, Kestila M, Wu J, Salminen A, Bohling T, Ruotsalainen V, et al. Loss-of-function mutations in TYROBP (DAP12) result in a presenile dementia with bone cysts. Nat Genet. 2000;25(3):357-61.

569. Paloneva J, Manninen T, Christman G, Hovanes K, Mandelin J, Adolfsson R, et al. Mutations in two genes encoding different subunits of a receptor signaling complex result in an identical disease phenotype. Am J Hum Genet. 2002;71(3):656-62.

570. Paloneva J, Autti T, Raininko R, Partanen J, Salonen O, Puranen M, et al. CNS manifestations of Nasu-Hakola disease: a frontal dementia with bone cysts. Neurology. 2001;56(11):1552-8.

571. Paloneva J, Mandelin J, Kiialainen A, Bohling T, Prudlo J, Hakola P, et al. DAP12/TREM2 deficiency results in impaired osteoclast differentiation and osteoporotic features. J Exp Med. 2003;198(4):669-75.

572. Bianchin MM, Martin KC, de Souza AC, de Oliveira MA, Rieder CR. Nasu-Hakola disease and primary microglial dysfunction. Nat Rev Neurol. 2010;6(9):2 p following 523.

573. Kiialainen A, Hovanes K, Paloneva J, Kopra O, Peltonen L. Dap12 and Trem2, molecules involved in innate immunity and neurodegeneration, are co-expressed in the CNS. Neurobiol Dis. 2005;18(2):314-22.

574. Guerreiro RJ, Lohmann E, Bras JM, Gibbs JR, Rohrer JD, Gurunlian N, et al. Using exome sequencing to reveal mutations in TREM2 presenting as a frontotemporal dementia-like syndrome without bone involvement. JAMA Neurol. 2013;70(1):78-84.

575. Kleinberger G, Yamanishi Y, Suarez-Calvet M, Czirr E, Lohmann E, Cuyvers E, et al. TREM2 mutations implicated in neurodegeneration impair cell surface transport and phagocytosis. Sci Transl Med. 2014;6(243):243ra86.

576. Guerreiro R, Wojtas A, Bras J, Carrasquillo M, Rogaeva E, Majounie E, et al. TREM2 variants in Alzheimer's disease. N Engl J Med. 2013;368(2):117-27.

577. Magno L, Bunney TD, Mead E, Svensson F, Bictash MN. TREM2/PLCgamma2 signalling in immune cells: function, structural insight, and potential therapeutic modulation. Mol Neurodegener. 2021;16(1):22.

578. Wang Y, Cella M, Mallinson K, Ulrich JD, Young KL, Robinette ML, et al. TREM2 lipid sensing sustains the microglial response in an Alzheimer's disease model. Cell. 2015;160(6):1061-71.

579. Tanzi RE. TREM2 and Risk of Alzheimer's Disease--Friend or Foe? N Engl J Med. 2015;372(26):2564-5.

580. Correale C, Genua M, Vetrano S, Mazzini E, Martinoli C, Spinelli A, et al. Bacterial sensor triggering receptor expressed on myeloid cells-2 regulates the mucosal inflammatory response. Gastroenterology. 2013;144(2):346-56 e3.

581. Genua M, Rutella S, Correale C, Danese S. The triggering receptor expressed on myeloid cells (TREM) in inflammatory bowel disease pathogenesis. J Transl Med. 2014;12:293.

582. Seno H, Miyoshi H, Brown SL, Geske MJ, Colonna M, Stappenbeck TS. Efficient colonic mucosal wound repair requires Trem2 signaling. Proc Natl Acad Sci U S A. 2009;106(1):256-61.

583. Chan G, White CC, Winn PA, Cimpean M, Replogle JM, Glick LR, et al. CD33 modulates TREM2: convergence of Alzheimer loci. Nat Neurosci. 2015;18(11):1556-8.

584. Griciuc A, Patel S, Federico AN, Choi SH, Innes BJ, Oram MK, et al. TREM2 Acts Downstream of CD33 in Modulating Microglial Pathology in Alzheimer's Disease. Neuron. 2019;103(5):820-35 e7.

585. Malik M, Parikh I, Vasquez JB, Smith C, Tai L, Bu G, et al. Genetics ignite focus on microglial inflammation in Alzheimer's disease. Mol Neurodegener. 2015;10:52.

586. Wang L, Aschenbrenner D, Zeng Z, Cao X, Mayr D, Mehta M, et al. Gain-of-function variants in SYK cause immune dysregulation and systemic inflammation in humans and mice. Nat Genet. 2021;53(4):500-10.

587. Wang D, Feng J, Wen R, Marine JC, Sangster MY, Parganas E, et al. Phospholipase Cgamma2 is essential in the functions of B cell and several Fc receptors. Immunity. 2000;13(1):25-35.

588. Martin-Nalda A, Fortuny C, Rey L, Bunney TD, Alsina L, Esteve-Sole A, et al. Severe Autoinflammatory Manifestations and Antibody Deficiency Due to Novel Hypermorphic PLCG2 Mutations. J Clin Immunol. 2020;40(7):987-1000.

589. Ombrello MJ, Remmers EF, Sun G, Freeman AF, Datta S, Torabi-Parizi P, et al. Cold urticaria, immunodeficiency, and autoimmunity related to PLCG2 deletions. N Engl J Med. 2012;366(4):330-8.

590. Chae JJ, Park YH, Park C, Hwang IY, Hoffmann P, Kehrl JH, et al. Connecting two pathways through Ca 2+ signaling: NLRP3 inflammasome activation induced by a hypermorphic PLCG2 mutation. Arthritis Rheumatol. 2015;67(2):563-7.

591. Gattorno M, Martini A. Beyond the NLRP3 inflammasome: autoinflammatory diseases reach adolescence. Arthritis Rheum. 2013;65(5):1137-47.

592. Aki D, Minoda Y, Yoshida H, Watanabe S, Yoshida R, Takaesu G, et al. Peptidoglycan and lipopolysaccharide activate PLCgamma2, leading to enhanced cytokine production in macrophages and dendritic cells. Genes Cells. 2008;13(2):199-208.

593. LaPorte SL, Juo ZS, Vaclavikova J, Colf LA, Qi X, Heller NM, et al. Molecular and structural basis of cytokine receptor pleiotropy in the interleukin-4/13 system. Cell. 2008;132(2):259-72.

594. Ring AM, Lin JX, Feng D, Mitra S, Rickert M, Bowman GR, et al. Mechanistic and structural insight into the functional dichotomy between IL-2 and IL-15. Nat Immunol. 2012;13(12):1187-95.

595. Wang X, Rickert M, Garcia KC. Structure of the quaternary complex of interleukin-2 with its alpha, beta, and gammac receptors. Science. 2005;310(5751):1159-63.

596. Ran FA, Hsu PD, Wright J, Agarwala V, Scott DA, Zhang F. Genome engineering using the CRISPR-Cas9 system. Nat Protoc. 2013;8(11):2281-308.

597. Yanagimachi MD, Niwa A, Tanaka T, Honda-Ozaki F, Nishimoto S, Murata Y, et al. Robust and highly-efficient differentiation of functional monocytic cells from human pluripotent stem cells under serum- and feeder cell-free conditions. PLoS One. 2013;8(4):e59243.

598. Niwa A, Heike T, Umeda K, Oshima K, Kato I, Sakai H, et al. A novel serum-free monolayer culture for orderly hematopoietic differentiation of human pluripotent cells via mesodermal progenitors. PLoS One. 2011;6(7):e22261.

599. Cormack B. Directed mutagenesis using the polymerase chain reaction. Curr Protoc Mol Biol. 2001;Chapter 8:Unit8 5.

600. Rapino F, Robles EF, Richter-Larrea JA, Kallin EM, Martinez-Climent JA, Graf T. C/EBPalpha induces highly efficient macrophage transdifferentiation of B lymphoma and leukemia cell lines and impairs their tumorigenicity. Cell Rep. 2013;3(4):1153-63.

601. Gaidt MM, Ebert TS, Chauhan D, Schmidt T, Schmid-Burgk JL, Rapino F, et al. Human Monocytes Engage an Alternative Inflammasome Pathway. Immunity. 2016;44(4):833-46.

602. Cartegni L, Chew SL, Krainer AR. Listening to silence and understanding nonsense: exonic mutations that affect splicing. Nat Rev Genet. 2002;3(4):285-98.

603. Yao H, Coppola K, Schweig JE, Crawford F, Mullan M, Paris D. Distinct Signaling Pathways Regulate TREM2 Phagocytic and NFkappaB Antagonistic Activities. Front Cell Neurosci. 2019;13:457.

604. Loke P, Allison JP. PD-L1 and PD-L2 are differentially regulated by Th1 and Th2 cells. Proc Natl Acad Sci U S A. 2003;100(9):5336-41.

605. Chan A, Scalchunes C, Boyle M, Puck JM. Early vs. delayed diagnosis of severe combined immunodeficiency: a family perspective survey. Clin Immunol. 2011;138(1):3-8.

606. Loeber JG, Platis D, Zetterstrom RH, Almashanu S, Boemer F, Bonham JR, et al. Neonatal Screening in Europe Revisited: An ISNS Perspective on the Current State and Developments Since 2010. Int J Neonatal Screen. 2021;7(1).

607. Matthews DJ, Hibbert L, Friedrich K, Minty A, Callard RE. X-SCID B cell responses to interleukin-4 and interleukin-13 are mediated by a receptor complex that includes the interleukin-4 receptor alpha chain (p140) but not the gamma c chain. Eur J Immunol. 1997;27(1):116-21.

608. Taylor N, Candotti F, Smith S, Oakes SA, Jahn T, Isakov J, et al. Interleukin-4 signaling in B lymphocytes from patients with X-linked severe combined immunodeficiency. J Biol Chem. 1997;272(11):7314-9.

609. McElroy CA, Dohm JA, Walsh ST. Structural and biophysical studies of the human IL-7/IL-7Ralpha complex. Structure. 2009;17(1):54-65.

610. Argudo-Ramirez A, Martin-Nalda A, Marin-Soria JL, Lopez-Galera RM, Pajares-Garcia S, Gonzalez de Aledo-Castillo JM, et al. First Universal Newborn Screening Program for Severe Combined Immunodeficiency in Europe. Two-Years' Experience in Catalonia (Spain). Front Immunol. 2019;10:2406.

611. Barbaro M, Ohlsson A, Borte S, Jonsson S, Zetterstrom RH, King J, et al. Newborn Screening for Severe Primary Immunodeficiency Diseases in Sweden-a 2-Year Pilot TREC and KREC Screening Study. J Clin Immunol. 2017;37(1):51-60.

612. Brown L, Xu-Bayford J, Allwood Z, Slatter M, Cant A, Davies EG, et al. Neonatal diagnosis of severe combined immunodeficiency leads to significantly improved survival outcome: the case for newborn screening. Blood. 2011;117(11):3243-6.

613. Van der Ploeg CPB, Blom M, Bredius RGM, van der Burg M, Schielen P, Verkerk PH, et al. Cost-effectiveness of newborn screening for severe combined immunodeficiency. Eur J Pediatr. 2019;178(5):721-9.

614. Walter RB. Expanding use of CD33-directed immunotherapy. Expert Opin Biol Ther. 2020;20(9):955-8.

615. Wood B. Multicolor immunophenotyping: human immune system hematopoiesis. Methods Cell Biol. 2004;75:559-76.

616. Chen Q, Ye W, Jian Tan W, Mei Yong KS, Liu M, Qi Tan S, et al. Delineation of Natural Killer Cell Differentiation from Myeloid Progenitors in Human. Sci Rep. 2015;5:15118.

617. Sconocchia G, Keyvanfar K, El Ouriaghli F, Grube M, Rezvani K, Fujiwara H, et al. Phenotype and function of a CD56+ peripheral blood monocyte. Leukemia. 2005;19(1):69-76.

618. Takahashi K, Prinz M, Stagi M, Chechneva O, Neumann H. TREM2-transduced myeloid precursors mediate nervous tissue debris clearance and facilitate recovery in an animal model of multiple sclerosis. PLoS Med. 2007;4(4):e124.

619. Piccio L, Buonsanti C, Mariani M, Cella M, Gilfillan S, Cross AH, et al. Blockade of TREM-2 exacerbates experimental autoimmune encephalomyelitis. Eur J Immunol. 2007;37(5):1290-301.

620. Jin SC, Benitez BA, Karch CM, Cooper B, Skorupa T, Carrell D, et al. Coding variants in TREM2 increase risk for Alzheimer's disease. Hum Mol Genet. 2014;23(21):5838-46.

621. Deczkowska A, Weiner A, Amit I. The Physiology, Pathology, and Potential Therapeutic Applications of the TREM2 Signaling Pathway. Cell. 2020;181(6):1207-17.

622. McQuade A, Kang YJ, Hasselmann J, Jairaman A, Sotelo A, Coburn M, et al. Gene expression and functional deficits underlie TREM2-knockout microglia responses in human models of Alzheimer's disease. Nat Commun. 2020;11(1):5370.

623. Ulland TK, Song WM, Huang SC, Ulrich JD, Sergushichev A, Beatty WL, et al. TREM2 Maintains Microglial Metabolic Fitness in Alzheimer's Disease. Cell. 2017;170(4):649-63 e13.

624. Wu K, Byers DE, Jin X, Agapov E, Alexander-Brett J, Patel AC, et al. TREM-2 promotes macrophage survival and lung disease after respiratory viral infection. J Exp Med. 2015;212(5):681-97.

625. Cella M, Buonsanti C, Strader C, Kondo T, Salmaggi A, Colonna M. Impaired differentiation of osteoclasts in TREM-2-deficient individuals. J Exp Med. 2003;198(4):645-51.

626. Cheng B, Li X, Dai K, Duan S, Rong Z, Chen Y, et al. Triggering Receptor Expressed on Myeloid Cells-2 (TREM2) Interacts With Colony-Stimulating Factor 1 Receptor (CSF1R) but Is Not Necessary for CSF1/CSF1R-Mediated Microglial Survival. Front Immunol. 2021;12:633796.

627. Sharif O, Gawish R, Warszawska JM, Martins R, Lakovits K, Hladik A, et al. The triggering receptor expressed on myeloid cells 2 inhibits complement component 1q effector mechanisms and exerts detrimental effects during pneumococcal pneumonia. PLoS Pathog. 2014;10(6):e1004167.

628. Sieber MW, Jaenisch N, Brehm M, Guenther M, Linnartz-Gerlach B, Neumann H, et al. Attenuated inflammatory response in triggering receptor expressed on myeloid cells 2 (TREM2) knock-out mice following stroke. PLoS One. 2013;8(1):e52982.

Apendix A: Permission for reprint of figures

Permission from Springer Nature Customer Service Centre GmbH for reprint of figures from Springer Nature, Journal of Clinical Immunology, Alternative Splicing Rescues Loss of Common Gamma Chain Function and Results in IL-21R-like Deficiency, Illig, D. et al. 2019.[255]

SPRINGER NATURE LICENSE
TERMS AND CONDITIONS

Nov 11, 2021

This Agreement between Mr. David Illig ("You") and Springer Nature ("Springer Nature") consists of your license details and the terms and conditions provided by Springer Nature and Copyright Clearance Center.

License Number	5186020171960
License date	Nov 11, 2021
Licensed Content Publisher	Springer Nature
Licensed Content Publication	Journal of Clinical Immunology
Licensed Content Title	Alternative Splicing Rescues Loss of Common Gamma Chain Function and Results in IL-21R-like Deficiency
Licensed Content Author	David Illig et al
Licensed Content Date	Mar 21, 2019
Type of Use	Thesis/Dissertation
Requestor type	academic/university or research institute
Format	print and electronic
Portion	figures/tables/illustrations
Number of figures/tables /illustrations	4

Will you be translating?	no
Circulation/distribution	500 - 999
Author of this Springer Nature content	yes
Title	Elucidation of novel monogenic disorders in children with intestinal inflammation
Institution name	Ludwig-Maximilians-Universität zu München
Expected presentation date	Nov 2021
Portions	All Figures
Requestor Location	Mr. David Illig Lindwurmstraße 2A Munich, 80337 Germany Attn: Mr. David Illig
Total	0.00 EUR

Terms and Conditions

Springer Nature Customer Service Centre GmbH
Terms and Conditions

This agreement sets out the terms and conditions of the licence (the **Licence**) between you and **Springer Nature Customer Service Centre GmbH** (the **Licensor**). By clicking 'accept' and completing the transaction for the material (**Licensed Material**), you also confirm your acceptance of these terms and conditions.

1. Grant of License

1. 1. The Licensor grants you a personal, non-exclusive, non-transferable, world-wide licence to reproduce the Licensed Material for the purpose specified in your order only. Licences are granted for the specific use requested in the order and for no other

use, subject to the conditions below.

1. 2. The Licensor warrants that it has, to the best of its knowledge, the rights to license reuse of the Licensed Material. However, you should ensure that the material you are requesting is original to the Licensor and does not carry the copyright of another entity (as credited in the published version).

1. 3. If the credit line on any part of the material you have requested indicates that it was reprinted or adapted with permission from another source, then you should also seek permission from that source to reuse the material.

2. Scope of Licence

2. 1. You may only use the Licensed Content in the manner and to the extent permitted by these Ts&Cs and any applicable laws.

2. 2. A separate licence may be required for any additional use of the Licensed Material, e.g. where a licence has been purchased for print only use, separate permission must be obtained for electronic re-use. Similarly, a licence is only valid in the language selected and does not apply for editions in other languages unless additional translation rights have been granted separately in the licence. Any content owned by third parties are expressly excluded from the licence.

2. 3. Similarly, rights for additional components such as custom editions and derivatives require additional permission and may be subject to an additional fee. Please apply to Journalpermissions@springernature.com/bookpermissions@springernature.com for these rights.

2. 4. Where permission has been granted **free of charge** for material in print, permission may also be granted for any electronic version of that work, provided that the material is incidental to your work as a whole and that the electronic version is essentially equivalent to, or substitutes for, the print version.

2. 5. An alternative scope of licence may apply to signatories of the STM Permissions Guidelines, as amended from time to time.

3. Duration of Licence

3. 1. A licence for is valid from the date of purchase ('Licence Date') at the end of the relevant period in the below table:

Scope of Licence	Duration of Licence
Post on a website	12 months
Presentations	12 months
Books and journals	Lifetime of the edition in the language purchased

4. Acknowledgement

4. 1. The Licensor's permission must be acknowledged next to the Licenced Material in print. In electronic form, this acknowledgement must be visible at the same time as the figures/tables/illustrations or abstract, and must be hyperlinked to the journal/book's homepage. Our required acknowledgement format is in the Appendix below.

5. Restrictions on use

5. 1. Use of the Licensed Material may be permitted for incidental promotional use and minor editing privileges e.g. minor adaptations of single figures, changes of format, colour and/or style where the adaptation is credited as set out in Appendix 1 below. Any other changes including but not limited to, cropping, adapting, omitting material that affect the meaning, intention or moral rights of the author are strictly prohibited.

5. 2. You must not use any Licensed Material as part of any design or trademark.

5. 3. Licensed Material may be used in Open Access Publications (OAP) before publication by Springer Nature, but any Licensed Material must be removed from OAP sites prior to final publication.

6. Ownership of Rights

6. 1. Licensed Material remains the property of either Licensor or the relevant third party and any rights not explicitly granted herein are expressly reserved.

7. Warranty

IN NO EVENT SHALL LICENSOR BE LIABLE TO YOU OR ANY OTHER PARTY OR ANY OTHER PERSON OR FOR ANY SPECIAL, CONSEQUENTIAL, INCIDENTAL OR INDIRECT DAMAGES, HOWEVER CAUSED, ARISING OUT OF OR IN CONNECTION WITH THE DOWNLOADING, VIEWING OR USE OF THE MATERIALS REGARDLESS OF THE FORM OF ACTION, WHETHER FOR BREACH OF CONTRACT, BREACH OF WARRANTY, TORT, NEGLIGENCE, INFRINGEMENT OR OTHERWISE (INCLUDING, WITHOUT LIMITATION, DAMAGES BASED ON LOSS OF PROFITS, DATA, FILES, USE, BUSINESS OPPORTUNITY OR CLAIMS OF THIRD PARTIES), AND
WHETHER OR NOT THE PARTY HAS BEEN ADVISED OF THE POSSIBILITY OF SUCH DAMAGES. THIS LIMITATION SHALL APPLY NOTWITHSTANDING ANY FAILURE OF ESSENTIAL PURPOSE OF ANY LIMITED REMEDY PROVIDED HEREIN.

8. Limitations

8. 1. ***BOOKS ONLY:*** Where **'reuse in a dissertation/thesis'** has been selected the following terms apply: Print rights of the final author's accepted manuscript (for clarity, NOT the published version) for up to 100 copies, electronic rights for use only on a personal website or institutional repository as defined by the Sherpa guideline (www.sherpa.ac.uk/romeo/).

8. 2. For content reuse requests that qualify for permission under the STM Permissions Guidelines, which may be updated from time to time, the STM Permissions Guidelines supersede the terms and conditions contained in this licence.

9. Termination and Cancellation

9. 1. Licences will expire after the period shown in Clause 3 (above).

9. 2. Licensee reserves the right to terminate the Licence in the event that payment is not received in full or if there has been a breach of this agreement by you.

Appendix 1 — Acknowledgements:

For Journal Content:
Reprinted by permission from **[the Licensor]**: **[Journal Publisher** (e.g. Nature/Springer/Palgrave)] **[JOURNAL NAME] [REFERENCE CITATION** (Article name, Author(s) Name), **[COPYRIGHT]** (year of publication)

For **Advance Online Publication papers:**
Reprinted by permission from **[the Licensor]**: **[Journal Publisher** (e.g. Nature/Springer/Palgrave)] **[JOURNAL NAME] [REFERENCE CITATION** (Article name, Author(s) Name), **[COPYRIGHT]** (year of publication), advance online publication, day month year (doi: 10.1038/sj.[JOURNAL ACRONYM].)

For Adaptations/Translations:
Adapted/Translated by permission from **[the Licensor]**: **[Journal Publisher** (e.g. Nature/Springer/Palgrave)] **[JOURNAL NAME] [REFERENCE CITATION** (Article name, Author(s) Name), **[COPYRIGHT]** (year of publication)

Note: For any republication from the British Journal of Cancer, the following credit line style applies:

Reprinted/adapted/translated by permission from **[the Licensor]**: on behalf of Cancer Research UK: : **[Journal Publisher** (e.g. Nature/Springer/Palgrave)] **[JOURNAL NAME] [REFERENCE CITATION** (Article name, Author(s) Name), **[COPYRIGHT]** (year of publication)

For **Advance Online Publication** papers:
Reprinted by permission from The **[the Licensor]**: on behalf of Cancer Research UK: **[Journal Publisher** (e.g. Nature/Springer/Palgrave)] **[JOURNAL NAME] [REFERENCE CITATION** (Article name, Author(s) Name), **[COPYRIGHT]** (year

of publication), advance online publication, day month year (doi: 10.1038/sj. [JOURNAL ACRONYM])

For Book content:
Reprinted/adapted by permission from [**the Licensor**]: [**Book Publisher** (e.g. Palgrave Macmillan, Springer etc) [**Book Title**] by [**Book author**(s)] [**COPYRIGHT**] (year of publication)

Other Conditions:

Version 1.3

Questions? customercare@copyright.com or +1-855-239-3415 (toll free in the US) or +1-978-646-2777.

Acknowledgements

I studied biochemistry to understand mechanisms and processes in the human body on a molecular level and my long-term goal was to use this knowledge and my experimental skills to help patients. In this thesis I could follow this dream and apply my research translationally. Therefore, sincere thanks are given to my supervisors Prof. Christoph Klein and Dr. Daniel Kotlarz, who gave me the opportunity to perform these very interesting translational experiments and work at the border of bench and bedside. I am very thankful for the excellent technical, financial, and intellectual environment that they provided at the CCRC Hauner. I learnt an indescribable number of techniques and skills in a scientific and personal perspective, which have prepared me extremely well for my future life as a scientist and as a person. I hope that I can use these skills in future to help patients and the society. I am also grateful for the fruitful discussions that we had to promote the projects and help our patients. In this line, I would like to also thank Prof. Carolin Daniel for spending the time to serve as my third TAC member and providing helpful feedback during our regular meetings. Furthermore, I would like to thank all my lab colleagues for their help in the lab, for their professional and personal advice, for the fun that they brought to the lab, and for all the nice memories that we made together.

A PhD thesis requires enthusiasm, motivation, and resilience, but also needs time to develop ideas, perform experiments, and advance science. Financial support by different sources provided me with the necessary security and freedom to complete this thesis. Equally important, non-material support by different institutions helped me to develop personally and mentally. In particular, I am very grateful for the Hanns-Seidel-Stiftung for financial and non-material support during this thesis, which gave me the freedom to focus on my experiments, but also broadened my interest in rhetorical, societal and political topics. Furthermore, I would like to thank the Studienstiftung des deutschen Volkes for their non-material support during my PhD, which helped me to develop personally and provided me mentorship. I would also like to express my gratitude to the Care-for-Rare Foundation, the Reinhard-Frank-Stiftung, and the Else-Kröner-Fresenius-Stiftung for personal funding and funding of my project during different phases of my thesis, which gave me security in pursuing this thesis and allowed to perform important experiments. I would like to thank the CRC1054 and its members for strengthening my interest and knowledge in immunity, providing a network of like-minded people, and giving me the opportunity to join interesting lectures, seminars, retreats, and discussions.

Last, but not less important, I would like to express my sincere gratitude to my wife Valery, my mother Heike, my father Andreas, my sister Jasmin, and all my close friends. Without their emotional and every day support I would have not been able to perform this challenging project and complete this thesis. I am thankful for all the talks that we have, for all the phone calls, for the holidays, for all the diversion that you provided and that you accept the challenges of the scientist life without hesitation.

Affidavit

LMU LUDWIG-MAXIMILIANS-UNIVERSITÄT MÜNCHEN | Promotionsbüro Medizinische Fakultät | MMRS

Affidavit

ILLIG, DAVID
Surname, first name

Lindwurmstraße 2A
Street

80337 München, Germany
Zip code, town, country

I hereby declare, that the submitted thesis entitled:

Elucidation of novel monogenic disorders in children with intestinal inflammation
……

is my own work. I have only used the sources indicated and have not made unauthorised use of services of a third party. Where the work of others has been quoted or reproduced, the source is always given.

I further declare that the submitted thesis or parts thereof have not been presented as part of an examination degree to any other university.

München, 27.04.2022 — David Illig

place, date — Signature doctoral candidate

Confirmation of congruency

LMU LUDWIG-MAXIMILIANS-UNIVERSITÄT MÜNCHEN

Promotionsbüro Medizinische Fakultät

MMRS

Confirmation of congruency between printed and electronic version of the doctoral thesis

ILLIG, DAVID

Surname, first name

Lindwurmstraße 2A

Street

80337 München, Germany

Zip code, town, country

I hereby declare, that the submitted thesis entitled:

Elucidation of novel monogenic disorders in children with intestinal inflammation

……

is congruent with the printed version both in content and format.

München, 27.04.2022

place, date

David Illig

Signature doctoral candidate

List of publications

1. **Illig D**, Navratil M, Kelecic J, Conca R, Hojsak I, Jadresin O, Coric M, Vukovic J, Rohlfs M, Hollizeck S, Bohne J, Klein C, Kotlarz D. Alternative Splicing Rescues Loss of Common Gamma Chain Function and Results in IL-21R-like Deficiency. J Clin Immunol. 2019;39(2):207-15.

2. Goettel JA, Kotlarz D, Emani R, Canavan JB, Konnikova L, **Illig D**, Frei SM, Field M, Kowalik M, Peng K, Gringauz J, Mitsialis V, Wall SM, Tsou A, Griffith AE, Huang Y, Friedman JR, Towne JE, Plevy SE, O'Hara Hall A, Snapper SB. Low-Dose Interleukin-2 Ameliorates Colitis in a Preclinical Humanized Mouse Model. Cell Mol Gastroenterol Hepatol. 2019;8(2):193-5.

3. Magg T, Shcherbina A, Arslan D, Desai MM, Wall S, Mitsialis V, Conca R, Unal E, Karacabey N, Mukhina A, Rodina Y, Taur PD, **Illig D**, Marquardt B, Hollizeck S, Jeske T, Gothe F, Schober T, Rohlfs M, Koletzko S, Lurz E, Muise AM, Snapper SB, Hauck F, Klein C, Kotlarz D. CARMIL2 Deficiency Presenting as Very Early Onset Inflammatory Bowel Disease. Inflamm Bowel Dis. 2019;25(11):1788-95.

4. Khoshnevisan R, Anderson M, Babcock S, Anderson S, **Illig D**, Marquardt B, Sherkat R, Schroder K, Moll F, Hollizeck S, Rohlfs M, Walz C, Adibi P, Rezaei A, Andalib A, Koletzko S, Muise AM, Snapper SB, Klein C, Thiagarajah JR, Kotlarz D. NOX1 Regulates Collective and Planktonic Cell Migration: Insights From Patients With Pediatric-Onset IBD and NOX1 Deficiency. Inflamm Bowel Dis. 2020;26(8):1166-76.